Application of Plasma Phenomena

Po-Yu Chang

Institute of Space and Plasma Sciences, National Cheng Kung University

Lecture 4

2025 fall semester

Thursday 9:00-12:00

Materials:

https://capst.ncku.edu.tw/PGS/index.php/teaching/

Online courses:
https://nckucc.webex.com/nckucc/j.php?MTID=m50e2008a7e216ef32c42db2d027415ec

2025/10/8 updated

Methods of plasma production

- DC electrical discharges
  - Dark electrical discharges in gases
  - DC electrical glow discharges in gases
  - DC electrical arc discharges in gases
- AC electrical discharges
  - RF electrical discharges in gases
  - Microwave electrical discharges in gases
  - Dielectric-barrier discharges (DBDs)
- Other mechanism
  - Laser produced plasma
  - Pulsed-power generated plasma

Reference

- Industrial plasma engineering, volume 1, by J. Reece Roth, Chapter 8 - 13.
- Plasma physics and engineering, by Alexander Fridman an Lawrence A. Kennedy.
- Plama medicine, by Alexander Fridman and Gary Frideman.

Methods of plasma production

- **DC electrical discharges**
  - **Dark electrical discharges in gases**
  - **DC electrical glow discharges in gases**
  - **DC electrical arc discharges in gases**
- **AC electrical discharges**
  - **RF electrical discharges in gases**
  - **Microwave electrical discharges in gases**
  - **Dielectric-barrier discharges (DBDs)**
- **Other mechanism**
  - **Laser produced plasma**
  - **Pulsed-power generated plasma**

Electrical discharge physics was studied using the classical low pressure electrical discharge tube

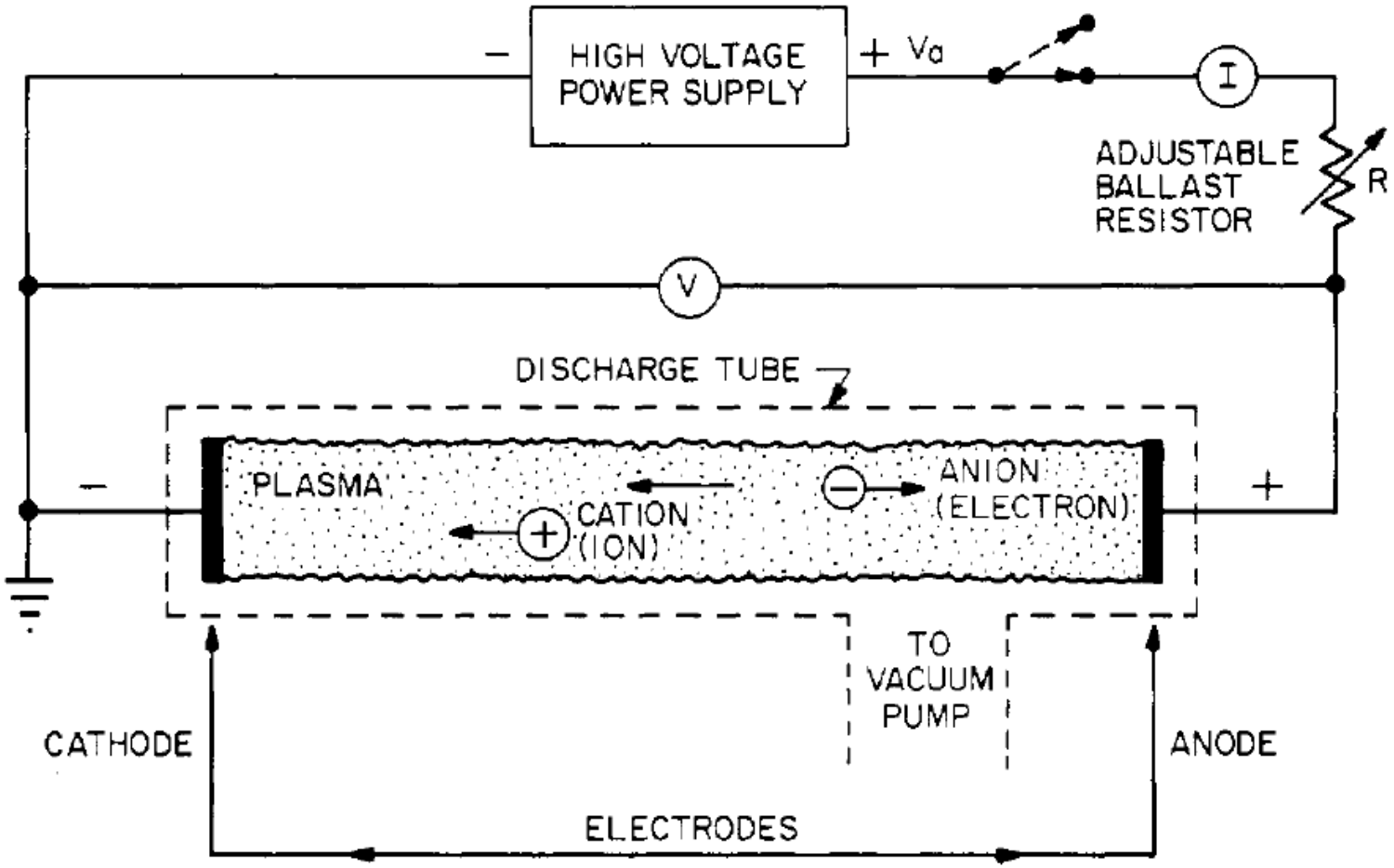

The V-I curve is nonlinear in a DC electrical discharge tube

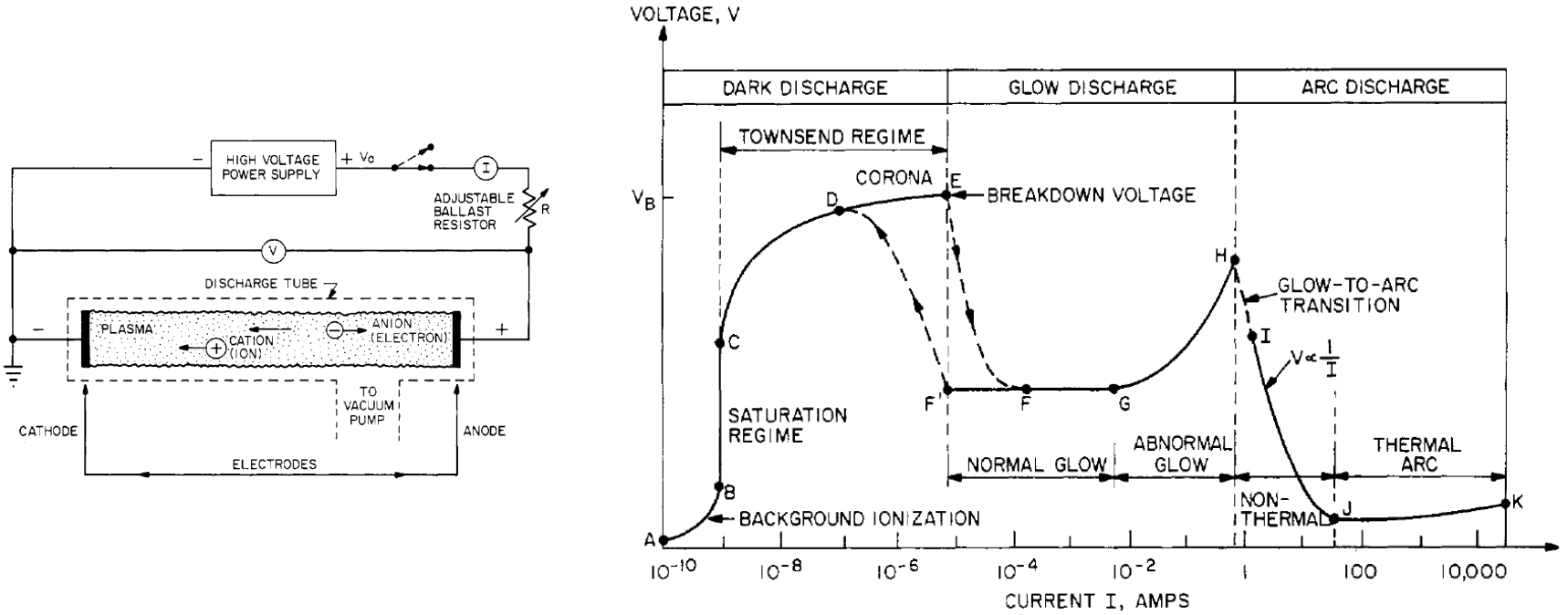

- Depends on the voltage, the adjustable ballast resistor, the voltage-current characteristic behaves differently in different regime.
  - Dark discharge
  - Glow discharge
  - Arc discharge

In a dark discharge, the excitation light is so little and is not visible

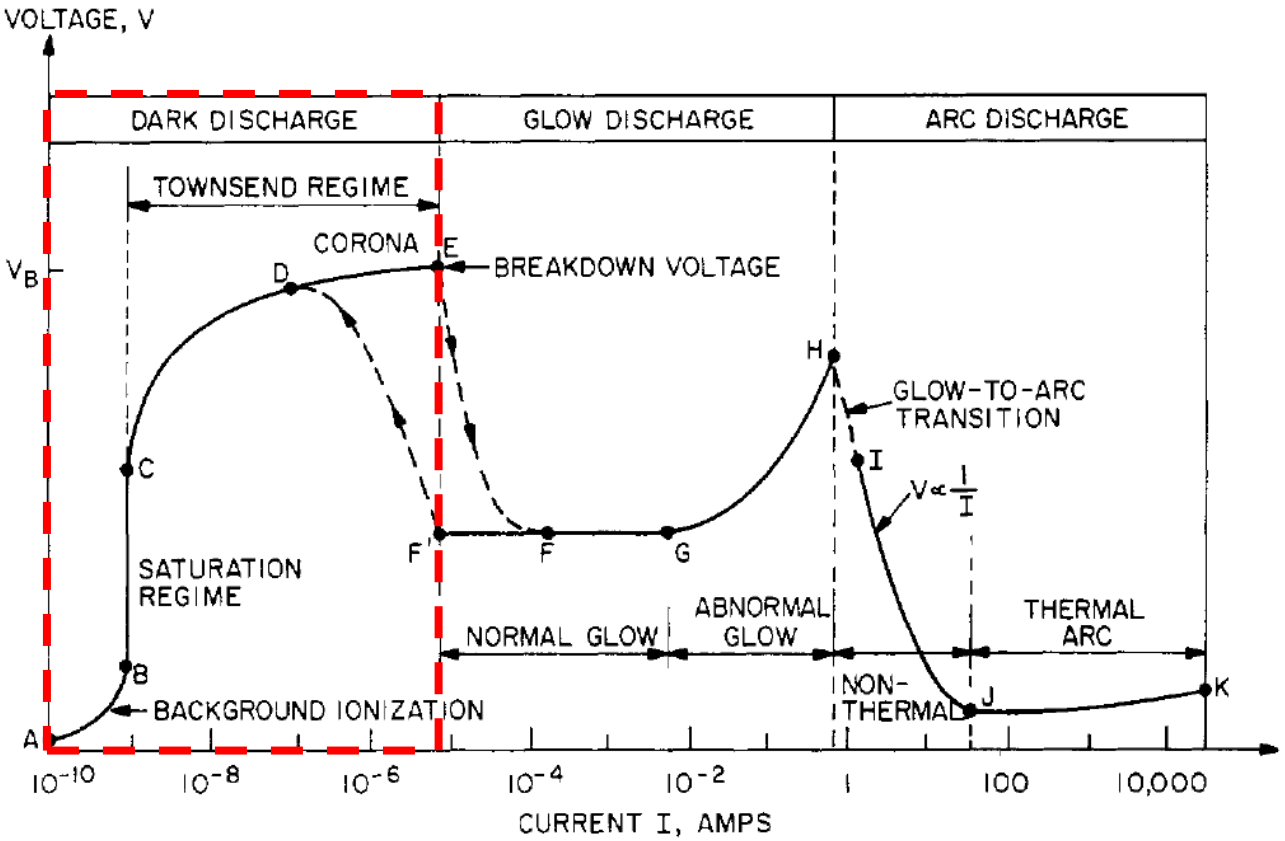

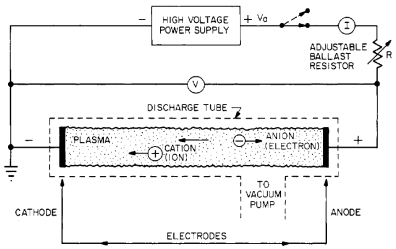

- In dark discharge, with the exception of the more energetic corona discharges, the number density of excited species is so small so that it does not emit enough light to be seen by a human observer.

In background ionization, ions and electrons are created by ionization from background radiation

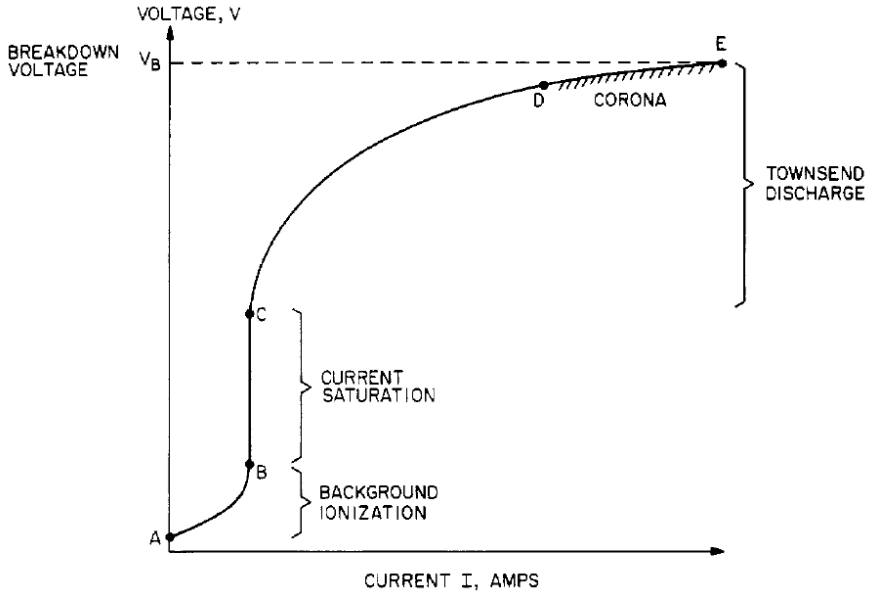

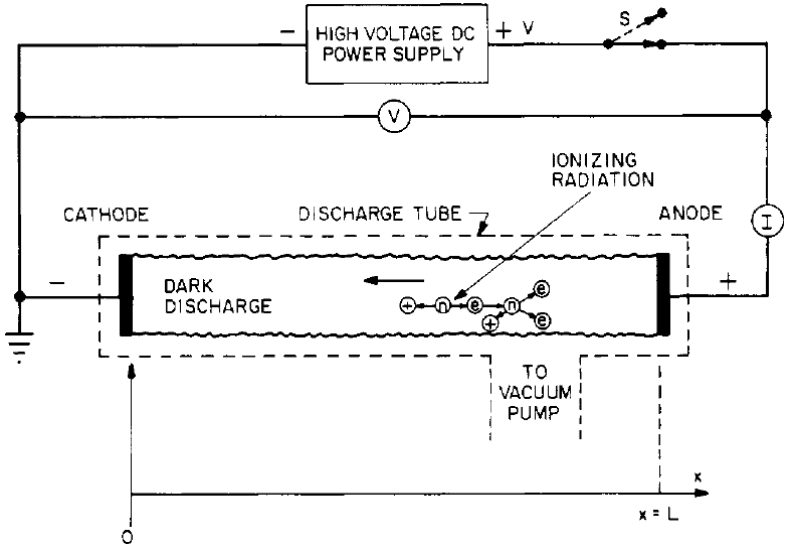

- **Sources of background radiation:**
  - **Cosmic rays**
  - **Radioactive minerals in the surroundings**
  - **Electrostatic charge**
  - **UV light illumination**
  - **Other sources**

Current saturation occurs when all ions and electrons produced between the electrodes are collected

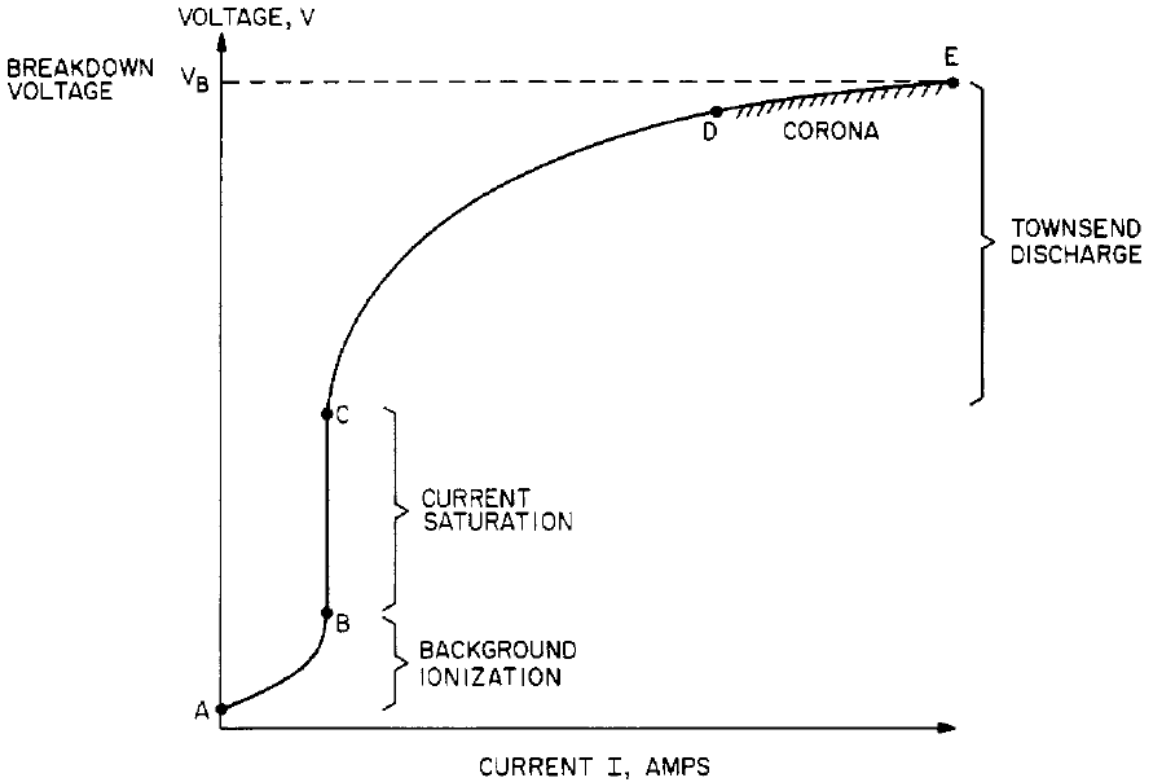

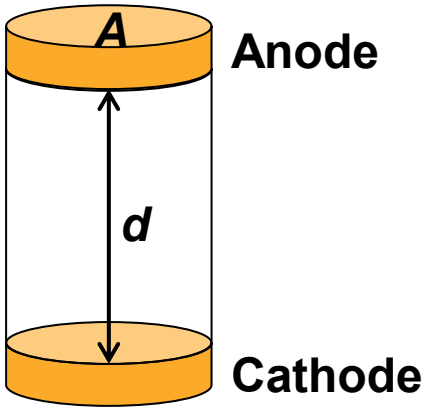

$$S = \frac{dn}{dt}\left(\text{electrons or ions/m}^3 - \text{s}\right)$$

$$I_s = eAdS \qquad J_s = edS$$

The region where the current exponentially increases is called the Townsend discharge

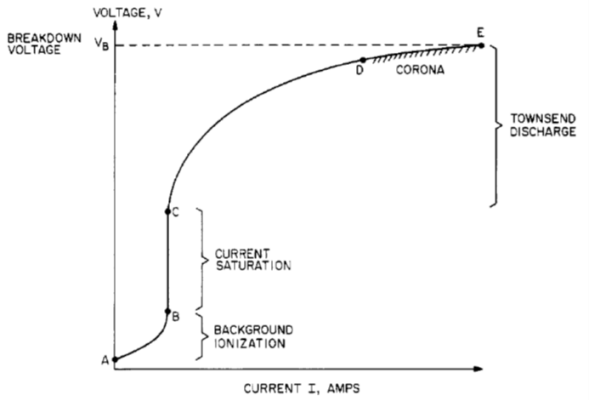

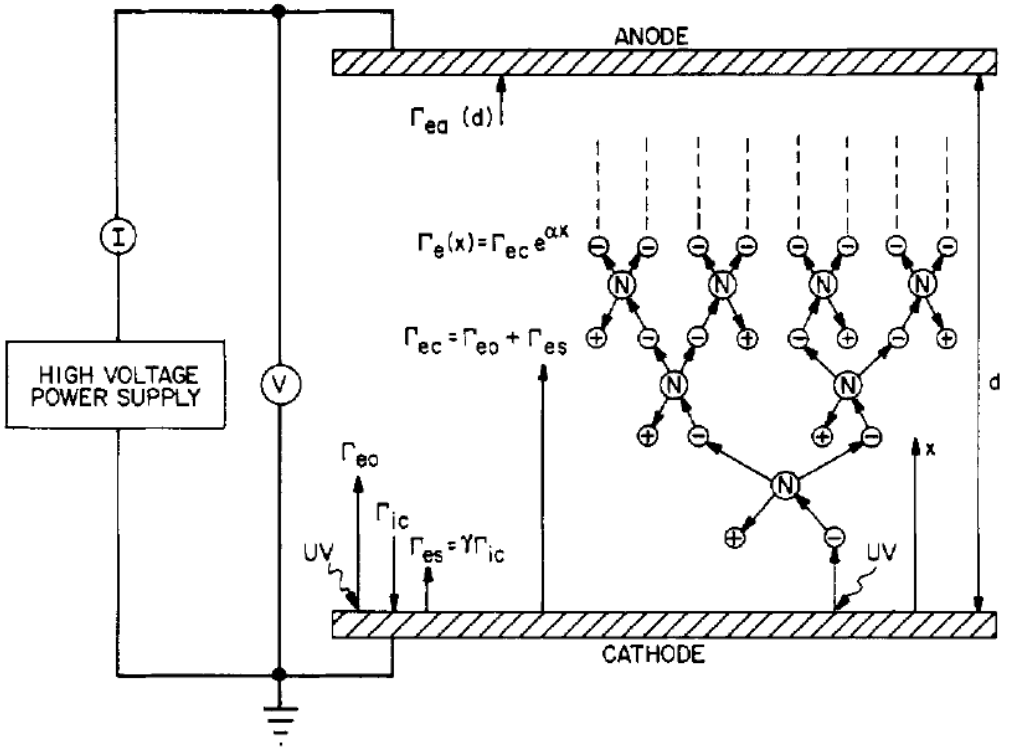

- **Electrons from photo- or secondary electron emission from the cathode:**

$$\boldsymbol{\Gamma_{ec} = \Gamma_{e0} + \Gamma_{es}\left(\text{electrons}/m^2 - s\right)}$$

- **Volume ionization source from the ionization of the background gas by energetic electrons accelerated in the electric field:**

$$\boldsymbol{S_e = R_e = n_e n_0 \langle \sigma v \rangle_{ne}}$$

Chain reaction or avalanche of electron and ion production occurs in a strong electric field

1. The electrons initially produced in the creation of ion-electron pairs by ionizing radiation or from other sources are accelerated in the electric field of the discharge tube.
2. If the electric field is high enough, the electrons can acquire sufficient energy before reaching the anode to ionize another neutral atom.
3. As the electric field becomes stronger, these secondary electrons may themselves ionize a third neutral atom leading to a chain reaction, or avalanche of electron and ion production.

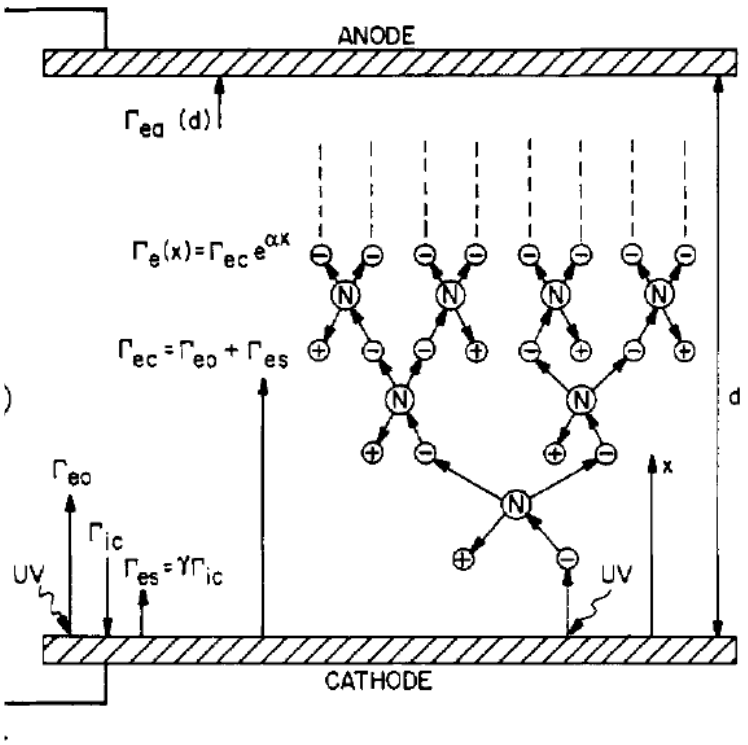

Special case I

- **Assumption:**
  - **No recombination or loss of electrons occurs.**
  - **Initiating electrons are emitted from the cathode, with no contribution by volume ionization.**
- **Townsend's first ionization coefficient, α: the number of ionizing collisions made on the average by an electron as it travels 1 m along the electric field:**

$$\alpha \sim \frac{1}{\lambda_i} = \frac{\nu_{ei}}{\bar{v}_e} = \frac{n_0 \langle \sigma v_e \rangle_{ne}}{\bar{v}_e}$$

- **Differential electron flux:**

$$d\Gamma_e = \alpha \Gamma_e dx$$

$$\int_{\Gamma_{e0}}^{\Gamma_e} \frac{d\Gamma_e}{\Gamma_e} = \int_0^x \alpha dx$$

$$\Gamma_e = \Gamma_{e0} e^{\alpha x}$$

$$J_e = e\Gamma_e = J_{e0} e^{\alpha x} \quad (A/m^2)$$

$$I_e = I_{e0} e^{\alpha x} = A J_{e0} e^{\alpha x} \quad (A)$$

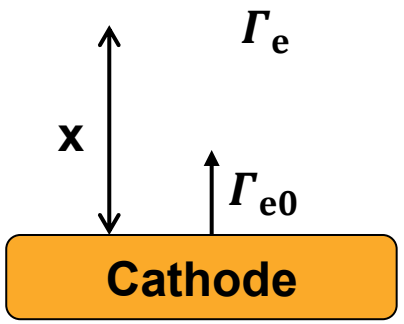

Special case II

- **Assumption:**
  - **No recombination or loss of electrons occurs.**
  - **No cathode emission, i.e., Γ_{e0}=0.**
  - **Significant volume source of electrons throughout the discharge volume.**
- **Differential electron flux:**

$$d\Gamma_e = \alpha\Gamma_e dx + S_e dx$$

$$\int_0^{\Gamma_e} \frac{1}{\alpha\Gamma_e + S_e}\, d\Gamma_e = \int_0^x \mathrm{d}x = \frac{\ln(\alpha\Gamma_e + S_e)}{\alpha}\Big|_0^{\Gamma_e}$$

$$\Gamma_e = \frac{S_e}{\alpha}(e^{\alpha x} - 1)$$

$$J_e = e\Gamma_e = \frac{eS_e}{\alpha}(e^{\alpha x} - 1)$$

$$J_e = \frac{J_s}{\alpha d}(e^{\alpha x} - 1)$$

$$J_s = edS_e$$

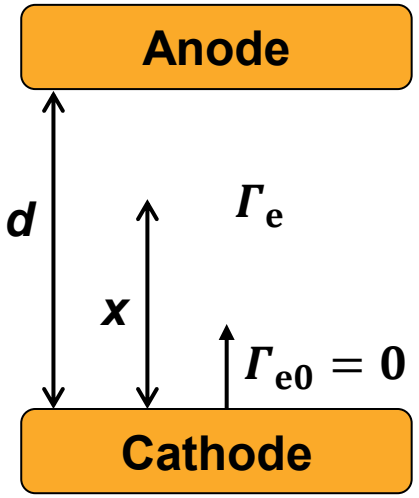

Derivation of Townsend's first ionization coefficient

$$\frac{1}{\lambda_i} = \frac{\nu_{ei}}{\bar{v}_e} = \frac{n_0\langle\sigma v_e\rangle_{ne}}{\bar{v}_e} = \frac{p}{T}\frac{\langle\sigma v\rangle_{ne}}{\bar{v}_e} \equiv Ap \qquad A \equiv \frac{1}{T}\frac{\langle\sigma v\rangle_{ne}}{\bar{v}_e}$$

- **Number of primary electrons with energy higher than the ionization potential:**

$$dn_e = -n_e\frac{dx_i}{\lambda_i} \quad \Rightarrow \quad \frac{n_e(x_i)}{n_{e0}} = \exp\left(-\frac{x_i}{\lambda_i}\right)$$

$$\alpha \equiv \frac{\#/\text{ ionization collisions}}{\text{per electron}} \times (\#/\text{electron with E} > \text{ionization potential})$$

$$= \frac{1}{\lambda_i}\frac{n_e(x_i)}{n_{e0}} = \frac{1}{\lambda_i}\exp\left(-\frac{x_i}{\lambda_i}\right)$$

$$\alpha = Ap\exp(-Apx_i)$$

$$\frac{\alpha}{p} = A\exp\left(-\frac{AV^*}{E/p}\right) \equiv A\exp\left(-\frac{C}{E/p}\right) \equiv f\left(\frac{E}{p}\right) \qquad x_i \approx \frac{V^*}{E} \text{ where } V^* > V_i$$

- **The parameters A and C must be experimentally determined.**

Phenomenological constants A and C of Townsend's first ionization coefficient for selected gases

Gas	*A* ion pairs/m-Torr	*C* V/m-Torr
A	1200	20 000
Air	1220	36 500
CO_2	2000*	46 600
H_2	1060	35 000
HCl	2500*	38 000
He	182	5 000
Hg	2000	37 000
H_20	1290*	28 900
Kr	1450	22 000
N_2	1060	34 200
Ne	400	10 000
Xe	2220	31 000

* These values may be high by as much as a factor of two.

Stoletow point is the pressure for maximum current

- **Stoletow experimentally found that for a given electric field between the plates, there is an air pressure in the Townsend discharge where the current is a maximum.**

$$p_{\max} = \frac{E}{37200}\ (\text{Torr})$$

$$\frac{\alpha}{p} = A\exp\left(-\frac{C}{E/p}\right)$$

$$\frac{d\alpha}{dp} = A\left[1 - p\frac{C}{E}\right]\exp\left(-\frac{Cp}{E}\right) = 0$$

$$p_{\max} = \frac{E}{C} = \frac{E}{36500}\ \text{for air}$$

$$\frac{\alpha}{p} = f\left(\frac{E}{p}\right)$$

$$\frac{d\alpha}{dp} = \frac{d}{dp}\left[pf\left(\frac{E}{p}\right)\right] \equiv 0$$

$$f\left(\frac{E}{p}\right) - p\frac{E}{p^2}f'\left(\frac{E}{p}\right) = \frac{\alpha}{p} - \frac{E}{p}f'\left(\frac{E}{p}\right) = 0$$

$$\left(\frac{\alpha/p}{E/p}\right) = f'\left(\frac{E}{p}\right) = \tan\theta$$

The current will be a maximum when the tangent to the α/p versus E/p curve intersects the origin

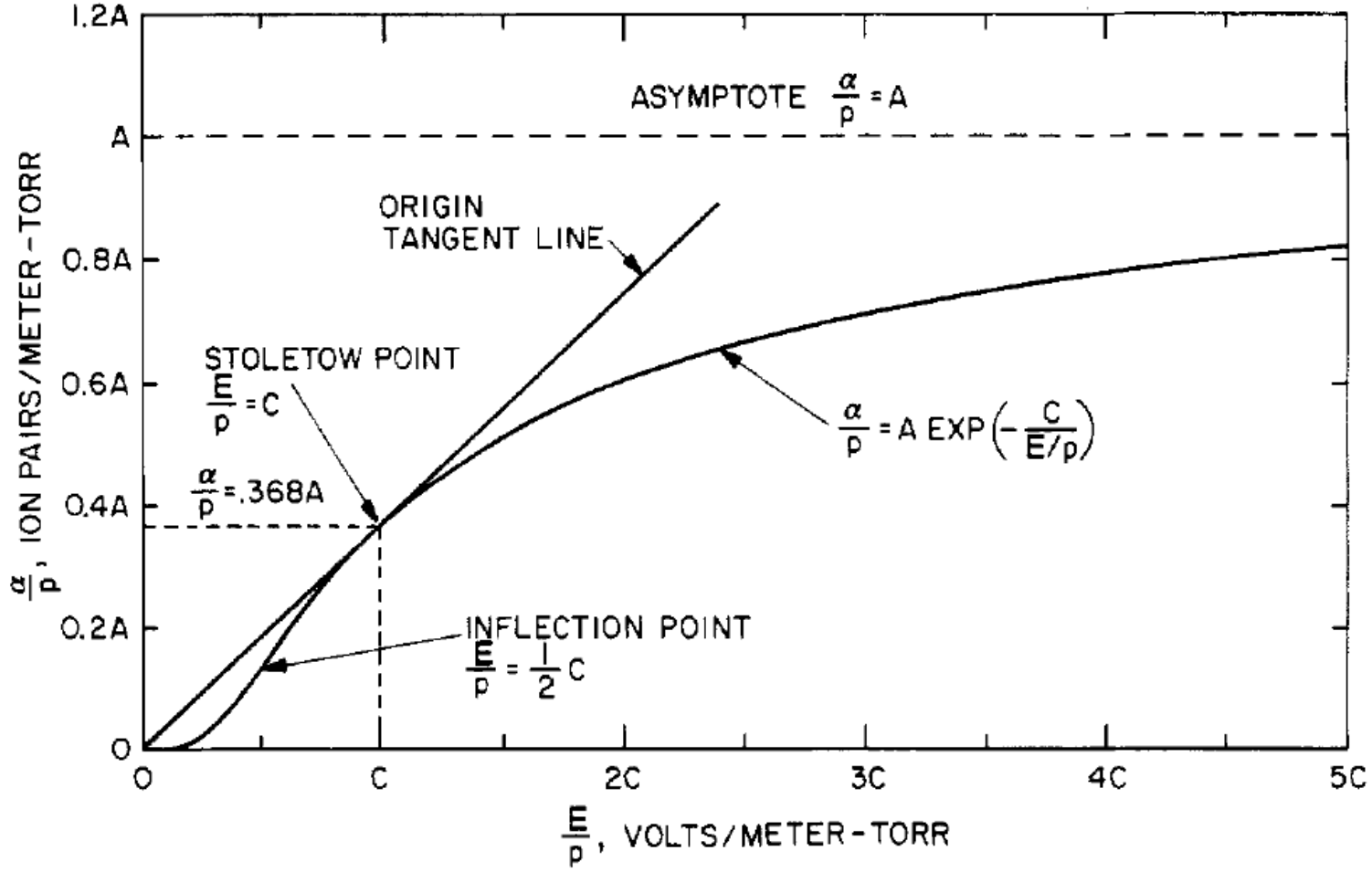

- **Stoletow point is the minimum of the Paschen breakdown curve for gases.**

Corona discharge (unipolar discharge) is a very low current, continuous phenomenon

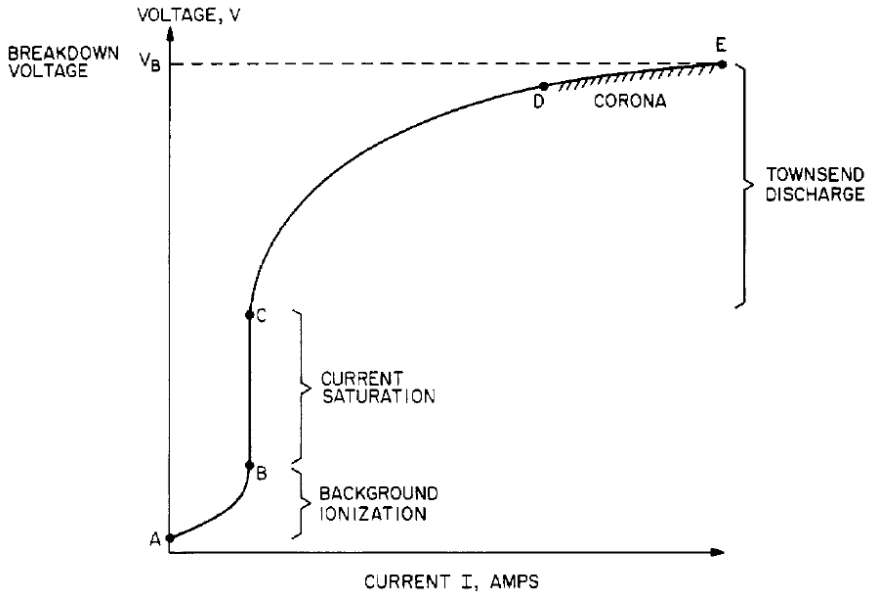

- **Break down condition for dry air:**

$$E_B = 3000 + \frac{1.35}{d}\,\mathrm{kV/m}$$

$$V_B = 3000d + 1.35\ \mathrm{kV}$$

- **Corona can initiate on sharp points at potentials as low as 5 kV.**
- **It can initiate from sharp points, fine wires, sharp edges, asperities, scratches or anything which creates a localized electric field greater than the breakdown electric field of the medium surrounding it.**
- **It can be a "glow discharge", i.e., visible to eyes. For low currents, the entire corona is dark.**

Phenomenology of corona generated by a fine wire

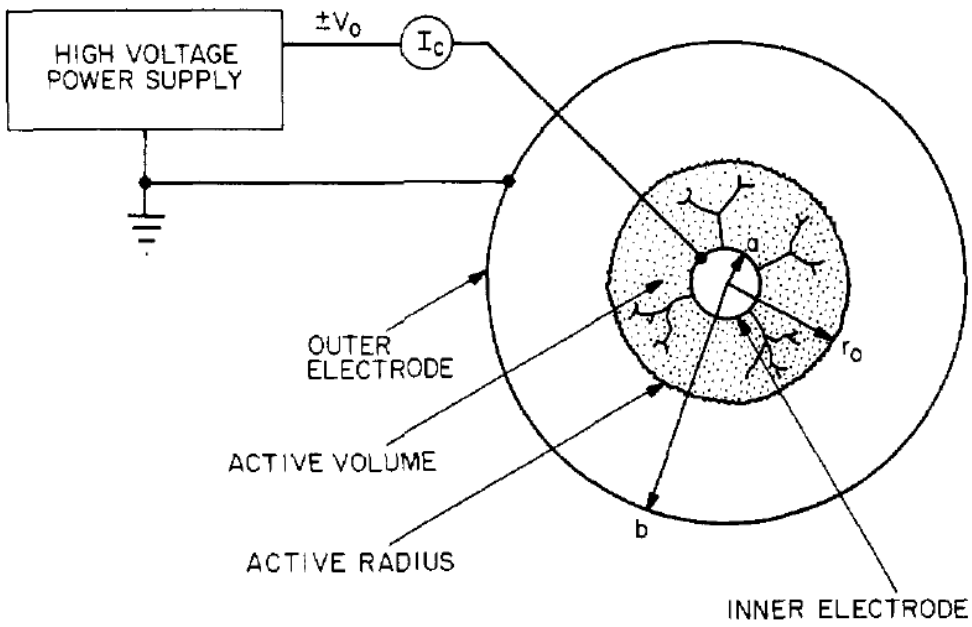

- **The point of corona initiation is that point at which the voltage on the inner conductor of radius a is high enough that corona is just detectable.**
- **The electric field will drop off to the breakdown value at a radius r_0 called the active radius.**

Corona can occur for both positive and negative polarity

- **Positive polarity**

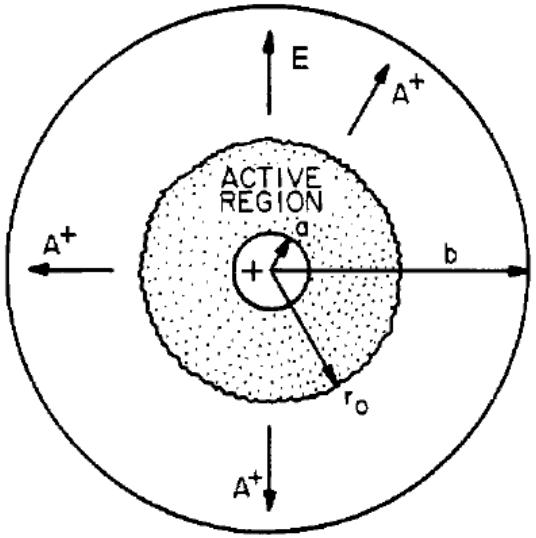

- **Negative polarity**

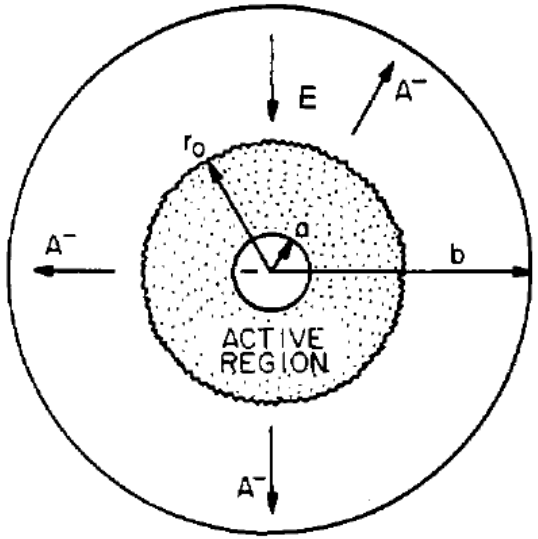

- **The initiation voltages or coronal current are slightly different between positive and negative polarity.**
- **A continuous (positive polarity, DC) or intermittent (negative polarity, usually) current, usually in the order of uA ~ mA per decimeter of length will flow to the power supply.**

Negative point corona, also known as Trichel pulses

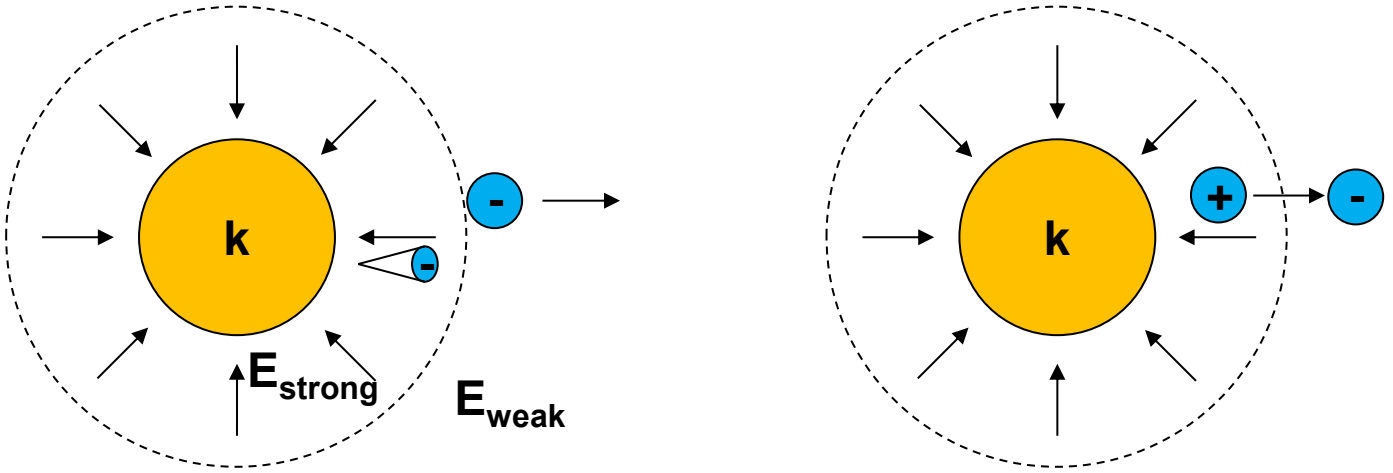

- Avalanche toward anode occurs in the strong electric field region.
- No further ionization occurs in the weak field region.
- Electrons are slow down by positively charged ions (ion+) behind.
- Electrons attach to gas molecules forming negatively charged ions (ion-).
- The presence of the negative ions reduces the electric field at the point electrode and the discharge extinguishes.
- When positively/negatively charged ions drifted away, the original high-field conditions are re-established

Positive point corona

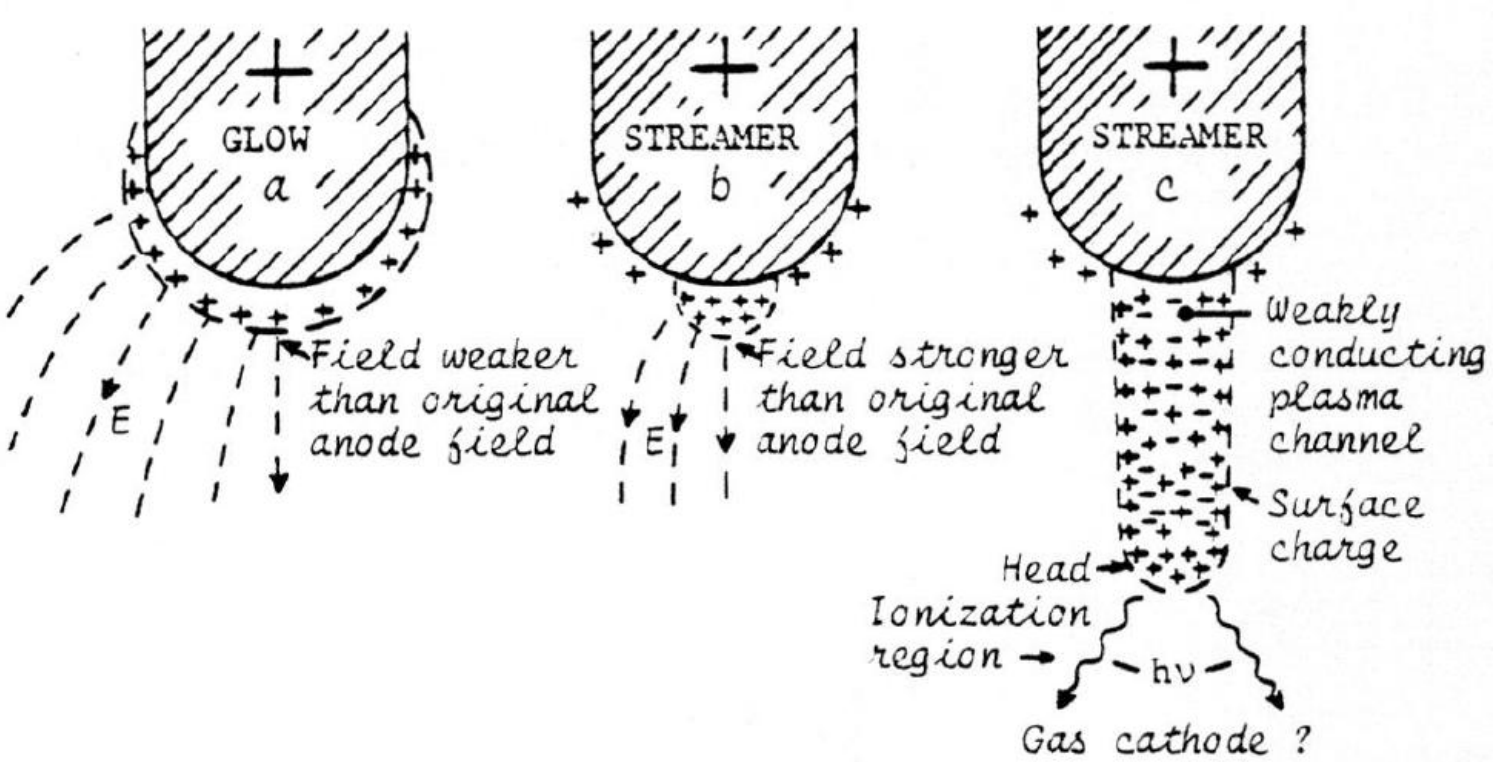

- **Electron avalanche initiated near the high-field region propagating toward anode.**
- **Streamer is developed.**
- **Lateral avalanches feed into the streamer core.**

M. Goldman and R. S. Sigmond, IEEE Trans. Elec. Insulation, **EI-17**, 90 (1982)

Don’t bring a long stick to a train station

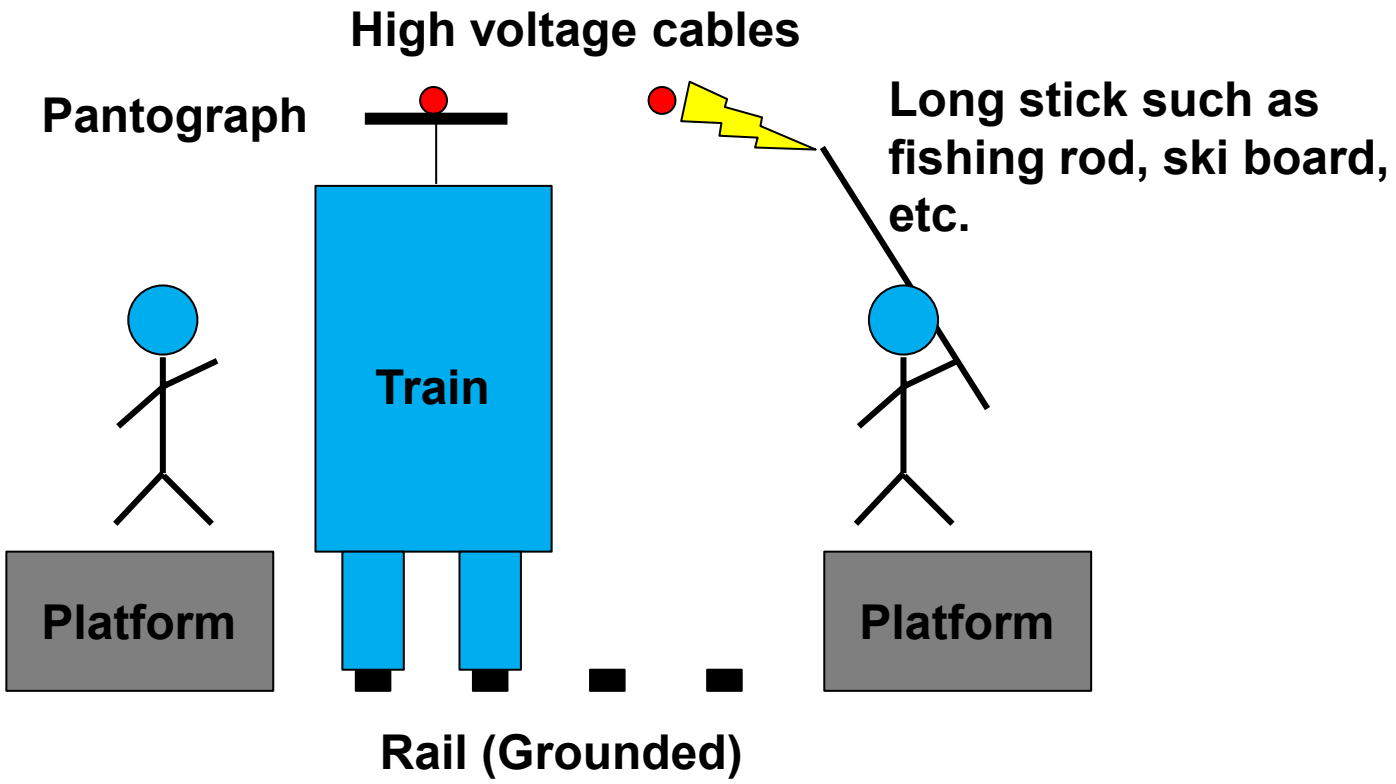

A corona discharge causes some problems even no breakdown occurs

- Ozone (O_3) is generated.
- Rubber is destroyed by O_3.
- NO_3^+ is generated with moisture.
- Disadvantage:
  - Power losses.
  - Radio frequency (RF) interference.
  - Reduce the service life of solid and liquid insulation via initiating partial discharge.
  - Chemical decomposition.
- Advantage:
  - Pseudospark discharge – fast switch.
  - Electrostatic precipitator (dust remover) using corona discharge.
  - Hair dryer

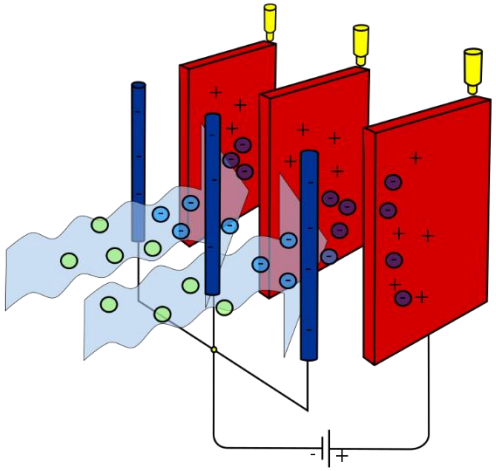

https://zh.wikipedia.org/wiki/%E9%9D%99%E7%94%B5%E9%99%A4%E5%B0%98

A corona shield is used to suppress corona

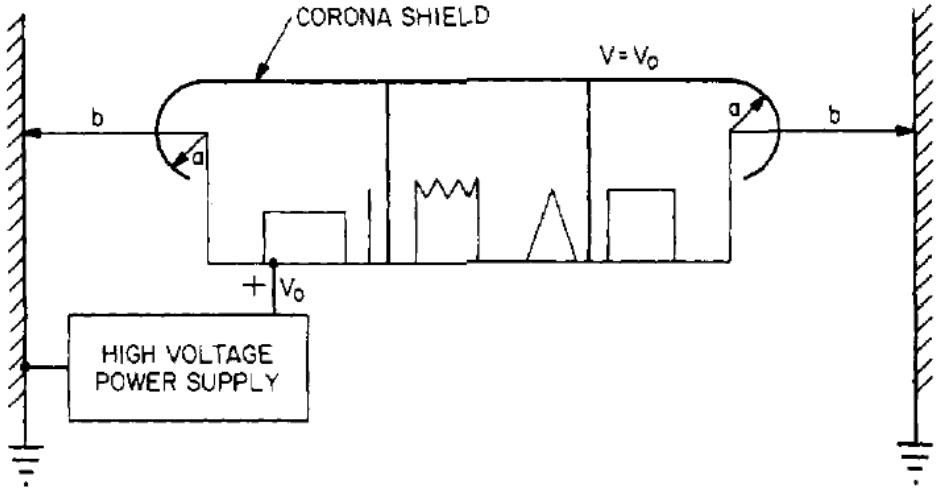

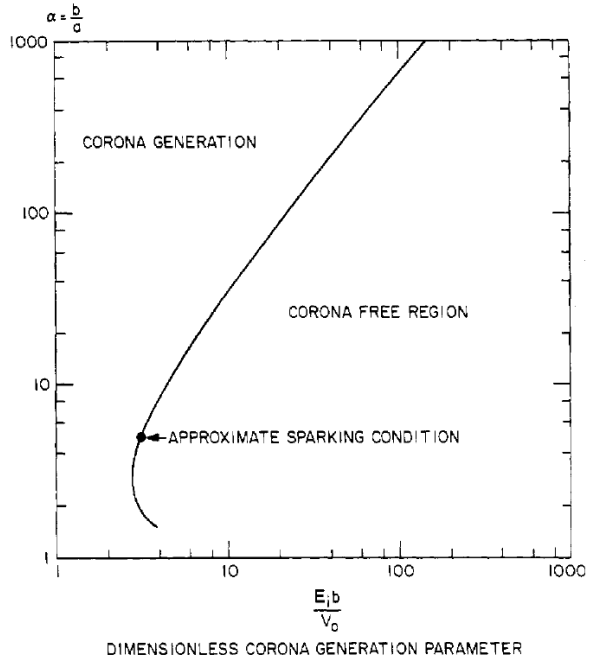

- **Cylindrical approximation:**

$$E_s = \frac{V_0}{a\ln(b/a)} = \frac{bV_0}{\mathrm{a\ b}\ln(b/a)} \qquad \chi \equiv \frac{b}{a}$$

$$\Rightarrow \quad \frac{E_i b}{V_0} = \frac{\chi}{\ln\chi}$$

$$E_s \equiv E_i \ \ (E@\ \text{surface for corona initiation})$$

- **For b=0.5 m, V_0=50 kV, E_i~E_B~3 MV/m**

$$\frac{E_B b}{V_0} = \frac{3\times10^6\times0.5}{5\times10^4} = 30 = \frac{\chi}{\ln\chi}$$

$$\chi \approx 150, i.e., a = 0.33\text{mm}$$

Electrical breakdown occurs when applied voltage is greater than the breakdown voltage

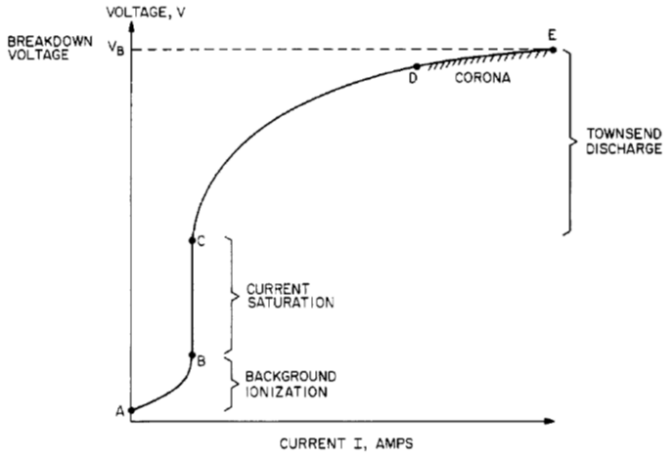

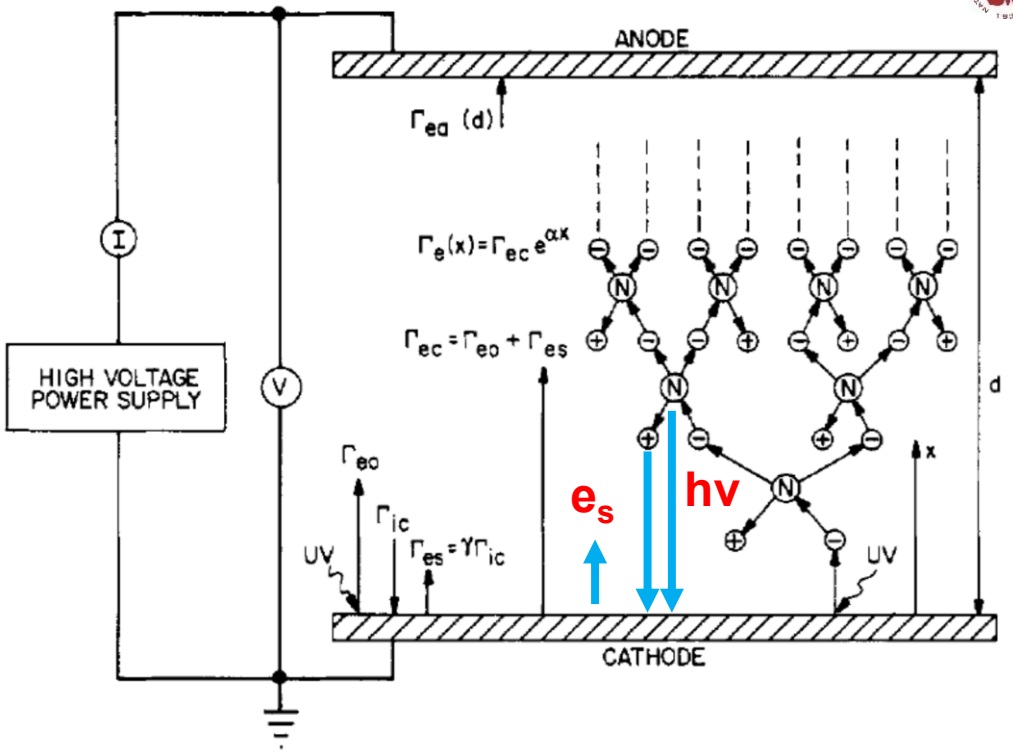

- **Primary electrons: electrons from the cathode due to photoemission, background radiation, or other processes.**
- **Secondary electrons: electrons emitted from the cathode per incident ion or photon created from ionization in gas.**

Derivation of electrical breakdown

- **Secondary electron emission coefficient:**

$$\gamma \equiv \frac{\#/\text{ of electrons emitted}}{\#/\text{ of incident ions or photons}}$$

$$\Gamma_{es} = \gamma\Gamma_{ic}$$

$$\Gamma_{ec} = \Gamma_{e0} + \Gamma_{es}$$

$$I_{ea} = I_{ec} + I_{ic} \quad \Rightarrow \quad \Gamma_{ea} = \Gamma_{ec} + \Gamma_{ic}$$

$$\Gamma_{ea} - \Gamma_{ec} = \Gamma_{ic} = \frac{\Gamma_{es}}{\gamma} \qquad (\Gamma_{ea} = \Gamma_{ec}e^{\alpha d})$$

$$\Gamma_{es} = \gamma(\Gamma_{ea} - \Gamma_{ec}) = \gamma\Gamma_{ec}\left(e^{\alpha d} - 1\right)$$

$$\Gamma_{ec} = \Gamma_{es} + \Gamma_{e0} = \gamma\Gamma_{ec}\left(e^{\alpha d} - 1\right) + \Gamma_{e0}$$

$$\Gamma_{ec} = \frac{\Gamma_{e0}}{1 - \gamma(e^{\alpha d} - 1)}$$

$$\Gamma_{ea} = \Gamma_{e0}\frac{e^{\alpha d}}{1 - \gamma(e^{\alpha d} - 1)}\left(\text{electrons}/m^2 - s\right)$$

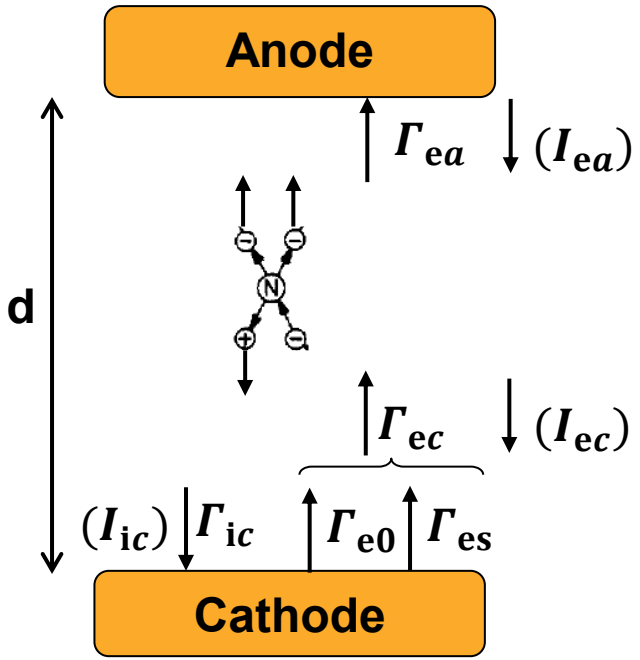

$$J = J_0\frac{e^{\alpha d}}{1 - \gamma(e^{\alpha d} - 1)}\left(A/m^2\right)$$

The Townsend condition for ignition (avalanche grows)

$$J = J_0 \frac{e^{\alpha d}}{1-\gamma(e^{\alpha d}-1)} \left(A/m^2\right)$$

- The Townsend condition for ignition or called avalanche grows occurs when

$$1-\gamma\left(e^{\alpha d}-1\right)=0$$

$$\gamma e^{\alpha d}=\gamma+1 \quad \text{or} \quad \ln\left(1+\frac{1}{\gamma}\right)=\alpha d$$

$$Apd\exp\left(-\frac{Cpd}{V_B}\right)=\ln\left(1+\frac{1}{\gamma}\right) \qquad \frac{\alpha}{p}=A\exp\left(-\frac{C}{E/p}\right) \quad E_B=\frac{V_B}{d}$$

$$V_B=\frac{Cpd}{\ln\left[\frac{Apd}{\ln\left(1+\frac{1}{\gamma}\right)}\right]}=f(pd)$$

$$(pd)_{min}=\frac{e}{A}\ln\left(1+\frac{1}{\gamma}\right)=\frac{2.718}{A}\ln\left(1+\frac{1}{\gamma}\right) \qquad V_{B,min}=2.718\frac{C}{A}\ln\left(1+\frac{1}{\gamma}\right)$$

Universal Paschen's curve

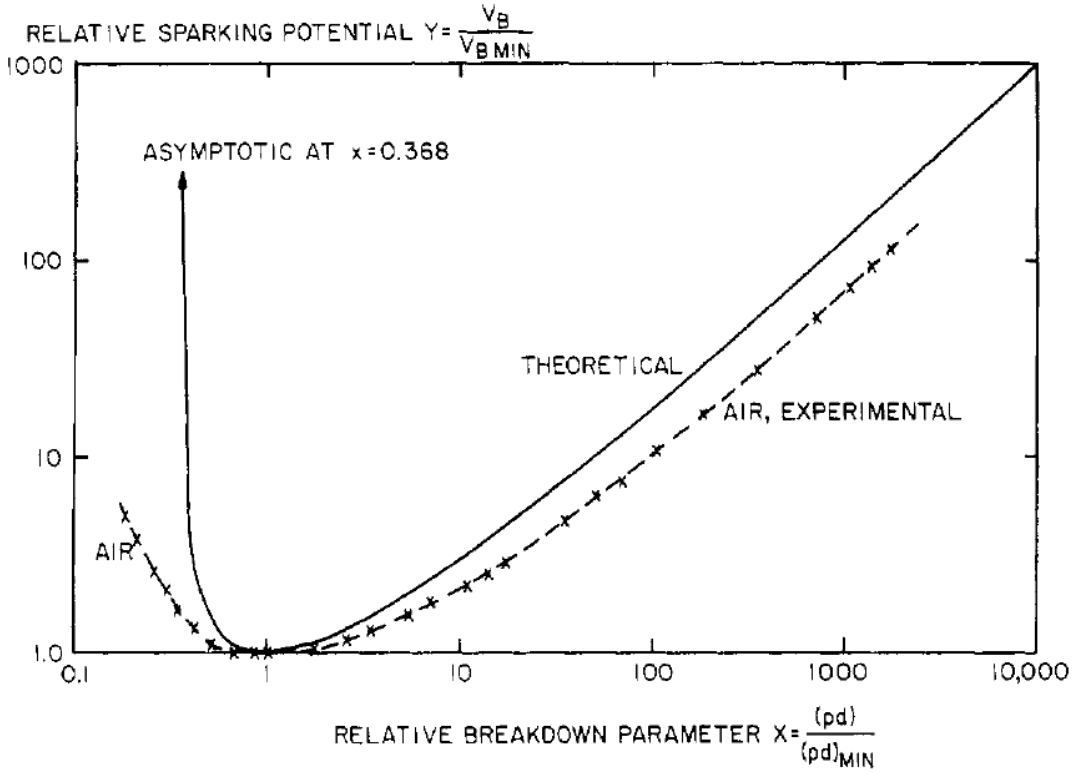

$$V_B = \frac{\mathrm{Cpd}}{\ln\left[\frac{\mathrm{Apd}}{\ln\left(1+\frac{1}{\gamma}\right)}\right]} = f(\mathrm{pd})$$

$$Y \equiv \frac{V_B}{V_{B,\min}} \qquad X \equiv \frac{\mathrm{pd}}{(\mathrm{pd})_{\min}}$$

$$Y = \frac{V_B}{V_{B,\min}} = \frac{X}{1+\ln X}$$

Collision frequency and electron energy gained from electric field are both important to electrical breakdown

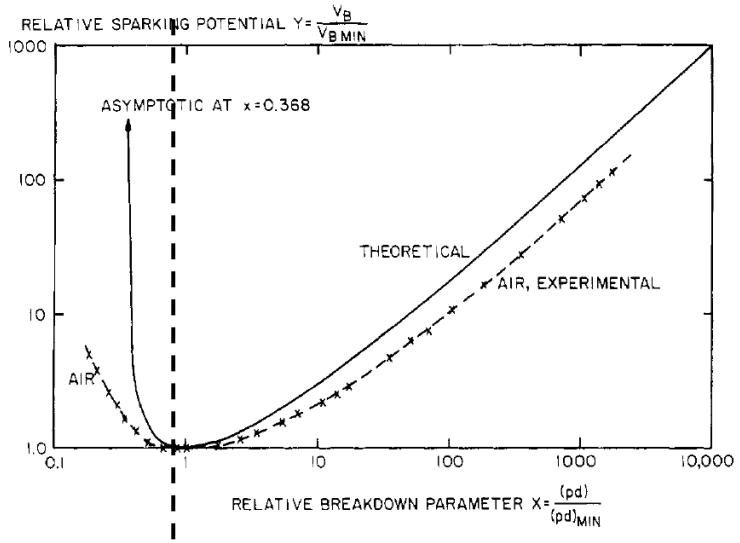

- **Collision is not frequent enough even the electrons gain large energy between each collision.**
- **Electrons do not gain enough energy between each collision even collisions happen frequently.**
- **The minimum of the Paschen's curve corresponds to the Stoletow point, the pressure at which the volumetric ionization rate is a maximum.**

Experimental Paschen's curve

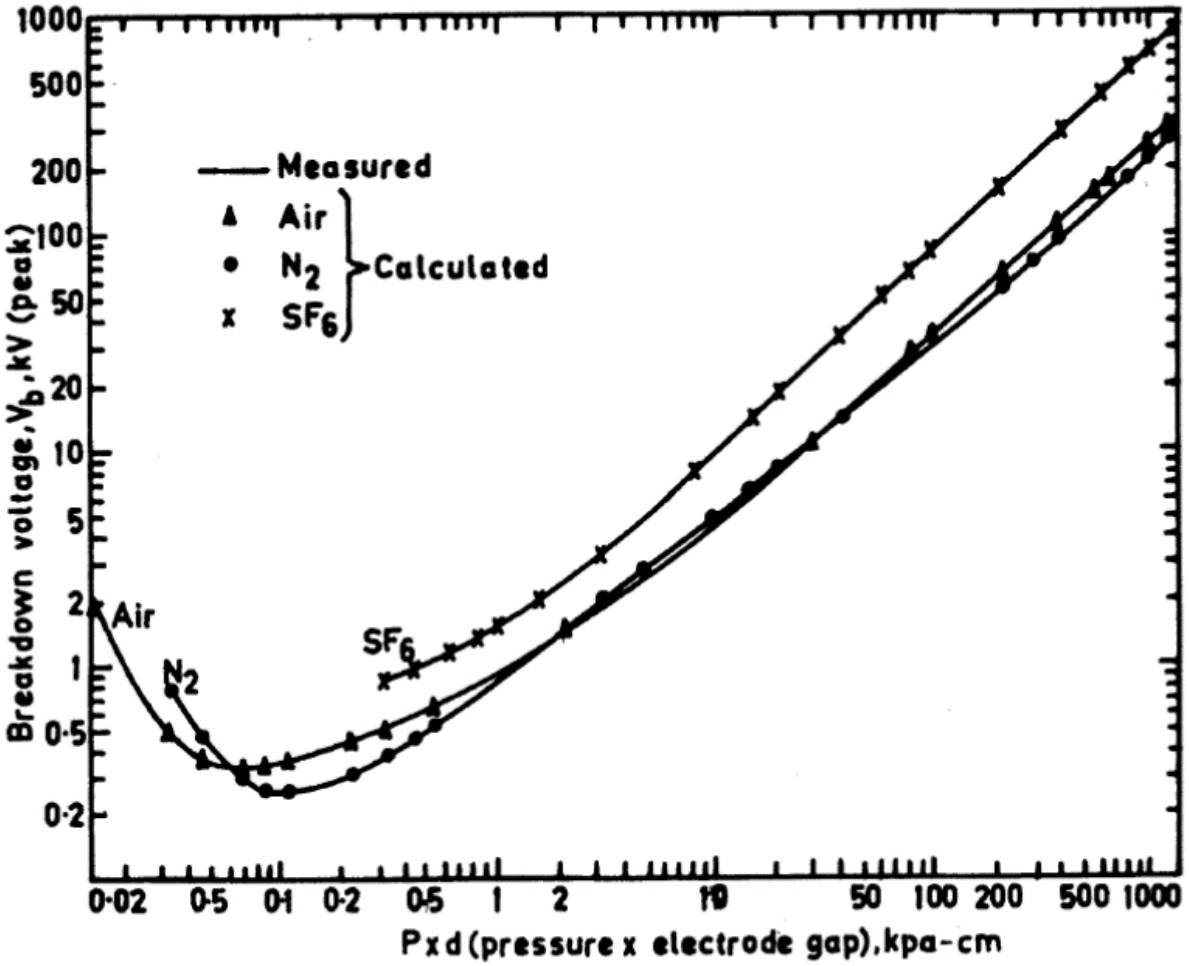

Paschen's curve is used to design different high voltage high current switches in pulsed-power system

- **Pulsed-power system**

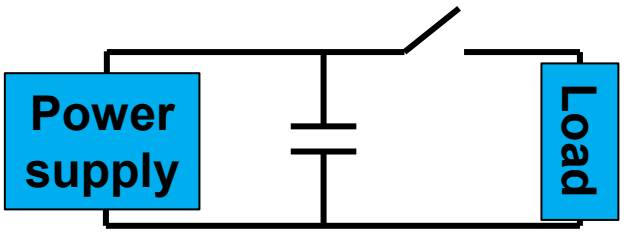

Low power **High power**

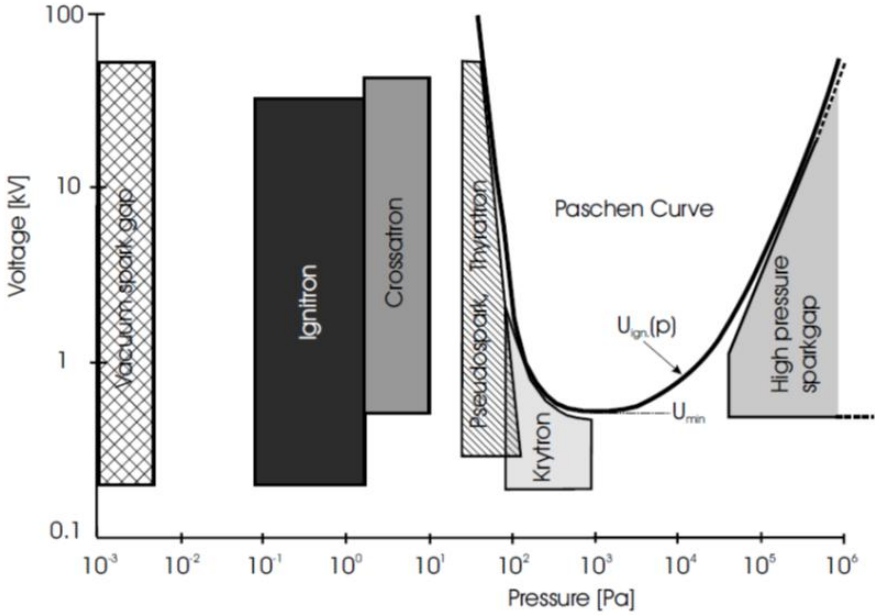

Driven piles - prefabricated steel, wood or concrete piles are driven into the ground using impact hammers

- **Driven piles**

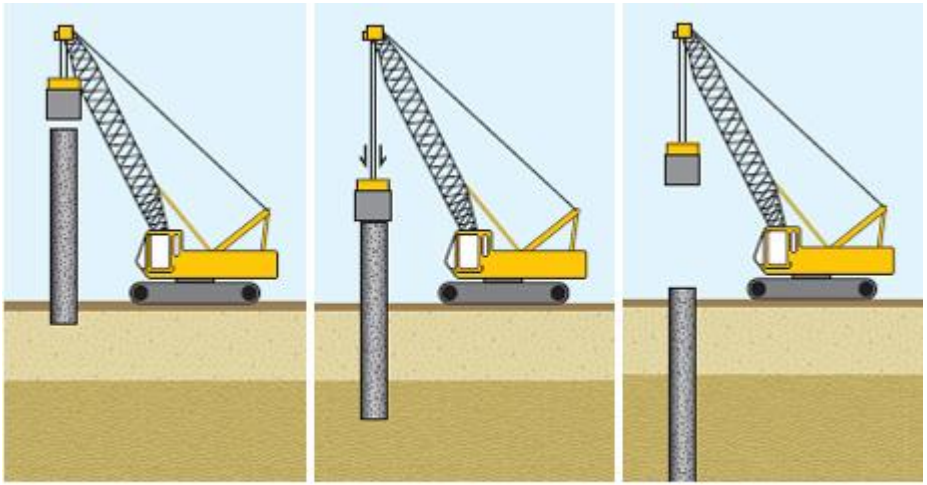

- **Hammer**

http://www.saudifoundations.com/driven.html
http://learnhowtowritesongs.com/tag/thesaurus/

Example of short pulses with a controllable repetition rate

https://www.youtube.com/watch?v=5fe8b4MlPYw

Spark-gap switch

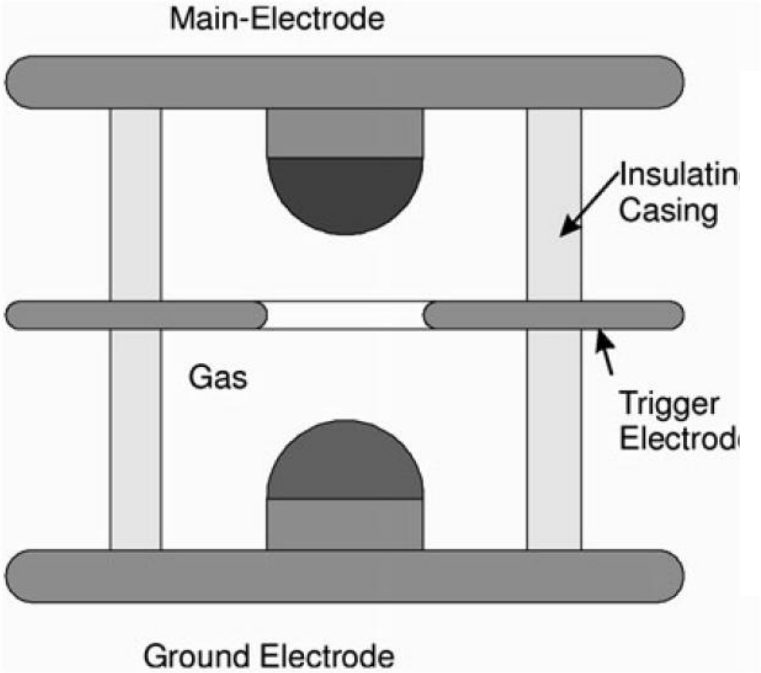

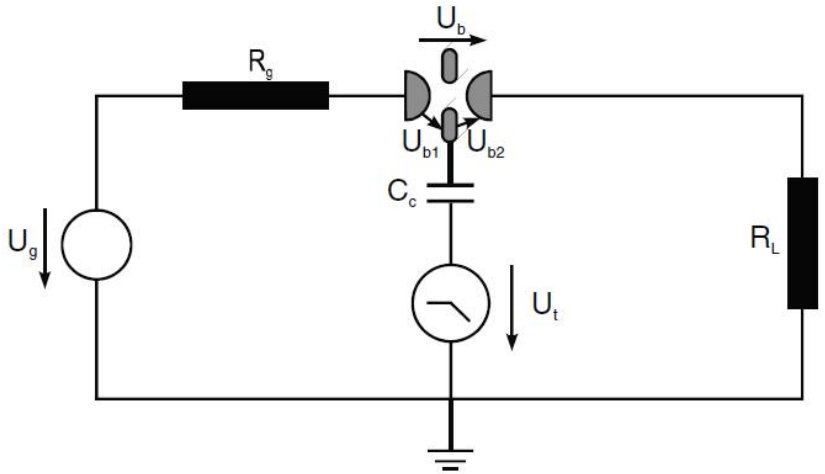

A spark gap switch is closed when electron breakdown occurs

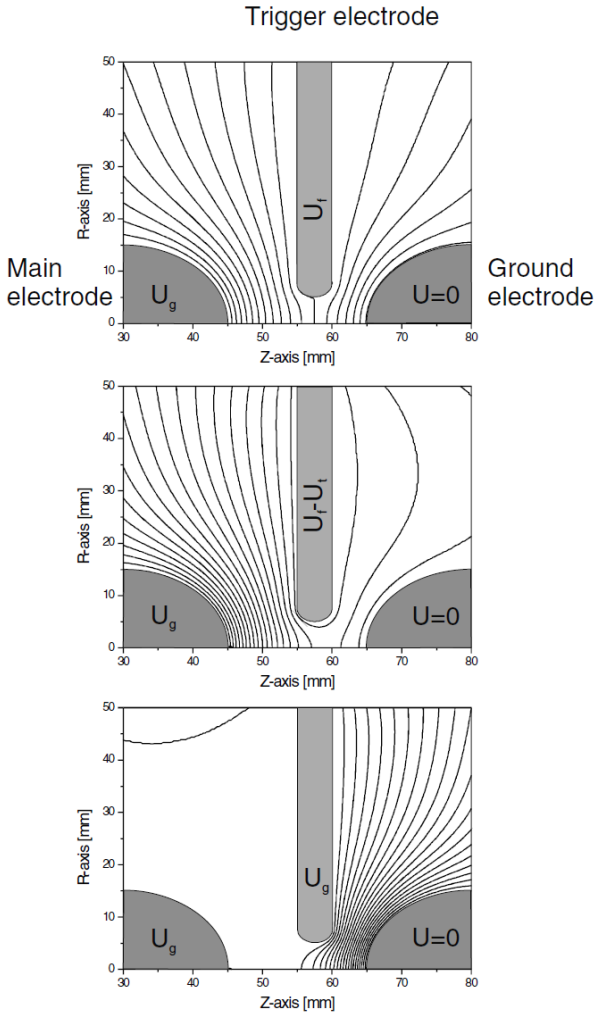

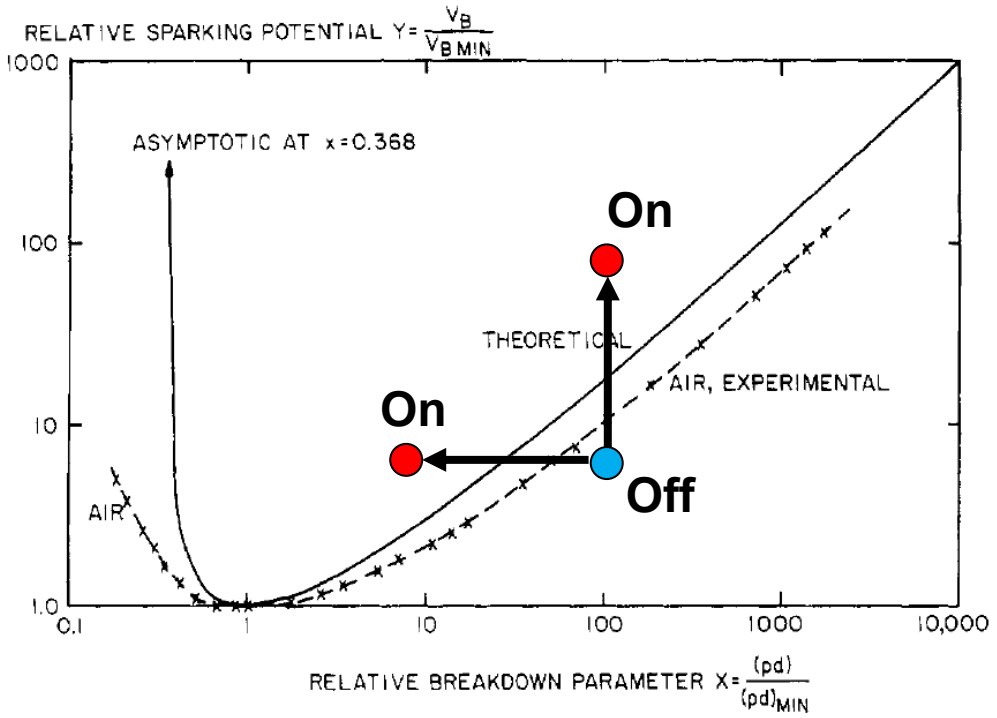

DC electrical glow discharges in gases

- **The internal resistance of the power supply is relatively low, then the gas will break down at the voltage V_B, and the discharge tube will move from the dark discharge regime into the low pressure normal glow discharge regime.**

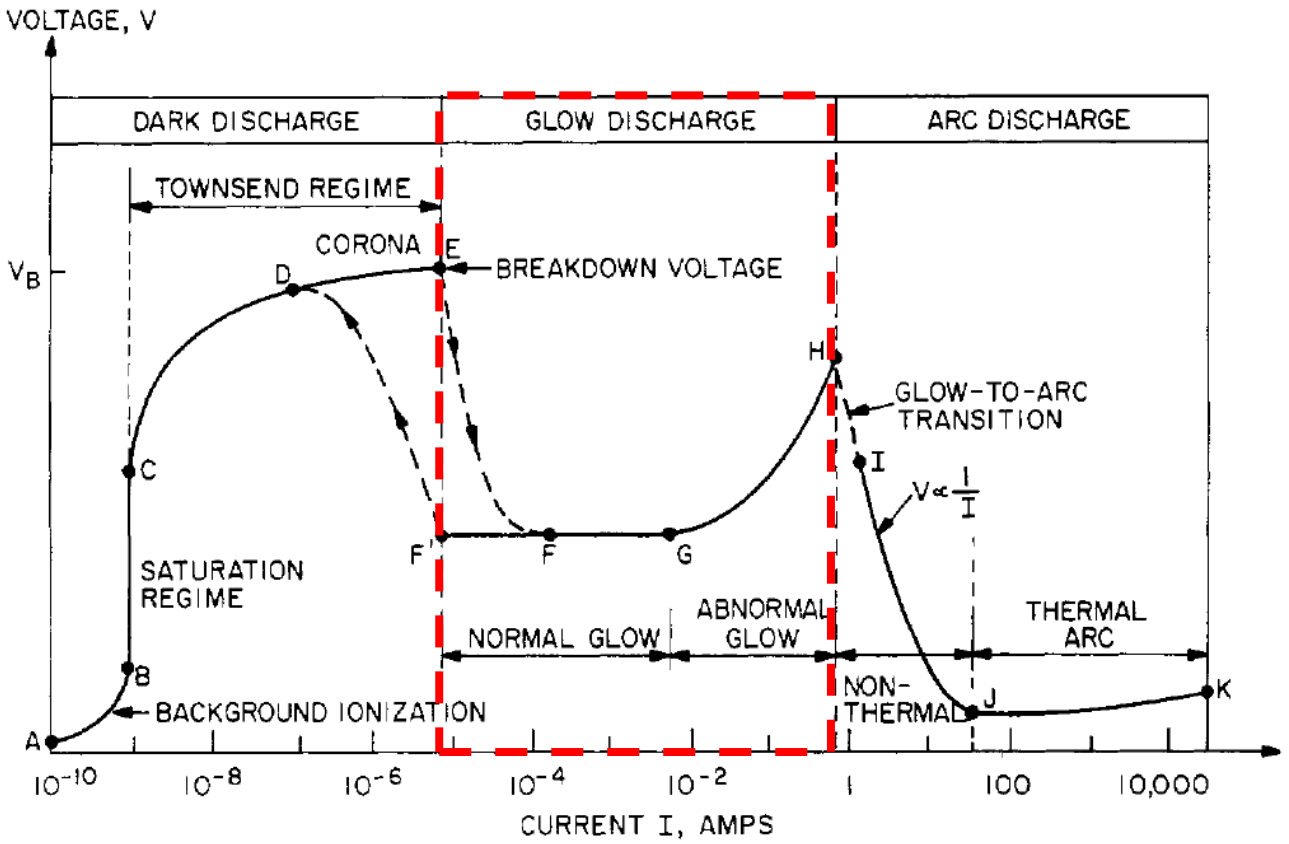

The plasma is luminous in the glow discharge regime

- **The luminosity arises because the electron energy and number density are high enough to generate visible light by excitation collisions.**

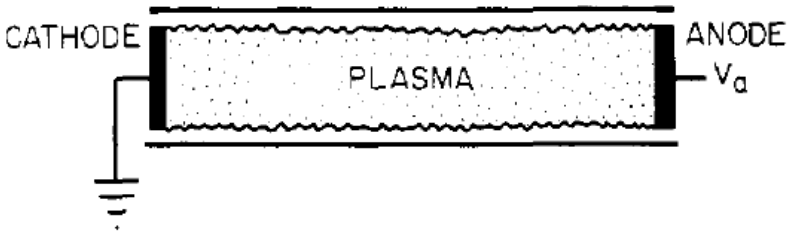

CLASSICAL DC ELECTRICAL DISCHARGE TUBE

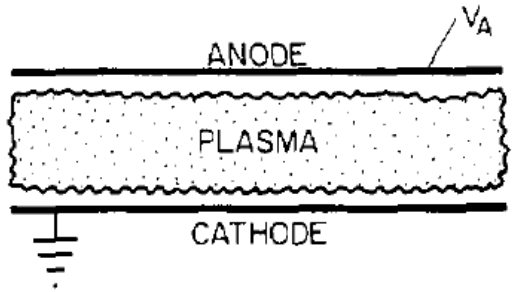

PARALLEL PLATE PLASMA REACTOR

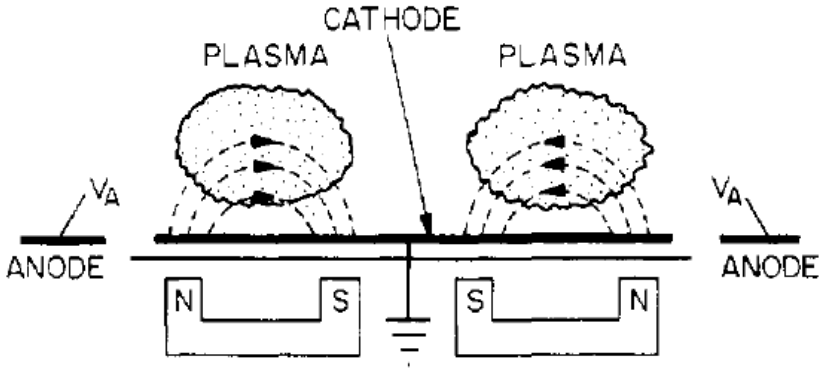

COPLANAR MAGNETRON REACTOR

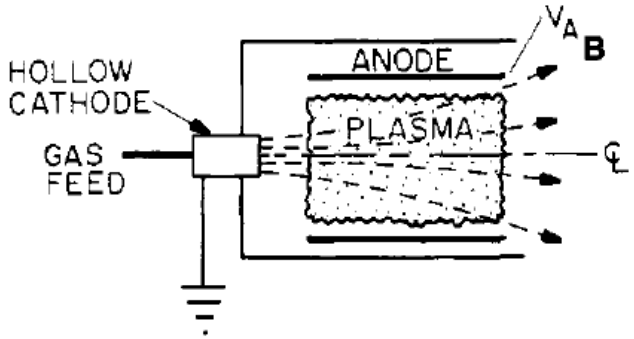

COAXIAL ELECTRON BOMBARDMENT DISCHARGE CHAMBER

Abnormal glow discharge occurs when the cross section of the plasma covers the entire surface of the cathode

$$R = \frac{V}{I}$$

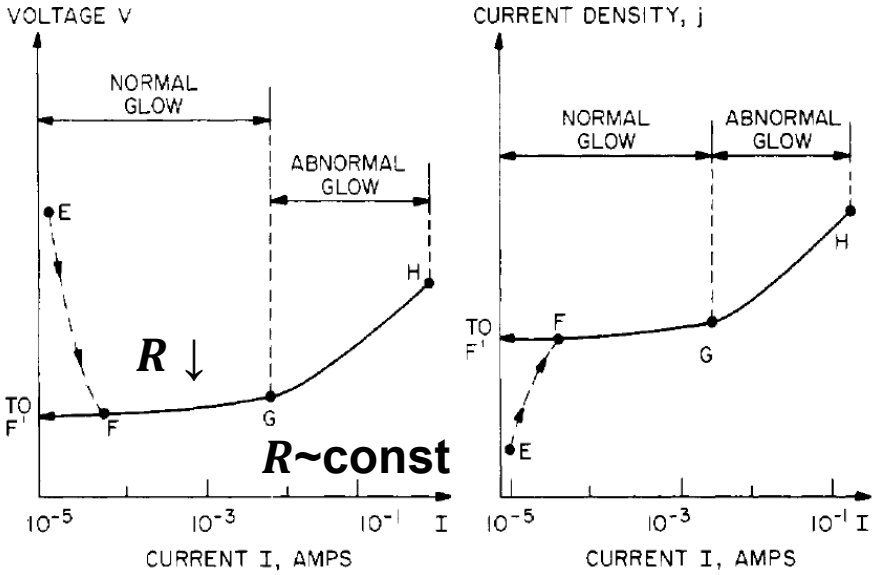

$$R = \eta \frac{l}{A}$$

- **Normal glow discharge:**

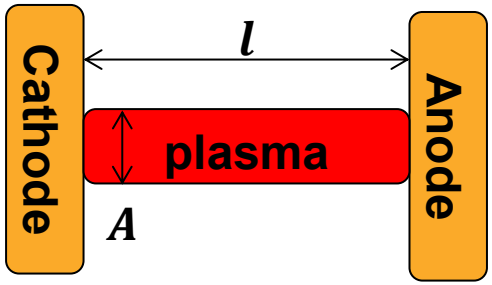

- **Abnormal glow discharge:**

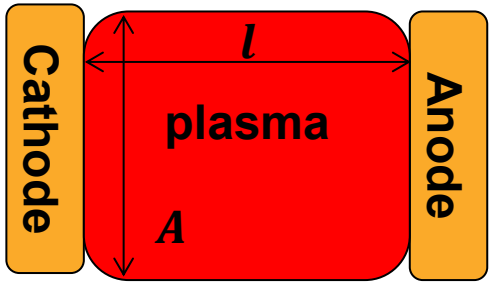

- **Surface cleaning using plasma needs to work in the abnormal glow discharge region.**

Plasma cleaning needs to work in the regime of abnormal glow discharge

- Top view

- Side view

Low pressure normal glow discharge

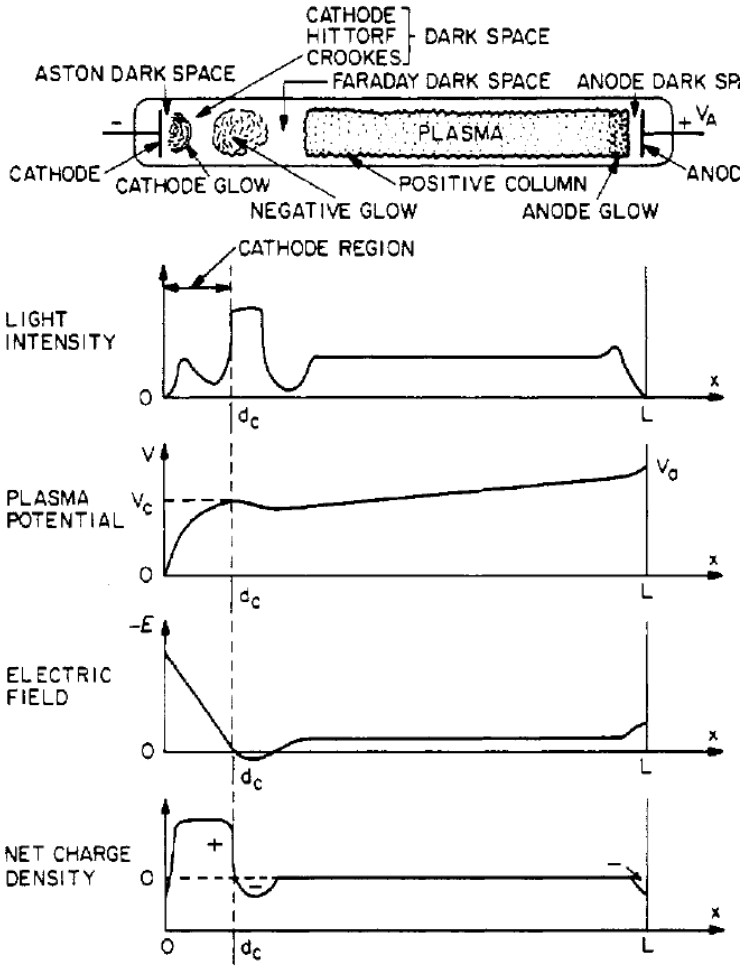

- **Cathode: made of an electrically conducting metal with 2nd e- emission γ, of which has a significant effect on the operation of the discharge tube.**
- **Aston dark space: a thin region with a strong electric field and a negative space charge. The electrons are of too low a density and/or energy to excite the gas, so it appears dark.**
- **Cathode glow: has a relatively high ion number density. The length depends on the type of gas and the gas pressure.**
- **Cathode (Crookes, Hittorf) dark space: has a moderate electric field, a positive space charge, and a relatively high ion density.**

Low pressure normal glow discharge

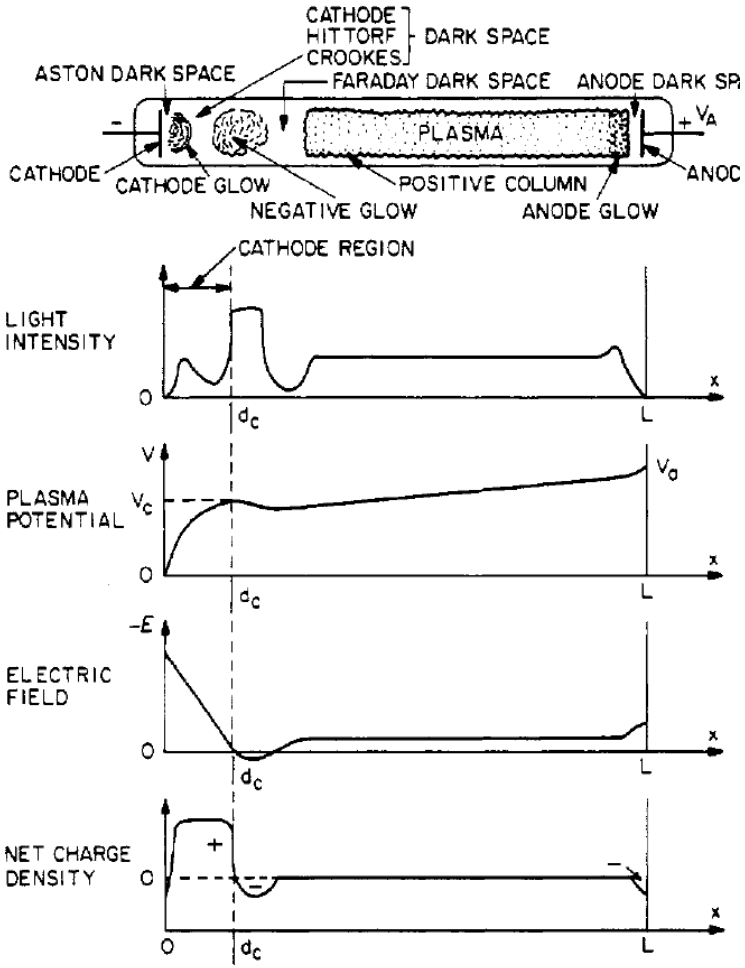

- **<u>Cathode region</u>: most of the voltage drop (cathode fall) across the discharge tube appears between the cathode and the boundary between the cathode dark space and the negative glow. Electrons are accelerated to energies high enough to produce ionization and avalanching in this region. The axial length will adjust itself such that $d_c p \sim (dp)_{min}$ where (dp) is the Paschen minimum.**

Low pressure normal glow discharge

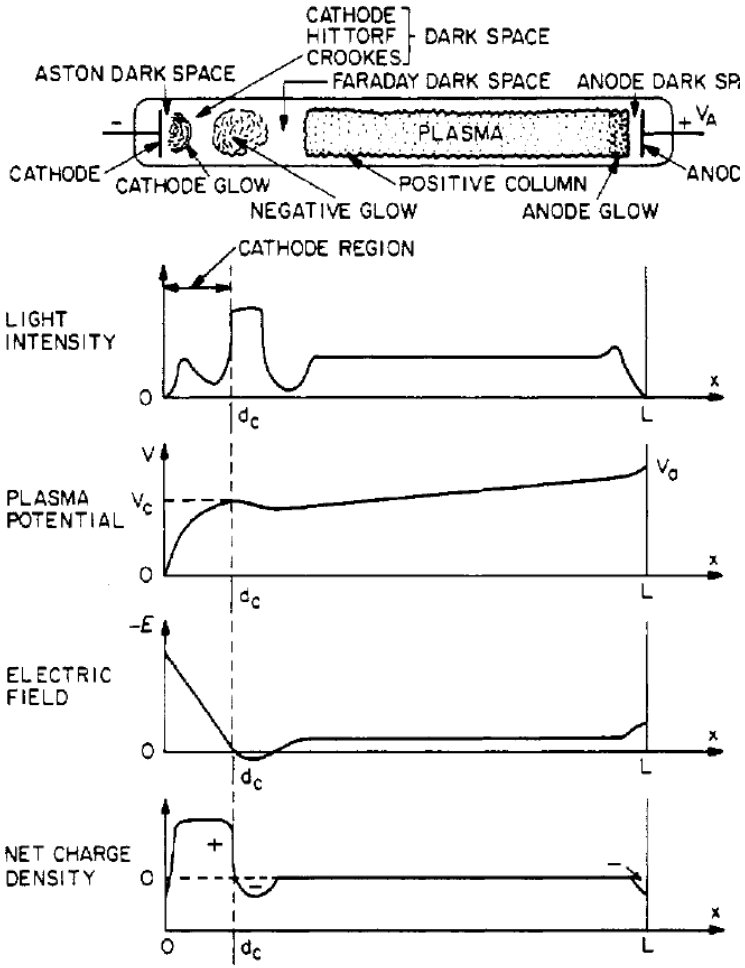

- **<u>Negative glow</u>: the brightest light intensity in the entire discharge. It has a relatively low electric field and is usually long compared to the cathode glow. Electrons carry almost the entire current in the negative glow region. Electrons which have been accelerated in the cathode region produce ionization and intense excitation in the negative glow, hence the bright light output observed.**

Low pressure normal glow discharge

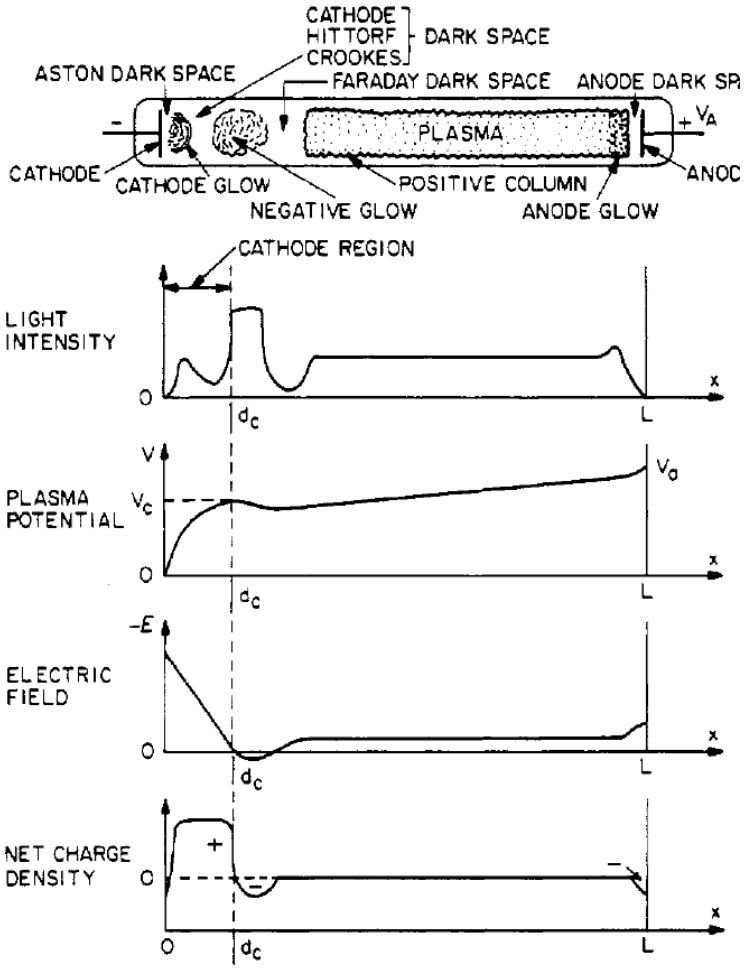

- **Faraday dark space: the electron energy in it is low as a result of ionization and excitation interactions in the negative glow. The electron number density decreases by recombination and radial diffusion, the net space charge is very low, and the axial electric field is relatively small.**

Low pressure normal glow discharge

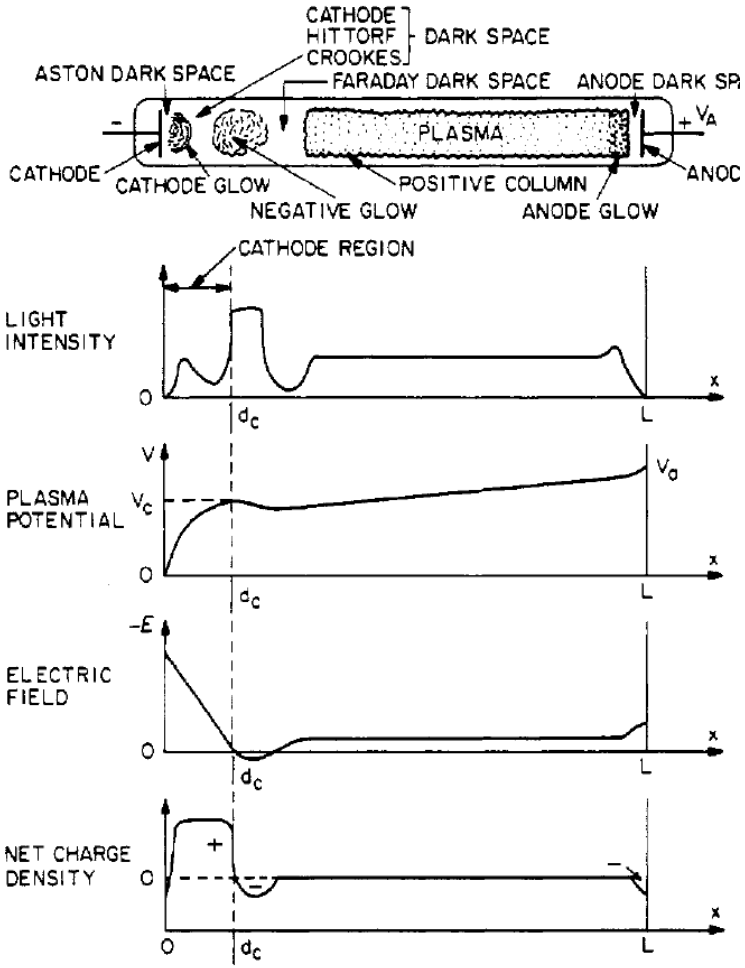

- **<u>Positive column</u>: quasi-neutral, the electric field is small and is just large enough to maintain the required degree of ionization at its cathode end. Since the length of cathode region remains constant, the positive column lengthens as the length of the discharge tube is increased.**

Low pressure normal glow discharge

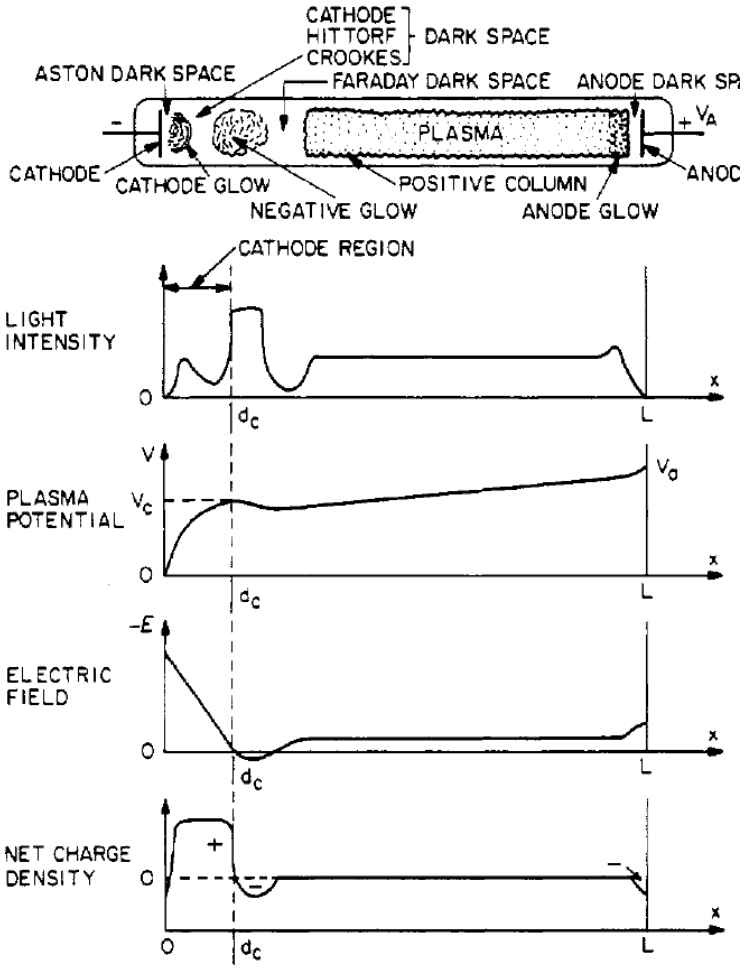

- **Anode glow: the boundary of the anode sheath, slightly more intense than the positive column.**
- **Anode dark space: has a negative space charge due to electrons traveling from the positive column to the anode and a higher electric field than the positive column. The anode pulls electrons out of the positive column and acts like a Langmuir probe in electron saturation in this respect.**

Striated discharges

- **Moving or standing striations are, respectively, traveling waves or stationary perturbations in the electron number density which occur in partially ionized gases, including the positive columns of DC normal glow discharge tubes.**
- **https://youtu.be/Be4RljMTOWE**

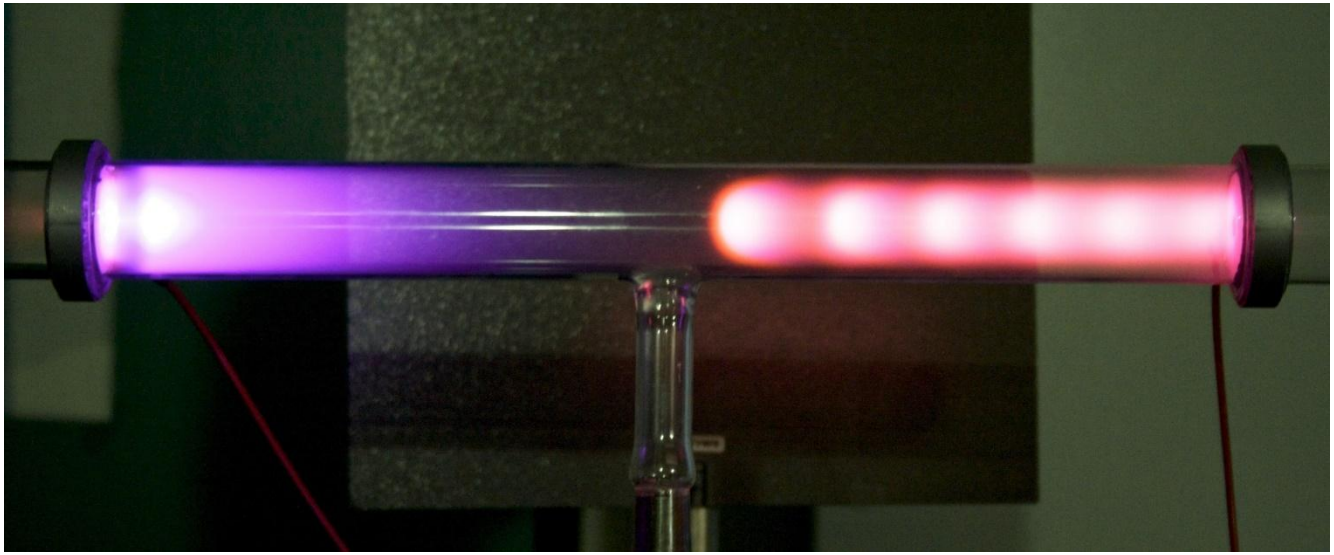

https://en.wikipedia.org/wiki/Glow_discharge

Obstructed discharges

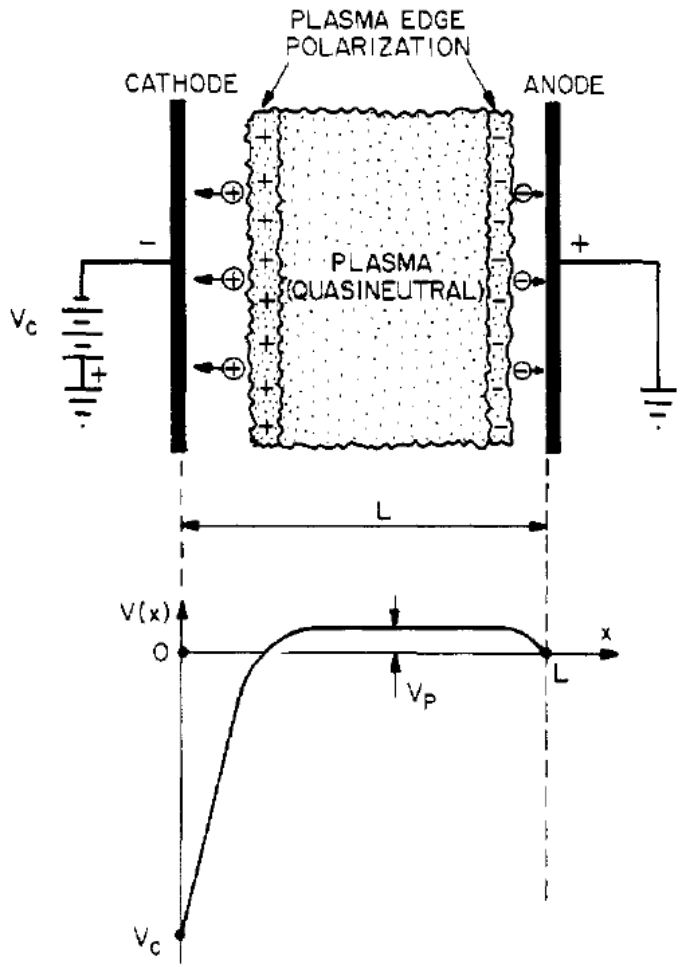

$$L < d_c$$

at the Paschen minimum, i.e., $(pd_c)_{min}$

$$V_c > V_{Paschen}$$

- **The obstructed glow discharge finds many uses in industry, where the high electron number densities generated by such discharge are desired. It will operate with a higher anode voltage. Such high voltage drops are sometimes desirable to accelerate ions into a wafer for deposition or etching purposes.**

Cylindrical glow discharge sources

- **This configuration is used in lighting devices, such as fluorescent lights and neon advertising signs.**

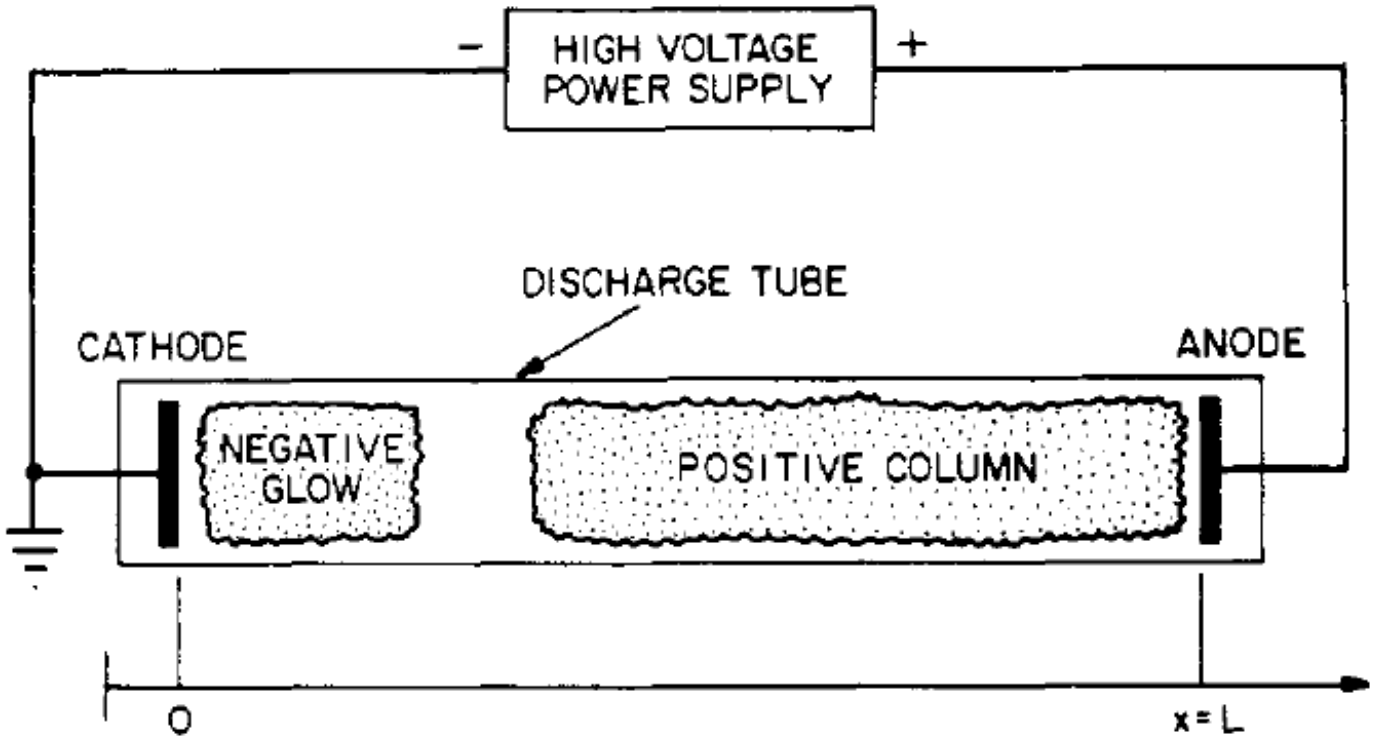

Parallel plate sources are widely used for plasma processing and plasma chemistry applications

- **Unobstructed operation**
- **Obstructed operation**

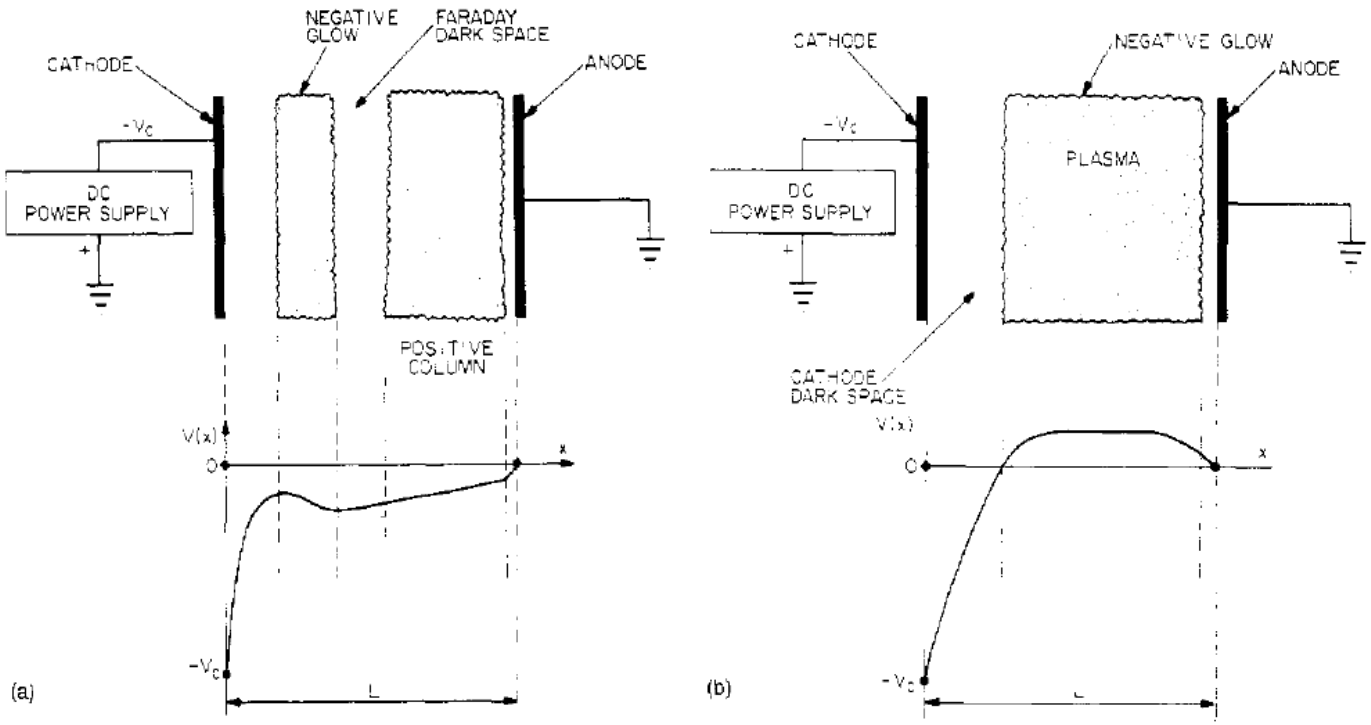

- **The obstructed configuration is used for plasma processing, where high ion energies bombarding the cathode, over large areas and at vertical incidence, are desired.**

Magnetron plasma source are used primarily for plasma-assisted sputtering and deposition

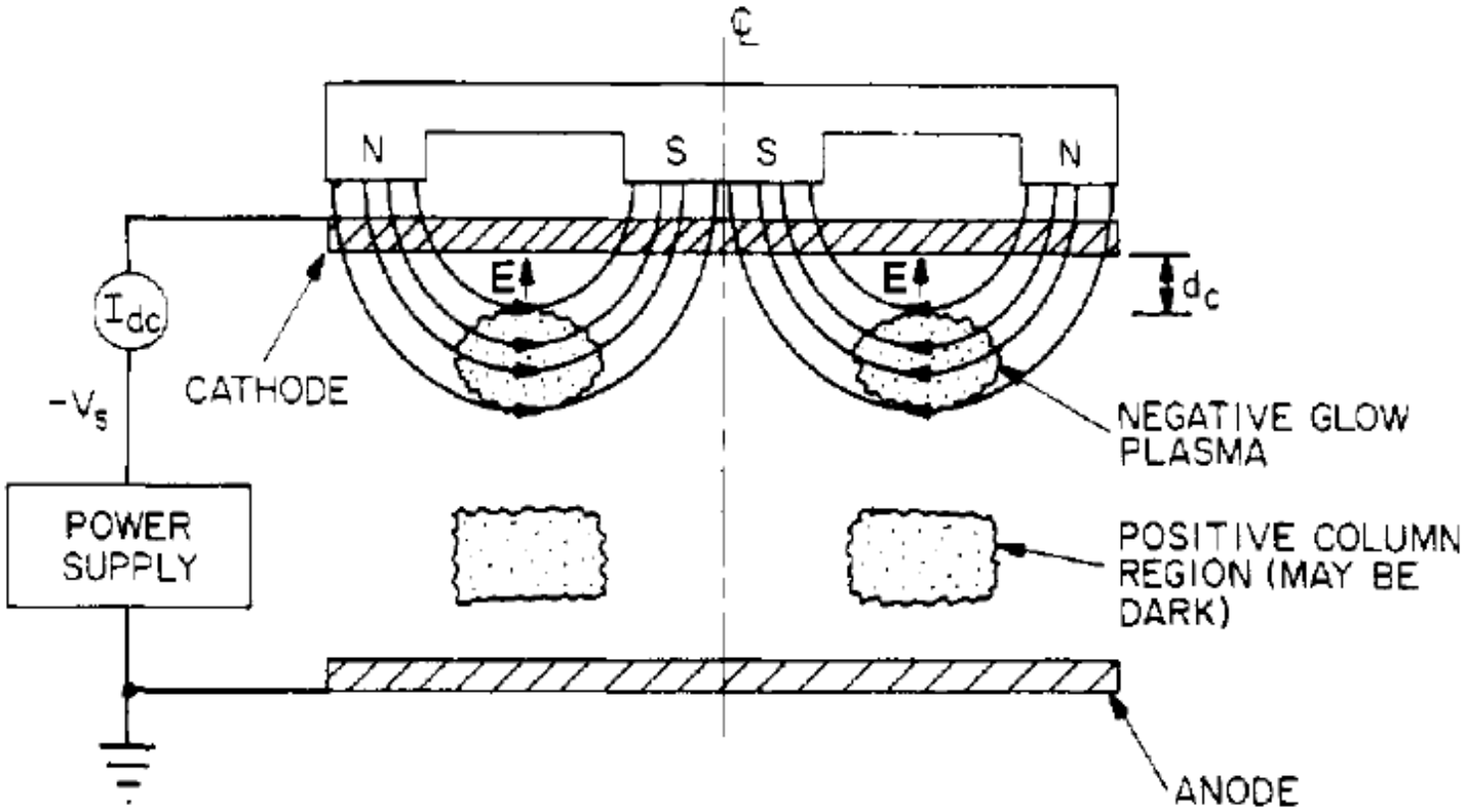

- When several hundred voltages are applied between the parallel plates, a glow discharge will form, with a negative glow plasma trapped in the magnetic mirrors above the magnet pole pieces.

Penning discharge plasma sources produce a dense plasma at pressures far below than most other glow discharges

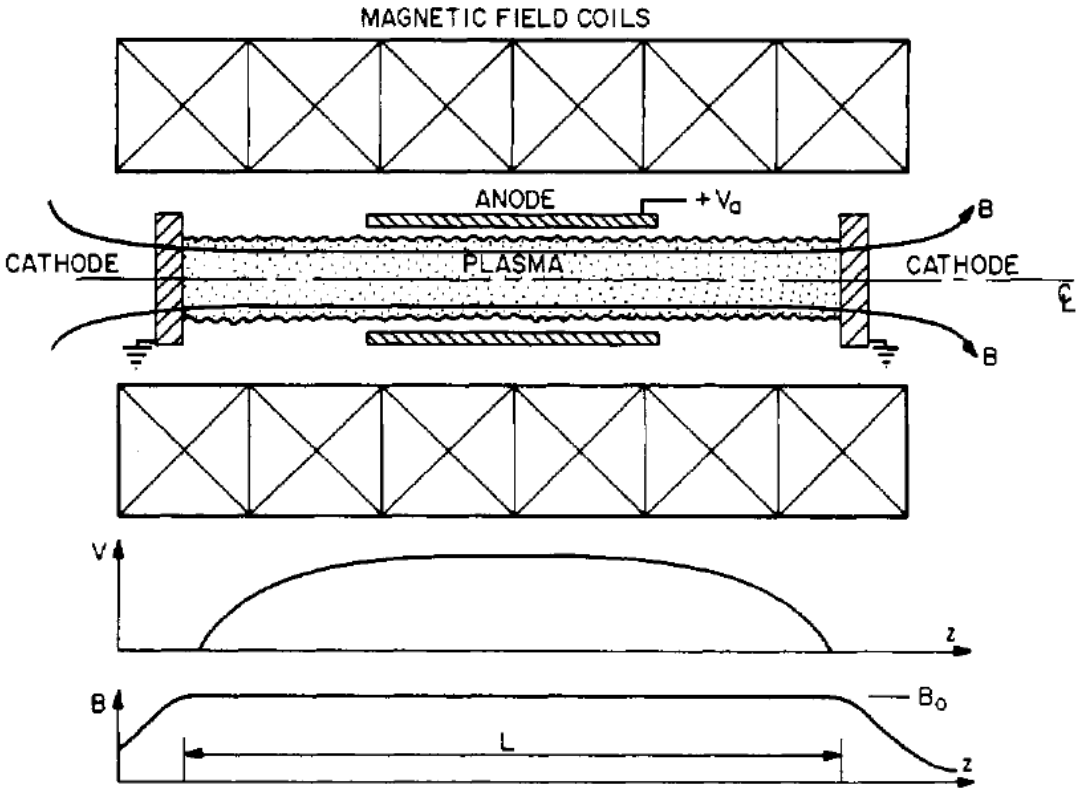

- **Strong axial magnetic fields: to prevent electrons from intercepting the anode.**
- **Axial electric fields: electrons are reflected by opposing cathodes.**
- **Multiple reflection of the electrons along axis.**

Discharge may enter glow-to-arc transition region if the cathode gets hot enough to emit electrons thermionically

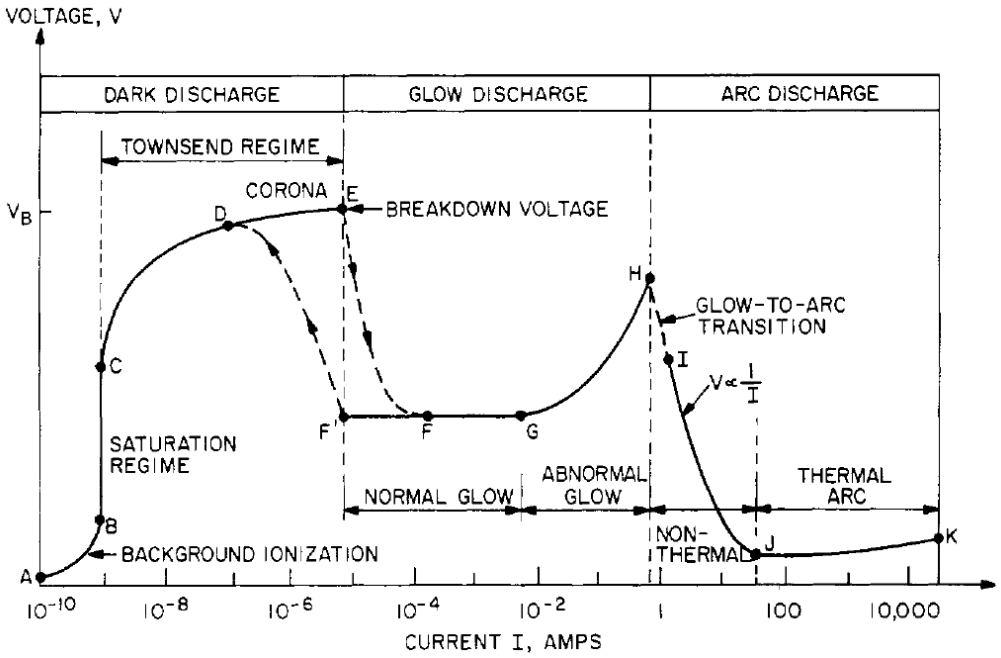

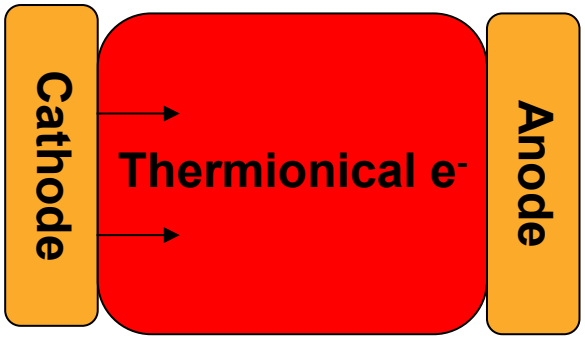

- If the cathode gets hot enough to emit electrons thermionically and the internal impedance of the power supply is sufficiently low, the discharge will make a transition into the arc regime.

DC electrical arc discharges in gases

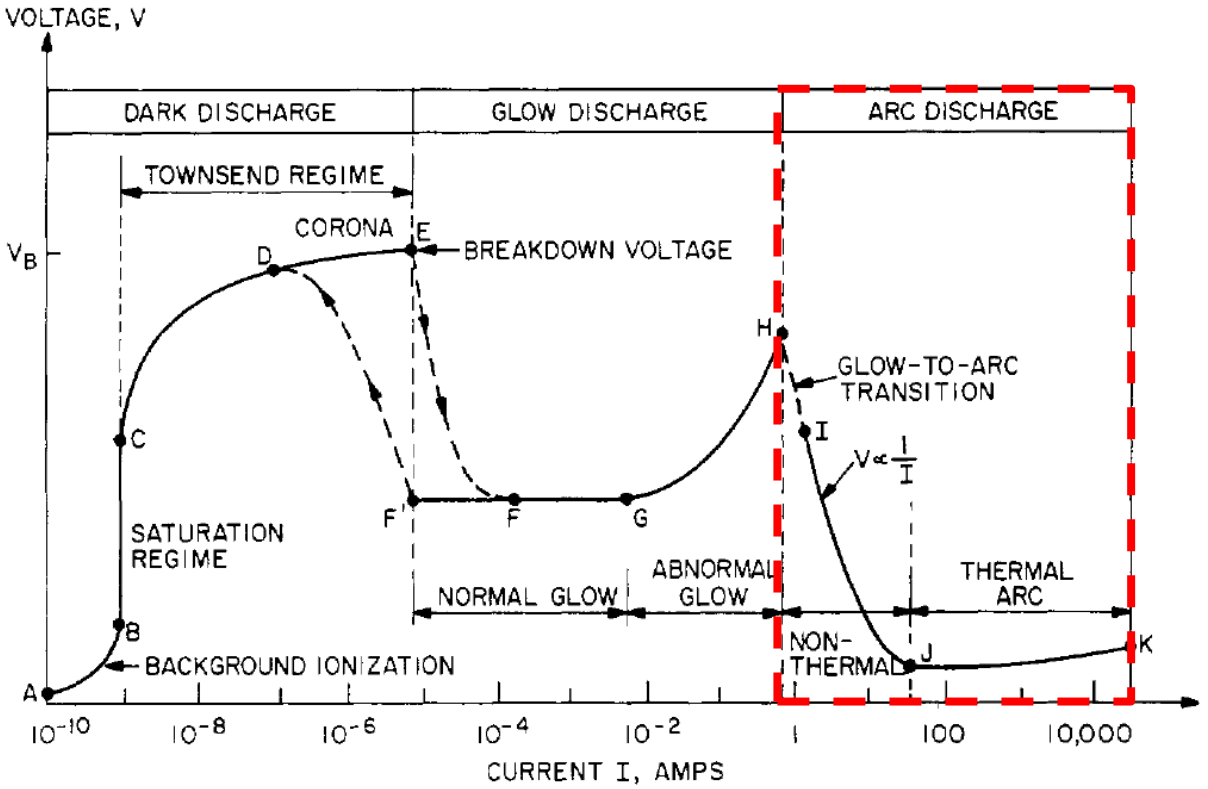

- **An arc is highly luminous and is characterized by high currents (> 1 A) and current densities (A=cm^2 t kA/cm^2).**
- **Cathode voltage fall is small (£10 V) in the region of high spatial gradients within a few mm of the cathode.**

An arc can be non-thermal or thermionic

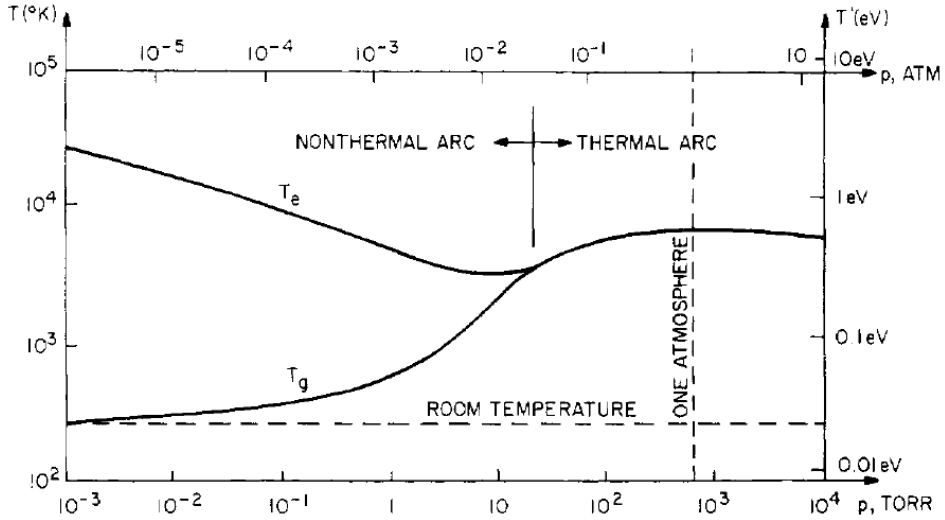

Plasma parameter	Non-thermal arc	Thermal arc
Equilibrium state	Kinetic	LTE
Electron density, n_e (electrons/m^3)	$10^{20} < n_e < 10^{21}$	$10^{22} < n_e < 10^{25}$
Gas pressure, p (Pa)	$0.1 < p < 10^5$	$10^4 < p < 10^7$
Electron temperature, T_e', (eV)	$0.2 < T_e' < 2.0$	$1.0 < T_e' < 10$
Gas temperature, T_g' (eV)	$0.025 < T_g' < 0.5$	$T_g' = T_e'$
Arc current, I (A)	$1 < I < 50$	$50 < I < 10^4$
E/p (V/m-Torr)	High	Low
IE (kW/cm)	$IE < 1.0$	$IE > 1.0$
Typical cathode emission	Thermonic	Field
Luminous intensity	Bright	Dazzling
Transparency	Transparent	Opaque
Ionization fraction	Indeterminate	Saha equation
Radiation output	Indeterminate	LTE

Classical arc were mostly used as lighting devices and operated as non-thermal arcs

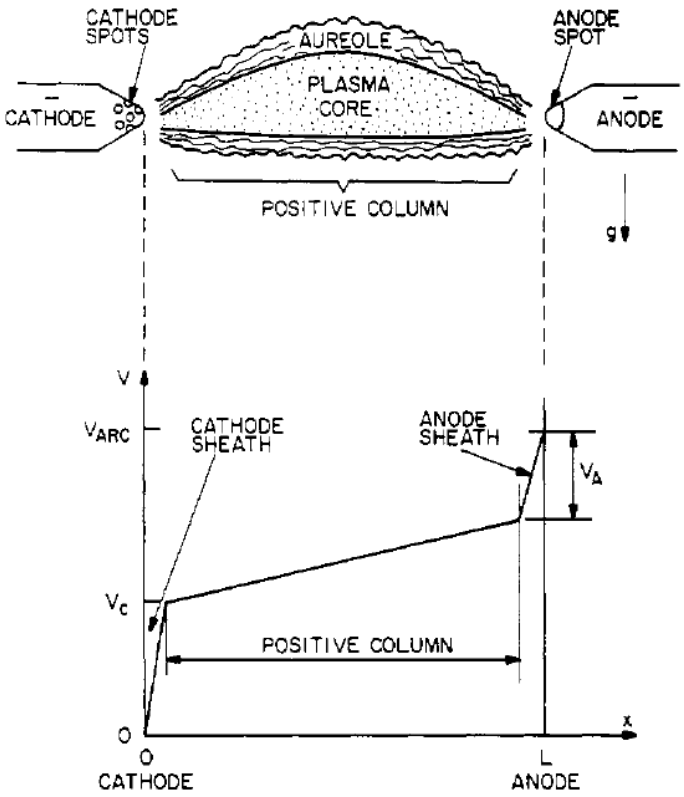

- <u>Cathode</u> - emits electrons thermionically
- <u>Cathode spots</u> - several hot spots causing material losses through vaporization and move over the cathode surface with a velocity ~ m/s.
- <u>Cathode sheath</u> - voltage drop (cathode fall) ~ 10 V in < 1 mm.
- <u>Positive column</u> - little drop in voltage.
- <u>Plasma core</u> - hot region in thermodynamic equilibrium and radiates like a black body.
- <u>Aureole</u> - flaming gases where plasma chemistry takes place.

Classical arc were mostly used as lighting devices and operated as non-thermal arcs

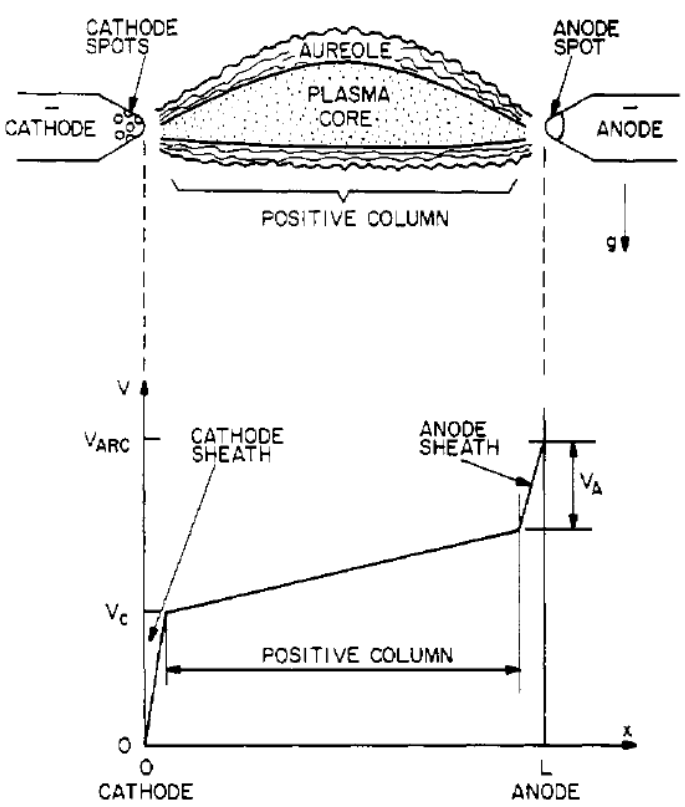

- <u>Anode sheath</u> - voltage drop (anode fall) ~ cathode fall and is comparable to or less than the ionization potential of the gas.
- <u>Anode spot</u> - a single 'hot spot' where the current density is high.
- <u>Anode</u> - usually made of a high melting point, refractory metal and is similar or slightly hotter than cathode.

Example

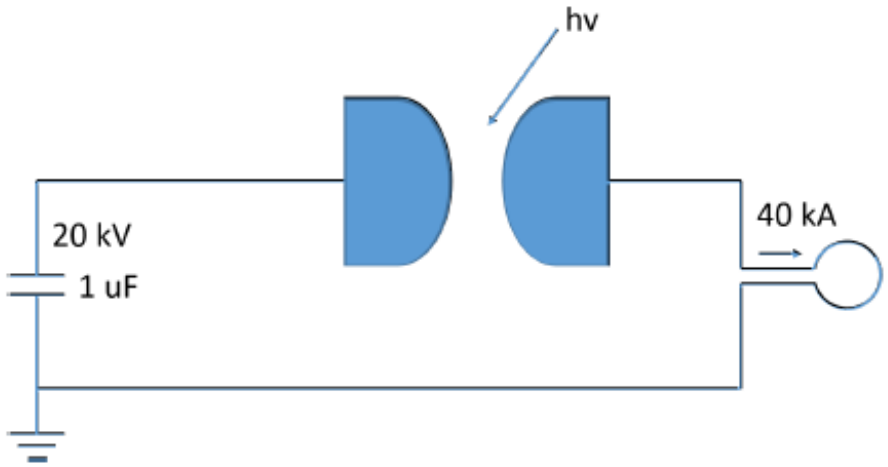

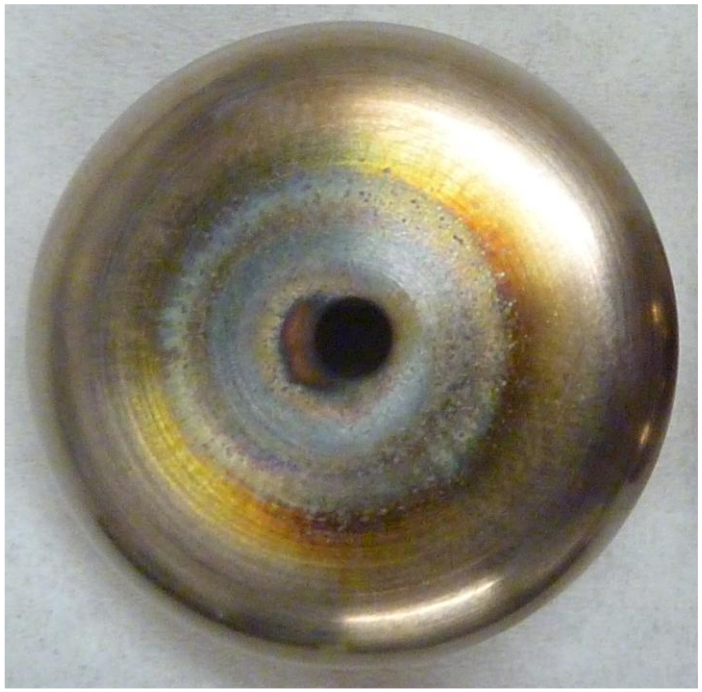

Note 1 - the cathode fall in arc is usually too small for secondary election emission so that the emission relies on thermionic and field emission

- Non-thermal, low intensity arcs - relies on thermionic emission
  - Non-self sustained thermionic emission - cathode must be heated externally.
  - Self sustained thermionic emission - cathode surface is raised to and maintained by the heat flux from the arc
- Thermal, high intensity arcs: relies on field emission
  - high current and current densities
  - cathode temperature is determined by the heat transfer to the cathode and the cathode cooling mechanism and is usually too cool to emit thermionically.

The arc tends to be pinched to smaller diameter

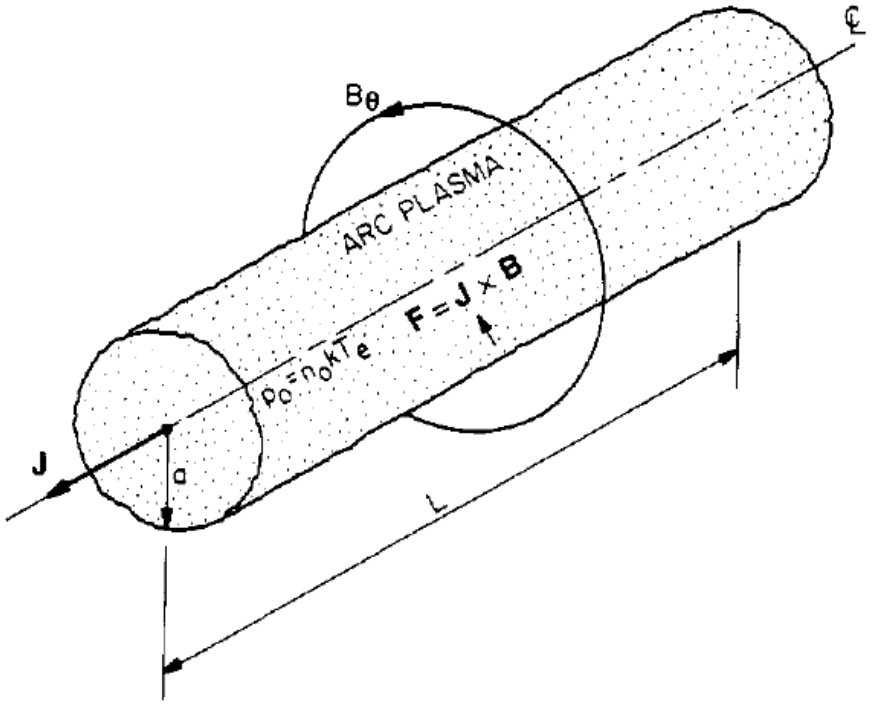

$$B_\theta = \frac{1}{2}\mu_0 J_z r \qquad r \le a$$

$$\vec{F} = \vec{J} \times \vec{B} = F_r \hat{r} = -\frac{1}{2}\mu_0 {J_z}^2 r\hat{r}\left(N/m^3\right)$$

Cathode jet is driven by the axial pressure gradient

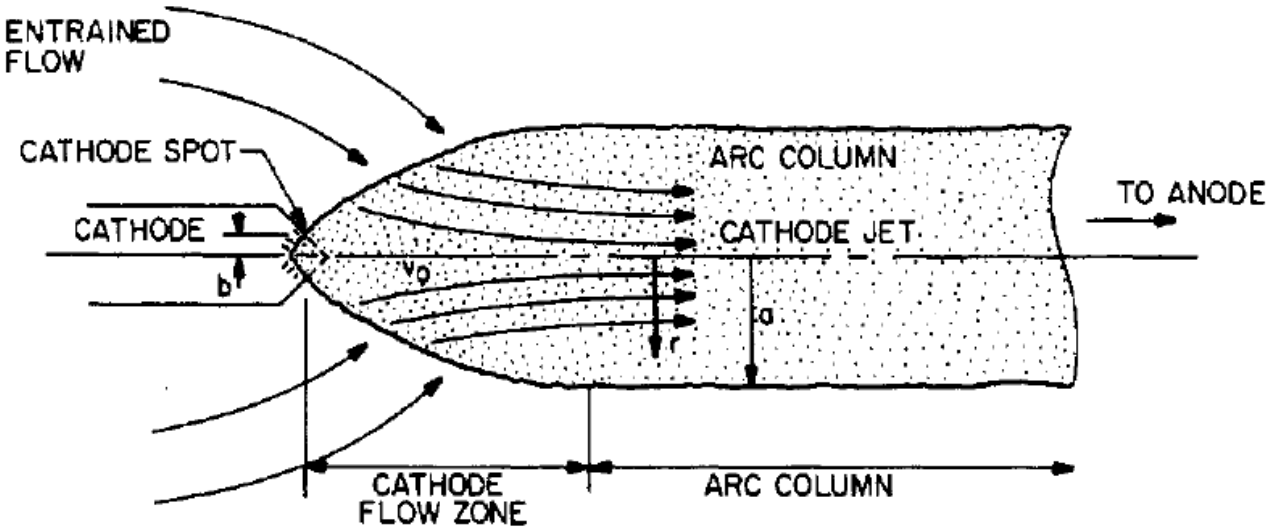

$$\nabla p = \vec{j} \times \vec{B} \qquad B_\theta = \frac{1}{2}\mu_0 J_z r \qquad r \le r_{\max}$$

$$p(r) = \int_r^{r_{\max}} J_z B_\theta \, dr = \frac{1}{4}\mu_0 {J_z}^2 \left({r_{\max}}^2 - r^2\right) \qquad p_0 = \frac{\mu_o I^2}{4\pi^2 {r_{\max}}^2} \qquad \text{where} \quad I = \pi {r_{\max}}^2 J_z$$

$$\because b < a \ , \therefore p_b > p_a$$

Example - Linear Arcs (free-burning arc)

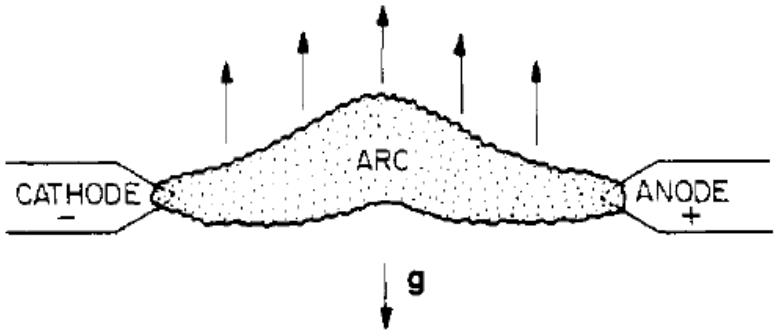

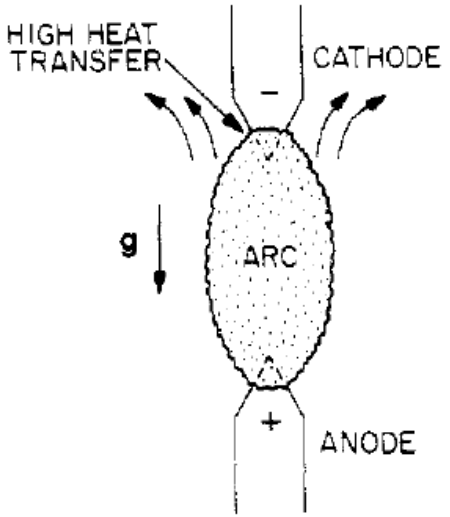

- **The buoyancy of the hot gases causes a horizontal linear arc to bow upward, resulting in an arched appearance that gave the ‘arc’ its name.**
- **The cathode is usually operated at the top, in order to better balance the heat loads on the two electrodes.**

Expanding Arcs

- **The gliding arc is used for toxic waste disposal and destructive plasma chemistry.**

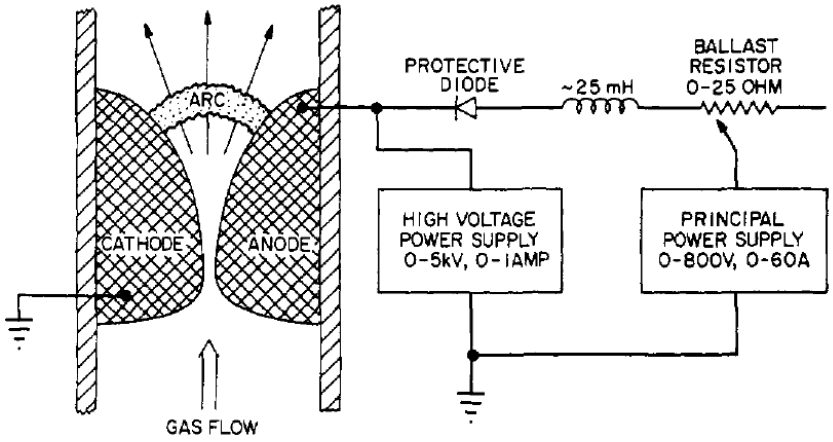

- **Heavy duty switchgear:**

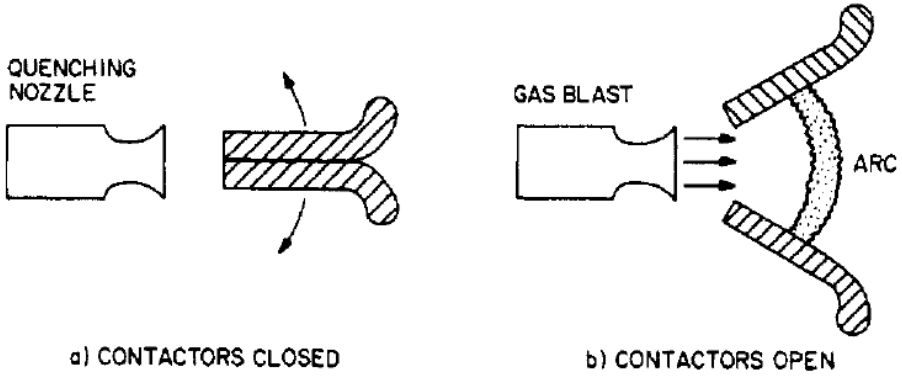

Wall-stabilized arc

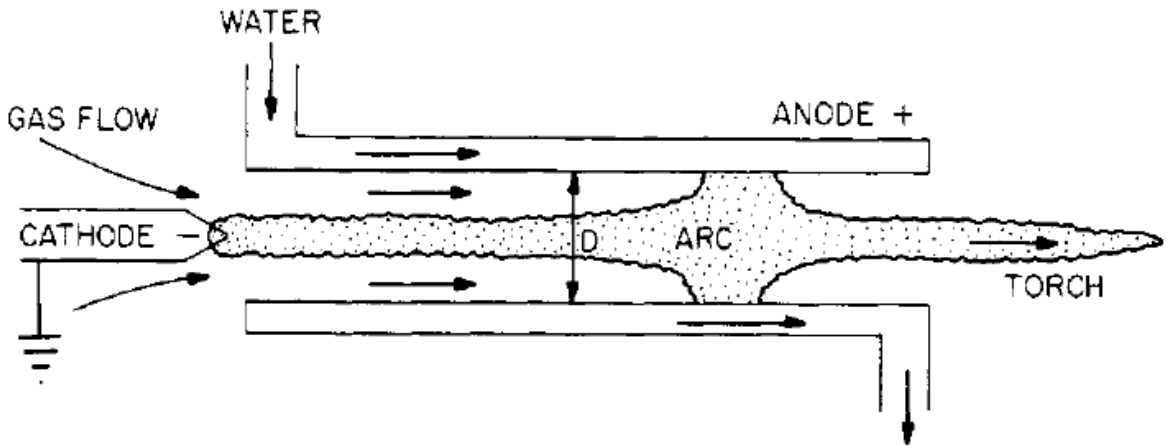

- **Radial power balance:**

$$\sigma E^2 = -\nabla \cdot (\kappa \nabla T) = -\frac{1}{r}\frac{d}{\mathrm{dr}}\left(r\kappa\frac{dT}{dr}\right)$$

- **Assume that the axial electric field E is constant σ and κ are not function of temperature:**

$$T_0 = T_{\mathrm{w}} + \frac{\sigma E^2 a^2}{4\kappa}$$

- **Wall-stabilized effect:**

$$T \downarrow \Rightarrow \kappa \downarrow \Rightarrow T_0 \uparrow \Rightarrow \sigma \uparrow \Rightarrow$$ **the arc will be pulled back on axis**

$$\tau_e = \frac{3\sqrt{m_e}(\mathrm{kT}_e)^{3/2}}{4\sqrt{2\pi}\mathrm{n}\lambda\mathrm{e}^4 z} \qquad \kappa = 3.2\frac{\mathrm{nkT}_e\tau_e}{m_e} \propto T_e{}^{5/2} \qquad \sigma = \frac{\mathrm{ne}^2\tau_e}{m_e} \propto T_e{}^{3/2}$$

Arc can be stabilized by air flow

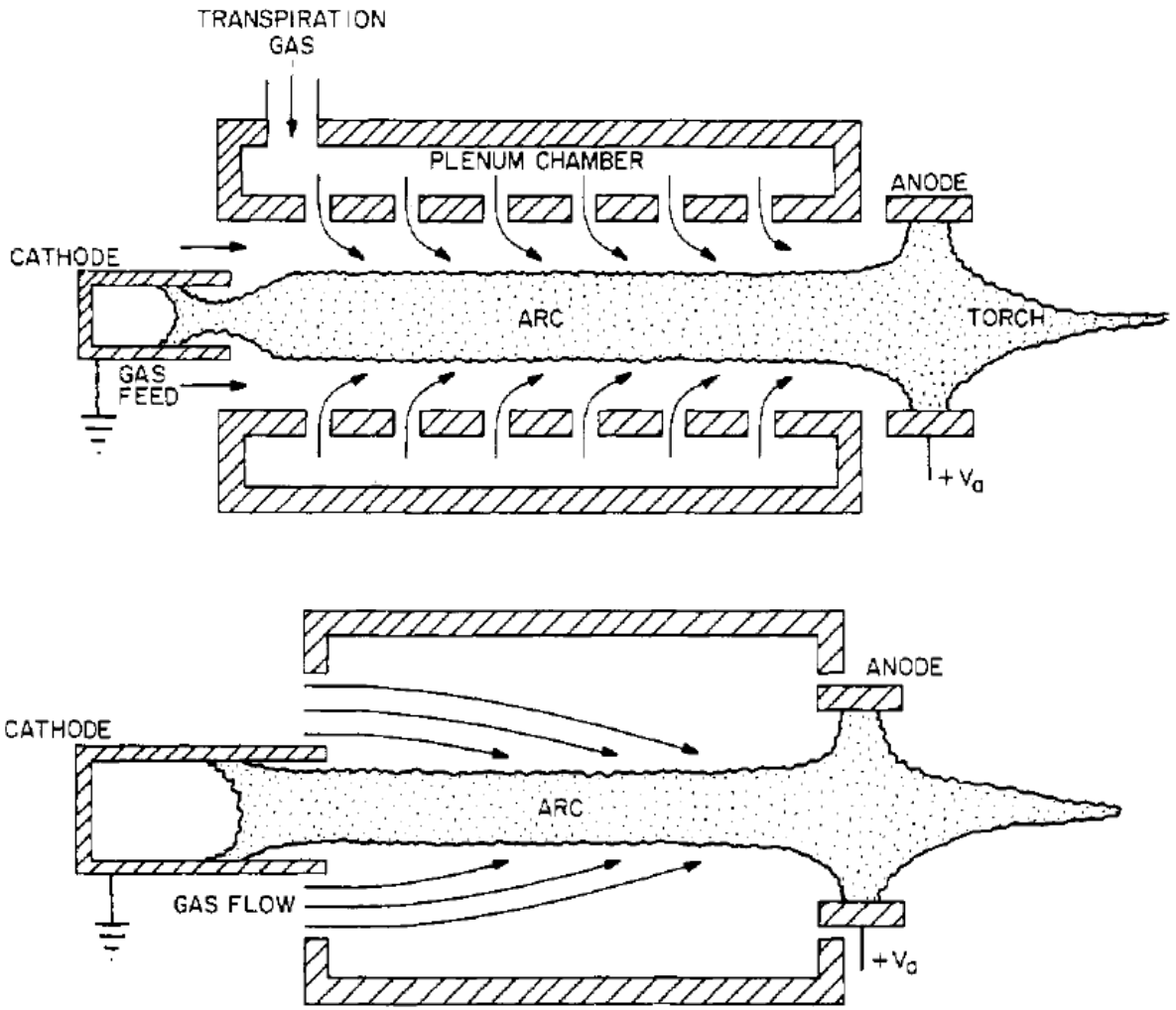

Arc can be stabilized by the vortex flow

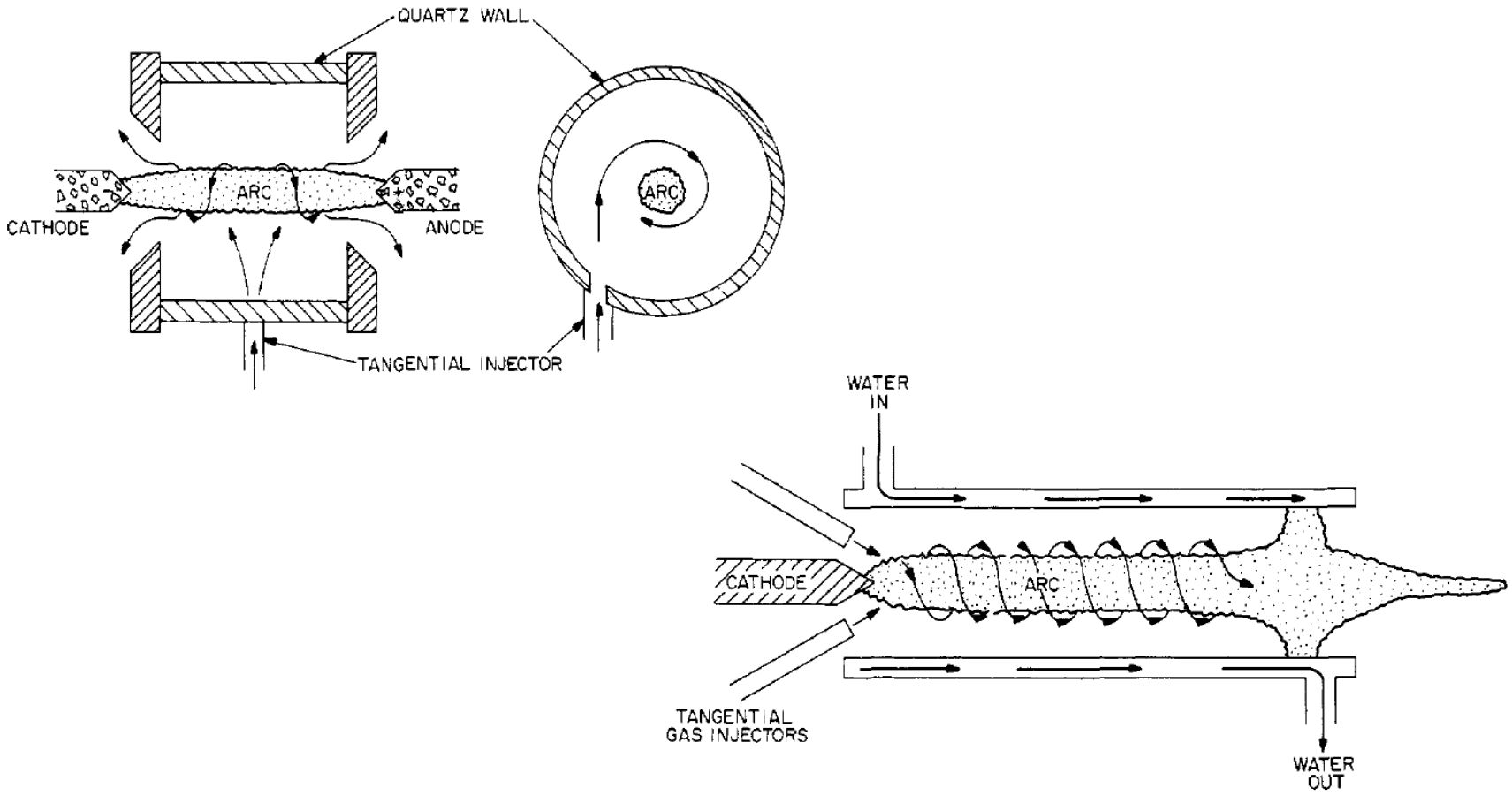

- **The vortex flow is very effective in reducing the heat flux to the wall.**

Magnetically stabilized arc

- **An axial magnetic field provides $\vec{J} \times \vec{B}$ forces which rotate the arc spoke to avoid high local heat loads on the anode.**

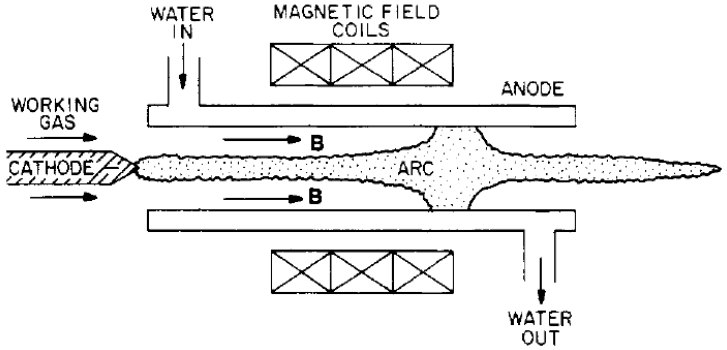

- **An axial magnetic mirror coaxial with the anode so that the magnetic field maximum is near the plane of the arc rotation.**

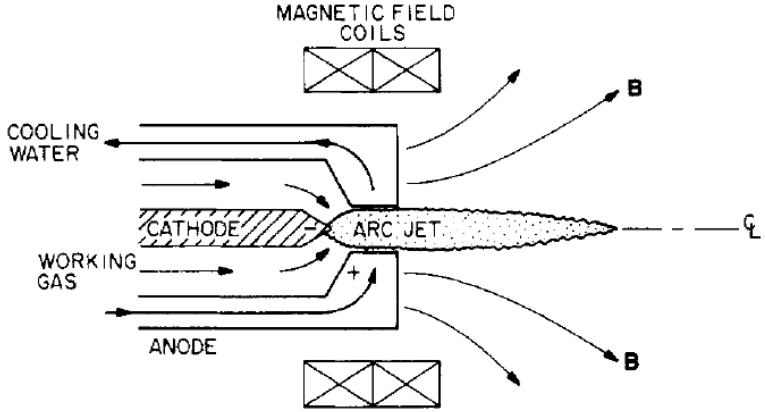

Transferred arc is good for metal melting and refining industry

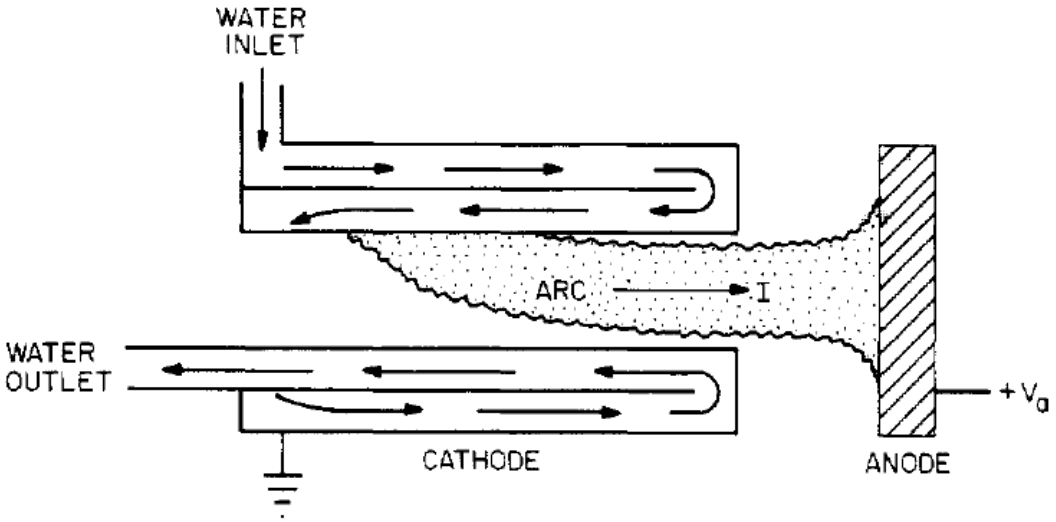

- **Capable of operating at the multi-megawatt level for duration (100s ~1000s hours) that are not possible for thermionically emitting cathodes or uncooled, incandescent cathodes operating in air.**
- **The arc root moves over the cathode surface, further reducing the cathode heat load and increasing the lifetime of the hardware.**
- **The object to be heated is used as the anode since the anode receives the heat deposition from the cathode jet.**

Non-transferred arc

- **Gas fed along the axis blows the arc out toward the material which is to be heated.**

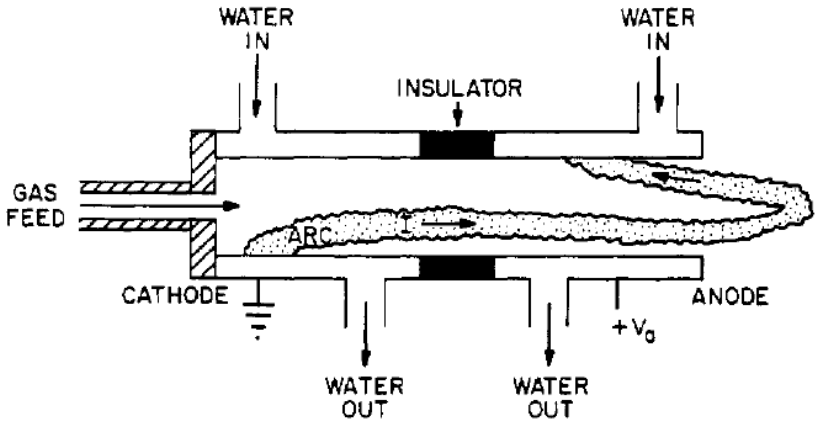

- **A working gas is fed in coaxially and forms a very hot arc jet, at supersonic velocities.**

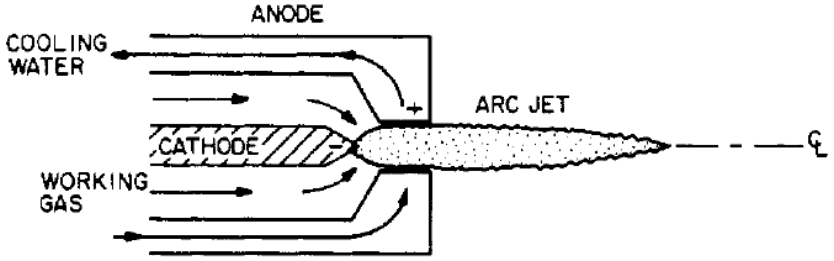

Application – Plasma torch (電漿熔融爐 by奧特拉斯/豐映科技)

- **Non-Transferred arc**

- **Transferred arc**

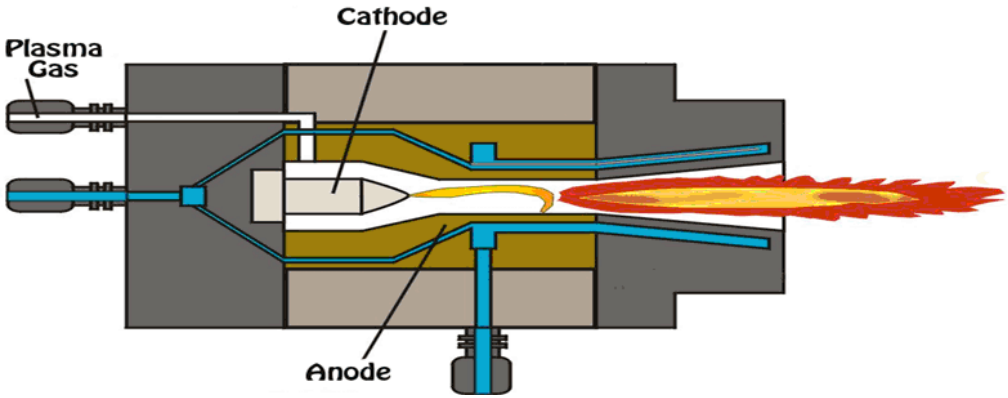

型式 / 特性	非傳輸型	傳輸型
電極結構	兩個電極皆在火炬本體上	一個電極在火炬本體上，另一電極在被處理物上(或爐底電極)
操作/安裝空間	較小	較大(尤其垂直高度)
氣流量	較大 (100%)	較小 (20%)
中心溫度(℃)	4,000～10,000	15,000～20,000
能量密度(MJ/kg)	5～40	20～200
功率控制參數	電流、氣流量	電流、氣流量、電弧長度
電能轉換熱能效率(%)	80～90	≧90
熔融機制	1.火焰直接加熱 2.電能使用效率較低(45%)	1.火焰直接加熱 2.熔漿電阻加熱 3.電能使用效率較高(60%)

https://www.atlas-innotek.com/projects/e6oFj63K47PYPqPe2
http://www.resi.com.tw/PlasmaTorch.htm

Methods of plasma production

- DC electrical discharges
  - Dark electrical discharges in gases
  - DC electrical glow discharges in gases
  - DC electrical arc discharges in gases
- **AC electrical discharges**
  - **RF electrical discharges in gases**
  - Microwave electrical discharges in gases
  - Dielectric-barrier discharges (DBDs)
- Other mechanism
  - Laser produced plasma
  - Pulsed-power generated plasma

RF can interact with plasma inductively or capacitively

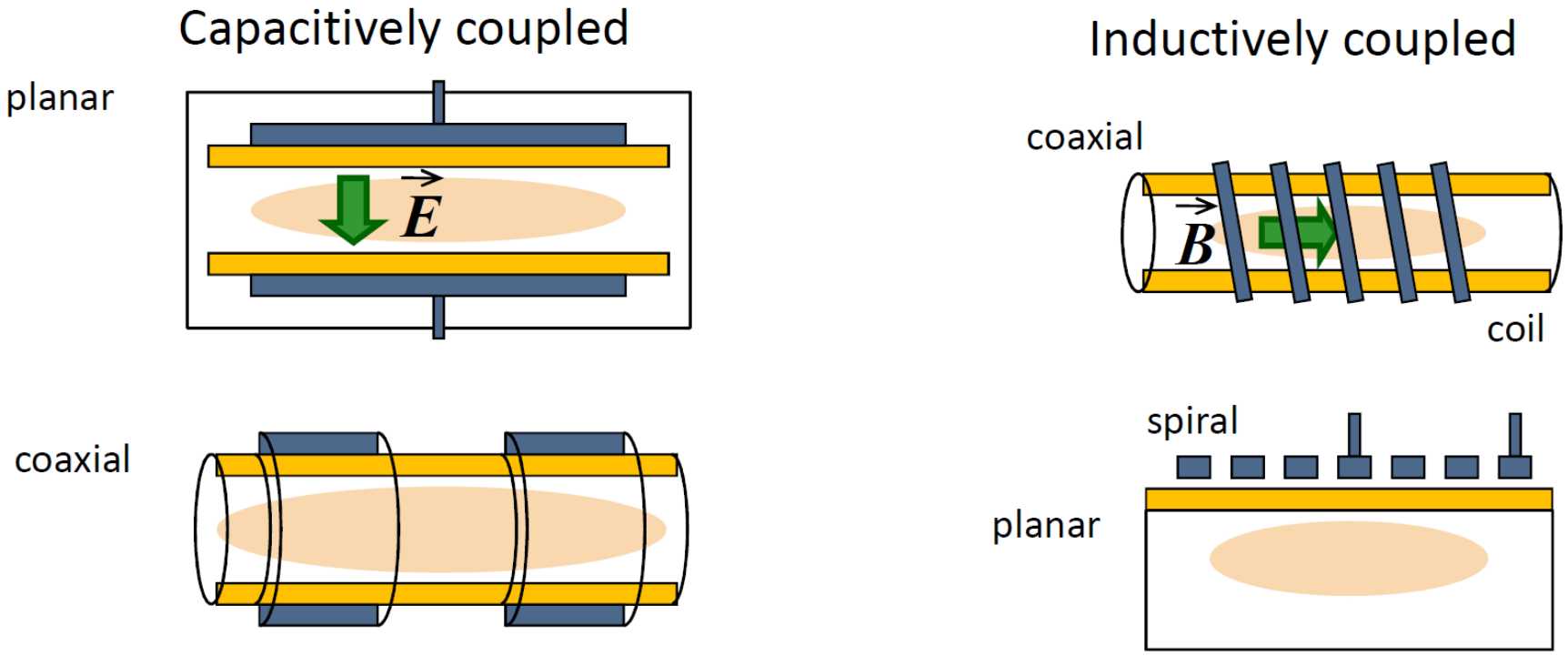

AC electrical discharges deliver energy to the plasma without contact between electrodes and the plasma

- **DC electrical discharge – a true current in the form of a flow of ions or electrons to the electrodes.**
- **AC electrical discharge – the power supply interacts with the plasma by displacement current.**
  - **Inductive radio frequency (RF) electrical discharges**
  - **Capacitive RF electrical discharges**
  - **Microwave electrical discharges**
  - **Dielectric-barrier discharges (DBDs)**
- **Other mechanism**
  - **Laser produced plasma**
  - **Pulsed-power generated plasma**

The plasma is generated by the induced electric field from the oscillating magnetic field

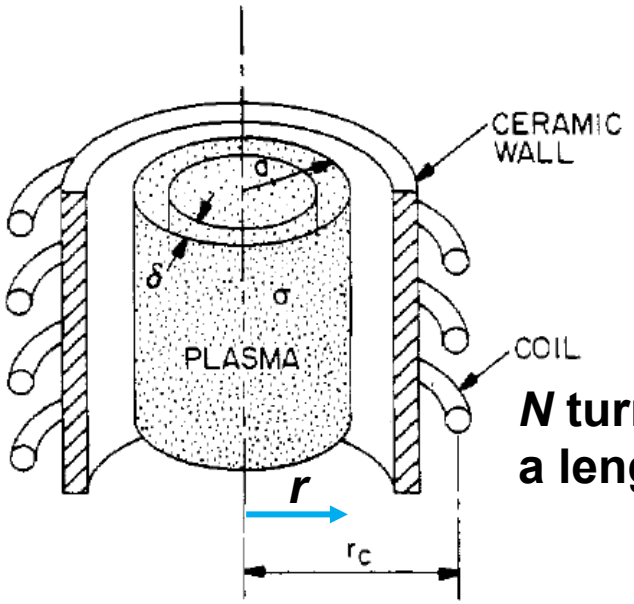

N **turn within a length of** ***l***

$$\nabla \times \vec{E} = -\frac{\partial \vec{B}}{\partial t}$$

$$\int (\nabla \times \vec{E})\, \mathrm{d}\vec{A} = \int \left(-\frac{\partial \vec{B}}{\partial t}\right) \mathrm{d}\vec{A}$$

$$2\pi r E = -\pi r^2 \frac{\partial B}{\partial t}$$

$$E = -\frac{r}{2}\frac{\partial B}{\partial t} \qquad B \times l = \mu_o N I$$

$$E = -\frac{r}{2}\mu_o \frac{N}{l}\frac{\partial I}{\partial t}$$

$$|E| = \frac{r}{2}\mu_o \frac{N}{l}\omega I$$

How an electromagnetic wave interacts with a plasma depends on its frequency

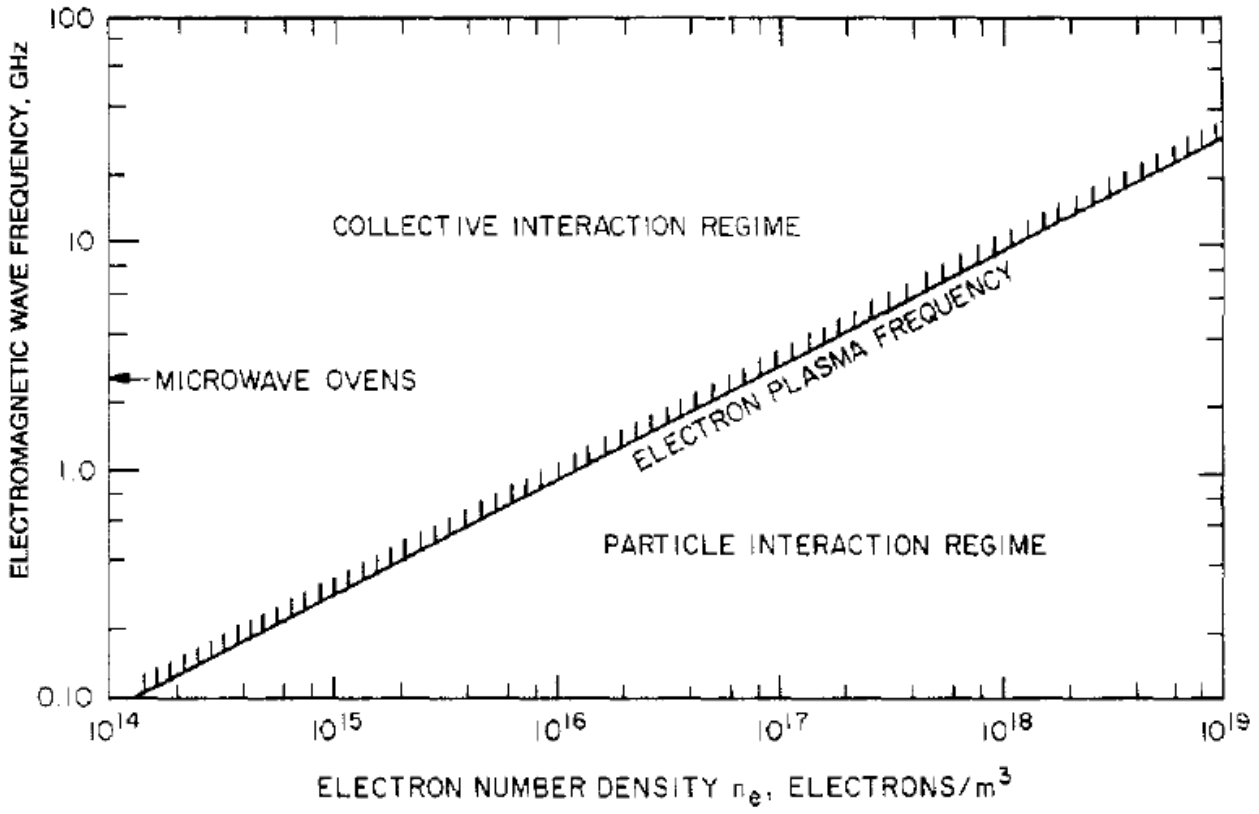

$$\omega_{pe} = \sqrt{\frac{n_e e^2}{\epsilon_0 m_e}} \, (\mathrm{rad}/s)$$

$$n_{cri} = \frac{\epsilon_0 m_e}{e^2} \omega_{pe}{}^2 \left(m^{-3}\right)$$

$n_{760\ \mathrm{Torr}\ /\ 300\mathrm{K}} = 2.45 \times 10^{25}\ \mathrm{m}^{-3}$ $\qquad$ $n_{0.1\ \mathrm{Torr},\ 1\ \%\ \mathrm{ionization}} = 3.2 \times 10^{19}\ \mathrm{m}^{-3}$

RF energy is strongly absorbed within the skin depth if the frequency is below the electron plasma frequency

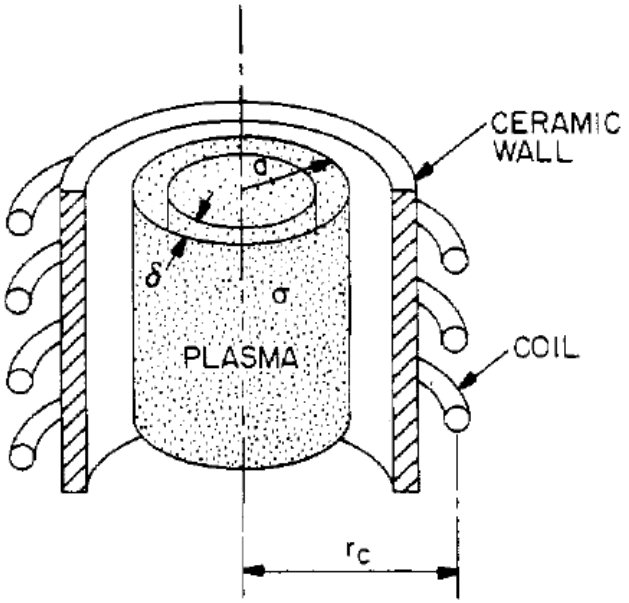

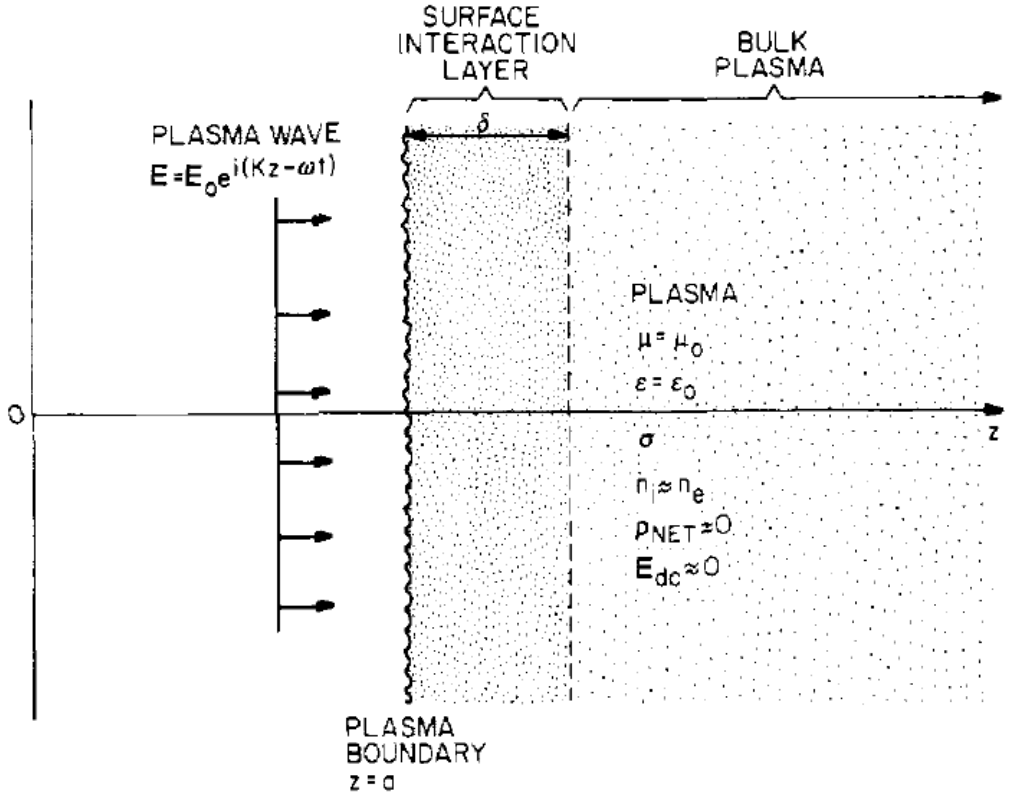

Skin depth is calculated using Maxwell's equations

$$\nabla \cdot \vec{E} \approx 0 (\text{quasi} - \text{neutral}) \qquad \nabla \cdot \vec{B} = 0$$

$$\vec{J} = \sigma \vec{E} \ (\text{Ohm}'\text{slaw})$$

$$\nabla \times \vec{E} = -\frac{\partial \vec{B}}{\partial t} \qquad \nabla \times \vec{B} = \mu_0 \vec{J} + \mu_0 \epsilon_0 \frac{\partial \vec{E}}{\partial t}$$

$$-\frac{\partial}{\partial t}(\nabla \times \vec{B}) = \nabla \times (\nabla \times \vec{E}) = \nabla(\nabla \cdot \vec{E}) - \nabla^2 \vec{E} \sim -\nabla^2 \vec{E}$$

$$\frac{\partial^2 \vec{E}}{\partial z^2} - \mu_0 \sigma \frac{\partial \vec{E}}{\partial t} - \mu_0 \epsilon_0 \frac{\partial^2 \vec{E}}{\partial t^2} = 0 \qquad \vec{E} = \vec{E}_0 \exp[-i(kz - \omega t)] \qquad k \equiv \alpha + \frac{i}{\delta}$$

$$\left(-k^2 + i\omega\mu_0\sigma + \mu_0\epsilon_0\omega^2\right)\vec{E} = 0$$

$$\alpha = \sqrt{\frac{\sigma\mu_0\omega}{2}}\left[\frac{\omega\epsilon_0}{\sigma} + \sqrt{1 + \left(\frac{\omega\epsilon_0}{\sigma}\right)^2}\right]^{1/2}$$

$$\frac{1}{\delta} = \sqrt{\frac{\sigma\mu_0\omega}{2}}\left[\sqrt{1 + \left(\frac{\omega\epsilon_0}{\sigma}\right)^2} - \frac{\omega\epsilon_0}{\sigma}\right]^{1/2}$$

Skin depth is calculated using Maxwell's equations

$$\alpha = \sqrt{\frac{\sigma\mu_0\omega}{2}}\left[\frac{\omega\epsilon_0}{\sigma} + \sqrt{1+\left(\frac{\omega\epsilon_0}{\sigma}\right)^2}\right]^{1/2} \qquad \frac{1}{\delta} = \sqrt{\frac{\sigma\mu_0\omega}{2}}\left[\sqrt{1+\left(\frac{\omega\epsilon_0}{\sigma}\right)^2} - \frac{\omega\epsilon_0}{\sigma}\right]^{1/2}$$

- In most industrial plasma, $\frac{\omega\epsilon_0}{\sigma} \ll 1$. Note that $\sigma = \frac{e^2 n_e}{m_e \nu_c} = \frac{\epsilon_0 {\omega_{pe}}^2}{\nu_c}$ so $\nu_c\omega << {\omega_{pe}}^2$ is required.

$$\alpha \approx \sqrt{\frac{\sigma\mu_0\omega}{2}}\left(m^{-1}\right)$$

skin depth: $$\delta \approx \sqrt{\frac{2}{\sigma\mu_0\omega}} = \frac{\sqrt{2}c}{\omega_{pe}}\sqrt{\frac{\nu_c}{\omega}} = \frac{c}{e}\sqrt{\frac{2m_e\epsilon_0}{n_e}}\sqrt{\frac{\nu_c}{\omega}} = \frac{c}{2\pi\nu_{pe}}\sqrt{\frac{\nu_c}{\pi f}}(m)$$

- The skin depth δ ~ the distance that an electromagnetic wave propagates into a medium during one period of the electron plasma frequency.

Skin depth needs to be carefully considered in the design of inductive industrial plasma reactors

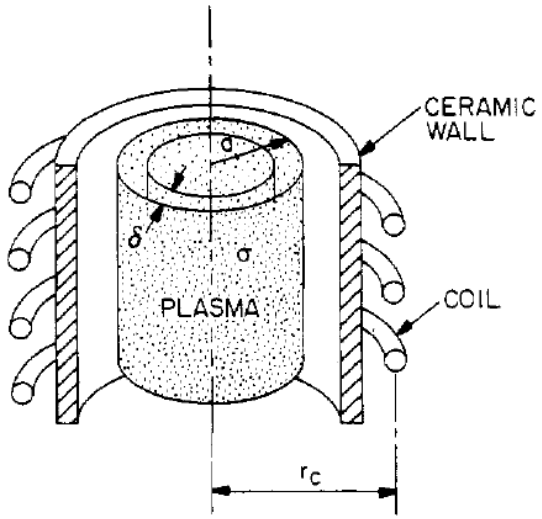

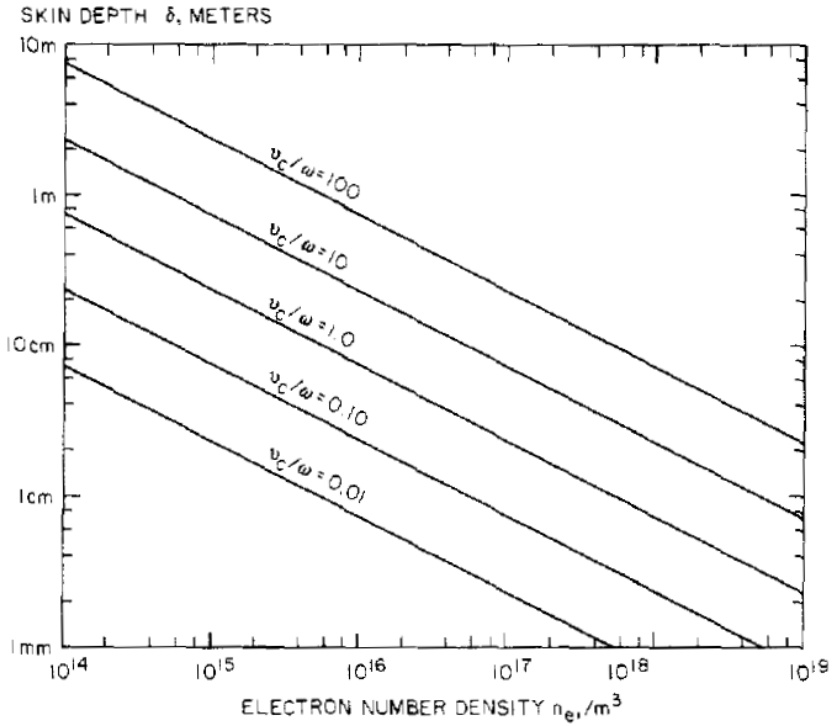

- **Boulos et al showed that the energy coupling parameter is maximum when $1.5\delta \leq a \leq 3\delta$. However, it doesn't mean the plasma will be uniformly heated.**

A kilowatt-level inductively coupled plasma torch is shown

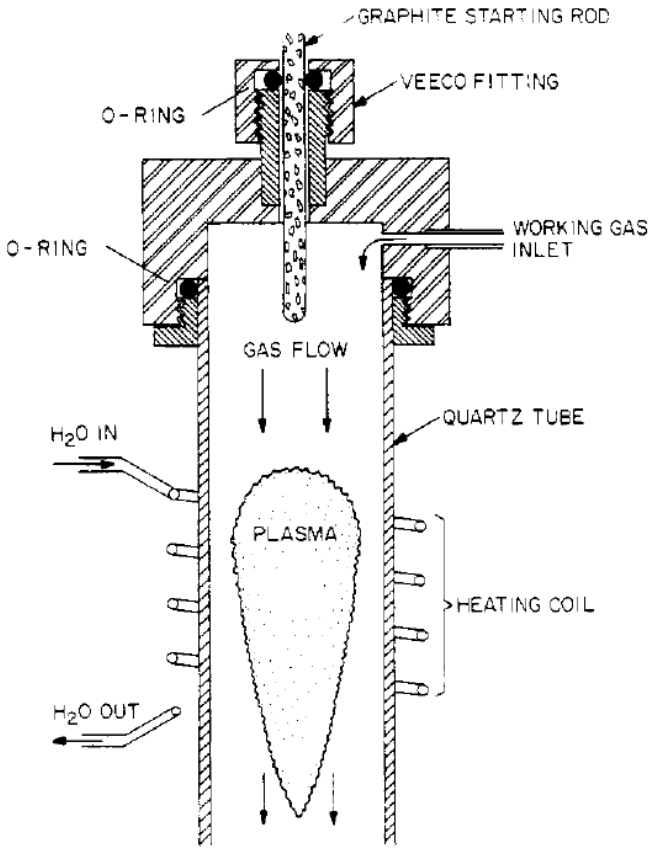

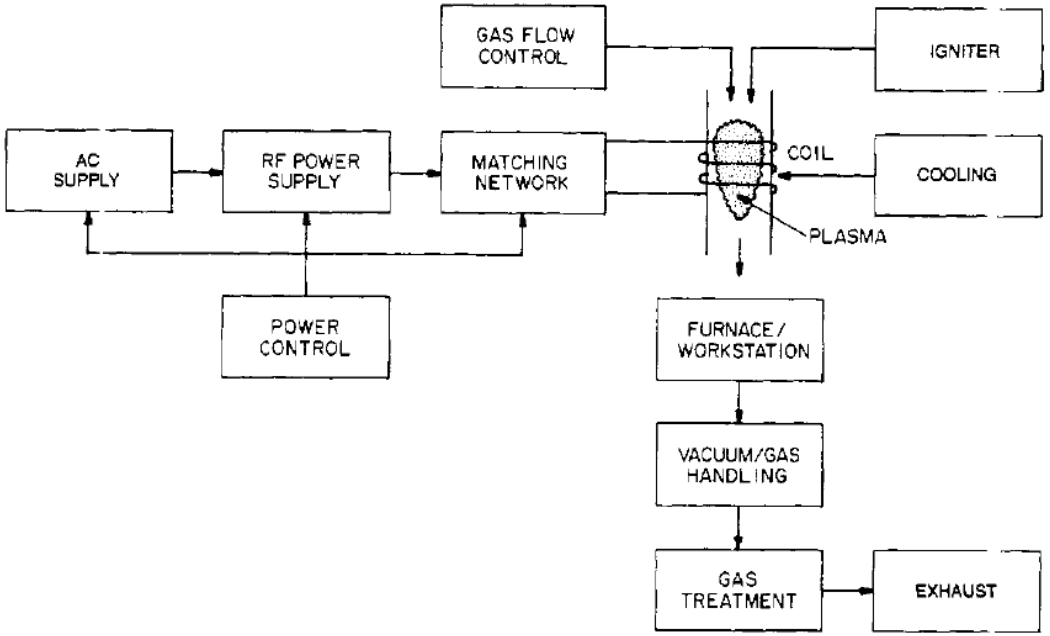

High voltage initiation is usually required for inductive RF plasma torches

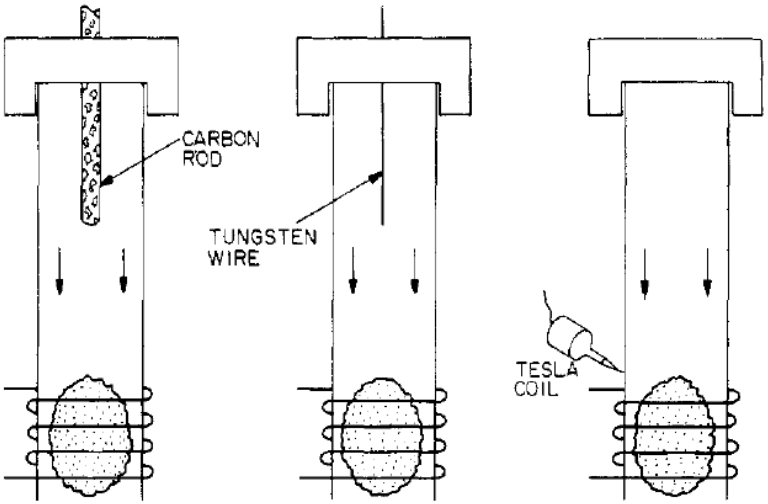

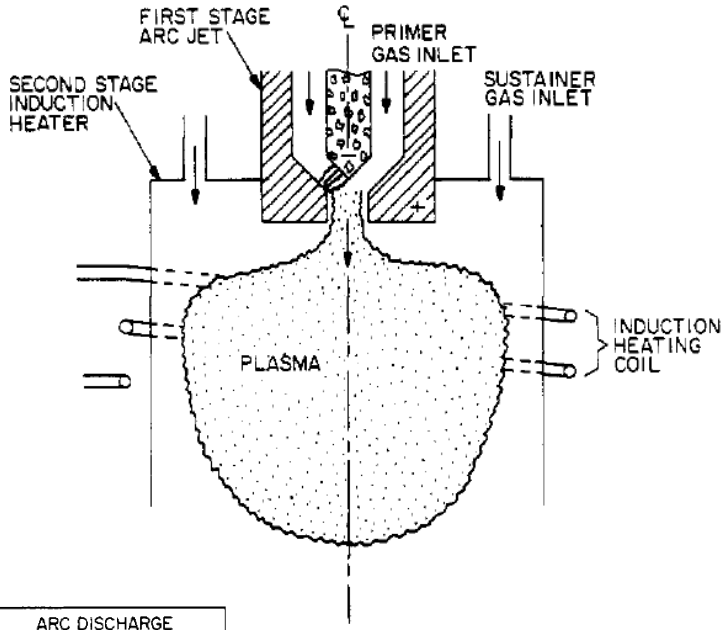

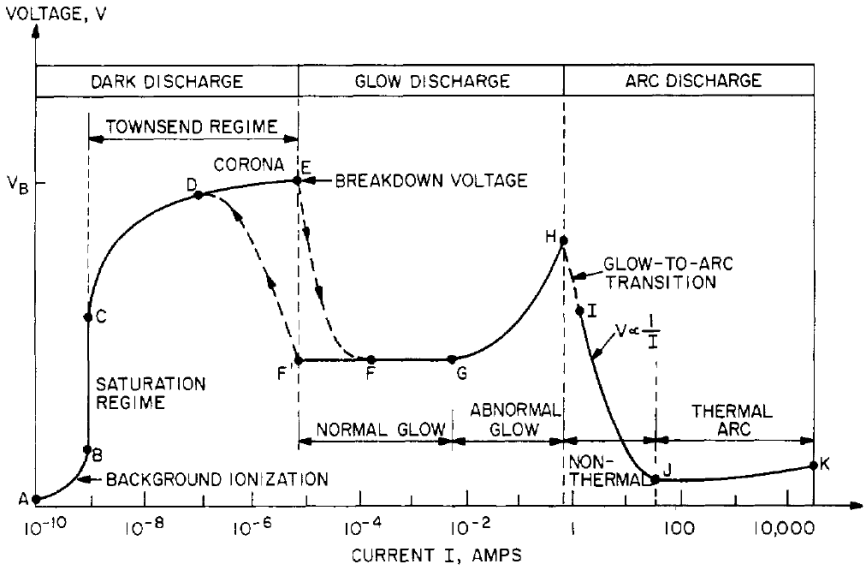

The power supplies are relatively inefficient

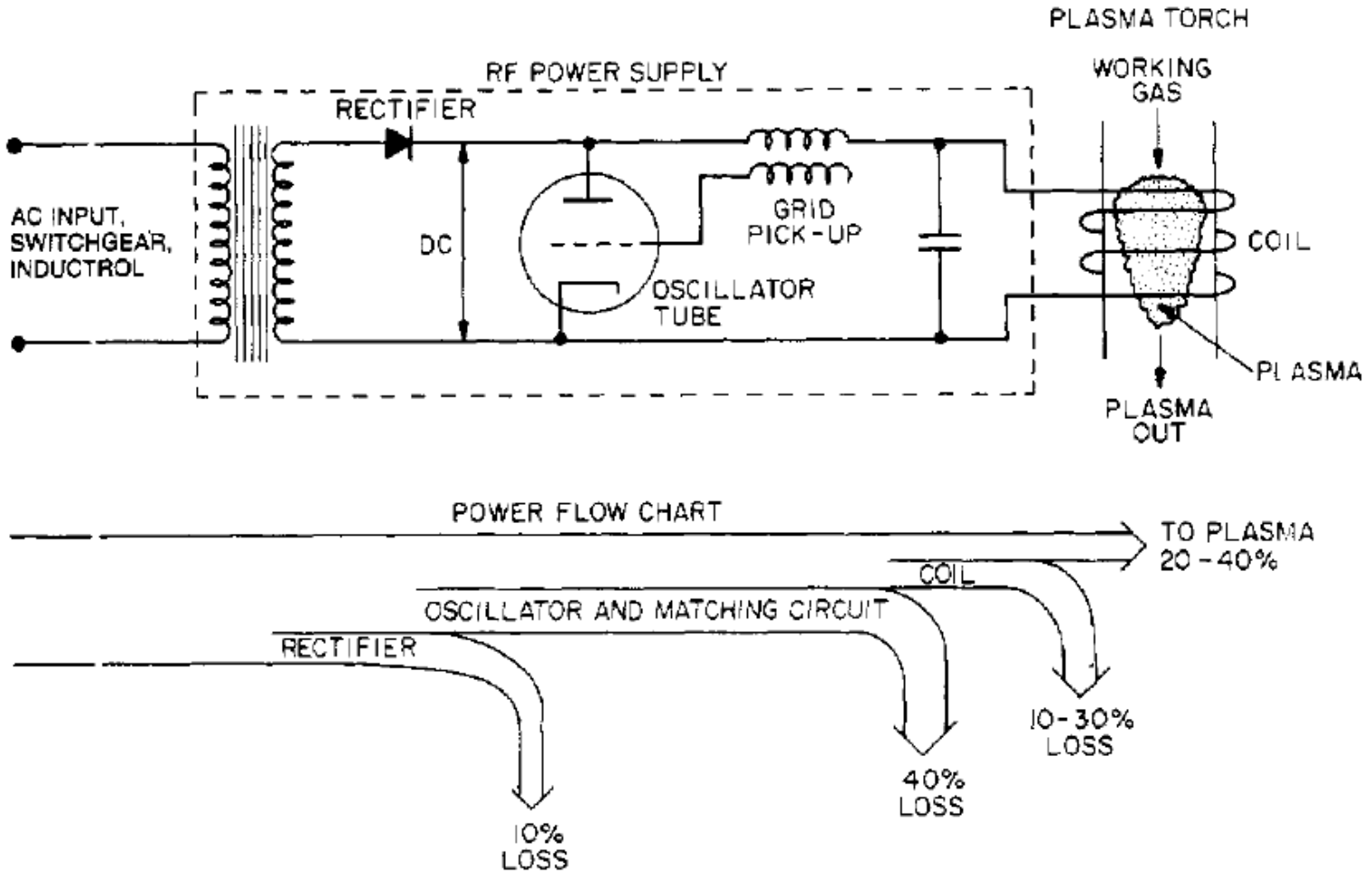

Operating regimes of inductively coupled plasma torches

Parameter	Low	Characteristic	High
Frequency	10 kHz	13.56 MHz	100 MHz
Power	1 kW	30 kW	1MW
Efficiency	20%	35%	50%
Pressure	10 Torr	1 atm	10 atm
Gas temperature	1000 K	10^4 K	2×10^4 K

Inductive RF coupling provides a plasma with less contamination from the electrode

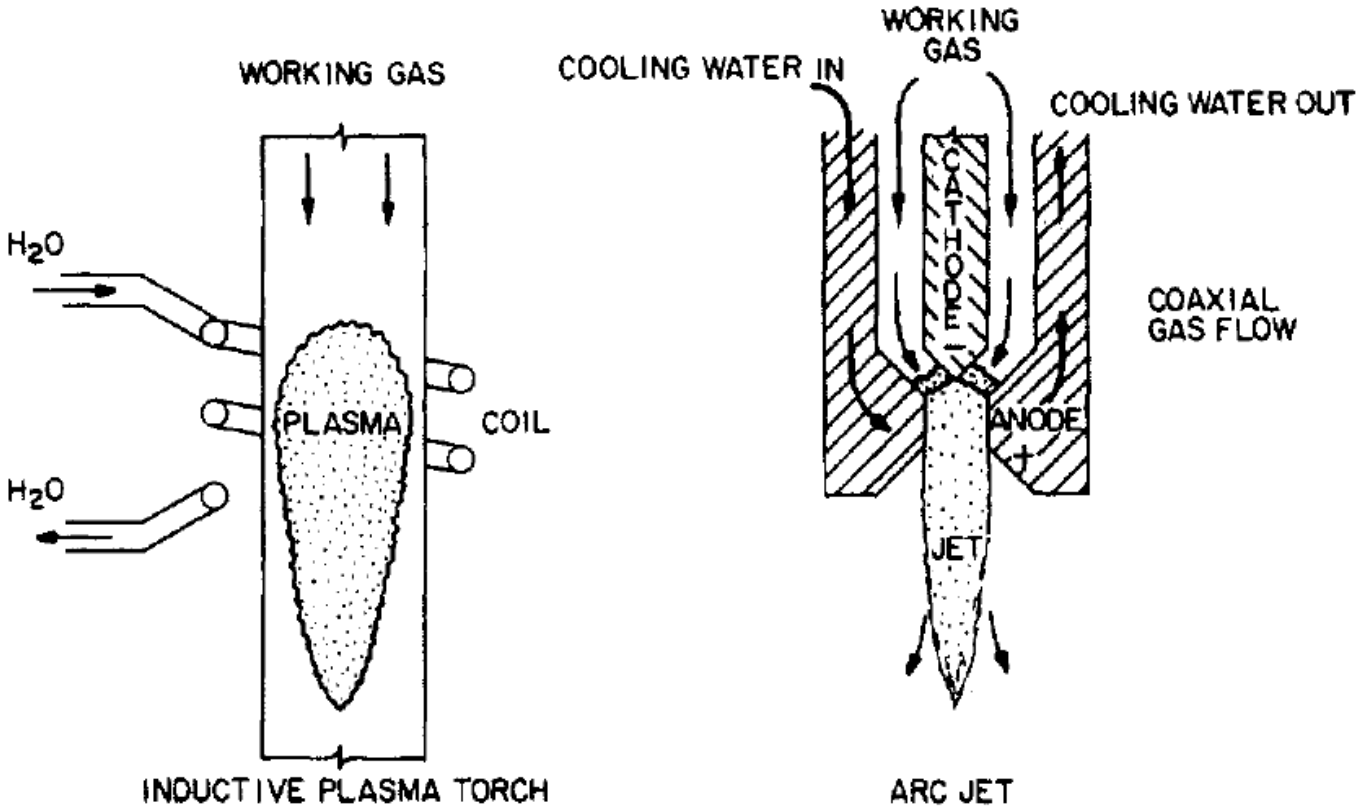

Several cooling configurations are shown

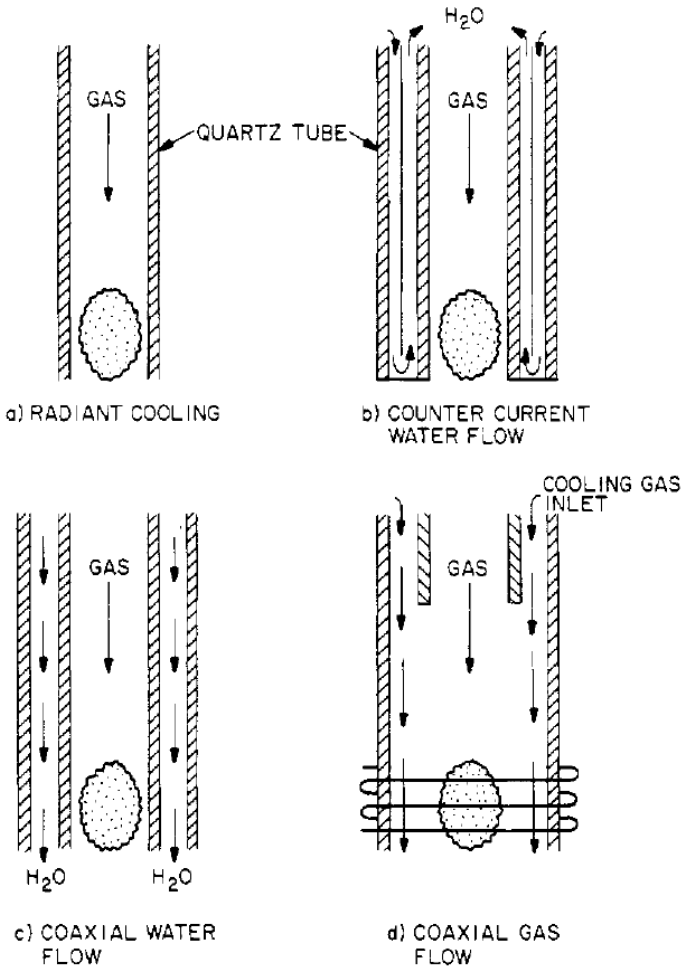

Inductive parallel plate reactor

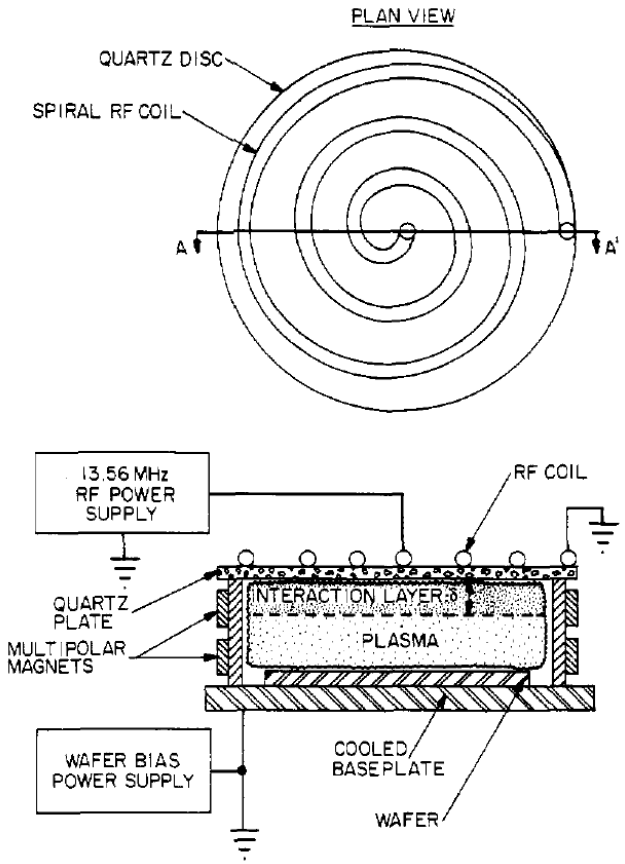

- **Uniform plasma source**
- **Higher power (2 kW) leading to higher plasma density (up to 10^{18} electrons/m^3)**
- **Lower gas pressure, i. e., longer mean free paths and little scattering of ions and is desired in deposition and etching applications.**

Rotamak

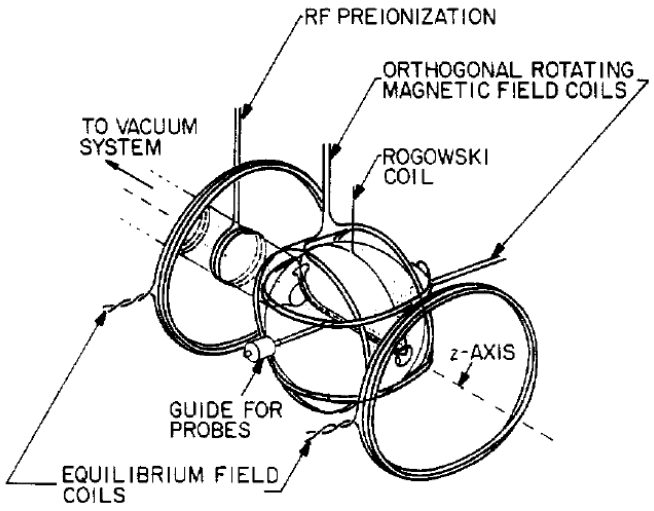

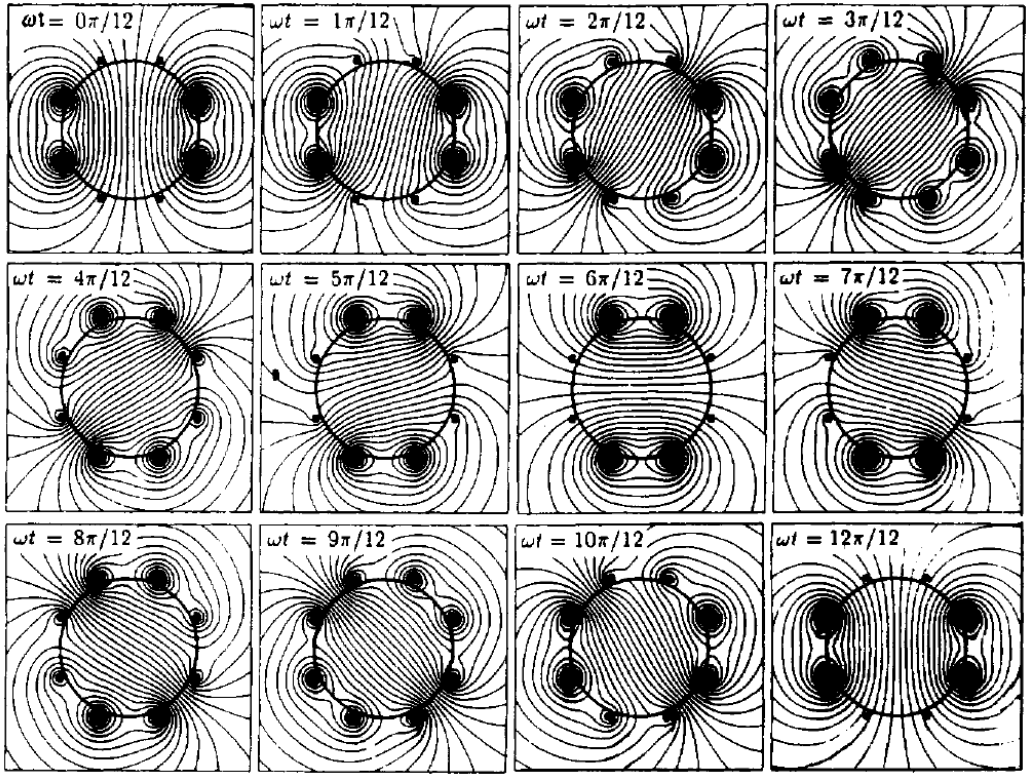

- **The rapidly rotating magnetic field generates large plasma currents, thus heating the plasma to densities and temperatures of interest in many industrial applications**

Inductively heated toroidal plasmas

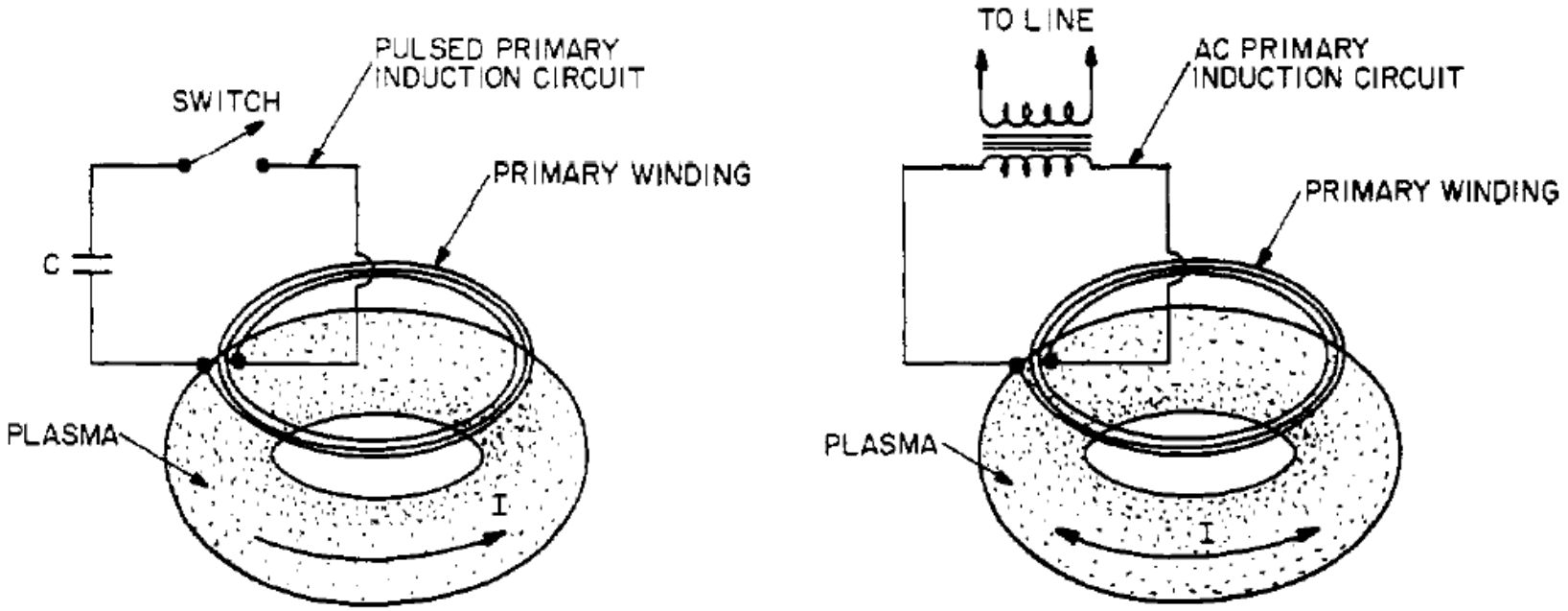

- **Large currents are induced in the plasma by transformer action from a ramped current in a pulsed primary induction circuit.**

Applications of inductive plasma torches

- High purity materials production
  - Silica and other refractories
  - Ultrafine powder
  - Spherical fine power
  - Refining/purification
- High temperature thermal treatment
  - Heat treatment
  - Plasma sintering
- Surface treatment
  - Oxidation
  - Nitriding

Applications of inductive plasma torches

- Surface coating
  - Plasma flame spraying
  - Surface coating of powder
- Chemical vapor deposition (CVD)
  - At atmospheric pressure
  - At reduced pressure
- Chemical synthesis and processing
- Experimental applications
  - Laboratory furnace
  - High intensity light source
  - Spectroscopic analysis
  - Isotope separation
  - Ion source
  - High power density plasma source

AC electrical discharges deliver energy to the plasma without contact between electrodes and the plasma

- DC electrical discharge – a true current in the form of a flow of ions or electrons to the electrodes.
- AC electrical discharge – the power supply interacts with the plasma by displacement current.
  - Inductive radio frequency (RF) electrical discharges
  - **Capacitive RF electrical discharges**
  - Microwave electrical discharges
  - Dielectric-barrier discharges (DBDs)
- Other mechanism
  - Laser produced plasma
  - Pulsed-power generated plasma

Capacitive RF coupling plasma without magnetic fields

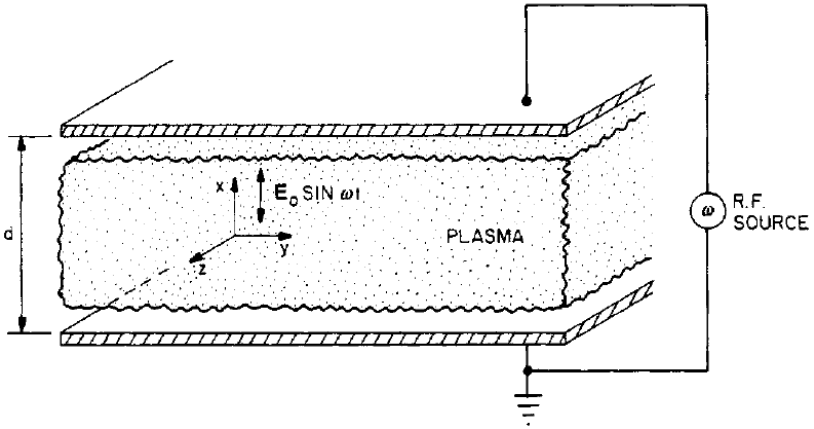

$$\vec{F} = m\,\vec{a} = -\nu_c m\,\vec{v} - e\,\vec{E}$$

$$m\frac{dv_y}{dt} + m\nu_c v_y = 0$$

$$v_y(t) = v_{y0}\exp(-\nu_c t)$$

$$m\frac{d^2x}{dt^2} + m\nu_c\frac{dx}{dt} = eE_0\sin(\omega t)$$

$$x = C_1\sin(\omega t) + C_2\cos(\omega t)$$

$$C_1 = -\frac{eE_0}{m}\frac{1}{\omega^2 + {\nu_c}^2}$$

$$C_2 = -\frac{\nu_c eE_0}{\omega m}\frac{1}{\omega^2 + {\nu_c}^2}$$

$$v_x(t) = -\frac{eE_0\omega}{m(\omega^2 + {\nu_c}^2)}\left[\cos(\omega t) - \frac{\nu_c}{\omega}\sin(\omega t)\right]$$

$$P = \frac{dW}{dt} = eE_0\sin(\omega t)v_x$$

$$\bar{P}_{tot} = n_e\bar{P} = \frac{1}{4}\epsilon_0{E_0}^2\frac{2n_e e^2}{m\epsilon_0}\frac{\nu_c}{\omega^2 + {\nu_c}^2}$$

Capacitive RF coupling plasma with magnetic fields

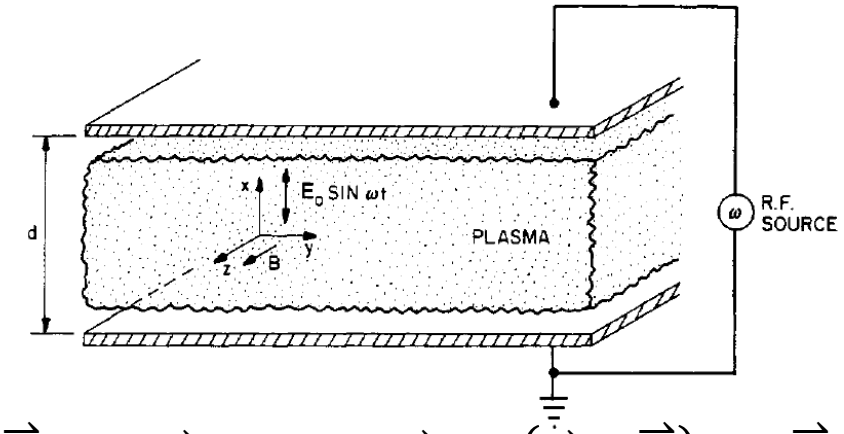

$$\vec{F} = m\,\vec{a} = -\nu_c m\,\vec{v} - e\left(\vec{v} \times \vec{B}\right) - e\,\vec{E}$$

$$m\frac{d^2x}{dt^2} + m\nu_c\frac{dx}{dt} + eB\frac{dy}{dt} = -eE_0\sin(\omega t)$$

$$m\frac{dv_y}{dt} + m\nu_c v_y - eB\frac{dx}{dt} = 0$$

$$m\frac{dv_z}{dt} + m\nu_c v_z = 0$$

$$v_z(t) = v_{z0}\exp(-\nu_c t)$$

$$\frac{d^2x}{dt^2} + \nu_c\frac{dx}{dt} + \omega_c\frac{dy}{dt} = -\frac{eE_0}{m}\sin(\omega t)$$

$$\frac{d^2y}{dt^2} + \nu_c\frac{dx}{dt} - \omega_c\frac{dy}{dt} = 0 \qquad \omega_c = \frac{eB}{m}$$

$$x = C_1\sin(\omega t) + C_2\cos(\omega t)$$

$$y = C_e\sin(\omega t) + C_4\cos(\omega t)$$

$$C_1 = -\frac{eE_0}{2m}\left[\frac{\omega+\omega_c}{(\omega+\omega_c)^2+\nu_c{}^2} + \frac{\omega-\omega_c}{(\omega-\omega_c)^2+\nu_c{}^2}\right]$$

$$C_2 = -\frac{\nu_c eE_0}{2\omega m}\left[\frac{1}{(\omega+\omega_c)^2+\nu_c{}^2} + \frac{1}{(\omega-\omega_c)^2+\nu_c{}^2}\right]$$

$$C_3 = \frac{\omega_c(C_1\nu_c + C_2\omega)}{\omega^2+\nu_c{}^2} \qquad C_4 = -\frac{\omega_c(C_1\omega - C_2\nu_c)}{\omega^2+\nu_c{}^2}$$

The coupling efficient for capacitive RF with magnetic fields is less than DC electrical discharge

$$P = \frac{dW}{dt} = eE_0 \sin(\omega t) v_x$$

$$\bar{P}_{tot} = n_e \bar{P} = \frac{1}{4}\epsilon_0 {E_0}^2 \frac{n_e e^2}{m\epsilon_0} \nu_c \left[\frac{1}{(\omega+\omega_c)^2+{\nu_c}^2} + \frac{1}{(\omega-\omega_c)^2+{\nu_c}^2}\right]$$

$$= \frac{1}{4}\epsilon_0 {E_0}^2 \times {\omega_{pe}}^2 \nu_c \left[\frac{1}{(\omega+\omega_c)^2+{\nu_c}^2} + \frac{1}{(\omega-\omega_c)^2+{\nu_c}^2}\right]$$

- DC, unmagnetized discharge ($\omega=\omega_c=0$): $\nu_{*0} = \frac{2{\omega_{pe}}^2}{\nu_c}$
- Low collisionality ($\omega_c >> \nu_c$):

$$\nu_* \approx \nu_{*0} {\nu_c}^2 \left[\frac{\omega^2+{\omega_c}^2}{(\omega^2-{\omega_c}^2)^2}\right] \rightarrow \nu_{*0}\frac{{\nu_c}^2}{{\omega_c}^2} \ll \nu_{*0} \quad (\omega, \nu_c \ll \omega_c)$$

- High collisionality ($\omega_c << \nu_c$):

$$\nu_* \approx \nu_{*0}\frac{{\nu_c}^2}{\omega^2+{\nu_c}^2} \approx \nu_{*0}(\omega, \omega_c << \nu_c)$$

- Resonant ($\omega=\omega_c$):

$$\nu_* = \nu_{*0}\frac{2{\omega_c}^2+{\nu_c}^2}{4{\omega_c}^2+{\nu_c}^2} \rightarrow \frac{1}{2}\nu_{*0}(\omega=\omega_c >> \nu_c)$$

Collision frequency can be measured using capacitive RF electrical discharges

$$\bar{P}(\omega_c) = \frac{1}{4}\epsilon_0 {E_0}^2 \times \nu_{*0}\frac{2+(\nu_c/\omega_c)^2}{4+(\nu_c/\omega_c)^2} = \frac{1}{4}\epsilon_0 {E_0}^2 \times \nu_{*0}\frac{2+\epsilon^2}{4+\epsilon^2}$$

$$\bar{P}(\omega_c \pm \Delta\omega) = \frac{1}{4}\epsilon_0 {E_0}^2 \times \frac{\nu_{*0}}{2}\left(\frac{\nu_c}{\omega_c}\right)^2\left[\frac{1}{(2\pm\Delta\omega/\omega_c)^2+(\nu_c/\omega_c)^2}+\frac{1}{(\Delta\omega/\omega_c)^2+(\nu_c/\omega_c)^2}\right]$$

$$= \frac{1}{4}\epsilon_0 {E_0}^2 \times \frac{\nu_{*0}}{2}\epsilon^2\left[\frac{1}{(2\pm\delta)^2+\epsilon^2}+\frac{1}{\delta^2+\epsilon^2}\right] \text{ where } \delta \equiv \frac{\Delta\omega}{\omega_c}, \epsilon \equiv \frac{\nu_c}{\omega_c}$$

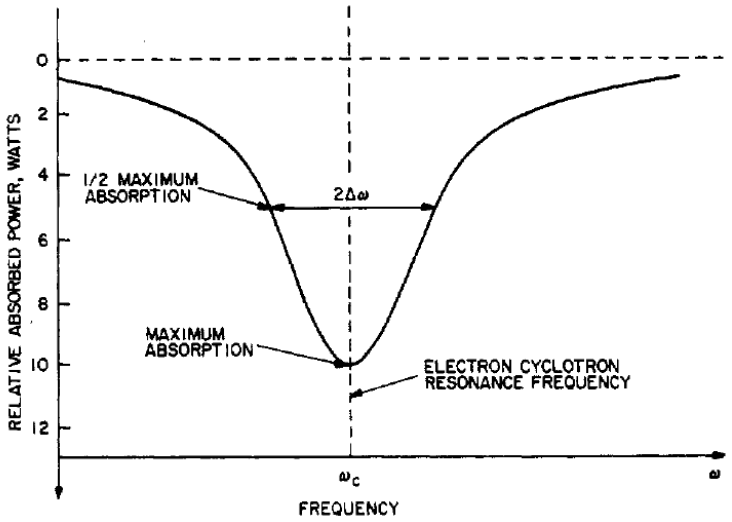

For $\delta \approx \epsilon << 1$,

$$\bar{P}(\omega_c \pm \nu_c) = \frac{1}{2}\bar{P}(\omega_c)$$

Symmetrical capacitive RF discharge model

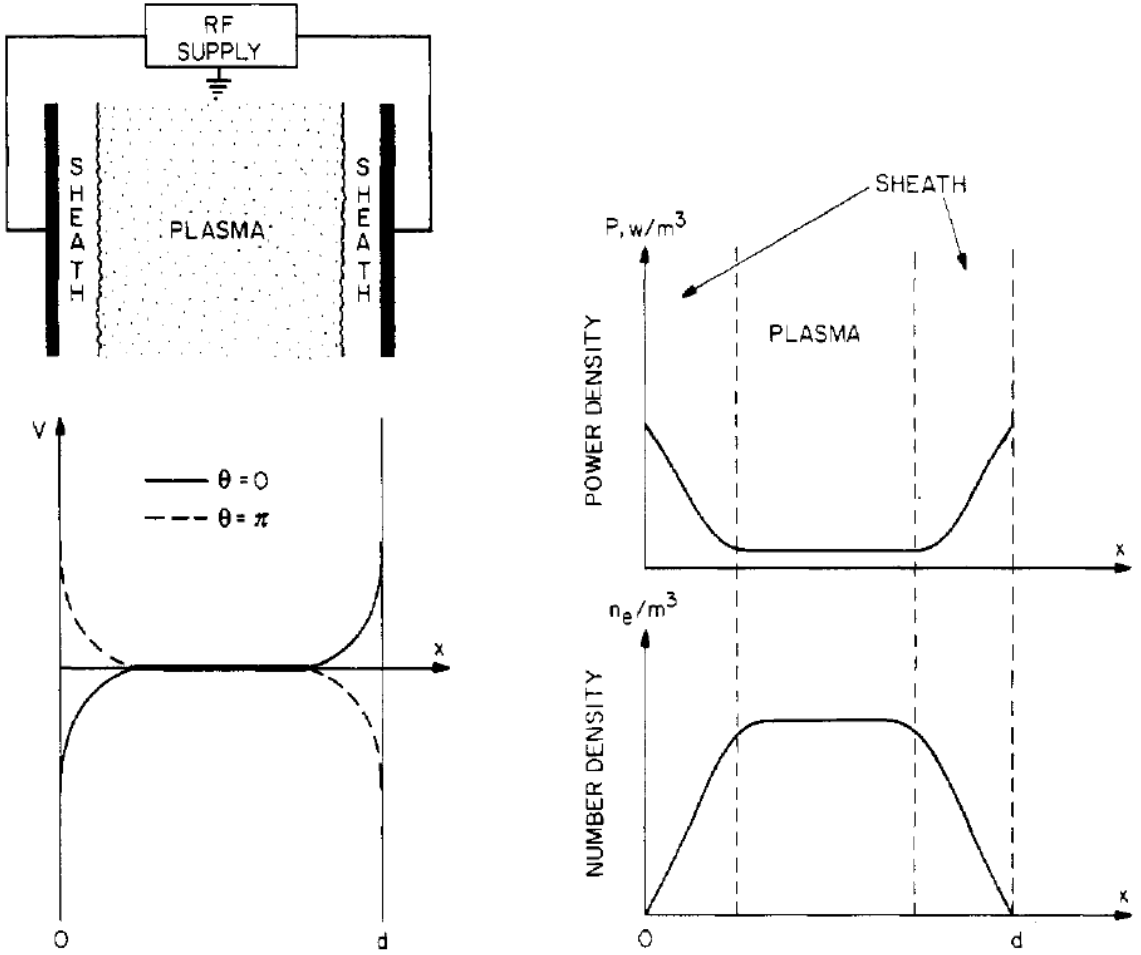

Empirical scaling of electrode voltage drop

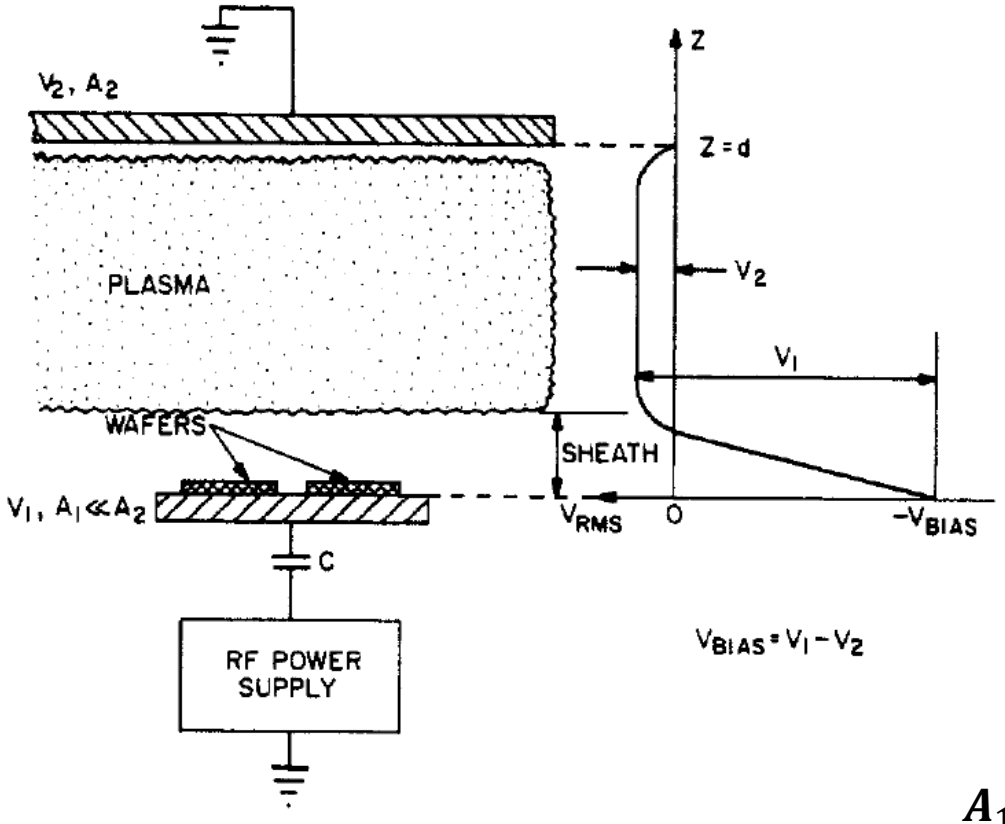

$$I_1 = A_1 J_1 = A_1 e n_{i1} \bar{v}_{i1}$$

$$I_2 = A_2 J_2 = A_2 e n_{i2} \bar{v}_{i2}$$

$$\bar{v}_{i1} = \sqrt{\left(\frac{2eV_1}{m_i}\right)}$$

$$\bar{v}_{i2} = \sqrt{\left(\frac{2eV_2}{m_i}\right)}$$

Assuming: $I_1 = I_2 \quad n_{i1} = n_{i2}$

$$A_1 e n_{i1} \sqrt{\left(\frac{2eV_1}{m_i}\right)} = A_2 e n_{i2} \sqrt{\left(\frac{2eV_2}{m_i}\right)}$$

$$\frac{V_1}{V_2} = \left(\frac{A_2}{A_1}\right)^2$$

$$\frac{V_1}{V_2} = \left(\frac{A_2}{A_1}\right)^q \text{ where } 1.0 \le q \le 2.5$$

Example of capacitively coupled RF plasma source 1

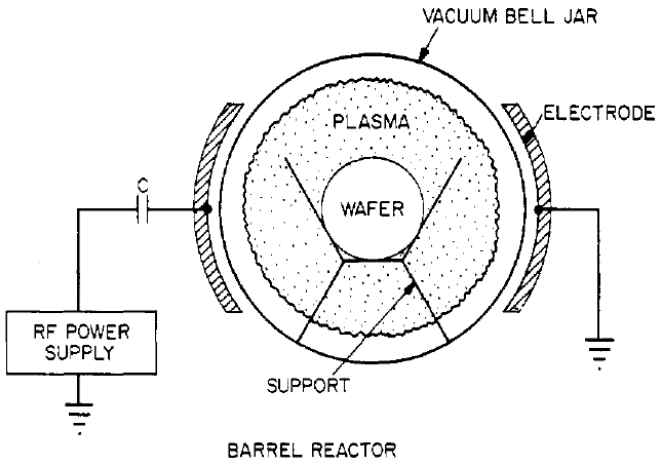

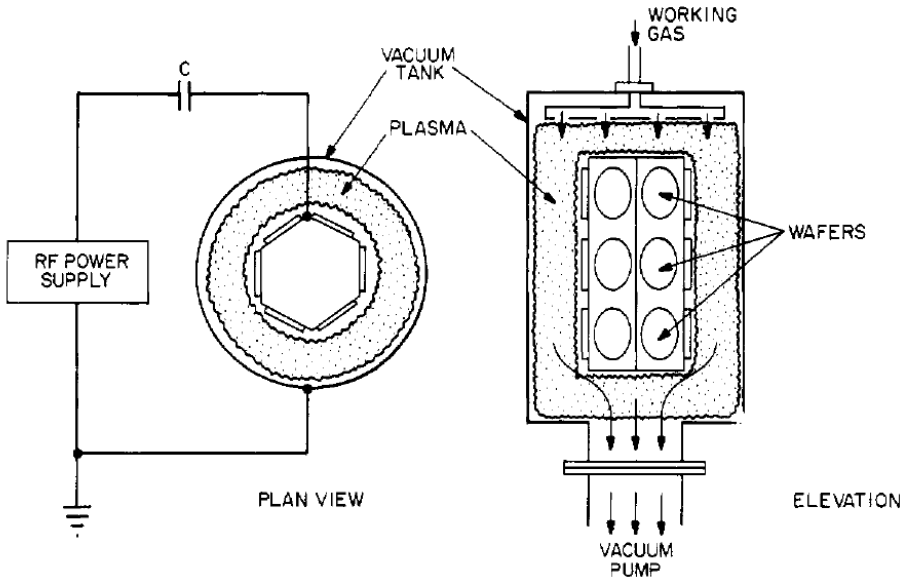

- **Barrier reactor – the wafers float electrically and have low ion bombardment energies**
- **Hexagonal reactor – the wafers develop a DC bias which leads to a relatively anisotropic, vertical etch.**

Example of capacitively coupled RF plasma source 2

- **Plane parallel reactor**

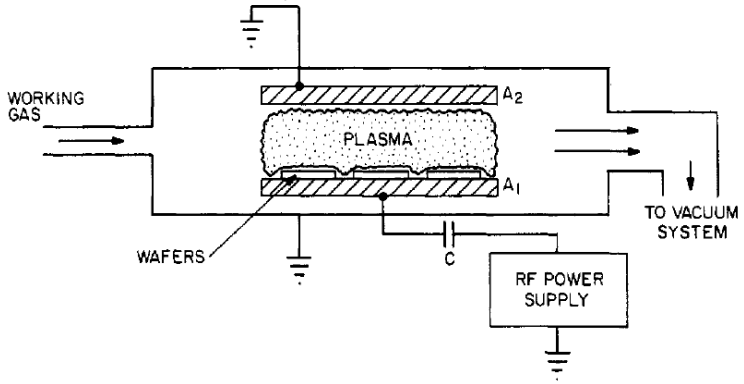

- **Multiple electrode system**

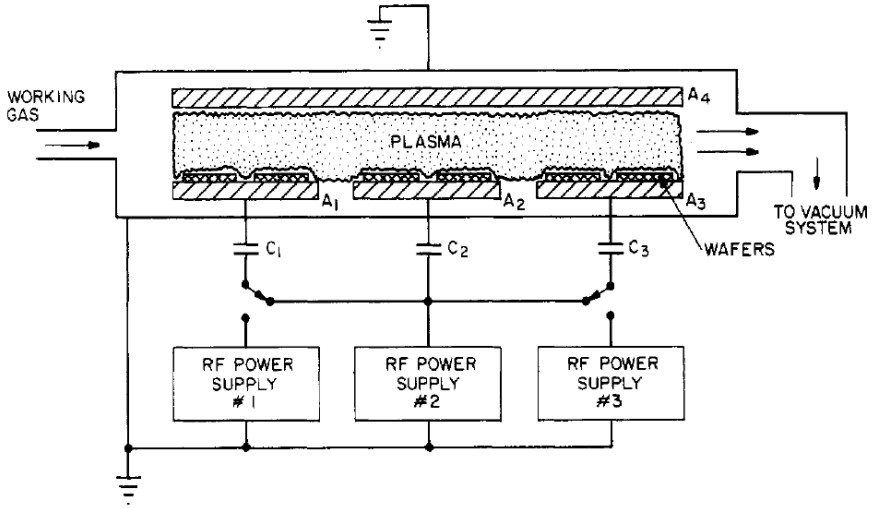

Operating regimes of capacitively coupled plasma reactors used for plasma processing

Parameter	Low value	Typical value	High value
Frequency	1 kHz	13.56 MHz	100 MHz
Gas pressure	3 mTorr	300 mTorr	5 Torr
Power level	50 W	$\approx$ 200 W	500 W
rms electrode voltage	100 V	$\approx$ 300 V	1000 V
Current density	0.1 mA/cm^2	$\approx$ 3 mA/cm^2	10 mA/cm^2
Electron temperature, T_e	3 eV	$\approx$ 5 eV	8 eV
Electron density, n_e	10^{15}/m^3	$\approx 5 \times 10^{15}$/m^3	3×10^{17}/m^3
Ion energy, $\mathcal{E}_i$	5 eV	50 eV	500 eV
Electrode separation, d	0.5 cm	4 cm	30 cm

AC electrical discharges deliver energy to the plasma without contact between electrodes and the plasma

- DC electrical discharge – a true current in the form of a flow of ions or electrons to the electrodes.
- AC electrical discharge – the power supply interacts with the plasma by displacement current.
  - Inductive radio frequency (RF) electrical discharges
  - Capacitive RF electrical discharges
  - **Microwave electrical discharges**
  - Dielectric-barrier discharges (DBDs)
- Other mechanism
  - Laser produced plasma
  - Pulsed-power generated plasma

Advantage of using microwave electrical discharges

- The wavelength of the microwave is in centimeters range. In contract, the wavelength is 22 m for RF frequency f = 13.6 MHz.
- The electron number density can approach the critical number density. ($7x10^{16}$ m^{-3}) at a frequency of 2.45 GHz.
- The plasma in microwave discharges is quasi-optical to microwave.
- Microwave-generated plasmas have a higher electron kinetic temperature (5 ~ 15 eV) than DC or low frequency RF-generated plasmas (1 or 2 eV).
- Capable of providing a higher fraction of ionization.
- Do not have a high voltage sheath.
- No internal electrodes.

Microwave frequency is determined for those used in communications and radar purposes

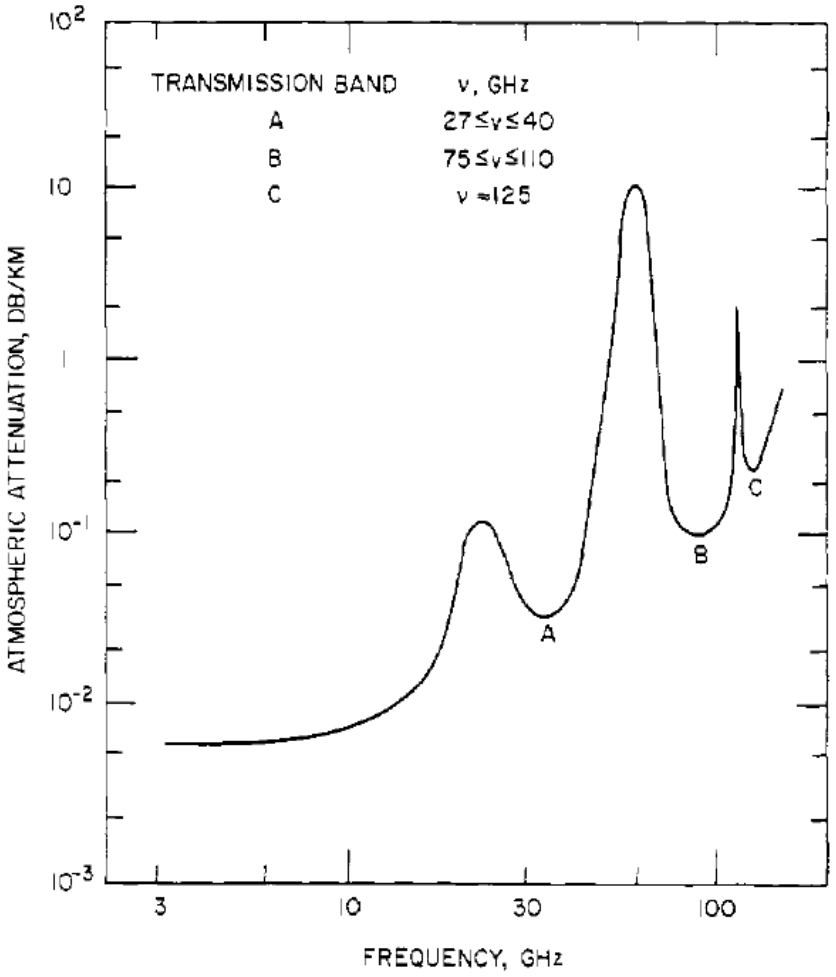

Internal of a magnetron

$$\omega_{LC} = \frac{1}{\sqrt{LC}} \equiv 4\omega_{ce}$$

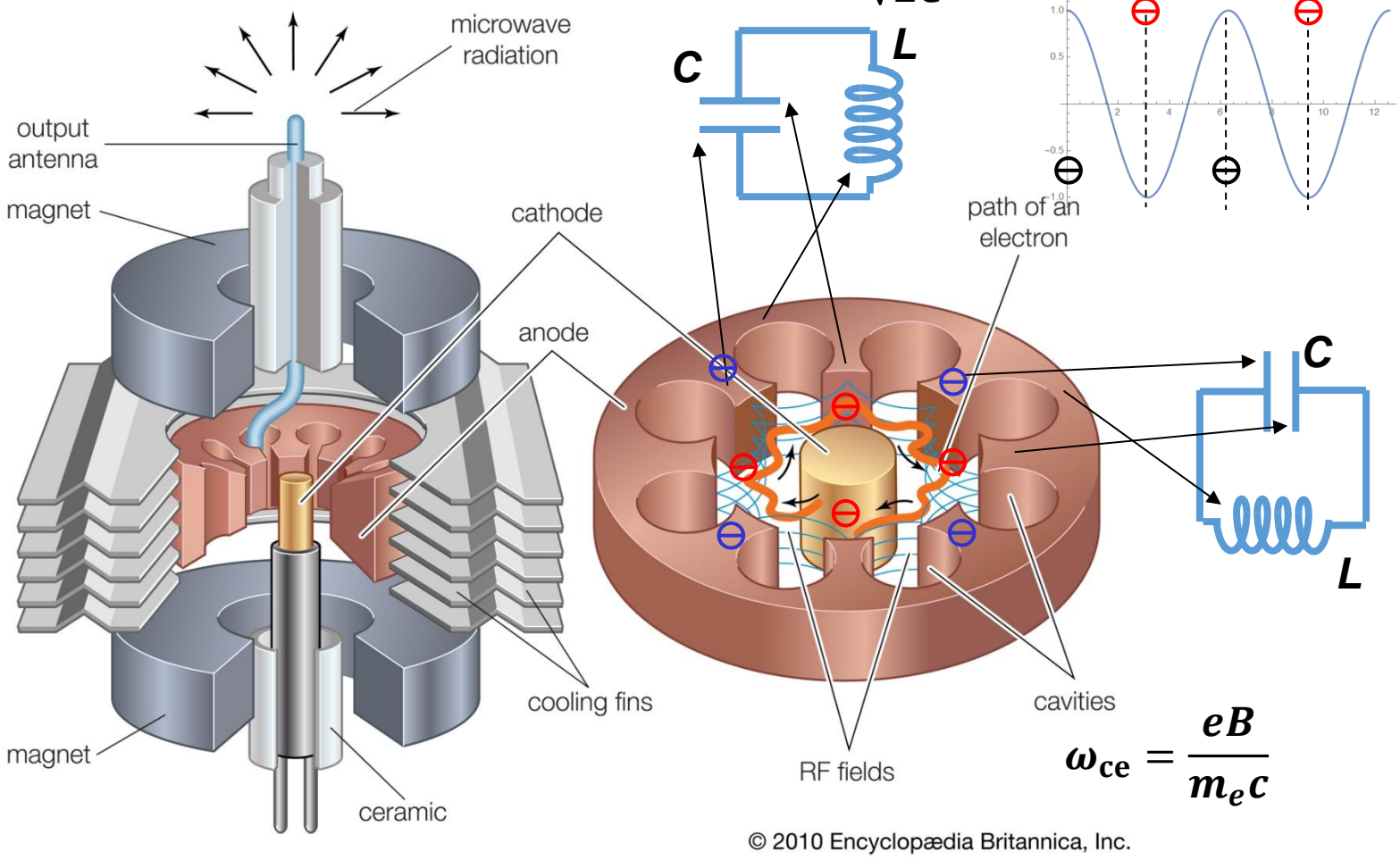

$$\omega_{ce} = \frac{eB}{m_e c}$$

https://kids.britannica.com/students/article/electron-tube/106024/media?assemblyId=137

Internal of a magnetron

$$\omega_{LC} = \frac{1}{\sqrt{LC}} \equiv 4\omega_{ce}$$

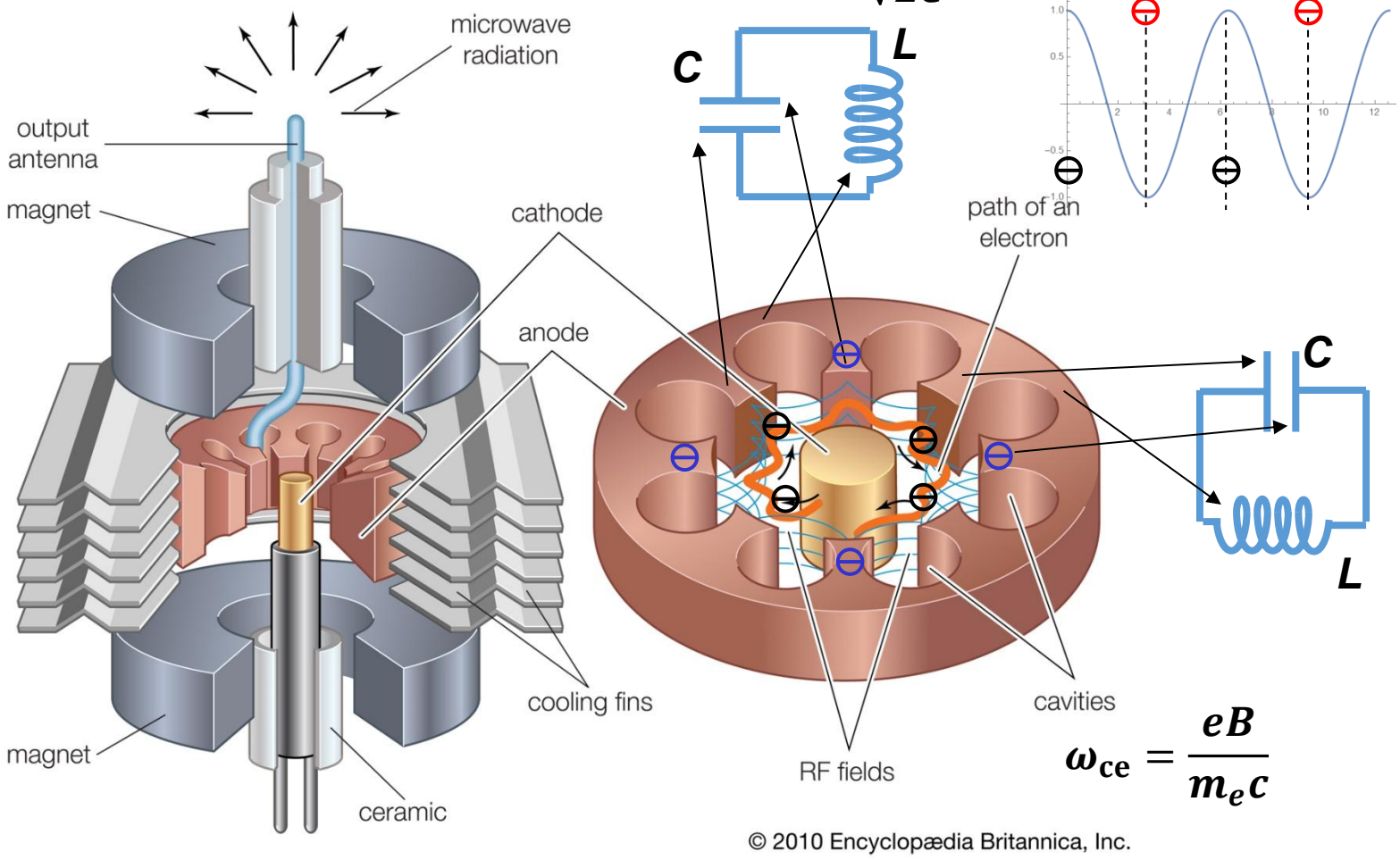

$$\omega_{ce} = \frac{eB}{m_e c}$$

https://kids.britannica.com/students/article/electron-tube/106024/media?assemblyId=137

Magnetron is a forced oscillation driven by electrons between the gap

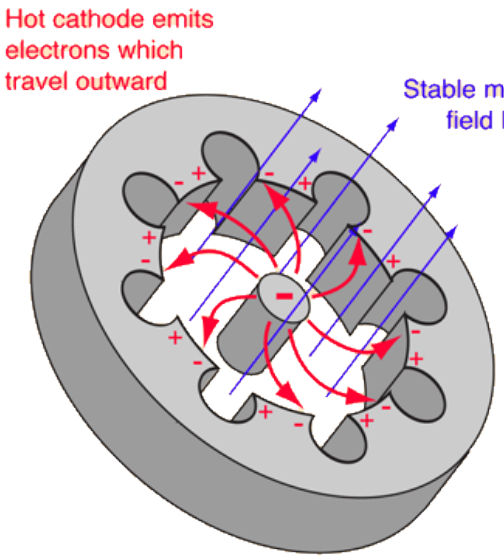

Electrons from a hot filament would travel radially to the outside ring if it were not for the magnetic field. The magnetic force deflects them in the sense shown and they tend to sweep around the circle. In so doing, they "pump" the natural resonant frequency of the cavities. The currents around the resonant cavities cause them to radiate electromagnetic energy at that resonant frequency.

Current around the cavity plays the role of an inductor.

Oscillating magnetic and electric fields produced in the cavity.

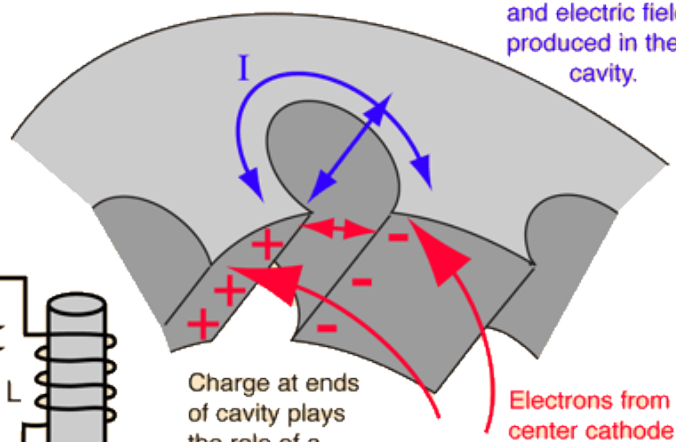

The cavity exhibits a resonance analogous to a parallel resonant circuit.

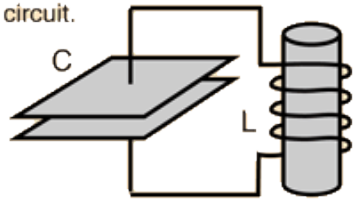

$$f_{resonance} \approx \frac{1}{2\pi}\sqrt{\frac{1}{LC}}$$

Charge at ends of cavity plays the role of a capacitor.

Electrons from the hot center cathode arriving at a negatively charged region tend to drive it back around the cavity, "pumping" the natural resonant frequency.

http://hyperphysics.phy-astr.gsu.edu/hbase/Waves/magnetron.html

Strong oscillation occurs when the electron cyclotron frequency match the LC oscillation frequency

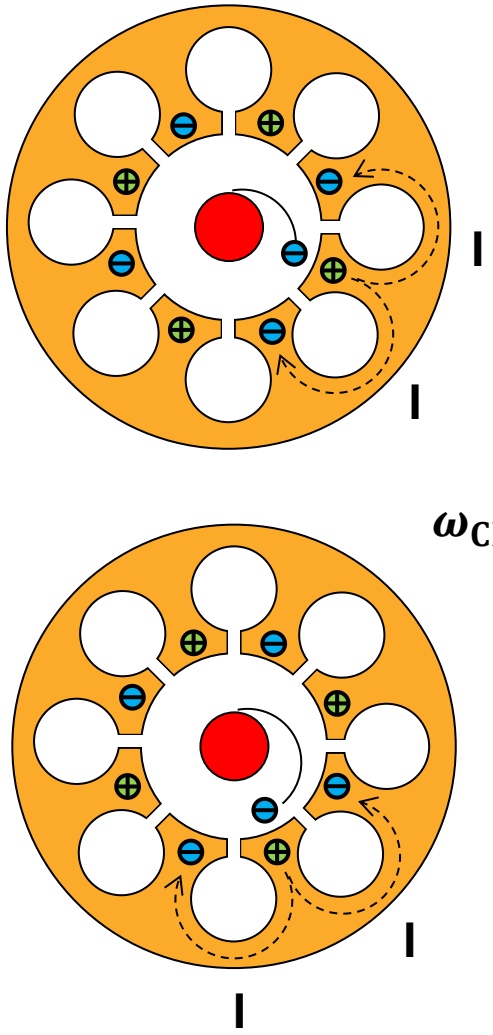

$$\omega_{CE} = \frac{eB}{mc}$$

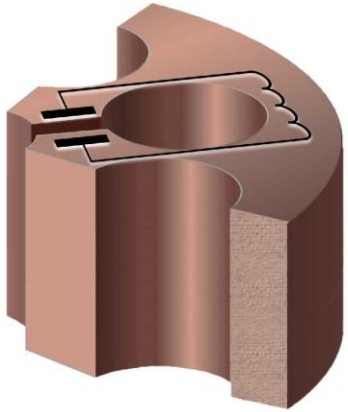

$$\omega = \frac{1}{\sqrt{LC}}$$

Resonance condition: $\omega_{CE} = \omega$

Resonance in a magnetron

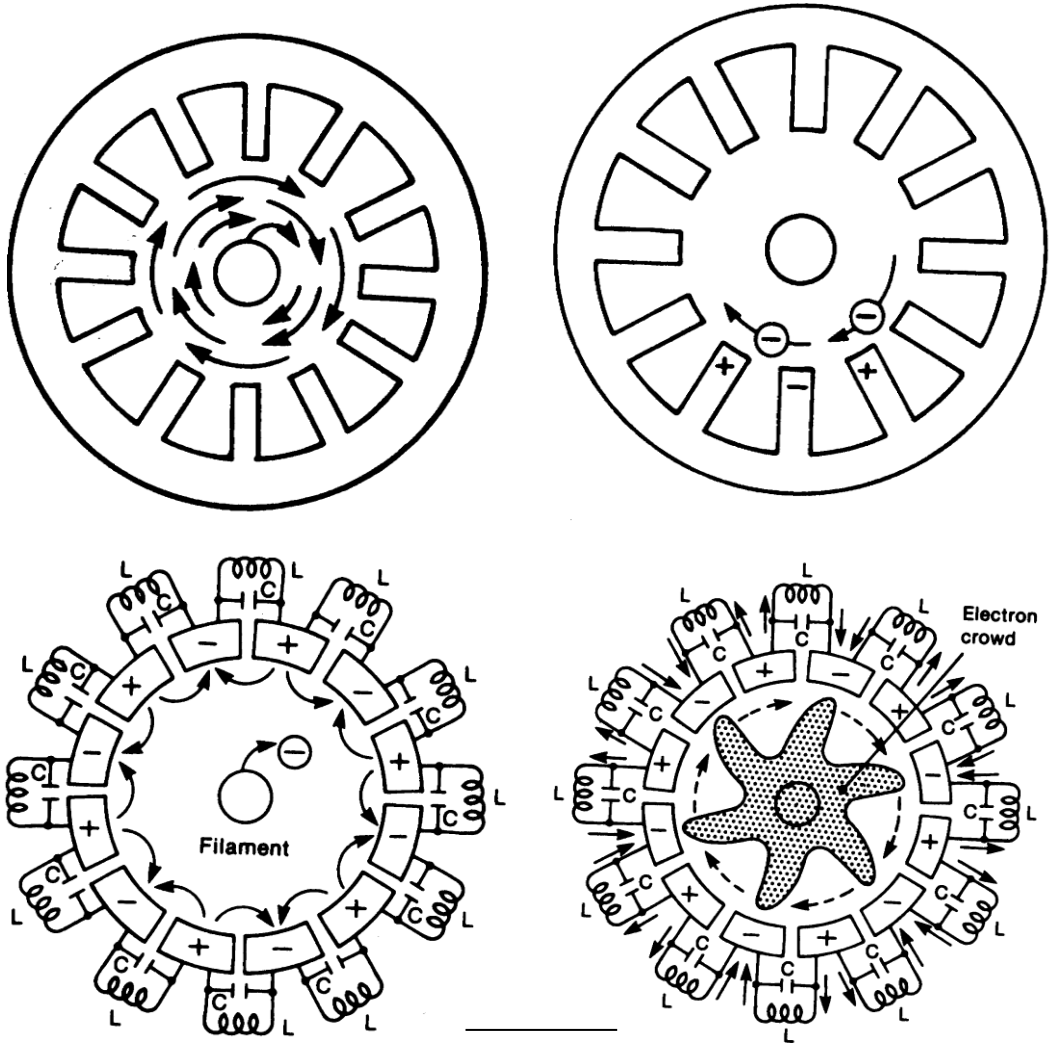

http://cdn.preterhuman.net/texts/government_information/intelligence_and_espionage/homebrew.military.and.espionage.electronics/servv89pn0aj.sn.sourcedns.com/_gbpprorg/mil/herf1/index.html

Magnetron schematic diagram

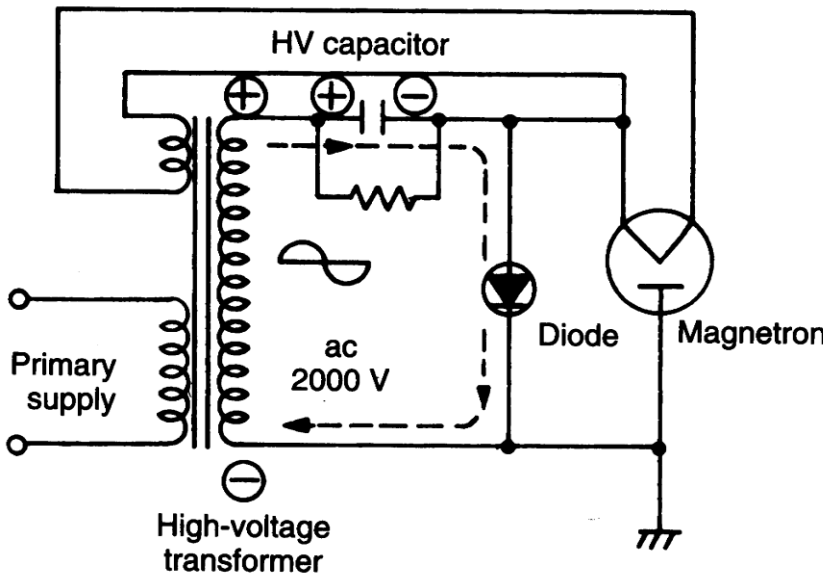

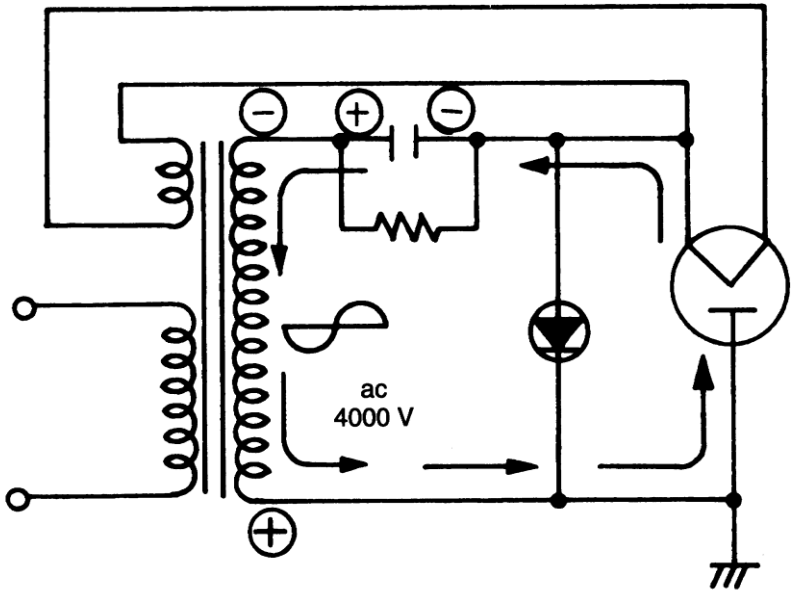

http://cdn.preterhuman.net/texts/government_information/intelligence_and_espionage/homebrew.military.and.espionage.electronics/servv89pn0aj.sn.sourcedns.com/_gbpprorg/mil/herf1/index.html

Magnetron schematic diagram

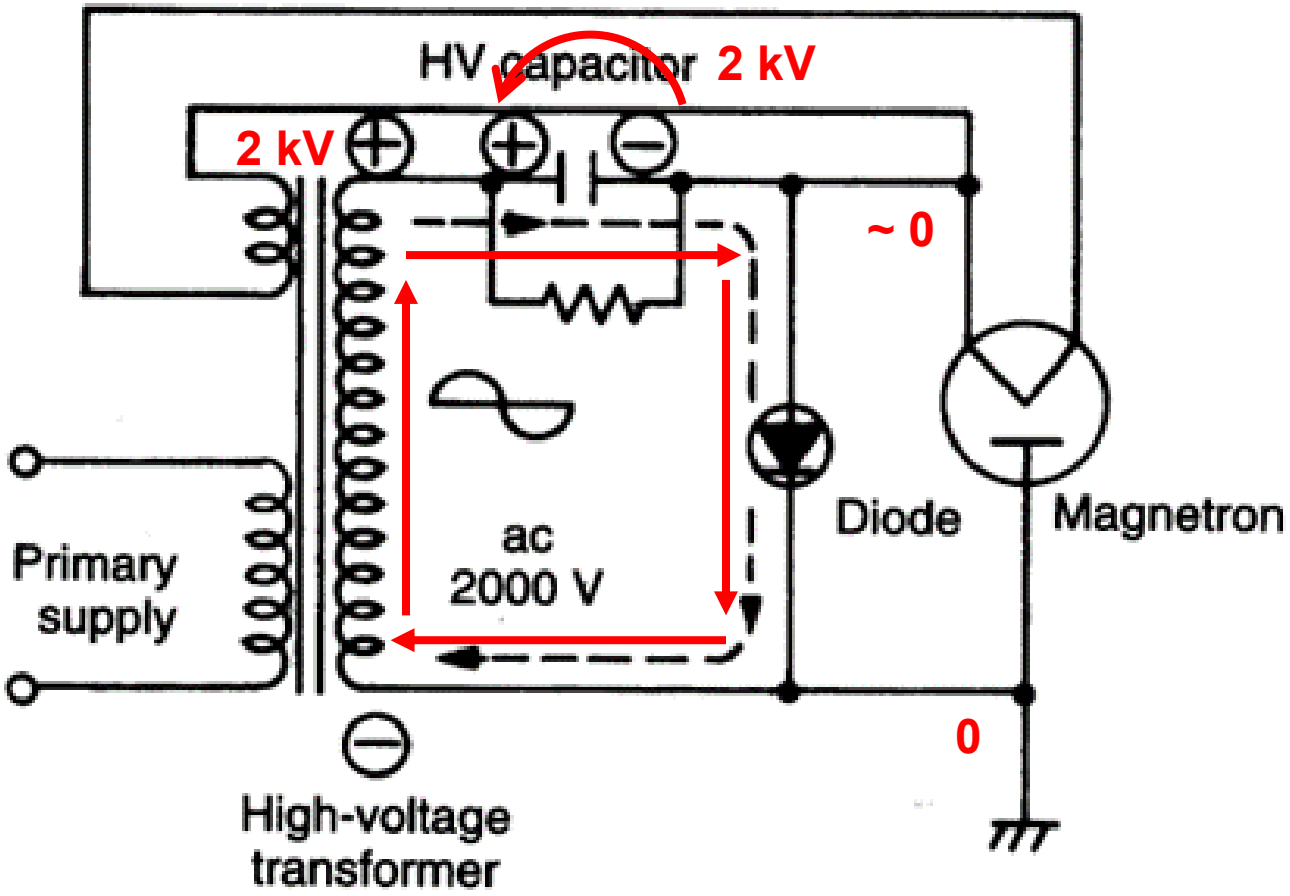

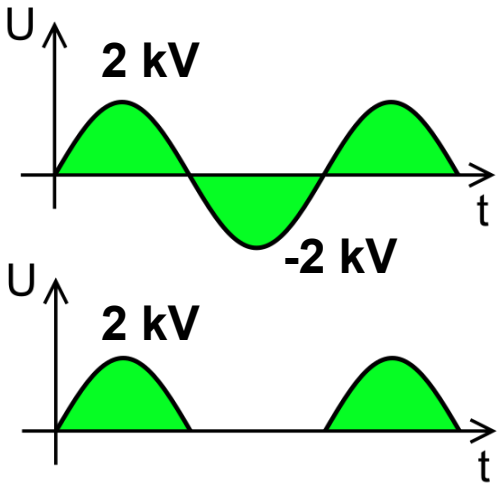

http://cdn.preterhuman.net/texts/government_information/intelligence_and_espionage/homebrew.military.and.espionage.electronics/servv89pn0aj.sn.sourcedns.com/_gbpprorg/mil/herf1/index.html

Magnetron schematic diagram

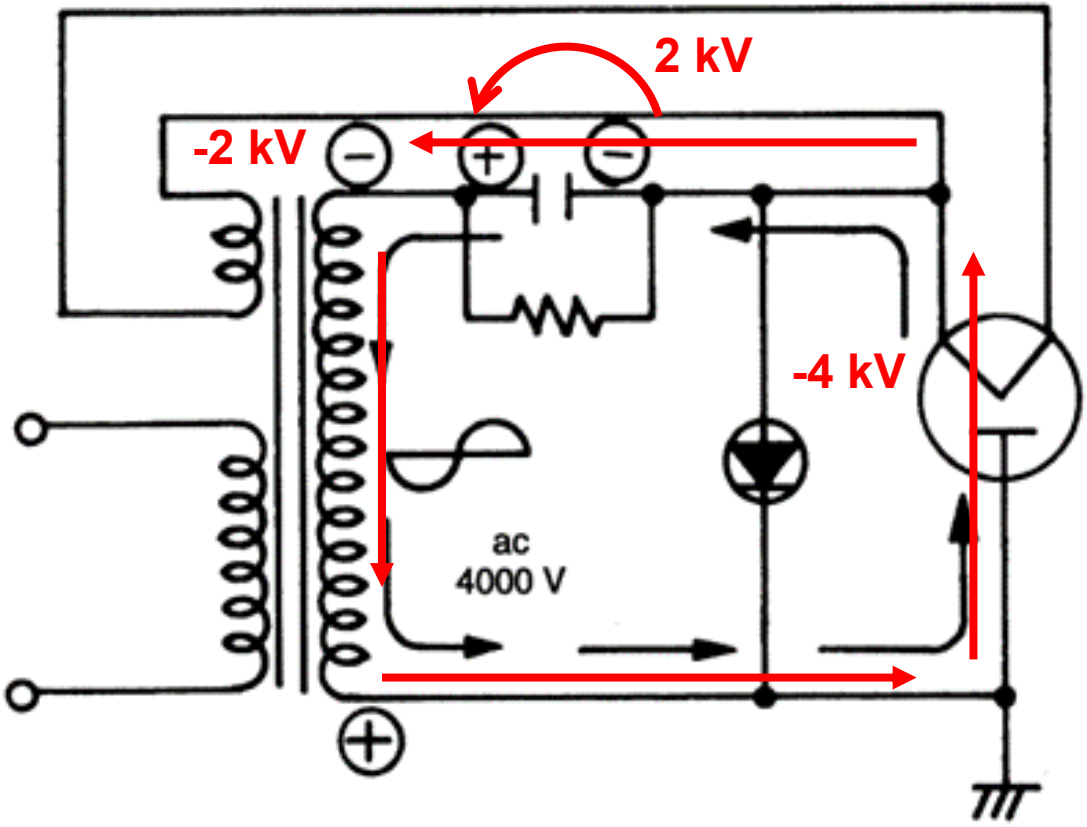

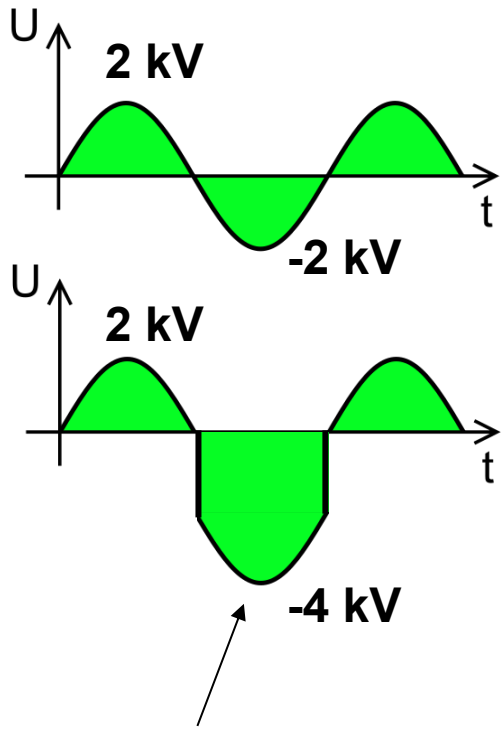

Microwave is generated.

---

http://cdn.preterhuman.net/texts/government_information/intelligence_and_espionage/homebrew.military.and.espionage.electronics/servv89pn0aj.sn.sourcedns.com/_gbpprorg/mil/herf1/index.html

The electrode of the microwave source is located at the location with the highest electric field

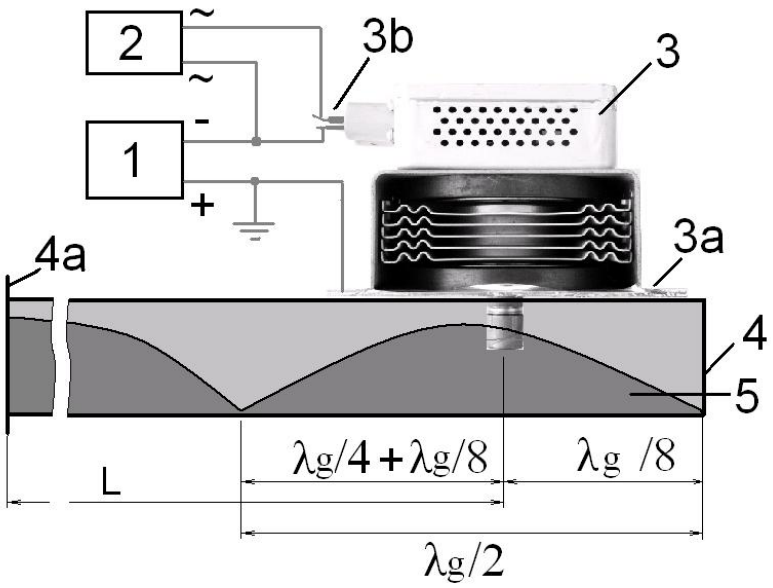

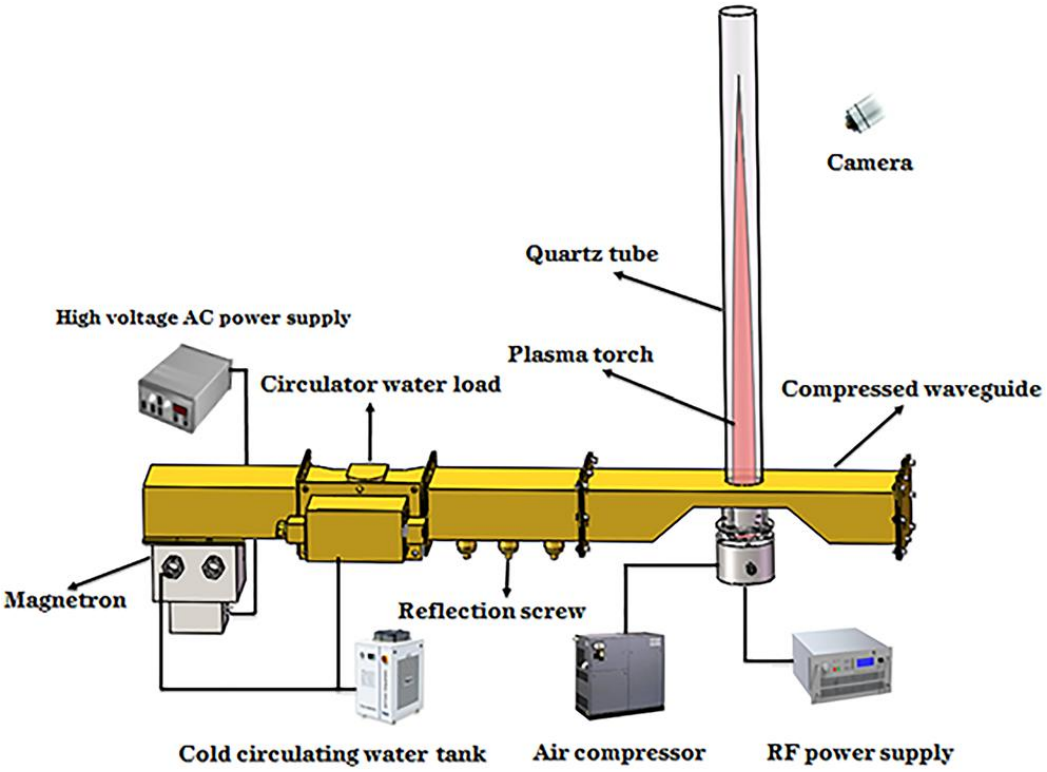

V. Surducan, etc., AIP Conference Proceedings 1425, 89 (2012)
Dan Ye, etc., AIP Advances 10, 055002 (2020

A 3-port circulator combining with a dump can be used as a isolator

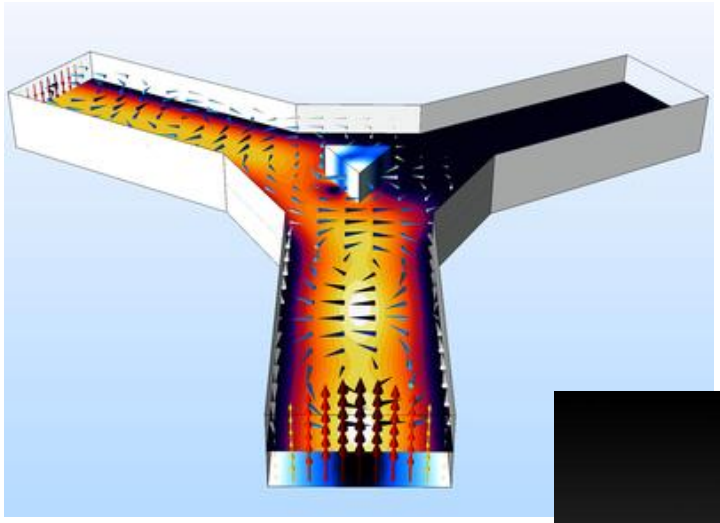

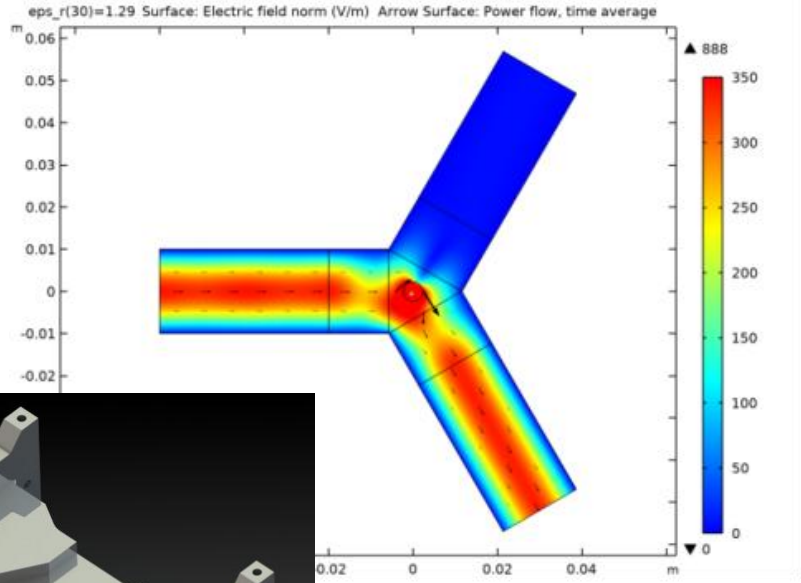

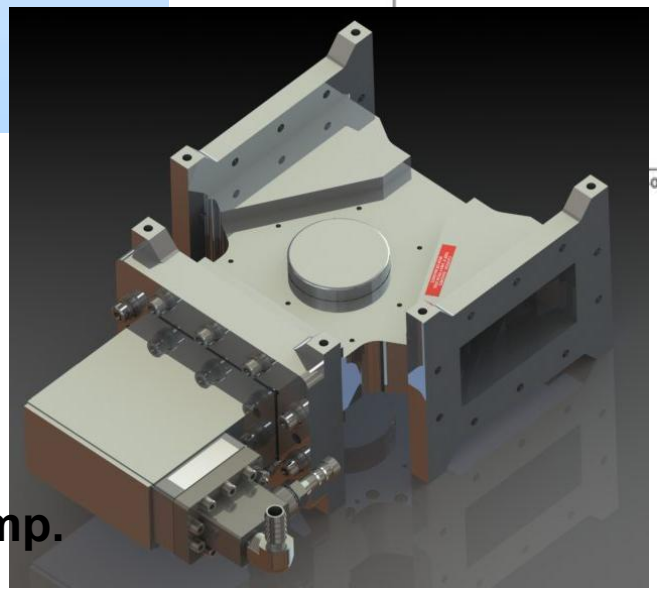

Water load as a dump.

https://cn.comsol.com/model/impedance-matching-of-a-lossy-ferrite-3-port-circulator-10302
https://doc.comsol.com/6.0/doc/com.comsol.help.models.rf.circulator/circulator.html
https://ferriteinc.com/high-power-microwave-circulators-isolators/wr340-waveguide-s-band/

Microwave plasma reactor configurations

- **Waveguide coupled reactor**

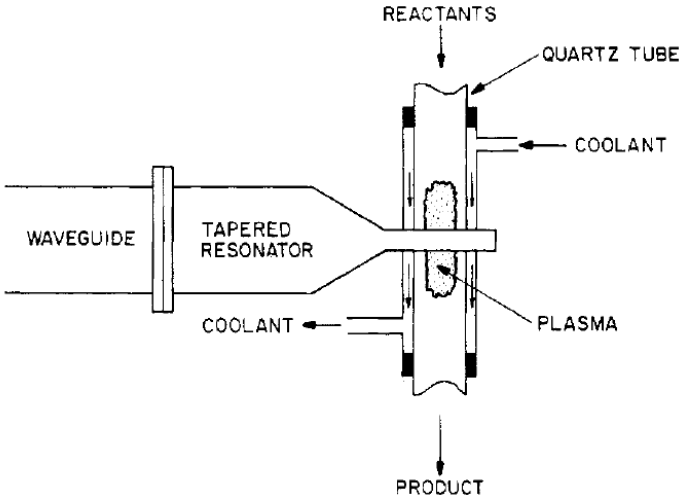

- **Resonant or multimode cavity – if the impedance matching is good, more energy can be fed into the cavity.**

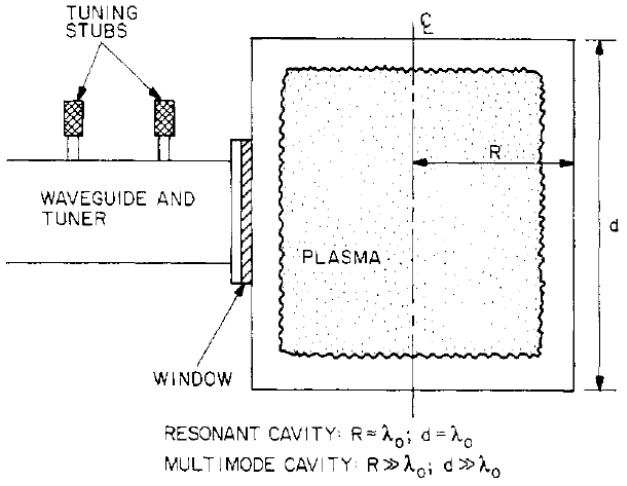

Strong absorption occurs when the frequency matches the electron cyclotron frequency

- **Electron cyclotron resonance (ECR) plasma reactor**

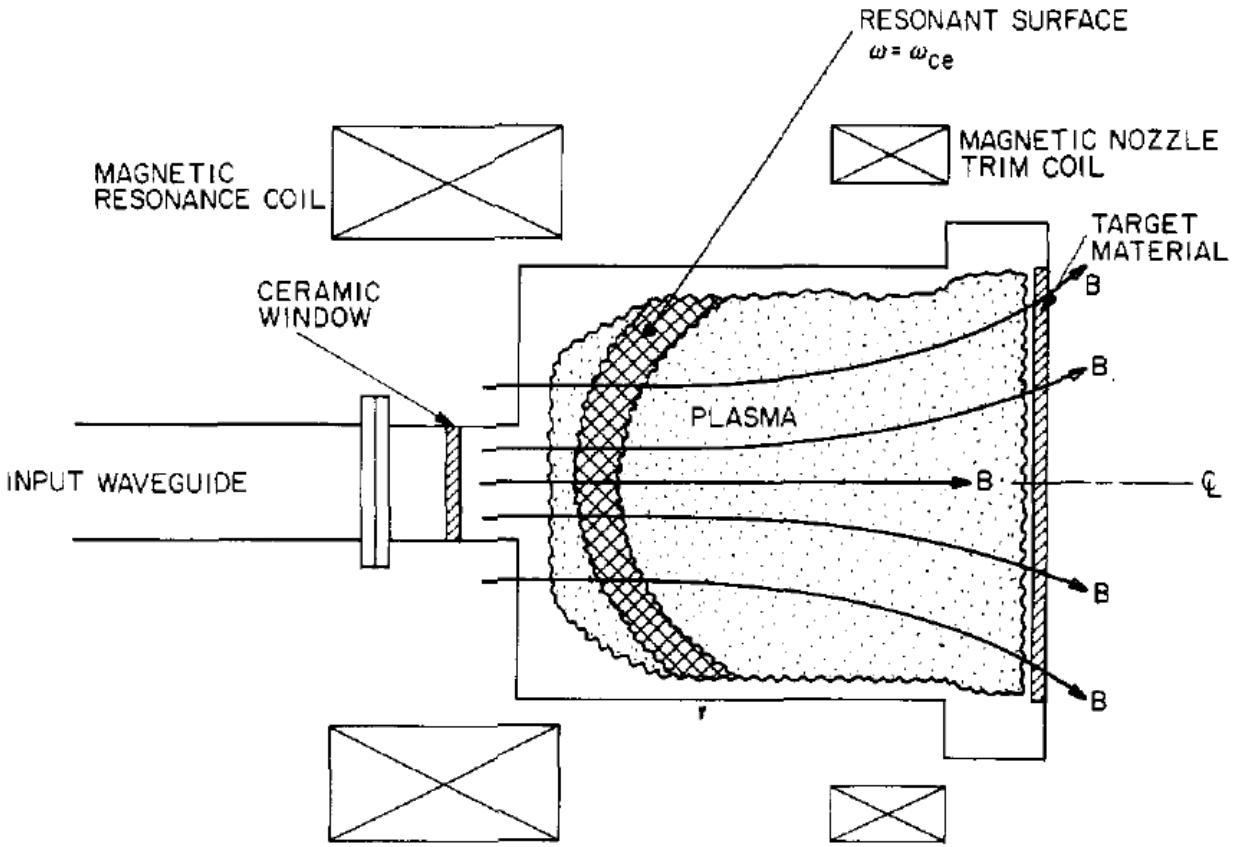

Electron cyclotron frequency depends on magnetic field only

$$m_e \frac{d\vec{v}}{dt} = -\frac{e}{c}\vec{v} \times \vec{B}$$

- Assuming $\vec{B} = B\hat{z}$ and the electron oscillates in x-y plane

$$\dot{m_e v_x} = -\frac{e}{c} B v_y \qquad \dot{m_e v_z} = 0$$

$$\dot{m_e v_y} = \frac{e}{c} B v_x$$

$$\ddot{v}_x = -\frac{eB}{m_e c}\dot{v}_y = -\left(\frac{eB}{m_e c}\right)^2 v_x$$

$$\ddot{v}_y = -\frac{eB}{m_e c}\dot{v}_x = -\left(\frac{eB}{m_e c}\right)^2 v_y$$

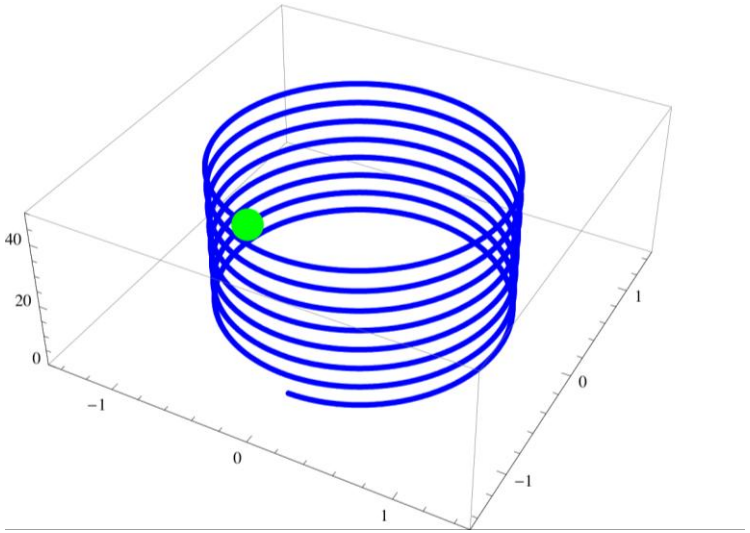

- Therefore

$$\omega_{ce} = \frac{eB}{m_e c}$$

Electrons keep getting accelerated when a electric field rotates in electron's gyrofrequency

$$m_e \frac{d\vec{v}}{dt} = -\frac{e}{c}\vec{v} \times \vec{B} - e\vec{E} \qquad \vec{B} = B_0\hat{z} \qquad \vec{E} = E_0[\hat{x}\cos(\omega t) + \hat{y}\sin(\omega t)]$$

$$m_e\dot{v}_x = -\frac{e}{c}Bv_y + E_0\cos(\omega t) \qquad m_e\dot{v}_y = \frac{e}{c}Bv_x + E_0\sin(\omega t) \qquad m_e\dot{v}_z = 0$$

$$\ddot{v}_x = -\frac{eB}{m_e c}\dot{v}_y - \frac{E_0}{m_e}\omega\sin(\omega t) = -\omega_{ce}{}^2 v_x - \frac{E_0}{m_e}(\omega_{ce} + \omega)\sin(\omega t)$$

$$\ddot{v}_y = -\frac{eB}{m_e c}\dot{v}_x + \frac{E_0}{m_e}\omega\cos(\omega t) = -\omega_{ce}{}^2 v_y + \frac{E_0}{m_e}(\omega_{ce} + \omega)\cos(\omega t)$$

$$\omega_{ce} = \frac{eB}{m_e c}$$

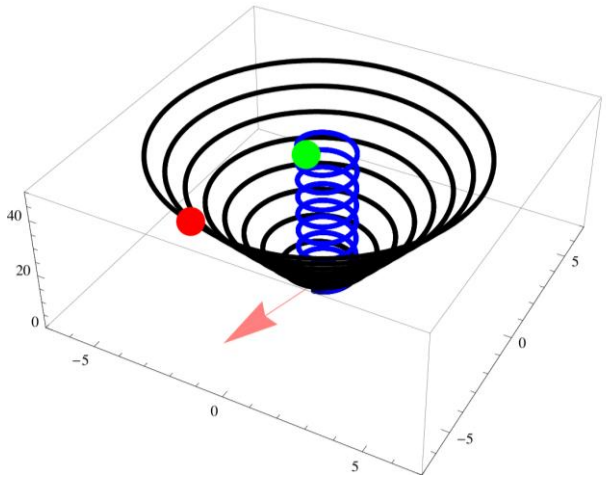

Electric field in a circular polarized electromagnetic wave keeps rotating as the wave propagates

- Right-handed polarization

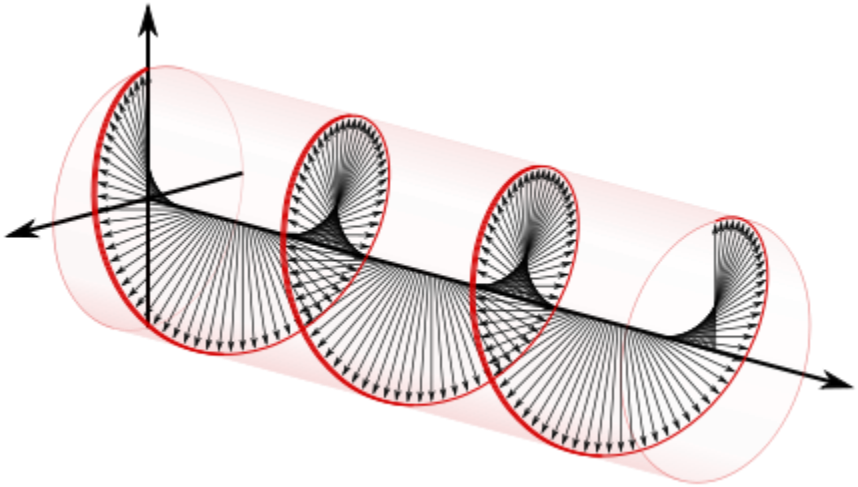

- Left-handed polarization

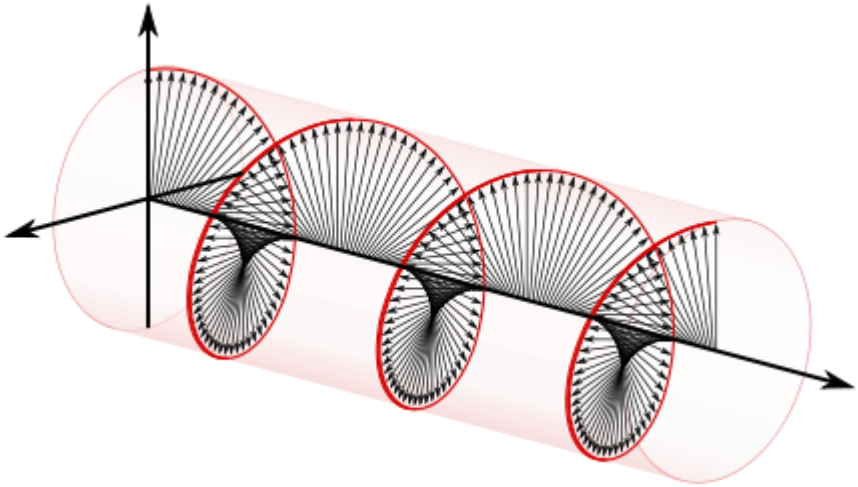

https://en.wikipedia.org/wiki/Circular_polarization

Electric field rotates in a circular polarization

$$E_x = E_o \exp(-i\omega t)$$

$$E_y = \pm iE_x = iE_o \exp(-i\omega t) = E_o \exp\left(\pm i\frac{\pi}{2}\right)\exp(-i\omega t) = E_o \exp\left[-i\left(\omega t \pm \frac{\pi}{2}\right)\right]$$

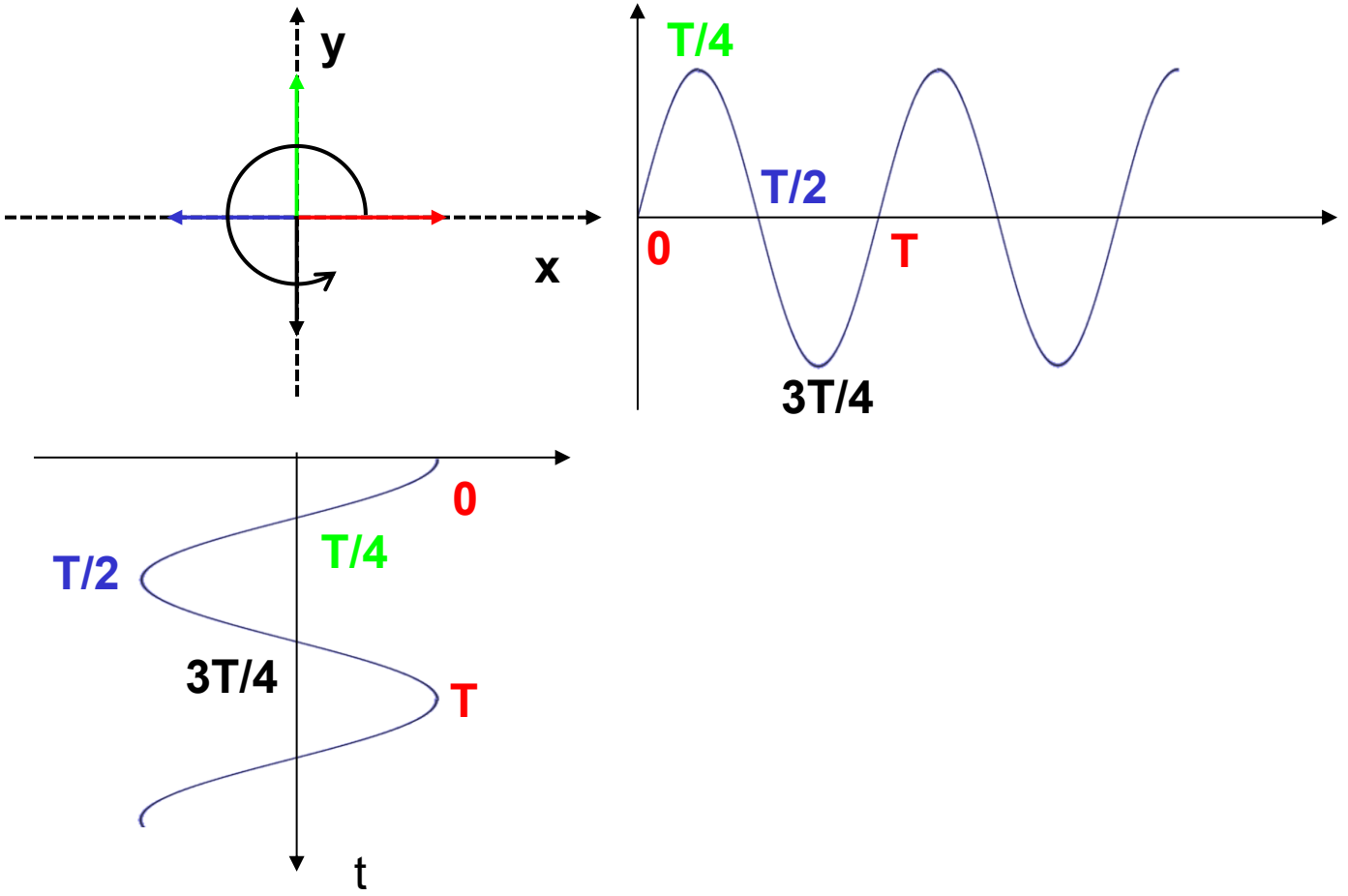

A linear polarized wave can be decomposed by a left-handed and a right-handed polarized wave

- Right-handed polarization

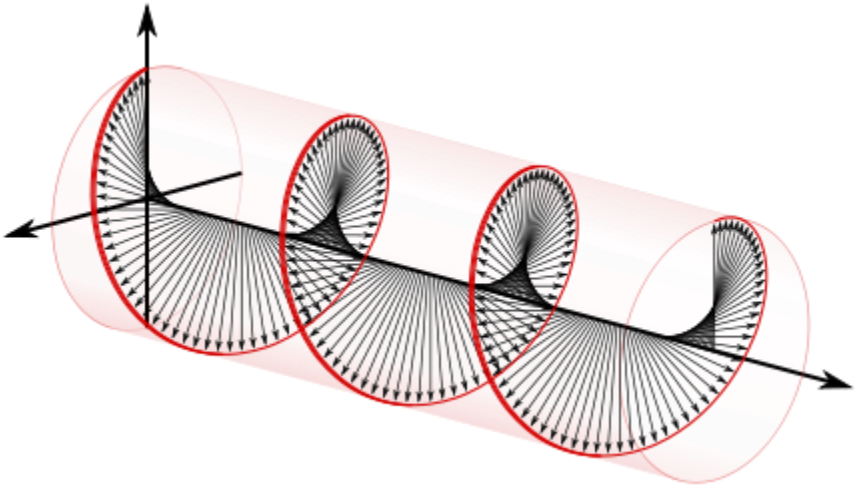

- Left-handed polarization

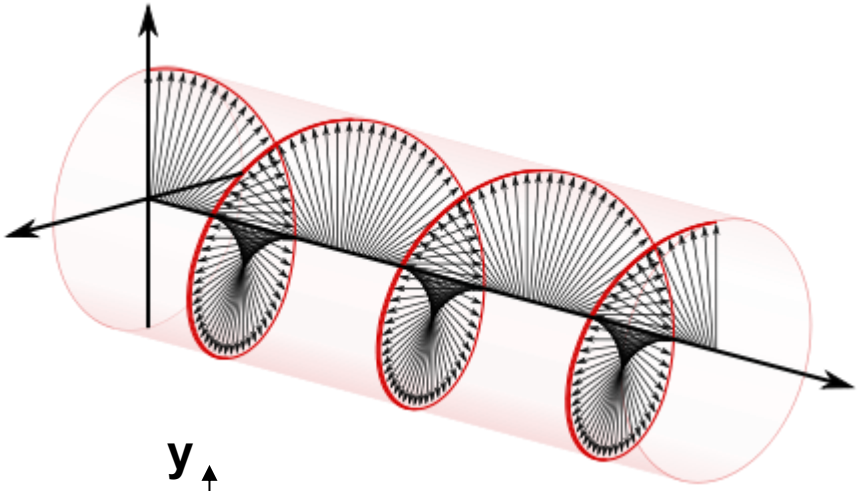

$$\vec{E} = E_0\hat{x} = \frac{E_0}{2}[(\hat{x} + i\hat{y}) + (\hat{x} - i\hat{y})]$$

RHC LHC

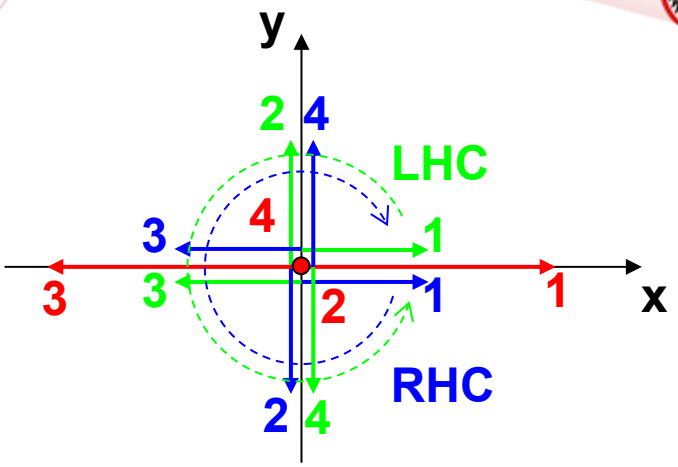

https://en.wikipedia.org/wiki/Circular_polarization

Only right-handed polarization can resonance with electron's gyromotion

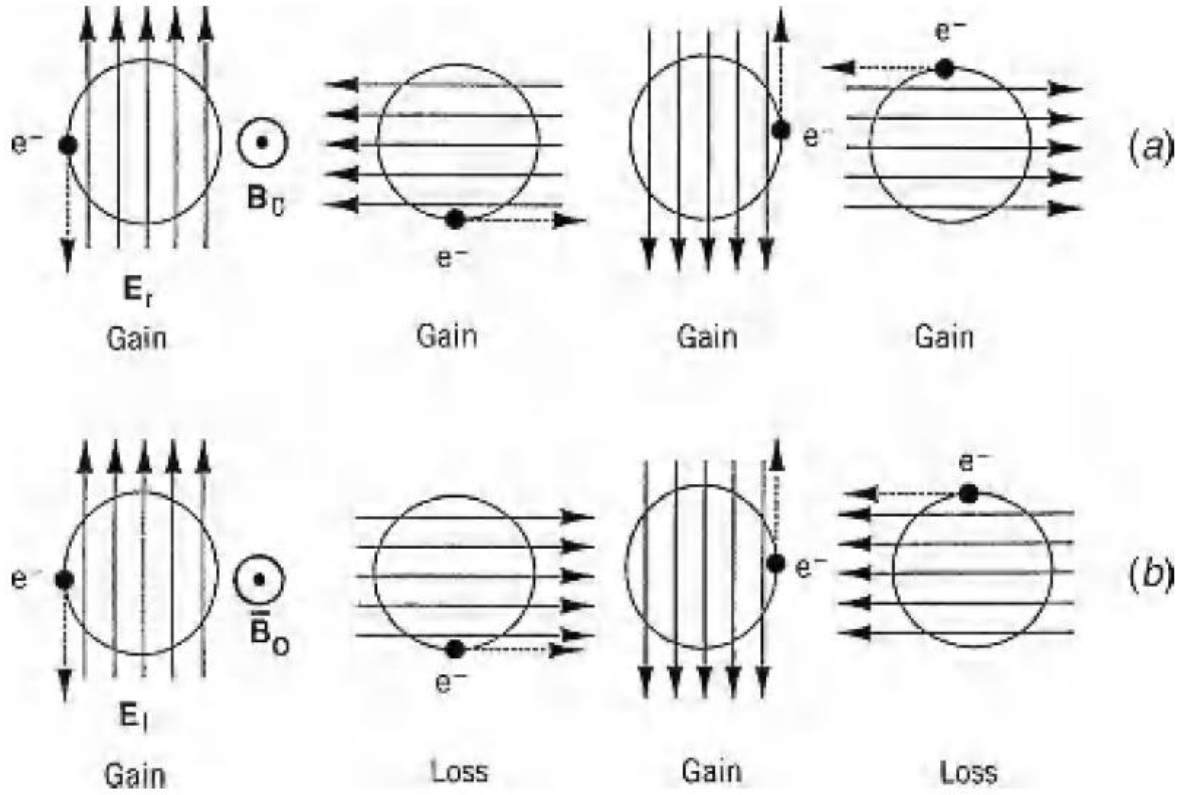

FIGURE 13.5. Basic principle of ECR heating: (*a*) continuous energy gain for right-hand polarization; (*b*) oscillating energy for left-hand polarization (after Lieberman and Gottscho, 1994).

Strong absorption occurs when the frequency matches the electron cyclotron frequency

- **Electron cyclotron resonance (ECR) plasma reactor**

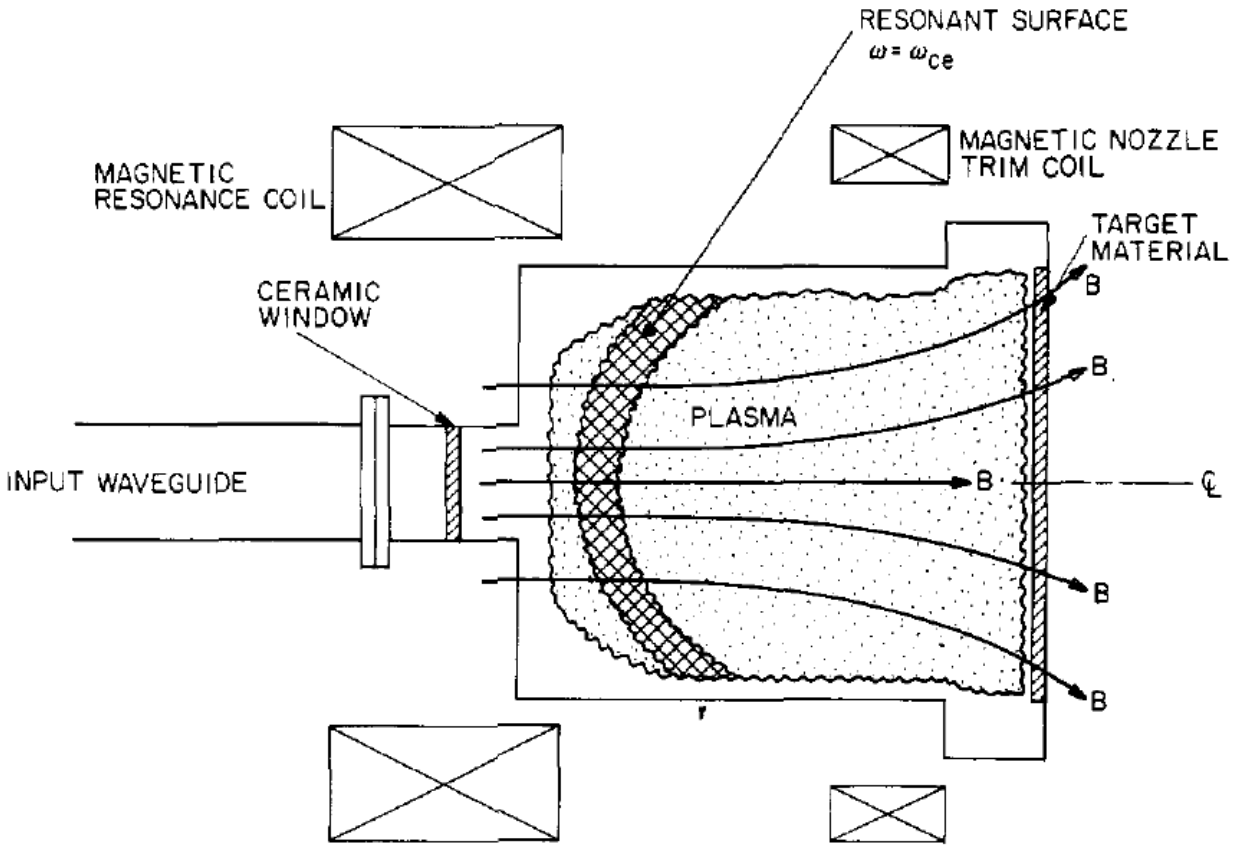

Electron cyclotron resonance (ECR) microwave systems

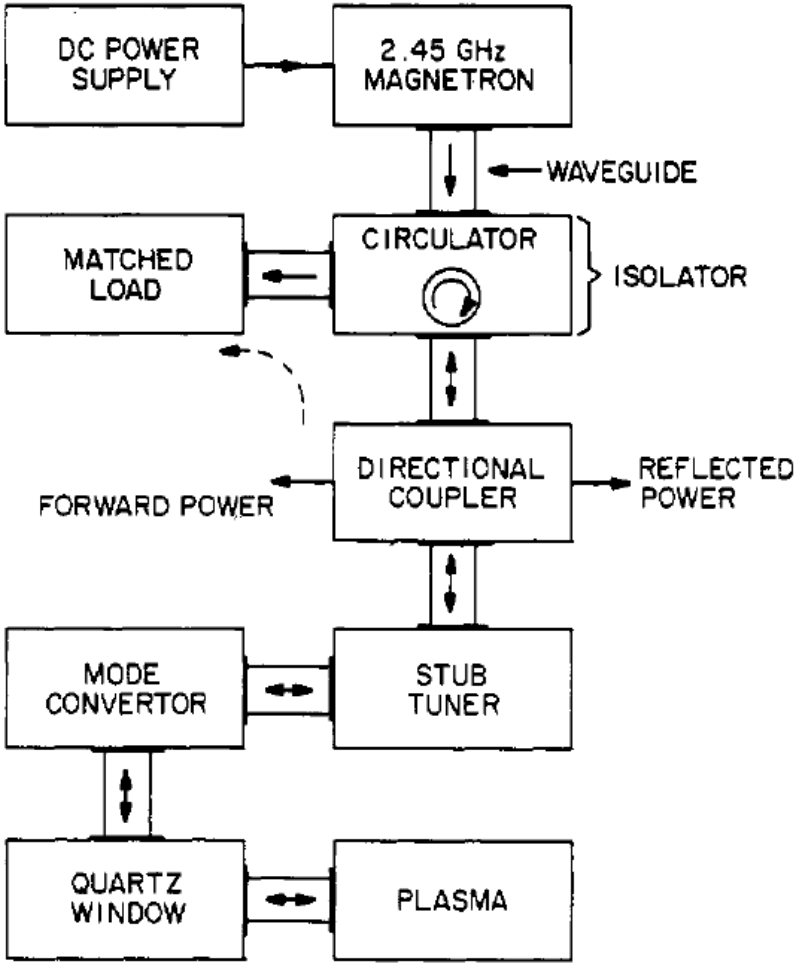

microwave systems

Immersed ECR plasma source

- **High particle fluxes on targets for diamond or other thin film deposition**
- **The ions in the plasma flux can be used for etching.**

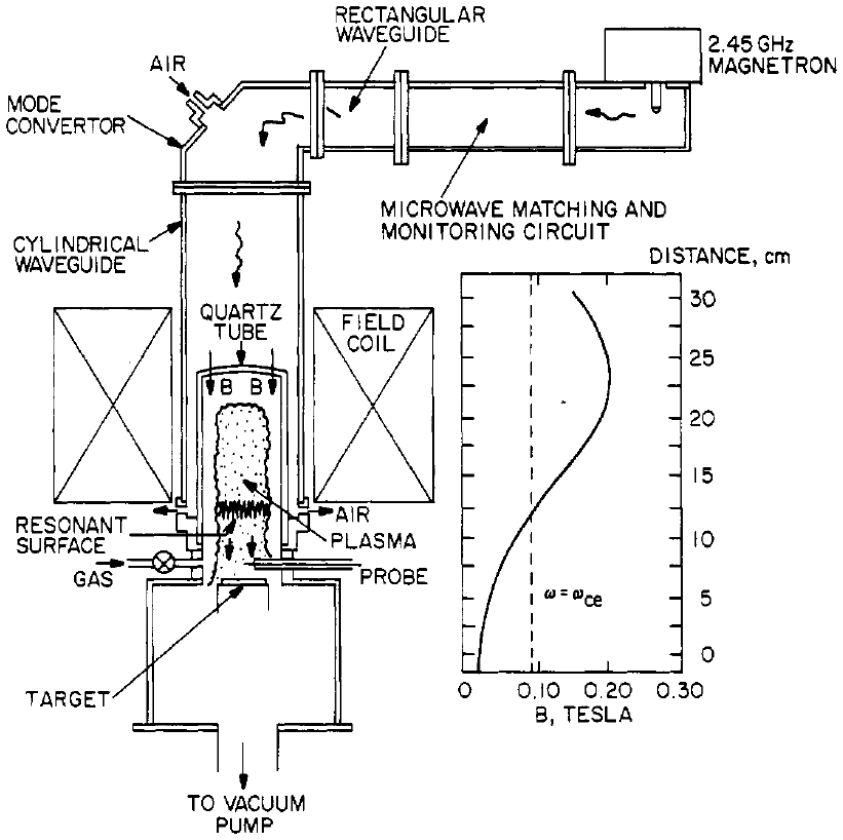

Distributed ECR system

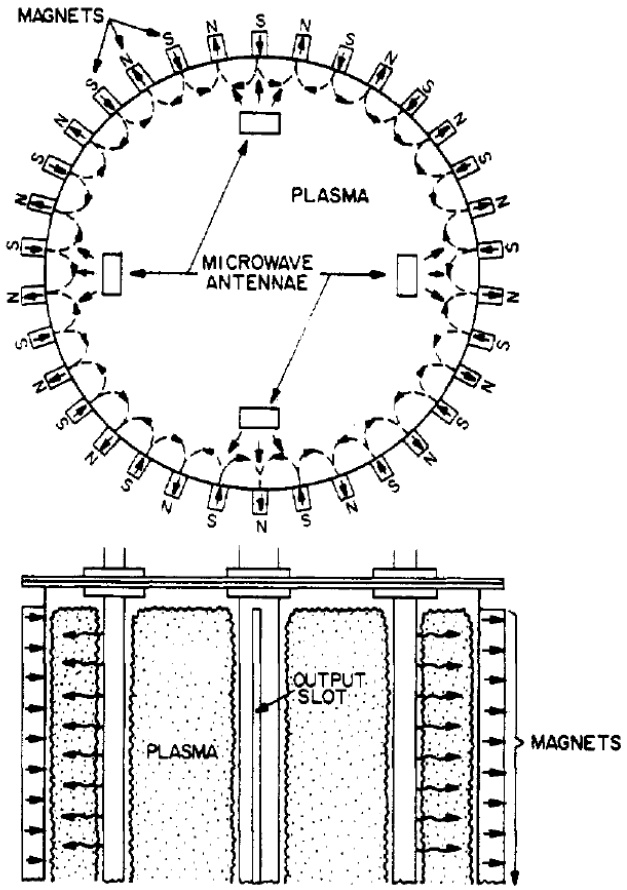

- **Function of the multipolar magnetic field at the tank boundary:**
  - **Provide a resonant surface for ECR absorption**
  - **Improve the confinement of the plasma**

Microwave plasma torch deposit a much faster rate than other types of plasma source for diamond film deposition

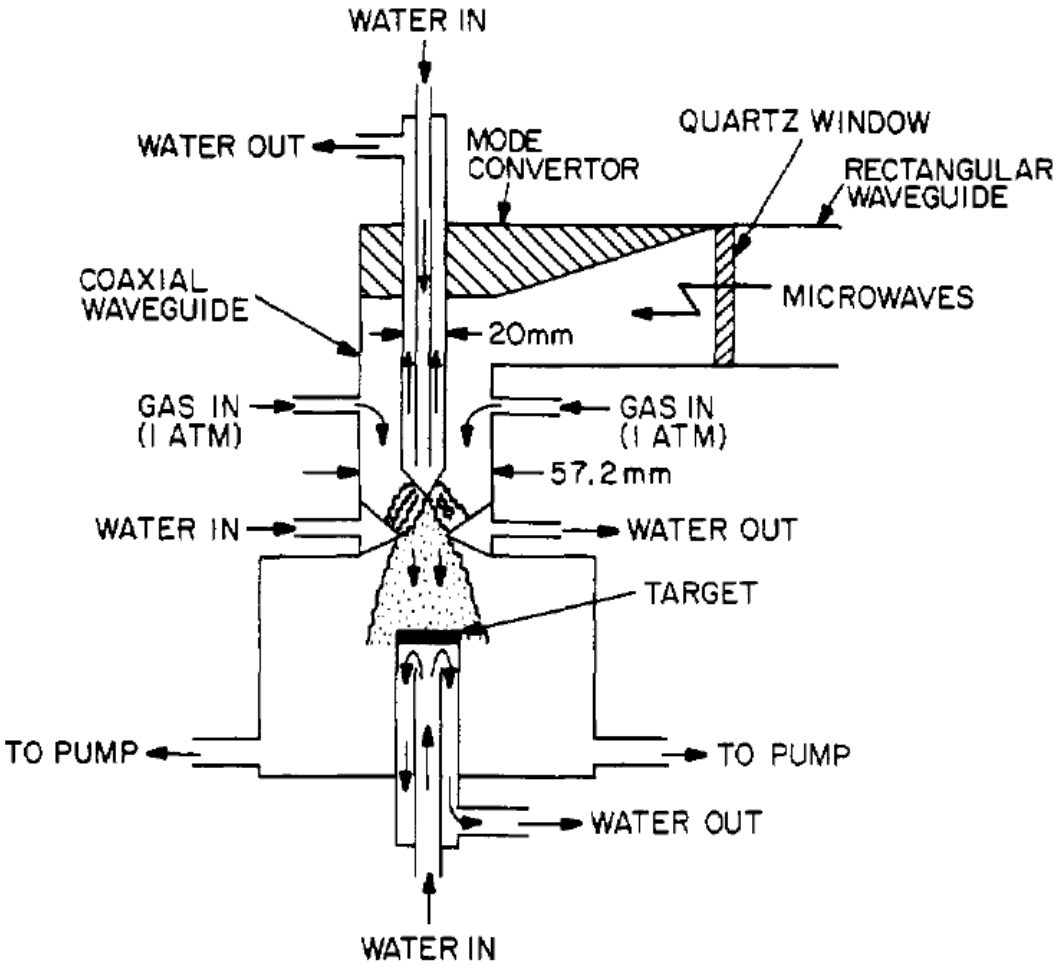

Microwave-generated plasmas have the capability of filling very large volumes with moderately high density

- Advantages
  - Lower neutral gas pressure, i.e., longer ion and neutral mean free paths.
  - Higher fraction ionize.
  - Higher electron density.
- Disadvantages
  - Lower ion bombardment energies.
  - Less control of the bombarding ion energy.
  - Difficult in tuning up and achieving efficient coupling.
  - Much more difficult and expensive to make uniform over a large area.
  - More expensive.

AC electrical discharges deliver energy to the plasma without contact between electrodes and the plasma

- DC electrical discharge – a true current in the form of a flow of ions or electrons to the electrodes.
- AC electrical discharge – the power supply interacts with the plasma by displacement current.
  - Inductive radio frequency (RF) electrical discharges
  - Capacitive RF electrical discharges
  - Microwave electrical discharges
  - **Dielectric-barrier discharges (DBDs)**
- Other mechanism
  - Laser produced plasma
  - Pulsed-power generated plasma

Dielectric-barrier discharges (DBDs)

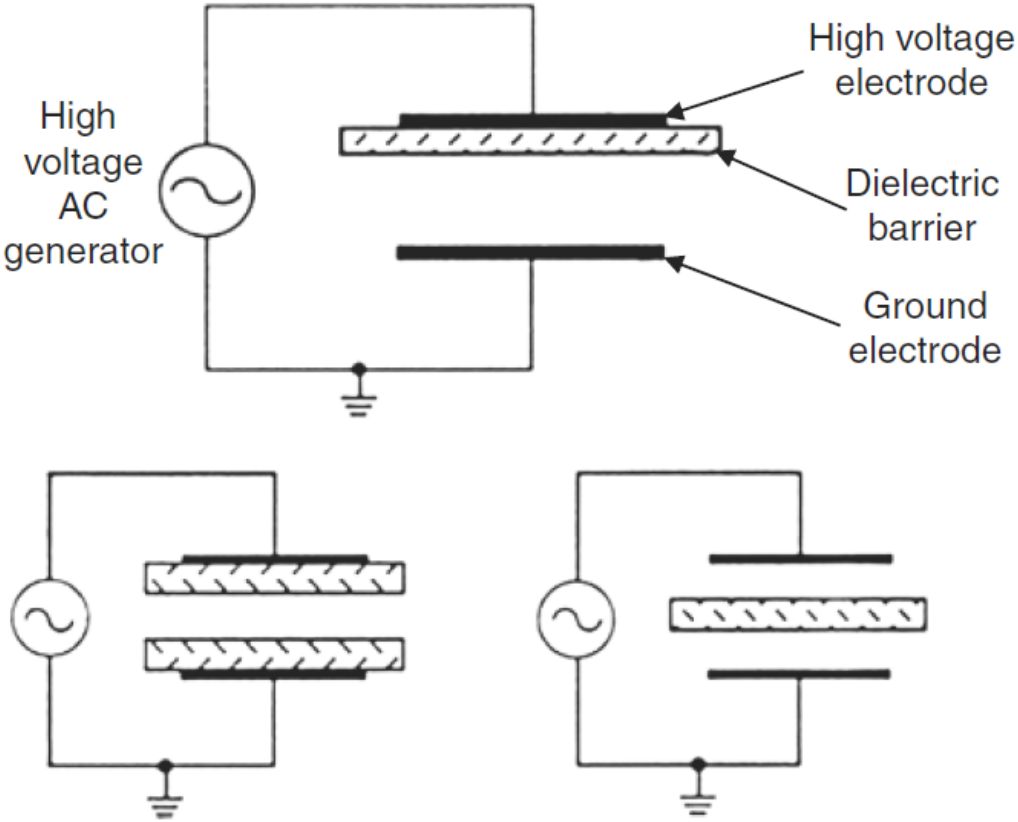

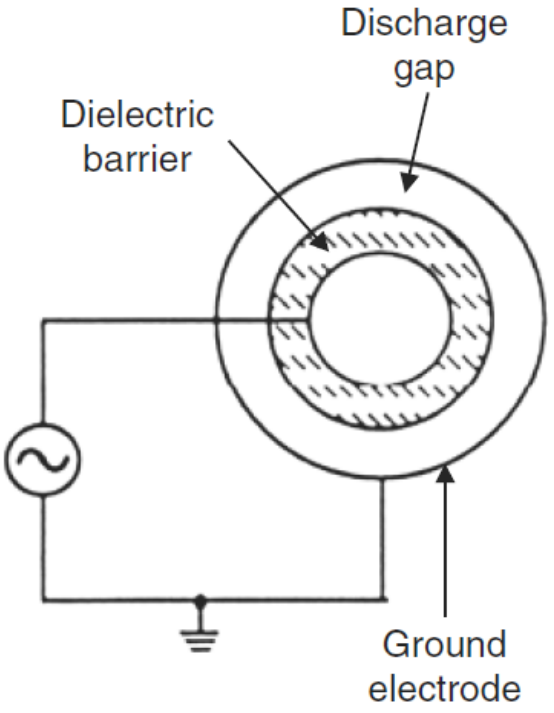

Space charge effect enhance the electric field

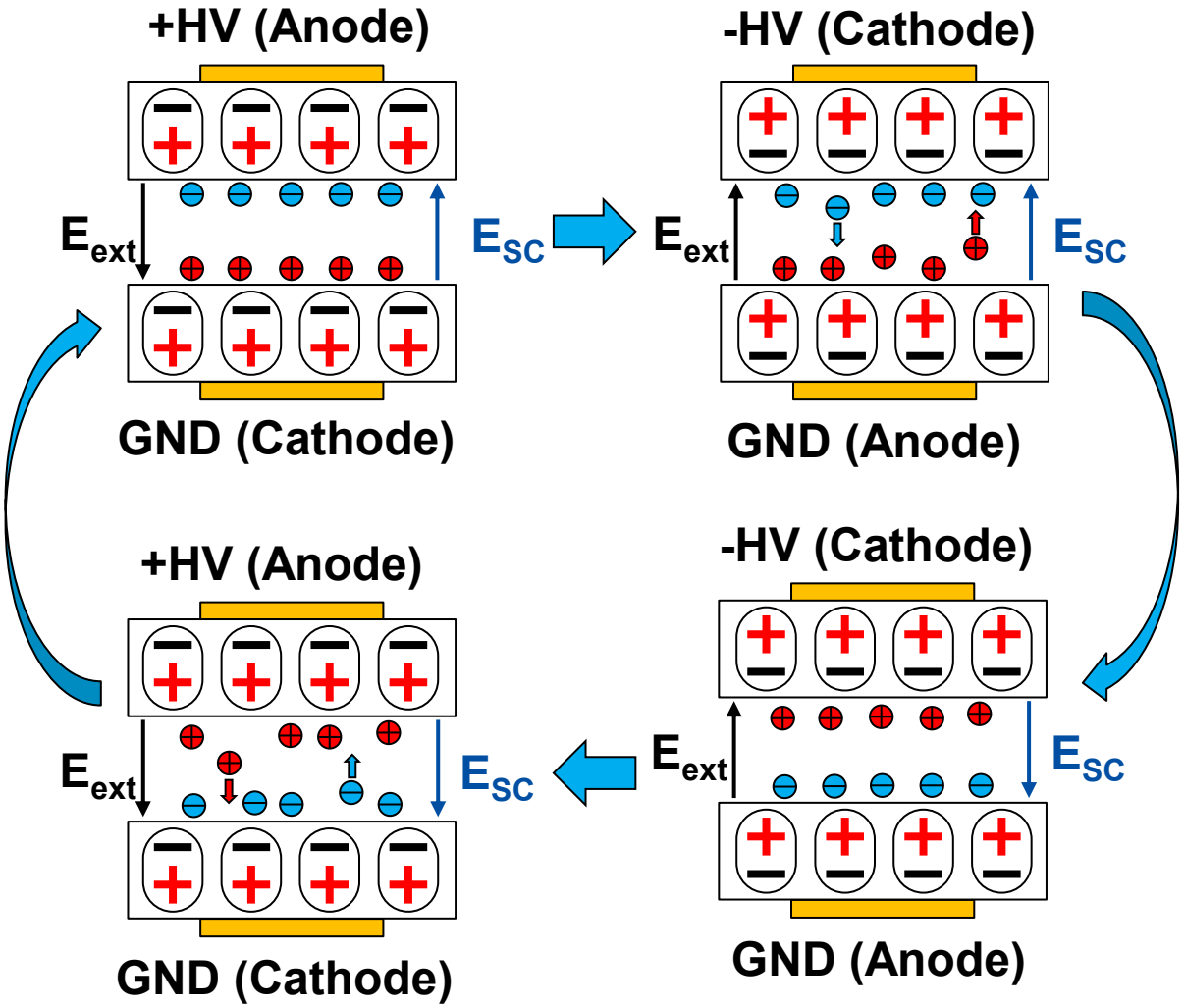

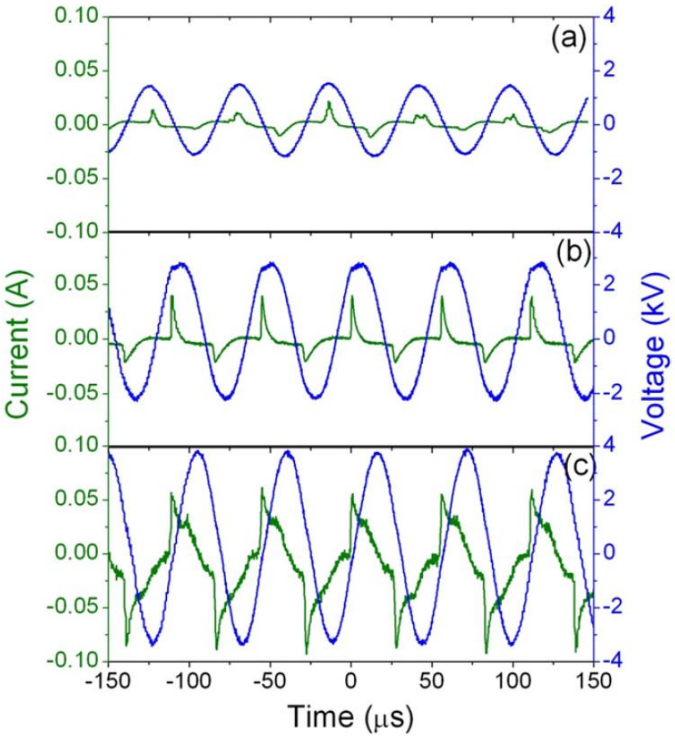

J. L. Walsh, *et al.*, J. Phys. D: Appl. Phys., **43**, 075201 (2010)

The foundation of AC discharge in plasma display panel

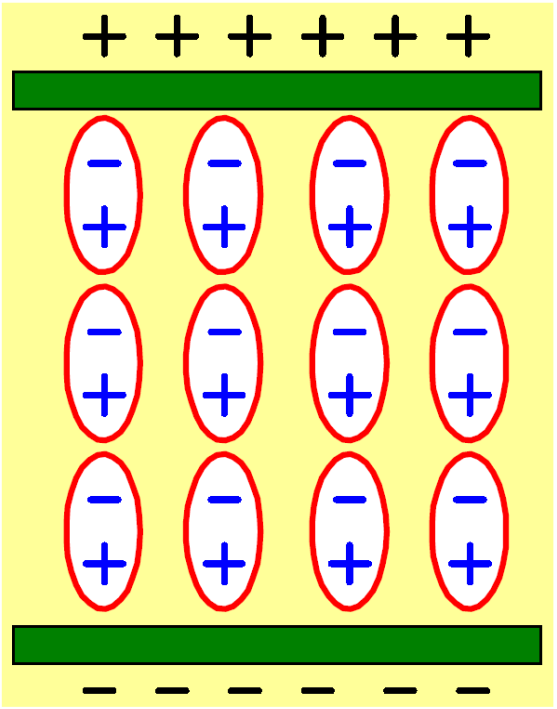

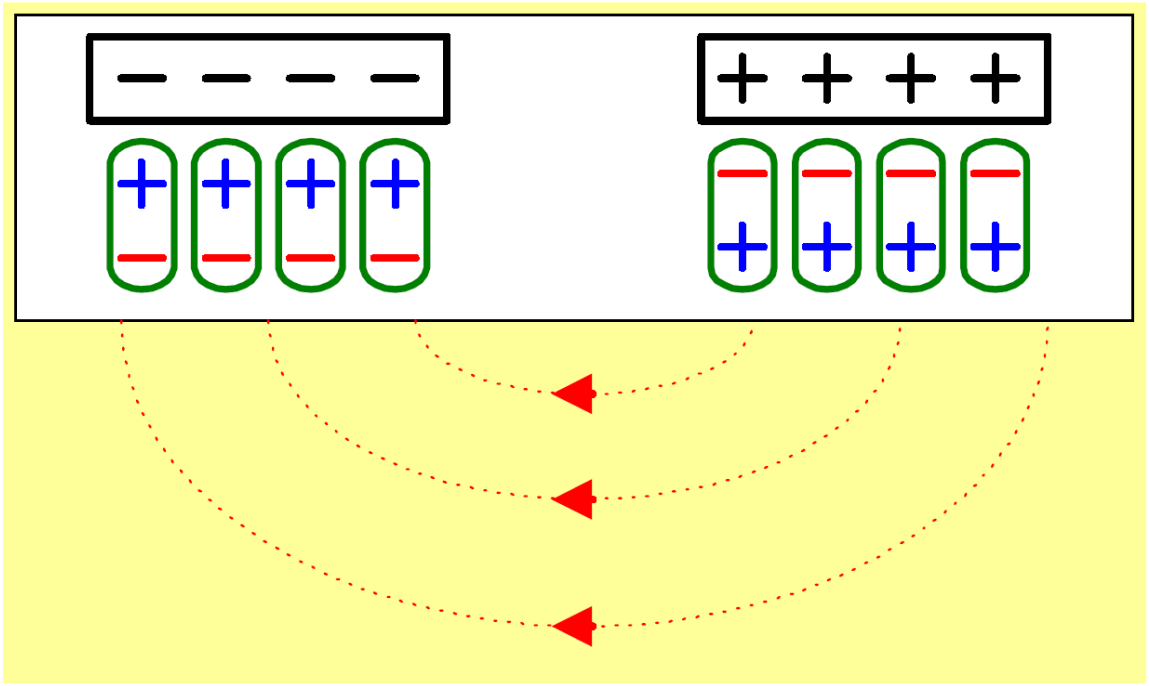

The plasma can be sustained using ac discharged in plasma display panel

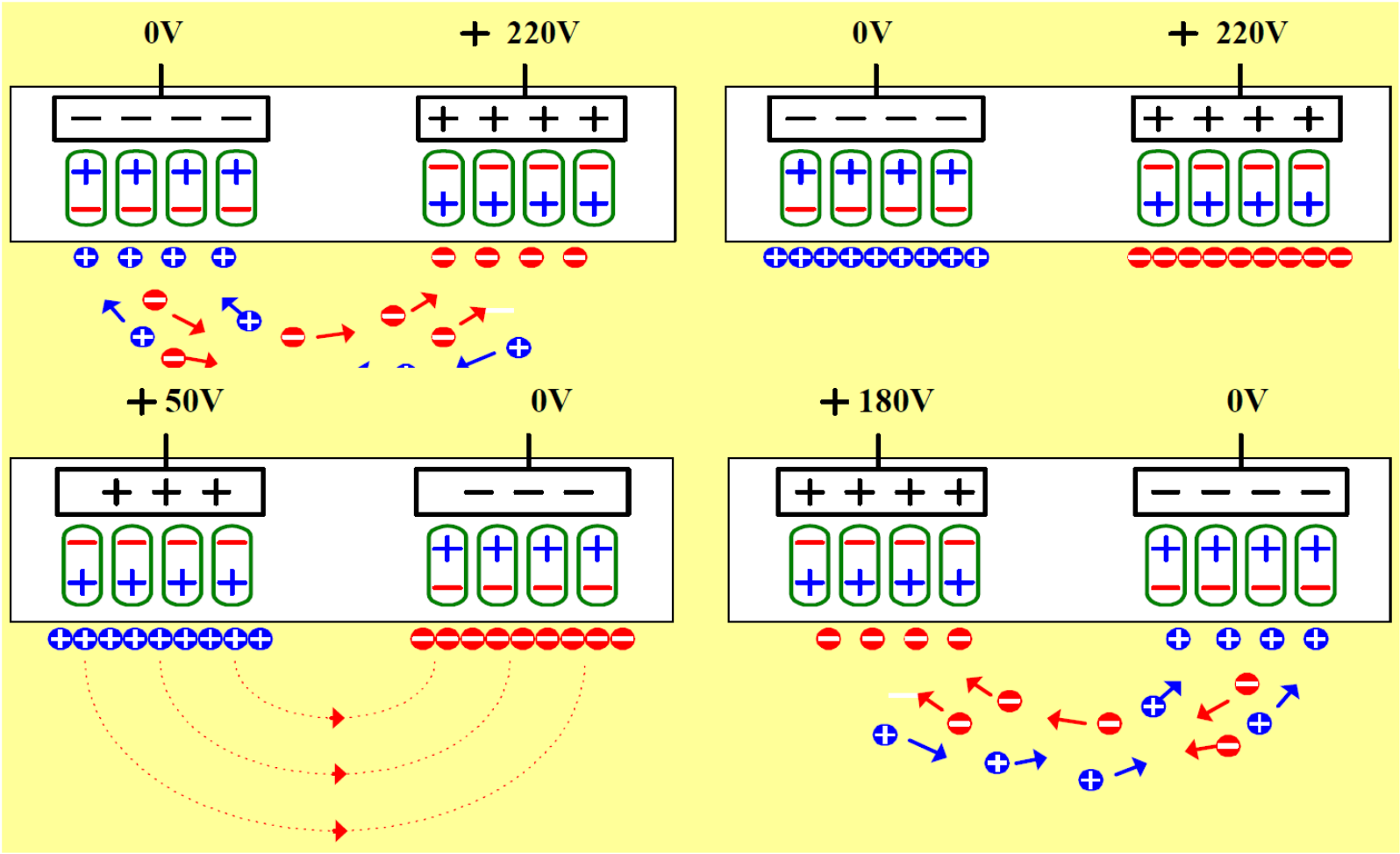

- **Wall discharge reduced the required discharge volta**

Plasma-needle discharge

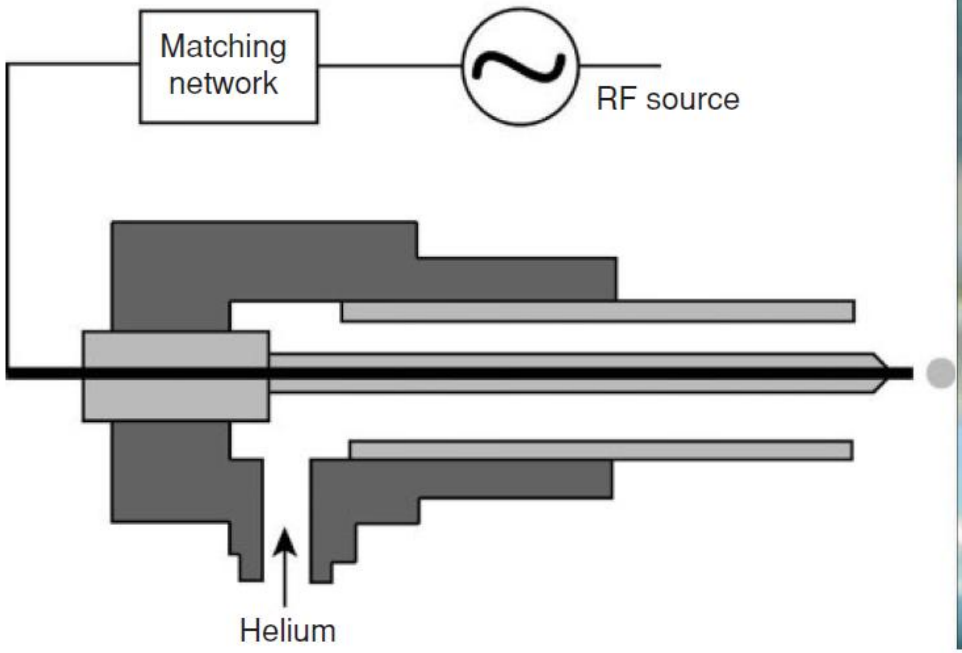

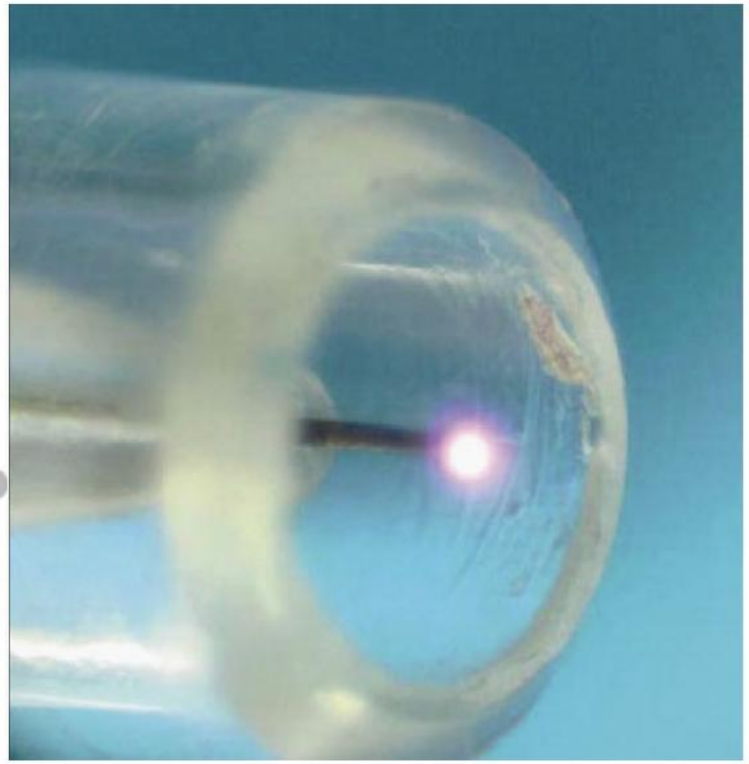

Atmospheric-pressure cold helium microplasma jets

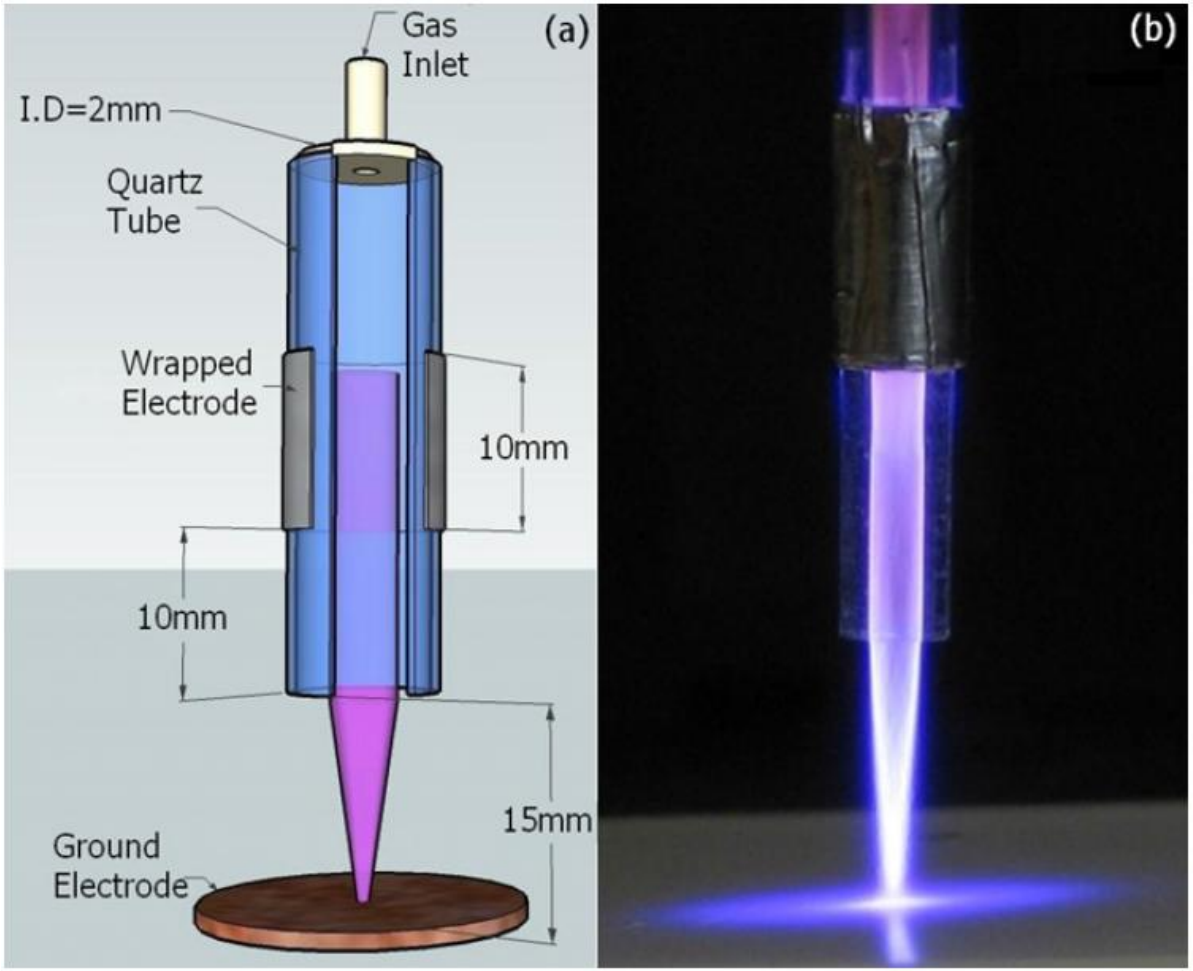

J. L. Walsh, *et al.*, J. Phys. D: Appl. Phys., **43**, 075201 (2010)

There are three different modes: chaotic, bullet, and continuous mode

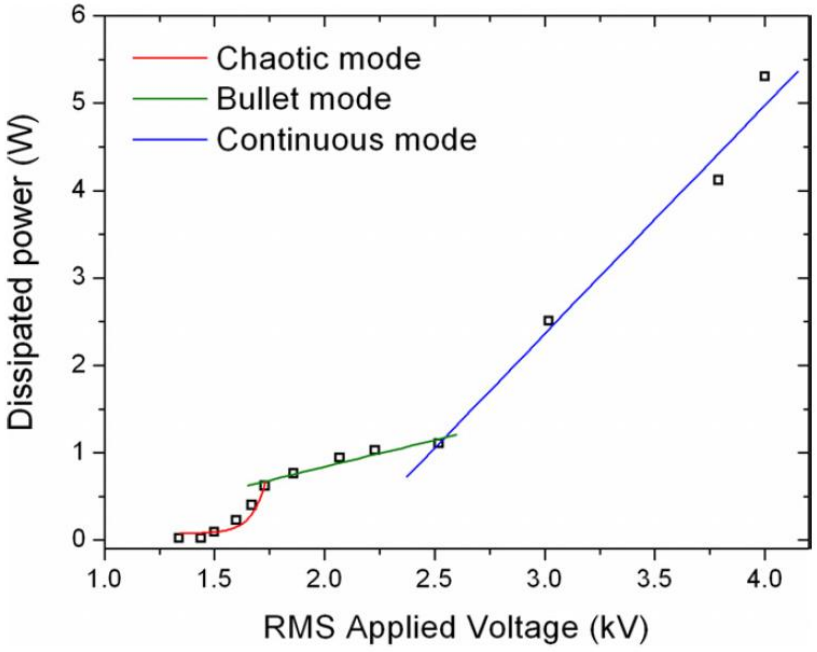

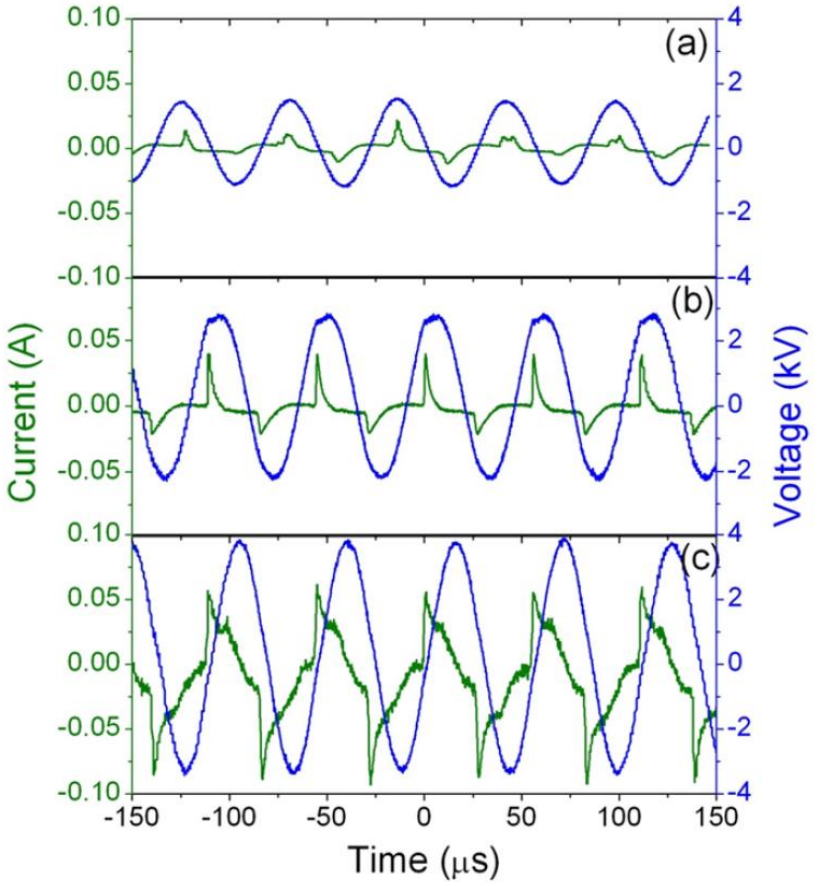

J. L. Walsh, *et al.*, J. Phys. D: Appl. Phys., **43**, 075201 (2010)

In bullet mode, the plasma jet comes out as a pulse

- **wavelength-integrated optical emission signal (350–800 nm)**

Bullet mode

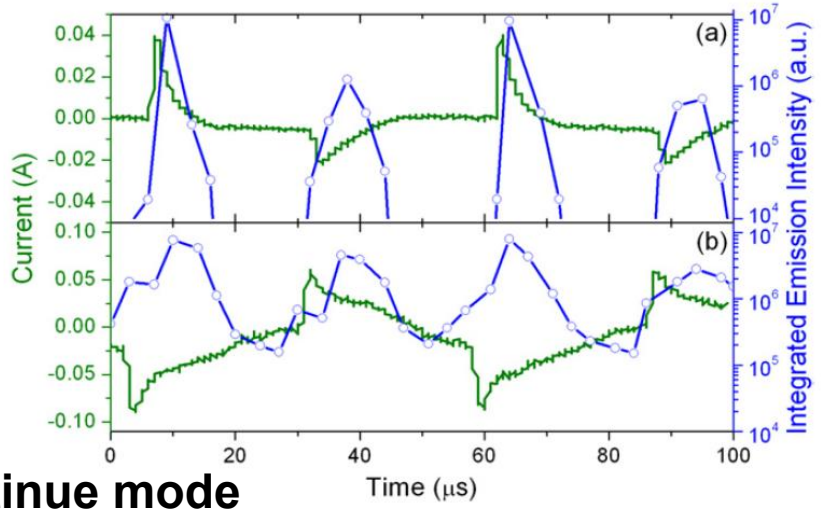

Continue mode

- **Images of bullet mode**

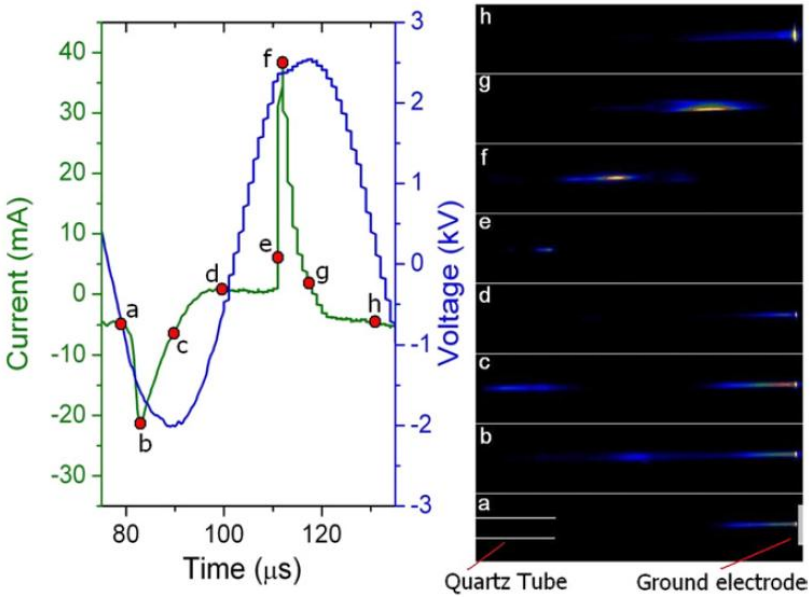

J. L. Walsh, *et al.*, J. Phys. D: Appl. Phys., **43**, 075201 (2010)

AC electrical discharges deliver energy to the plasma without contact between electrodes and the plasma

- DC electrical discharge – a true current in the form of a flow of ions or electrons to the electrodes.
- AC electrical discharge – the power supply interacts with the plasma by displacement current.
  - Inductive radio frequency (RF) electrical discharges
  - Capacitive RF electrical discharges
  - Microwave electrical discharges
  - Dielectric-barrier discharges (DBDs)
- Other mechanism
  - **Laser produced plasma**
  - Pulsed-power generated plasma

Electric field of a high-power laser can perturb the potential of a nuclear and thus ionize the atom directly

- For $I < 10^{18}$ w/cm^2

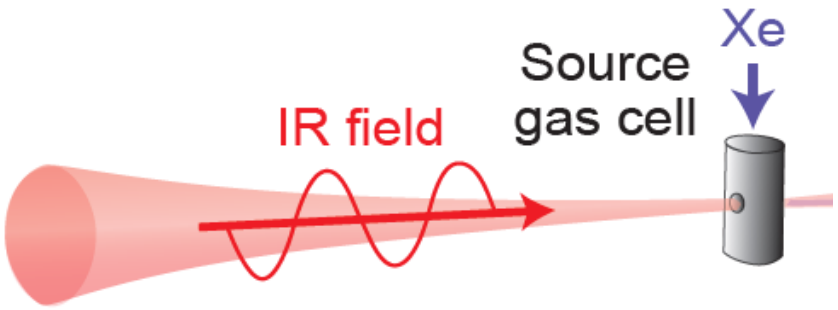

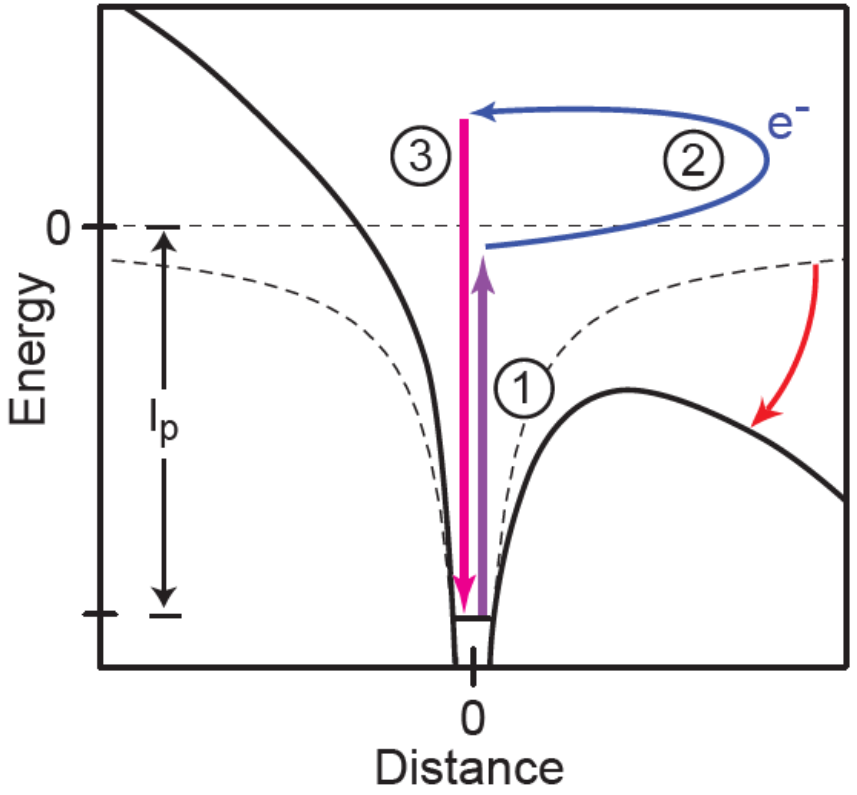

M. Krüger, etc., Appl. Sci. 9, 378 (2019)

Laser is absorbed in underdense plasma through collisional process called inverse bremsstrahlung

- **Bremsstrahlung**

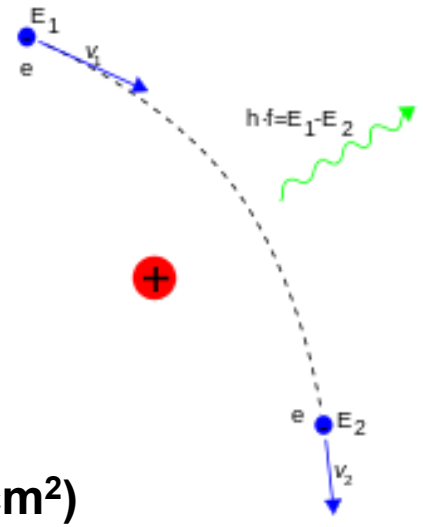

- **Inverse bremsstrahlung (For I < 10^{18} w/cm^2)**

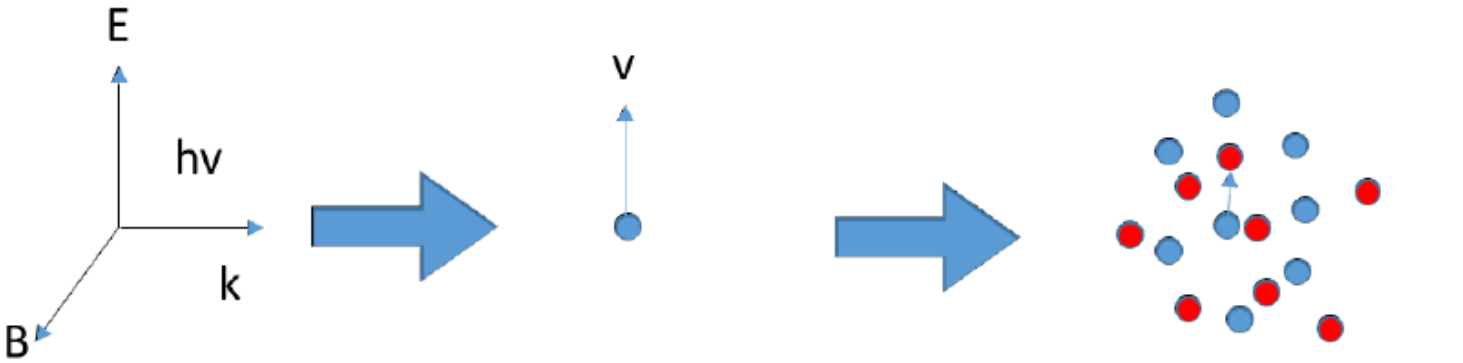

AC electrical discharges deliver energy to the plasma without contact between electrodes and the plasma

- DC electrical discharge – a true current in the form of a flow of ions or electrons to the electrodes.
- AC electrical discharge – the power supply interacts with the plasma by displacement current.
  - Inductive radio frequency (RF) electrical discharges
  - Capacitive RF electrical discharges
  - Microwave electrical discharges
  - Dielectric-barrier discharges (DBDs)
- Other mechanism
  - Laser produced plasma
  - **Pulsed-power generated plasma – it will be introduced later.**

Diagnostics

- Single/double Langmuir probe – n_e, T_e
- Interferometer – n_e
- Schlieren – dn_e/dx
- Faraday rotator – B
- Bdot probe – B
- Charged particle – B
- Spectroscopy – T_e, n_e
- Thomson scattering – T_e, n_e, T_i, n_i
- Faraday cup – dn_i/dt
- Retarding Potential Analyzer - v_i
- Intensified CCD – 2D image
- Framing camera – 2D image
- Streak camera – 1D image
- VISAR – shock velocity
- Neutron time of fligh (NToF)
  - Neutron yield, T_i
- Thomson parabola – e/m
- Stimulated brillouin scattering
  - Laser pulse compression

All plasmas are separated from the walls surrounding them by a sheath

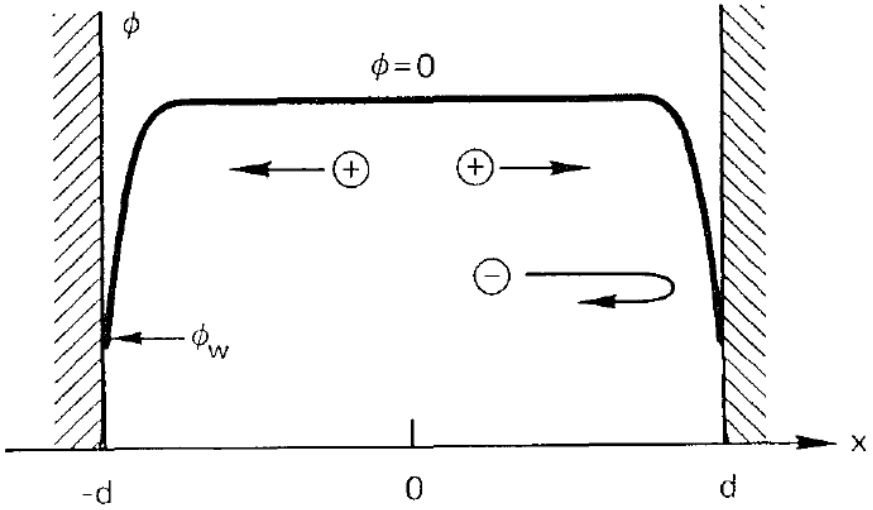

- When ions and electrons hit the wall, they recombine and are lost.
- Since electrons have much higher thermal velocities than ions, they are lost faster and leave the plasma with a net positive charge.
- Debye shielding will confine the potential variation to a layer of the order of several Debye lengths in thickness.
- A potential barrier is formed to confine electrons electrostatically.
- The flux of electrons is just equal to the flux of ions reaching the wall.

The planar sheath equation

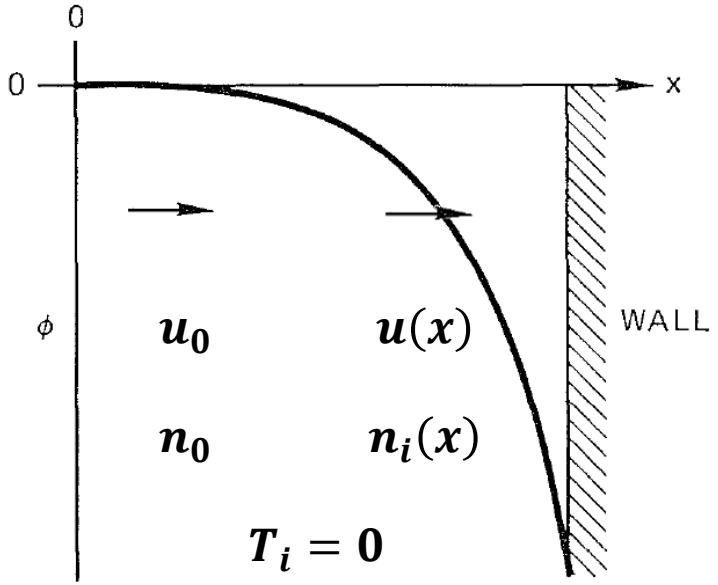

$$\frac{1}{2}mu^2 = \frac{1}{2}mu_0{}^2 - e\phi(x)$$

$$u = \left(u_0{}^2 - \frac{2e\phi}{m}\right)^{1/2}$$

$$n_0 u_0 = n_i(x)u(x)$$

$$n_i(x) = n_0\left(1 - \frac{2e\phi}{mu_0{}^2}\right)^{-1/2}$$

- **Boltzmann relation:**

$$n_e(x) = n_0 \exp\left(\frac{e\phi}{KT_e}\right)$$

- **Poisson's equation:**

$$\epsilon_0 \frac{d^2\phi}{dx^2} = e(n_e - n_i)$$

$$= en_0\left[\exp\left(\frac{e\phi}{KT_e}\right) - \left(1 - \frac{2e\phi}{mu_0{}^2}\right)^{-1/2}\right]$$

$$\chi \equiv -\frac{e\phi}{KT_e}, \xi \equiv \frac{x}{\lambda_D}, M \equiv \frac{u_0}{(KT_e/m)^{1/2}}$$

$$\lambda_D = \left(\frac{KT_e}{4\pi ne^2}\right)^{1/2}$$

$$\chi'' = \left(1 + \frac{2\chi}{M^2}\right)^{-1/2} - e^{-\chi}$$

The Bohm sheath criterion

$$\chi'' = \left(1 + \frac{2\chi}{M^2}\right)^{-1/2} - e^{-\chi}$$

$$\chi'\chi'' = \chi'\left(1 + \frac{2\chi}{M^2}\right)^{-1/2} - \chi' e^{-\chi}$$

$$\frac{d}{d\xi}\left(\frac{\chi'^2}{2}\right) = \frac{d\chi}{d\xi}\left(1 + \frac{2\chi}{M^2}\right)^{-1/2} - \frac{d\chi}{d\xi} e^{-\chi}$$

$$\chi_0 = 0\,, \chi_0' = 0, @\ \xi = 0$$

$$\int_{\chi_0'}^{\chi'} d\left(\frac{\chi'^2}{2}\right) = \int_0^{\chi}\left(1 + \frac{2\chi}{M^2}\right)^{-1/2} d\chi - \int_0^{\chi} e^{-\chi}\, d\chi$$

$$\frac{1}{2}\left(\chi'^2 - {\chi_0}'^2\right) = M^2\left[\left(1 + \frac{2\chi}{M^2}\right)^{1/2} - 1\right] + e^{-\chi} - 1$$

- Needs to be solved numerically
- The right-hand side must be positive for all χ .

The Bohm sheath criterion - continued

$$\frac{1}{2}\left(\chi'^2 - {\chi_0}'^2\right) = M^2\left[\left(1+\frac{2\chi}{M^2}\right)^{1/2} - 1\right] + e^{-\chi} - 1$$

- for $\chi \ll 1$

$$\left(1+\frac{2\chi}{M^2}\right)^{1/2} - 1 = 1 + \frac{\chi}{M^2} - \frac{1}{2}\left(\frac{\chi}{M^2}\right)^2 + \cdots - 1 \approx \frac{\chi}{M^2} - \frac{1}{2}\left(\frac{\chi}{M^2}\right)^2$$

$$e^{-\chi} - 1 = 1 - \chi + \frac{1}{2}\chi^2 + \cdots - 1 \approx -\chi + \frac{1}{2}\chi^2$$

$$M^2\left[\left(1+\frac{2\chi}{M^2}\right)^{1/2} - 1\right] + e^{\chi} - 1 \approx M^2\left[\frac{\chi}{M^2} - \frac{1}{2}\left(\frac{\chi}{M^2}\right)^2\right] - \chi + \frac{1}{2}\chi^2 = \frac{1}{2}\chi^2\left(-\frac{1}{M^2}+1\right) > 0$$

$$M^2 > 1 \text{ or } \boxed{mu_0{}^2 > KT_e}$$

- Ions must enter the sheath region with a velocity greater than the acoustic velocity v_s.
- There must be a finite electric field in the plasma.
- The scale of the sheath region is usually much smaller than the scale of the main plasma region in which the ions are accelerated.

The Child-Langmuir law

- The electron density can be neglected in the region of large χ next to the wall.

$$\chi'' = \left(1 + \frac{2\chi}{M^2}\right)^{-1/2} - e^{-\chi} \approx \left(1 + \frac{2\chi}{M^2}\right)^{-1/2} \approx \frac{M}{(2\chi)^{1/2}}$$

$$\frac{1}{2}\left(\chi'^2 - \chi_s'^2\right) = \int_{\chi_s}^{\chi} \frac{M}{(2\chi)^{1/2}}\, d\chi = \sqrt{2}M\left(\chi^{1/2} - \chi_s^{1/2}\right)$$

$n_e \approx 0 @ \xi = \xi_s$, $\chi_s << \chi$ and $\chi_s' << \chi'$, $\chi'^2 = 2^{3/2} M \chi^{1/2}$

$$\frac{d\chi}{\chi^{1/4}} = 2^{3/4} M^{1/2} d\xi$$

- Integrating from $\xi = \xi_s$ to $\xi_s + \frac{d}{\lambda_D} = \xi_{\text{wall}}$

$$\frac{4}{3}\chi_w^{3/4} = 2^{3/4} M^{1/2} \frac{d}{\lambda_D} \qquad M = \frac{4\sqrt{2}}{9} \frac{\chi_w^{3/2}}{d^2} \lambda_D$$

$$\chi \equiv -\frac{e\phi}{KT_e}, M \equiv \frac{u_0}{(KT_e/m)^{1/2}}$$

$$J = en_0u_0$$

$$J = \frac{4}{9}\left(\frac{2e}{m}\right)^{1/2} \frac{\epsilon_0 |\phi_w|^{3/2}}{d^2}$$

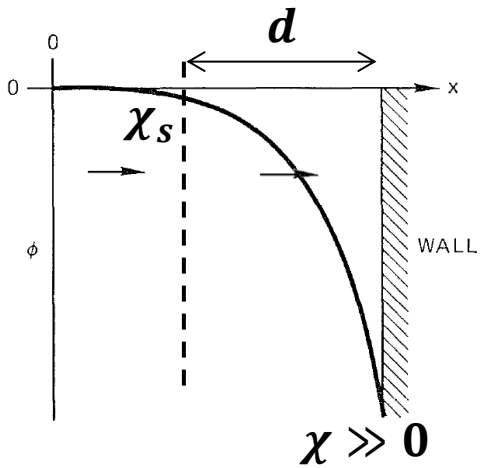

The potential variation in a plasma-wall system can be divided into three parts

- **Electron-free region:**

$$J = \frac{4}{9}\left(\frac{2e}{M}\right)^{1/2} \frac{\epsilon_0 |\phi_w|^{3/2}}{d^2}$$

  - **J is determined by the ion production rate**
  - **Φ_w is determined by the equality of electron and ion fluxes.**
- **Sheath:**
  - **~Debye length, n_e is appreciable.**
  - **A dark layers where no electrons were present to excite atoms to emission.**
  - **It has been measured by the electrostatic deflection of a thin electron beam shot parallel to a wall**

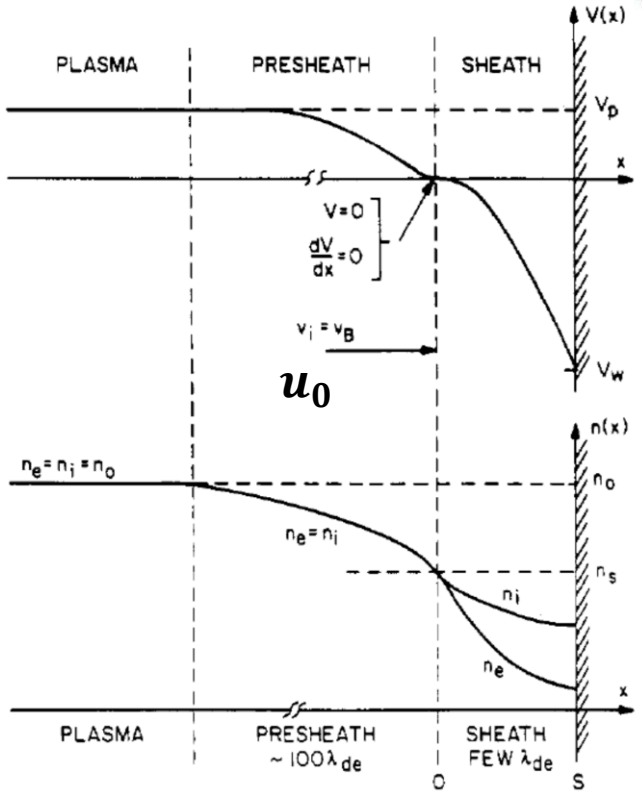

- **Presheath: ions are accelerated to the required velocity u_0 by a potential drop** $|\phi| \geq \frac{1}{2}\frac{KT_e}{e}$.

$$\frac{1}{2}mu_0^2 = |e\phi|,\ mu_0^2 > KT_e$$

Electrostatic probes

- **The electron current can be neglected if the probe is sufficiently negative relative to the plasma to repel most electrons.**

$$mu_0{}^2 > KT_e \qquad J = enu \qquad I = n_s eA\left(\frac{KT_e}{m}\right)^{1/2}$$

$$|\phi| \simeq \frac{1}{2}\frac{KT_e}{e}$$

$$n_s = n_0 \exp\left(\frac{e\phi}{KT_e}\right) = n_0 e^{-1/2} = 0.61 n_0$$

Bohm current: $I_B \simeq 0.5 n_0 eA\left(\frac{KT_e}{m}\right)^{1/2}$

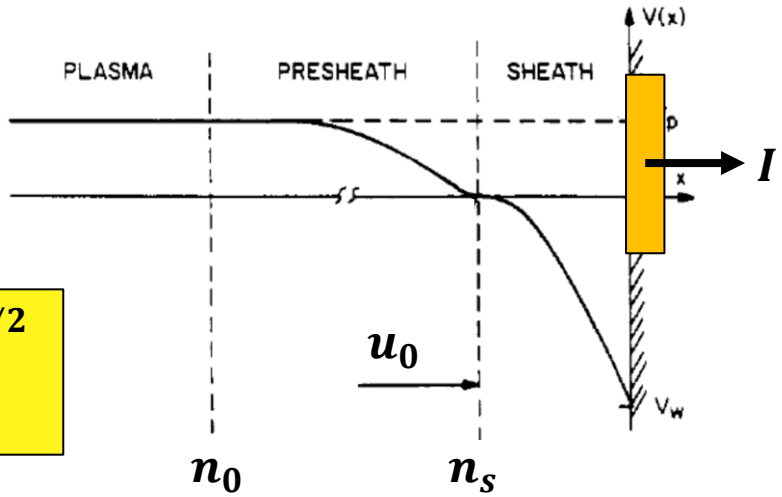

- **The plasma density can be obtained once the temperature is known.**

A plasma sheaths is formed when plasma is contact to a surface

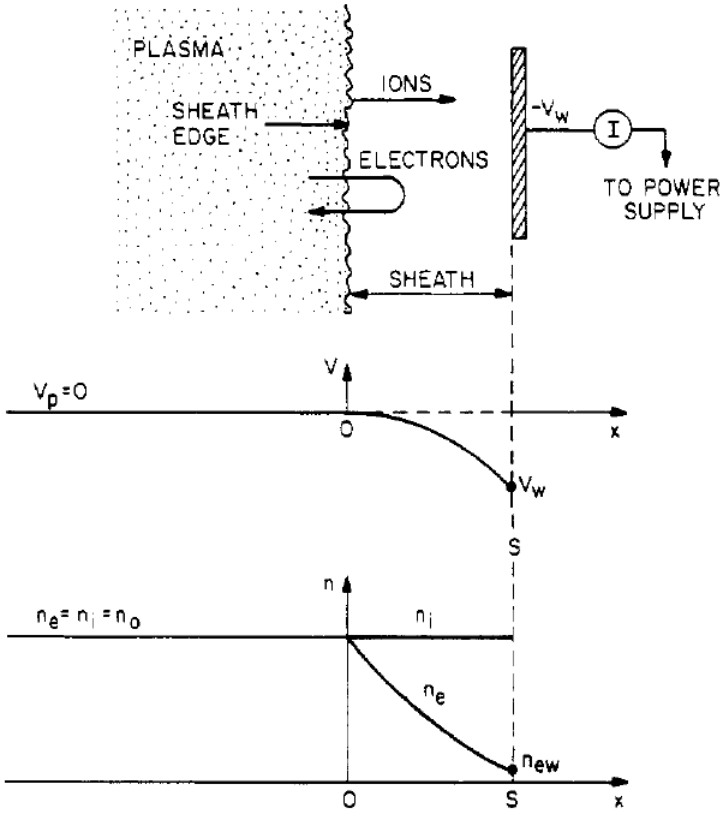

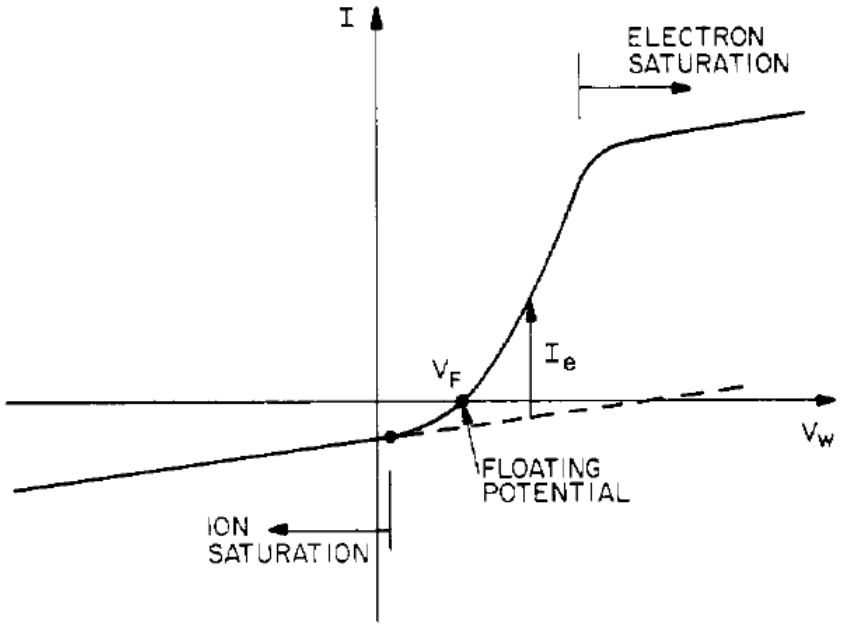

Floating voltage is determined when ion flux is balanced by electron flux

- **Wall flux of ions:**

$$\Gamma_i = \frac{1}{4} n_0 \bar{v}_i = n_0 \sqrt{\frac{8KT_i}{\pi m_i}}$$

- **Wall flux of electrons due to random motion:**

$$n_{ew} = n_0 \exp\left(\frac{e\Phi_w}{KT_e}\right) \qquad \text{(Boltzman equation)}$$

$$\Gamma_e = \frac{1}{4} n_{ew} \bar{v}_e = n_0 \exp\left(\frac{e\Phi_w}{KT_e}\right) \sqrt{\frac{8KT_e}{\pi m_e}}$$

- **Balance between electron and ion flux (current)**

$$I = \mathrm{eA}(\Gamma_i - \Gamma_e) = 0$$

$$\Phi_w = -\frac{KT_e}{2e} \ln\left(\frac{m_i T_e}{m_e T_i}\right)$$

Floating voltage can also be calculated using Bohm's velocity

- **Wall flux of ions using Bohm's velocity:**

$$u_0 = \sqrt{\frac{KT_e}{m_i}} \qquad \Gamma_i = n_s u_0$$

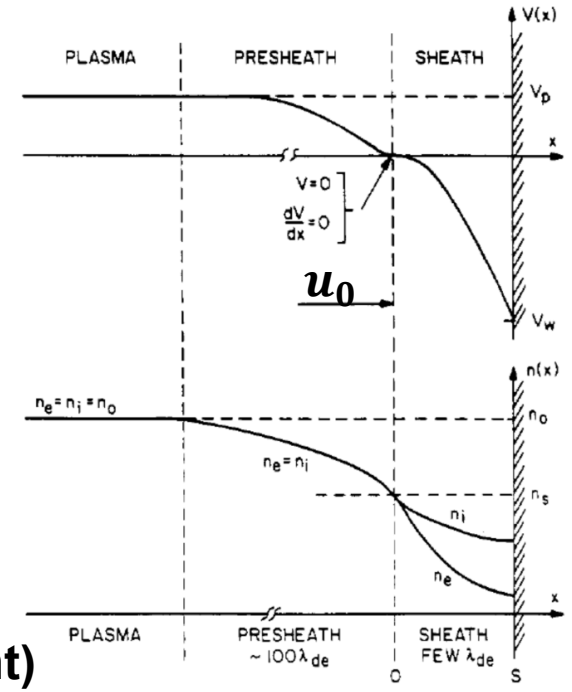

- **Wall flux of electrons due to random motion:**

$$n_{ew} = n_s \exp\left(\frac{e\Phi_w}{KT_e}\right)$$

$$\Gamma_e = \frac{1}{4} n_w \bar{v}_e = \frac{1}{4} n_s \exp\left(\frac{e\Phi_w}{KT_e}\right) \sqrt{\frac{8KT_e}{\pi m_e}}$$

- **Balance between electron and ion flux (current)**

$$I = \mathrm{eA}(\Gamma_i - \Gamma_e) = 0$$

$$\Phi_{wB} = -\frac{KT_e}{2e} \ln\left(\frac{m_i}{2\pi m_e}\right) \quad \Leftrightarrow \quad \Phi_w = -\frac{KT_e}{2e} \ln\left(\frac{m_i T_e}{m_e T_i}\right)$$

Electron temperature can be determined by the slope of the I-V curve between ion and electron saturation

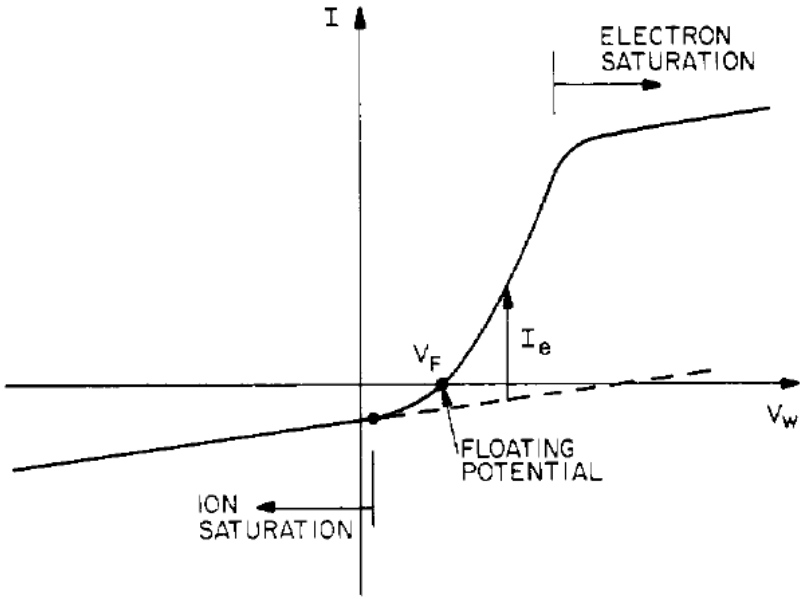

- **Ion saturation current:**

$$I_{is} = AJ_{is} = eA\Gamma_{is}$$
$$= eA\frac{1}{4}n_i\bar{v}_i$$
$$= \frac{eAn_i}{4}\sqrt{\frac{8KT_i}{\pi m_i}}$$

$$n_i = \frac{4I_{is}}{eA}\sqrt{\frac{\pi m_i}{8KT_i}}$$

- **Total current:** $I = I_{is} + I_e = I_{is} + \frac{1}{4}n_s\exp\left(\frac{eV}{KT_e}\right)\bar{v}_e eA \qquad V \equiv \Phi$

Assuming: $\frac{dI_{is}}{dV} \ll \frac{dI}{dV}$

$$\frac{dI}{dV} = \frac{dI_{is}}{dV} + \frac{1}{4}\frac{e}{KT_e}n_s\exp\left(\frac{eV}{KT_e}\right)\bar{v}_e eA = \frac{dI_{is}}{dV} + \frac{e}{KT_e}I_e = \frac{dI_{is}}{dV} + \frac{e}{KT_e}(I - I_{is})$$
$$\approx \frac{e}{KT_e}(I - I_{is})$$

$$T_e = \frac{e(I - I_{is})}{dI/dV}$$

Electron temperature can be obtained alternatively by finding the slope of I-V curve in Log-Linear plot

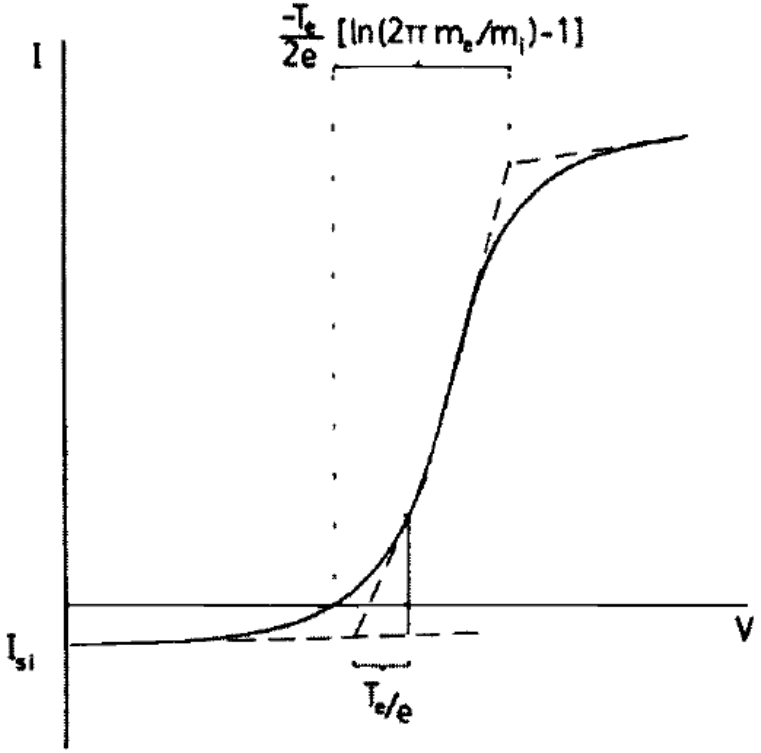

- **Electron saturation**

$$V = V_p \qquad I_{es} = \frac{1}{4} n_s \exp\left(\frac{eV_p}{KT_e}\right) \bar{v}_e eA$$

$$I = I_e + I_{is} \approx I_{es} = \frac{1}{4} n_s \exp\left(\frac{eV}{KT_e}\right) \bar{v}_e eA$$

$$= \frac{1}{4} n_s \exp\left(\frac{eV - eV_p + eV_p}{KT_e}\right) \bar{v}_e eA$$

$$= \frac{1}{4} n_s \exp\left(\frac{eV_p}{KT_e}\right) \exp\left(e\frac{V - V_p}{KT_e}\right) \bar{v}_e eA$$

$$= I_{es} \exp\left(e\frac{V - V_p}{KT_e}\right)$$

$$T_e = \frac{e(V - V_p)}{K(\ln I_{es} - \ln I)}$$

Plasma density can be obtained by finding the electron saturation current

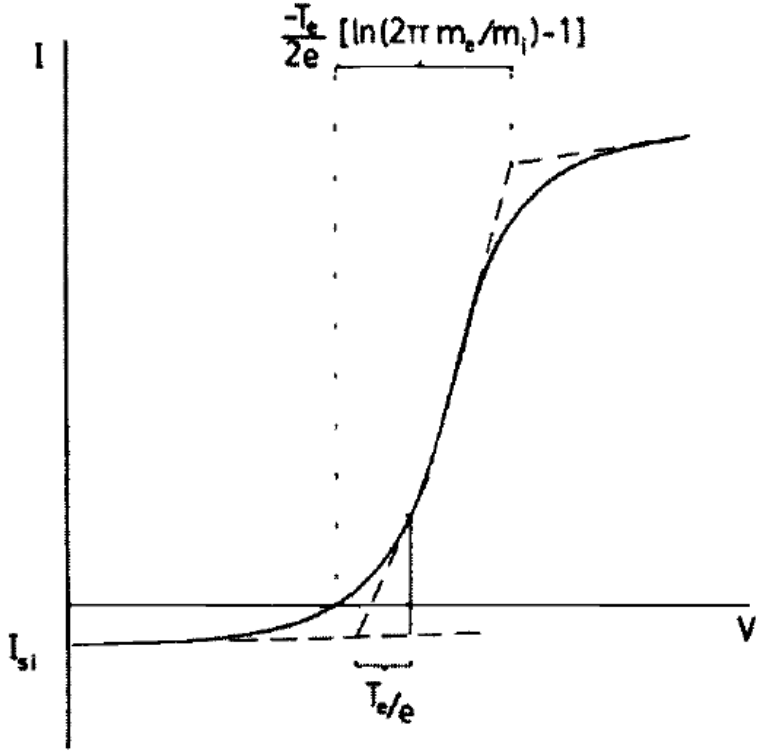

- **Electron saturation current:**

$$I_{es} = \frac{1}{4} n_s \exp\left(\frac{eV_p}{KT_e}\right) \bar{v}_e eA$$

$$= \frac{1}{4} n_0 eA \sqrt{\frac{8KT_e}{\pi m_e}}$$

$$n_0 = \frac{4I_{es}}{eA}\sqrt{\frac{\pi m_e}{8T_e}}$$

Two Langmuir probes can be operated simultaneously

Single Probe

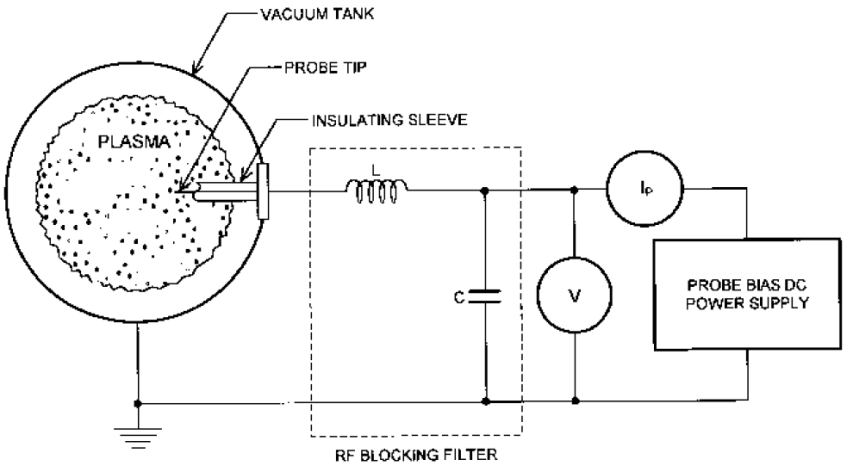

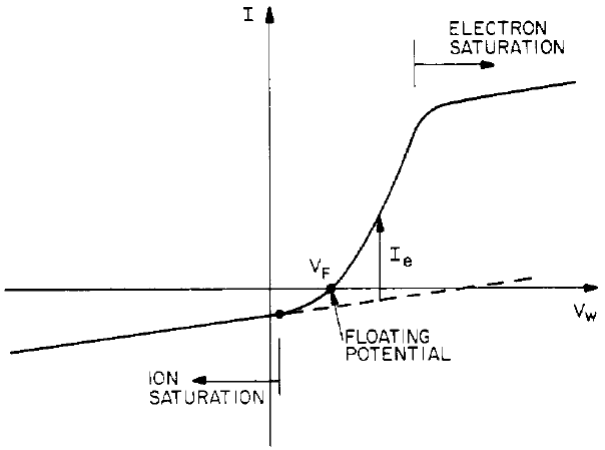

Double Probe

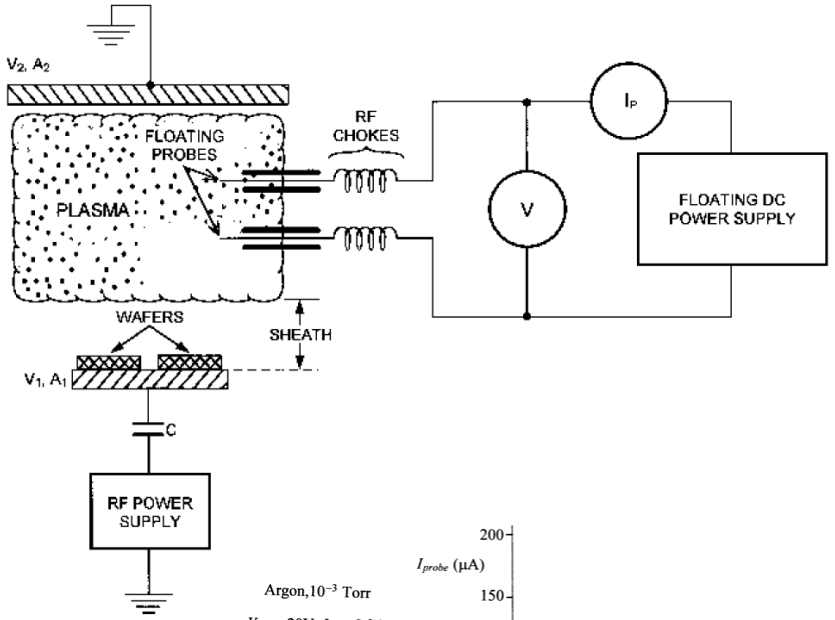

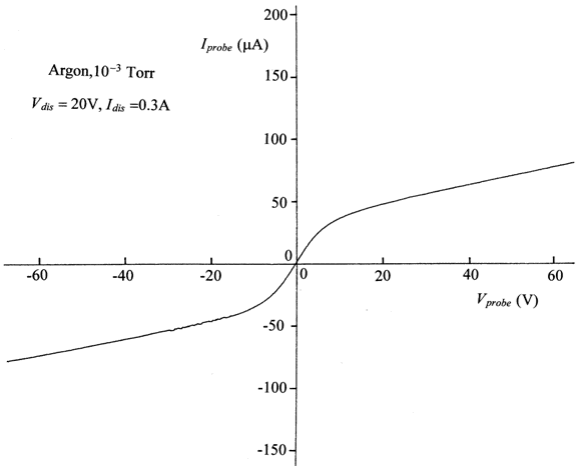

Double Langmuir probe is not disturbed by the discharge

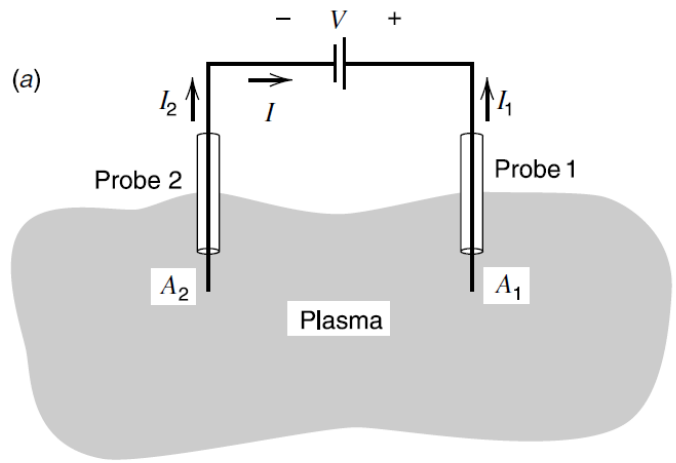

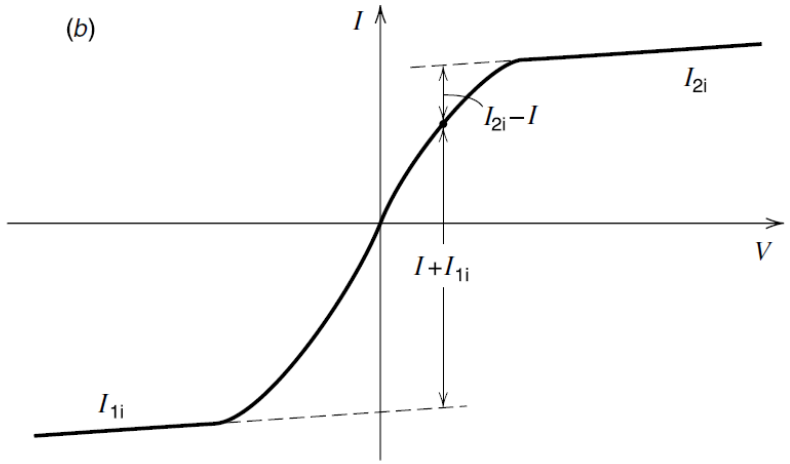

$$I = I_{1e} - I_{1i} = I_{2i} - I_{2e}$$

$$I_{1e} = A_1 \frac{\bar{v}_e e}{4} n_s \exp\left(\frac{eV_1}{KT_e}\right)$$

$$I_{2e} = A_2 \frac{\bar{v}_e e}{4} n_s \exp\left(\frac{eV_2}{KT_e}\right)$$

$$I_{1e} = I + I_{1i} \qquad I_{2e} = I_{2i} - I$$

$$\frac{I + I_{1i}}{I_{2i} - I} = \frac{A_1}{A_2} \exp\left(\frac{V_1 - V_2}{T_e}\right)$$

$$= \frac{A_1}{A_2} \exp\left(\frac{V}{T_e}\right)$$

$$I = I_i \tanh\left(\frac{V}{2T_e}\right) \qquad \frac{dI}{dV}\Big|_{v=0} = \frac{I_i}{2T_e}$$

- **The net current never exceeds the ion saturation current, minimizing the disturbance to the discharge.**

An electromagnetic wave is described using Maxwell's equation

$$\begin{cases} \nabla \times \vec{E} &= -\dfrac{\partial \vec{B}}{\partial t} \\ \nabla \times \vec{B} &= \mu_0 \vec{j} + \epsilon_0 \mu_0 \dfrac{\partial \vec{E}}{\partial t} \end{cases}$$

$$\nabla \times \left(\nabla \times \vec{E} \right) = -\frac{\partial}{\partial t} \left(\nabla \times \vec{B} \right) = -\frac{\partial}{\partial t} \left(\mu_0 \vec{j} + \epsilon_0 \mu_0 \frac{\partial \vec{E}}{\partial t} \right)$$

Conductivity: $\vec{j} = \overleftrightarrow{\sigma} \cdot \vec{E}$

$$\nabla \times \left(\nabla \times \vec{E} \right) = -\frac{\partial}{\partial t} \left(\nabla \times \vec{B} \right) = -\frac{\partial}{\partial t} \left(\mu_0 \overleftrightarrow{\sigma} \cdot \vec{E} + \epsilon_0 \mu_0 \frac{\partial \vec{E}}{\partial t} \right)$$

Plane wave: $\vec{E} = \vec{E} \exp \left[i \left(\vec{k} \cdot \vec{x} - \omega t \right) \right]$

$$i\vec{k} \times \left(i\vec{k} \times \vec{E} \right) = i\omega \left(\mu_0 \overleftrightarrow{\sigma} \cdot \vec{E} - i\omega \epsilon_0 \mu_0 \vec{E} \right)$$

Dispersion relation is determined by the determinant of the matrix of coefficient

$$-\vec{k}\times\left(\vec{k}\times\vec{E}\right) = -\left[\left(\vec{k}\cdot\vec{E}\right)\vec{k}-\left(\vec{k}\cdot\vec{k}\right)\vec{E}\right] = -\left(\vec{k}:\vec{k}\right)\vec{E}+k^2\vec{E}$$

$$\begin{aligned} i\omega\left(\mu_0\overleftrightarrow{\sigma}\cdot\vec{E}-i\omega\epsilon_0\mu_0\vec{E}\right) &= i\omega\left(\mu_0\overleftrightarrow{\sigma}\cdot\vec{E}-\frac{i\omega}{c^2}\vec{E}\right) = \frac{\omega^2}{c^2}\left[-\frac{c^2}{i\omega}\mu_0\overleftrightarrow{\sigma}\cdot\vec{E}+\vec{E}\right] \\ &= \frac{\omega^2}{c^2}\left(\overleftrightarrow{1}+\frac{i}{\omega\epsilon_0}\overleftrightarrow{\sigma}\right)\vec{E}\equiv\frac{\omega^2}{c^2}\overleftrightarrow{\varepsilon}\vec{E} \end{aligned}$$

Dielectric tensor: $\overleftrightarrow{\varepsilon}\equiv\overleftrightarrow{1}+\frac{i}{\omega\epsilon_0}\overleftrightarrow{\sigma}$

$$\left(\vec{k}:\vec{k}-k^2\overleftrightarrow{1}+\frac{\omega^2}{c^2}\overleftrightarrow{\varepsilon}\right)\vec{E}=0$$

$$\det\left(\vec{k}:\vec{k}-k^2\overleftrightarrow{1}+\frac{\omega^2}{c^2}\overleftrightarrow{\varepsilon}\right)=0$$

Two mode can propagate in the plasma

$$\det\left(\vec{k}:\vec{k}-k^2\overleftrightarrow{1}+\frac{\omega^2}{c^2}\overleftrightarrow{\varepsilon}\right)=0$$

Assuming the wave propagates along the z direction and isotropic medium:

$$\vec{k}=k\hat{z}$$

$$\overleftrightarrow{\varepsilon}=\varepsilon\overleftrightarrow{1}$$

$$\begin{pmatrix} -k^2+\frac{\omega^2}{c^2}\varepsilon & 0 & 0 \\ 0 & -k^2+\frac{\omega^2}{c^2}\varepsilon & 0 \\ 0 & 0 & \frac{\omega^2}{c^2}\varepsilon \end{pmatrix}=0$$

$$\left(-k^2+\frac{\omega^2}{c^2}\varepsilon\right)^2\frac{\omega^2}{c^2}\varepsilon=0$$

$$\frac{\omega^2}{c^2}\varepsilon=0$$

Longitudinal wave

$$\left(-k^2+\frac{\omega^2}{c^2}\varepsilon\right)^2=0$$

Transverse wave

The reflective index is determined by the dielectric

- **Longitudinal wave:** $\frac{\omega^2}{c^2}\varepsilon = 0$

$$\begin{pmatrix} -k^2+\frac{\omega^2}{c^2}\varepsilon & 0 & 0 \\ 0 & -k^2+\frac{\omega^2}{c^2}\varepsilon & 0 \\ 0 & 0 & 0 \end{pmatrix} \begin{pmatrix} E_\mathrm{x} \\ E_\mathrm{y} \\ E_\mathrm{z} \end{pmatrix} = 0 = \begin{pmatrix} \left(-k^2+\frac{\omega^2}{c^2}\varepsilon\right)E_\mathrm{x} \\ \left(-k^2+\frac{\omega^2}{c^2}\varepsilon\right)E_\mathrm{y} \\ 0 \end{pmatrix}$$

$$E_\mathrm{x} = E_\mathrm{y} = 0$$

- **Transverse wave:** $\left(-k^2+\frac{\omega^2}{c^2}\varepsilon\right)^2 = 0$

$$\begin{pmatrix} 0 & 0 & 0 \\ 0 & 0 & 0 \\ 0 & 0 & \frac{\omega^2}{c^2}\varepsilon \end{pmatrix} \begin{pmatrix} E_\mathrm{x} \\ E_\mathrm{y} \\ E_\mathrm{z} \end{pmatrix} = 0$$

$$E_\mathrm{z} = 0$$

Reflective index: $n \equiv \frac{kc}{\omega} = \varepsilon^{1/2}$

Conductivity tensor can be determined from equation of motion for electron

$$m_e \frac{\partial \vec{v}}{\partial t} = -e\left(\vec{E} + \vec{v} \times \vec{B}\right)$$

$$\vec{v} = \vec{v}\exp\left[i\left(\vec{k}\cdot\vec{x} - \omega t\right)\right]$$

$$\begin{cases} -i\omega m_e v_x &= -eE_x - eB_0 v_y \\ -i\omega m_e v_y &= -eE_y + eB_0 v_x \\ -i\omega m_e v_z &= -eE_z \end{cases}$$

$$\Omega \equiv \frac{eB_0}{m_e}$$

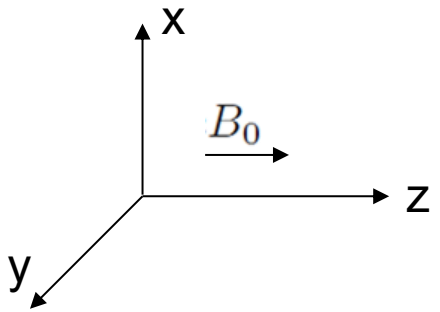

$$\begin{cases} v_x &= -\dfrac{ie}{\omega m_e}\dfrac{1}{1-\Omega^2/\omega^2}\left(E_x - i\dfrac{\Omega}{\omega}E_y\right) \\ v_y &= -\dfrac{ie}{\omega m_e}\dfrac{1}{1-\Omega^2/\omega^2}\left(i\dfrac{\Omega}{\omega}E_x + E_y\right) \\ v_z &= -\dfrac{ie}{\omega m_e}E_z \end{cases}$$

$$\vec{j} = -en_e\vec{v}_e \equiv \overleftrightarrow{\sigma}\vec{E}$$

$$\overleftrightarrow{\sigma} = -en_e\left(\frac{-ie}{\omega m_e}\right)\frac{1}{1-\Omega^2/\omega^2}\begin{pmatrix} 1 & -i\frac{\Omega}{\omega} & 0 \\ i\frac{\Omega}{\omega} & 1 & 0 \\ 0 & 0 & 1-\frac{\Omega^2}{\omega^2} \end{pmatrix}$$

$$= i\frac{n_e e^2}{\omega m_e}\frac{1}{1-\Omega^2/\omega^2}\begin{pmatrix} 1 & -i\frac{\Omega}{\omega} & 0 \\ i\frac{\Omega}{\omega} & 1 & 0 \\ 0 & 0 & 1-\frac{\Omega^2}{\omega^2} \end{pmatrix}$$

Dielectric tensor is obtained from conductivity tensor

$$\frac{i}{\omega\epsilon_0}\overleftrightarrow{\sigma} = -\frac{n_e e^2}{\epsilon_0 m_e}\frac{1}{\omega^2}\frac{1}{1-\Omega^2/\omega^2}\begin{pmatrix} 1 & -i\frac{\Omega}{\omega} & 0 \\ i\frac{\Omega}{\omega} & 1 & 0 \\ 0 & 0 & 1-\frac{\Omega^2}{\omega^2} \end{pmatrix}$$

$$= -\frac{\omega_p^2}{\omega^2-\Omega^2}\begin{pmatrix} 1 & -i\frac{\Omega}{\omega} & 0 \\ i\frac{\Omega}{\omega} & 1 & 0 \\ 0 & 0 & 1-\frac{\Omega^2}{\omega^2} \end{pmatrix} \qquad \omega_p^2 = \frac{n_e e^2}{\epsilon_0 m_e}$$

$$= \begin{pmatrix} -\frac{\omega_p^2}{\omega^2-\Omega^2} & i\frac{\Omega}{\omega}\frac{\omega_p^2}{\omega^2-\Omega^2} & 0 \\ -i\frac{\Omega}{\omega}\frac{\omega_p^2}{\omega^2-\Omega^2} & -\frac{\omega_p^2}{\omega^2-\Omega^2} & 0 \\ 0 & 0 & -\frac{\omega_p^2}{\omega^2} \end{pmatrix}$$

$$\overleftrightarrow{\varepsilon} = \overleftrightarrow{1} + \frac{i}{\omega\epsilon_0}\overleftrightarrow{\sigma} = \begin{pmatrix} 1-\frac{\omega_p^2}{\omega^2-\Omega^2} & i\frac{\Omega}{\omega}\frac{\omega_p^2}{\omega^2-\Omega^2} & 0 \\ -i\frac{\Omega}{\omega}\frac{\omega_p^2}{\omega^2-\Omega^2} & 1-\frac{\omega_p^2}{\omega^2-\Omega^2} & 0 \\ 0 & 0 & 1-\frac{\omega_p^2}{\omega^2} \end{pmatrix}$$

Assuming the wave is on the yz plane

let $X \equiv \dfrac{\omega_{\rm p}^2}{\omega^2}$ $\qquad Y \equiv \dfrac{\Omega}{\omega}$ $\qquad \overleftrightarrow{\varepsilon} = \begin{pmatrix} 1-\frac{X}{1-Y^2} & i\frac{XY}{1-Y^2} & 0 \\ -i\frac{XY}{1-Y^2} & 1-\frac{X}{1-Y^2} & 0 \\ 0 & 0 & 1-X \end{pmatrix}$

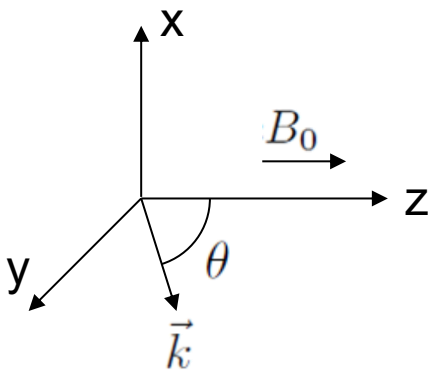

$$\vec{k} = k\,(0, \sin\theta, \cos\theta)$$

$$k_{\rm i} = 0\ ,\ k_{\rm j} = k\sin\theta\ ,\ k_{\rm k} = k\cos\theta$$

$$\vec{k}\,\vec{k} = \begin{pmatrix} 0 \\ k\sin\theta \\ k\cos\theta \end{pmatrix} \cdot \begin{pmatrix} 0 & k\sin\theta & k\cos\theta \end{pmatrix} = \begin{pmatrix} 0 & 0 & 0 \\ 0 & \sin^2\theta & \sin\theta\cos\theta \\ 0 & \sin\theta\cos\theta & \cos^2\theta \end{pmatrix}$$

$$n \equiv \frac{kc}{\omega} \qquad \frac{\omega^2}{c^2}\overleftrightarrow{\varepsilon} = \frac{k^2\omega^2}{k^2c^2}\overleftrightarrow{\varepsilon} = \frac{k^2}{n^2}\overleftrightarrow{\varepsilon}$$

$$\det\left(\vec{k}\,\vec{k} - k^2\overleftrightarrow{1} + \frac{\omega^2}{c^2}\overleftrightarrow{\varepsilon}\right) = 0$$

Reflective index

$$\begin{vmatrix} -k^2+\frac{k^2}{n^2}\left(1-\frac{X}{1-Y^2}\right) & i\frac{k^2}{n^2}\frac{XY}{1-Y^2} & 0 \\ -i\frac{k^2}{n^2}\frac{XY}{1-Y^2} & k^2\sin^2\theta-k^2+\frac{k^2}{n^2}\left(1-\frac{X}{1-Y^2}\right) & k^2\sin\theta\cos\theta \\ 0 & k^2\sin\theta\cos\theta & k^2\cos^2\theta-k^2+\frac{k^2}{n^2}\left(1-X\right) \end{vmatrix} = 0$$

$$\begin{vmatrix} -n^2+1-\frac{X}{1-Y^2} & i\frac{XY}{1-Y^2} & 0 \\ -i\frac{XY}{1-Y^2} & -n^2\cos^2\theta+1-\frac{X}{1-Y^2} & n^2\sin\theta\cos\theta \\ 0 & n^2\sin\theta\cos\theta & -n^2\sin^2\theta+1-X \end{vmatrix} = 0$$

$$n^2 = 1 - \frac{X\left(1-X\right)}{1-X-\frac{1}{2}Y^2\sin^2\theta \pm \left[\left(\frac{1}{2}Y^2\sin^2\theta\right)^2+\left(1-X\right)^2Y^2\cos^2\theta\right]^{1/2}}$$

Wave is circular polarized propagating along the magnetic field

- **Parallel to B_0** $(\theta = 0)$

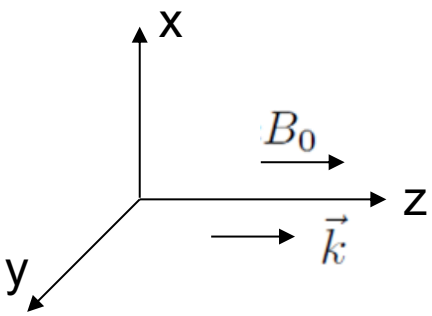

$$n^2 = 1 - \frac{X\left(1-X\right)}{1-X \pm \left[\left(1-X\right)^2 Y^2\right]^{1/2}} = 1 - \frac{X}{1 \pm Y} = 1 - \frac{\omega_{\mathrm{p}}^2/\omega^2}{1 \pm \Omega/\omega} = 1 - \frac{\omega_{\mathrm{p}}^2}{\omega\left(\omega \pm \Omega\right)}$$

$$\begin{pmatrix} -n^2 + 1 - \frac{X}{1-Y^2} & i\frac{XY}{1-Y^2} & 0 \\ -i\frac{XY}{1-Y^2} & -n^2\cos^2\theta + 1 - \frac{X}{1-Y^2} & 0 \\ 0 & 0 & 1-X \end{pmatrix} \begin{pmatrix} E_{\mathrm{x}} \\ E_{\mathrm{y}} \\ E_{\mathrm{z}} \end{pmatrix} = 0$$

$$\left(-n^2 + 1 - \frac{X}{1-Y^2}\right) E_{\mathrm{x}} + i\frac{XY}{1-Y^2} E_{\mathrm{y}} = \frac{\mp XY}{1-Y^2} E_{\mathrm{x}} + i\frac{XY}{1-Y^2} E_{\mathrm{y}} = 0$$

$$\frac{E_{\mathrm{x}}}{E_{\mathrm{y}}} = \pm i$$ **Left hang circular (LHC) or right hang circular (RHC) polarized.**

Electric field is not necessary parallel to the propagating direction which is perpendicular to B_0

- **Perpendicular to B_0** $\left(\theta = \frac{\pi}{2}\right)$

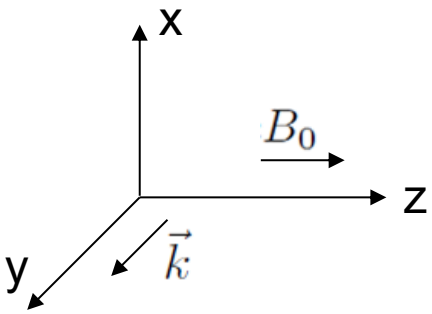

$$n^2 = 1 - \frac{X(1-X)}{1 - X - \frac{1}{2}Y^2 \pm \frac{1}{2}Y^2} = 1 - X \text{ or } 1 - \frac{X(1-X)}{1-X-Y^2}$$

$$\begin{pmatrix} -n^2 + 1 - \frac{X}{1-Y^2} & i\frac{XY}{1-Y^2} & 0 \\ -i\frac{XY}{1-Y^2} & 1 - \frac{X}{1-Y^2} & 0 \\ 0 & 0 & -n^2 + 1 - X \end{pmatrix} \begin{pmatrix} E_x \\ E_y \\ E_z \end{pmatrix} = 0$$

$$n^2 = 1 - \frac{\omega_p^2}{\omega^2} \qquad E_x = E_y = 0$$ **Ordinary wave (O-wave)**

$$n^2 = 1 - \frac{\omega_p^2\left(1 - \omega_p^2/\omega^2\right)}{\omega^2 - \omega_p^2 - \Omega^2} \qquad \frac{E_x}{E_y} = -i\omega\left(\frac{\omega^2 - \omega_p^2 - \Omega^2}{\omega_p^2 \Omega}\right) \qquad E_z = 0$$

Extraordinary wave (E-wave)

The electric field of an extraordinary wave rotates elliptically

Ordinary wave (O-wave)

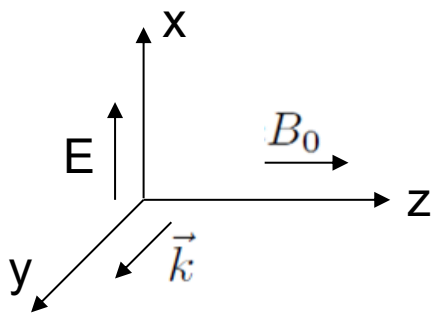

Extraordinary wave (E-wave)

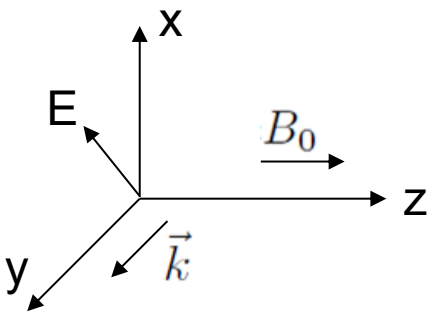

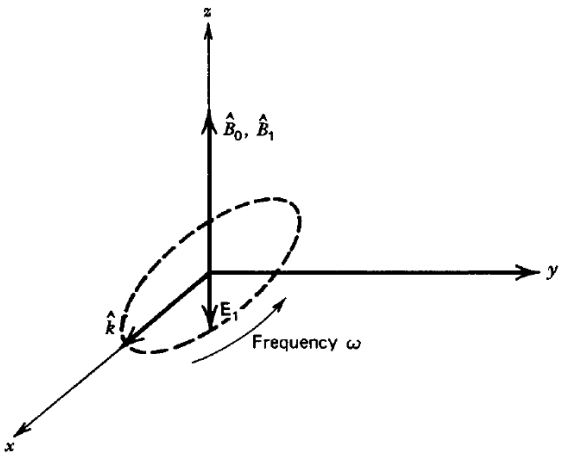

Electromagnetic wave can be used to measure the density or the magnetic field in the plasma

- **Nonmagnetized isotropic plasma (interferometer needed):**

$$n^2 = 1 - \frac{X\left(1-X\right)}{1-X-\frac{1}{2}Y^2\sin^2\theta \pm \left[\left(\frac{1}{2}Y^2\sin^2\theta\right)^2 + \left(1-X\right)^2 Y^2\cos^2\theta\right]^{1/2}}$$

$$= 1 - X = 1 - \frac{\omega_{\mathrm{p}}^2}{\omega^2} = 1 - \frac{n_{\mathrm{e}}}{n_{\mathrm{cr}}} \qquad \left(\boldsymbol{Y \equiv \frac{\Omega}{\omega} \equiv 0}\right)$$

Note: $\omega_{\mathrm{p}}^2 = \dfrac{n_{\mathrm{e}}e^2}{\epsilon_0 m_{\mathrm{e}}}$ $\quad n_{\mathrm{cr}} = \dfrac{\epsilon_0 m_{\mathrm{e}}\omega^2}{e^2}$

- **Magnetized isotropic plasma (Polarization detected needed):**

Parallel to B_0

$$n^2 = 1 - \frac{\omega_{\mathrm{p}}^2}{\omega\left(\omega \pm \Omega\right)} \qquad \frac{E_{\mathrm{x}}}{E_{\mathrm{y}}} = \pm i \qquad \Omega \equiv \frac{eB_0}{m_{\mathrm{e}}}$$

Faraday rotation: linear polarization rotation caused by the difference between the speed of LHC and RHC polarized wave.

Electromagnetic wave can be used to measure the density or the magnetic field in the plasma

- **Nonmagnetized isotropic plasma (interferometer needed):**

$$n^2 = 1 - \frac{X\left(1-X\right)}{1-X-\frac{1}{2}Y^2\sin^2\theta \pm \left[\left(\frac{1}{2}Y^2\sin^2\theta\right)^2 + \left(1-X\right)^2 Y^2\cos^2\theta\right]^{1/2}}$$

$$= 1 - X = 1 - \frac{\omega_{\mathrm{p}}^2}{\omega^2} = 1 - \frac{n_{\mathrm{e}}}{n_{\mathrm{cr}}} \qquad \left(\boldsymbol{Y \equiv \frac{\Omega}{\omega} \equiv 0}\right)$$

Note: $\omega_{\mathrm{p}}^2 = \dfrac{n_{\mathrm{e}}e^2}{\epsilon_0 m_{\mathrm{e}}}$ $\qquad n_{\mathrm{cr}} = \dfrac{\epsilon_0 m_{\mathrm{e}}\omega^2}{e^2}$

- **Magnetized isotropic plasma (Polarization detected needed):**

Parallel to B_0

$$n^2 = 1 - \frac{\omega_{\mathrm{p}}^2}{\omega\left(\omega \pm \Omega\right)} \qquad \frac{E_{\mathrm{x}}}{E_{\mathrm{y}}} = \pm i \qquad \Omega \equiv \frac{eB_0}{m_{\mathrm{e}}}$$

Faraday rotation: linear polarization rotation caused by the difference between the speed of LHC and RHC polarized wave.

There are two main style of interferometer

Michelson interferometer

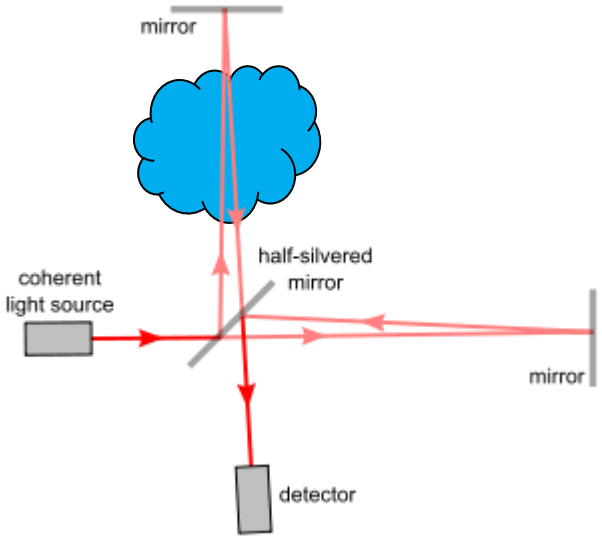

Mach-zehnder interferometer

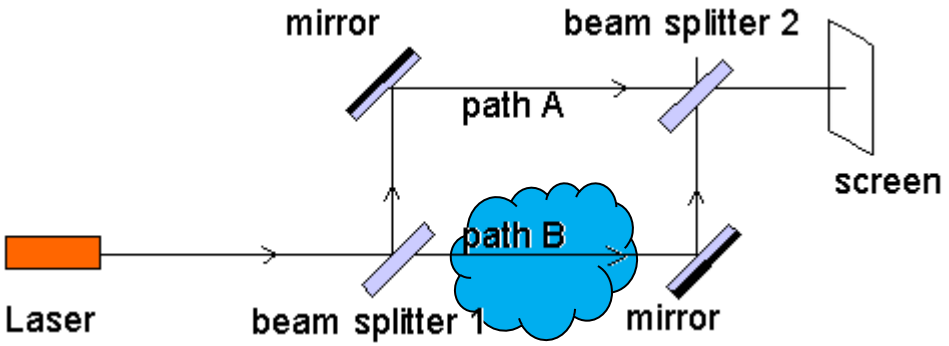

Interference pattern are due to the phase difference between two different path

$$E_1 = E_1 \exp(-i\omega t)$$

$$E_2 = E_2 \exp(-i\omega t + i\phi)$$

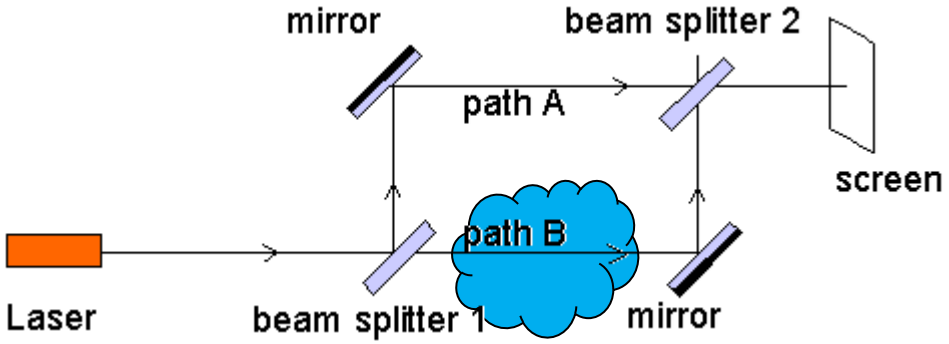

$$E = E_1 + E_2 = [E_1 + E_2 \exp(i\phi)] \exp(-i\omega t)$$

$$\begin{aligned} I &= |E|^2 = E^* E = [E_1 + E_2 \exp(-i\phi)] \exp(i\omega t) [E_1 + E_2 \exp(i\phi)] \exp(-i\omega t) \\ &= E_1^2 + E_2^2 + E_1 E_2 \exp(i\phi) + E_1 E_2 \exp(-i\phi) \\ &= E_1^2 + E_2^2 + 2E_1 E_2 \cos\phi \\ &= (E_1^2 + E_2^2)\left(1 + \frac{2E_1 E_2}{E_1^2 + E_2^2} \cos\phi\right) \end{aligned}$$

The intensity on screen depends on the phase different between two paths

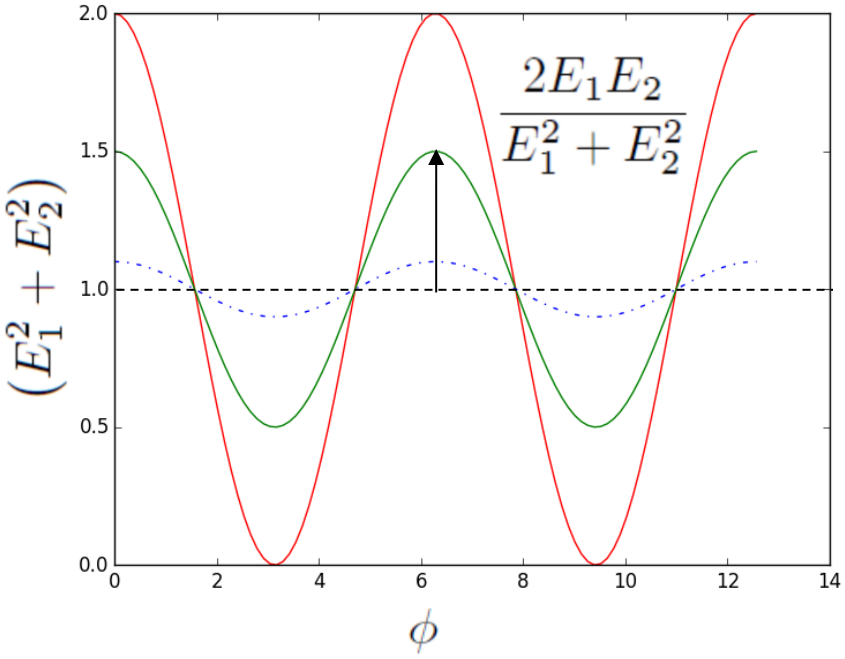

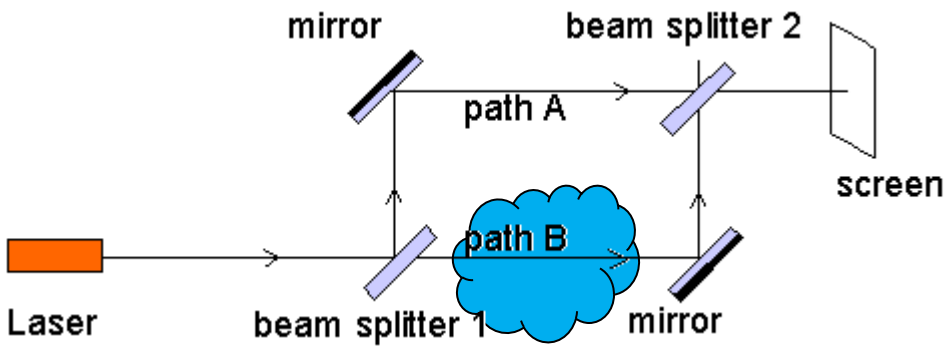

$$I = (E_1^2+E_2^2)\left(1+\frac{2E_1E_2}{E_1^2+E_2^2}\cos\phi\right)$$

The phase different depends on the line integral of the electron density along the path

$$\phi = \int k dl = \int n \frac{\omega}{c} dl$$

$$n^2 = 1 - \frac{n_e}{n_{cr}} \qquad n_{cr} = \frac{\epsilon_0 m_e \omega^2}{e^2}$$

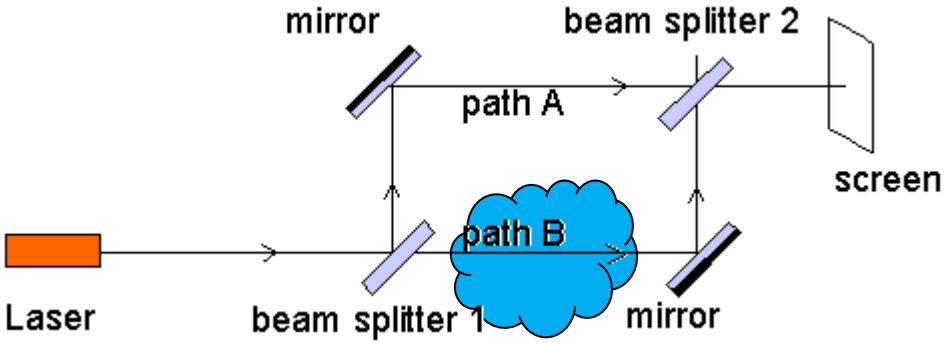

$$\begin{aligned}
\Delta\phi &= \int (k_{\text{plasma}} - k_0)\, dl = \frac{\omega}{c} \int (n-1)\, dl \\
&= \frac{\omega}{c} \int \left(\sqrt{1 - \frac{n_e}{n_c}} - 1 \right) dl \approx \frac{\omega}{c} \int \left(1 - \frac{1}{2}\frac{n_e}{n_c} - 1 \right) dl \\
&= -\frac{\omega}{2cn_c} \int n_e dl
\end{aligned}$$

Note that $n_e << n_{cr}$ **is assumed,** $\sqrt{1 - \frac{n_e}{n_{cr}}} \approx 1 - \frac{1}{2}\frac{n_e}{n_{cr}}$

The phase is determined by comparing to the pattern without the phase shift

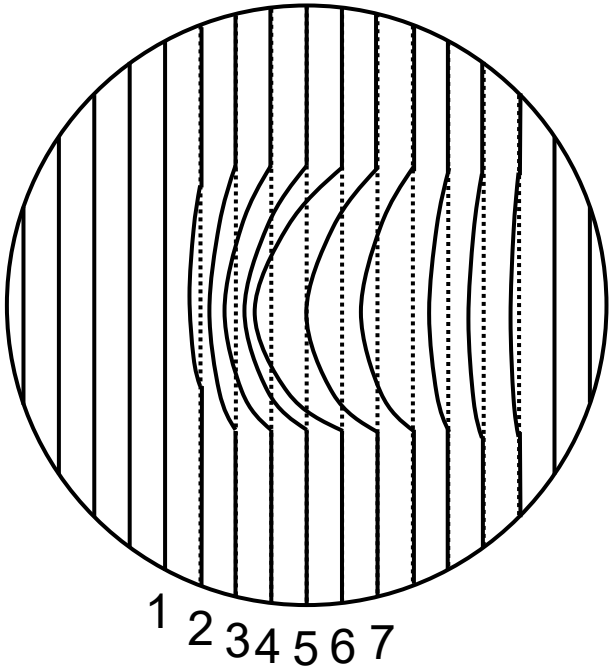

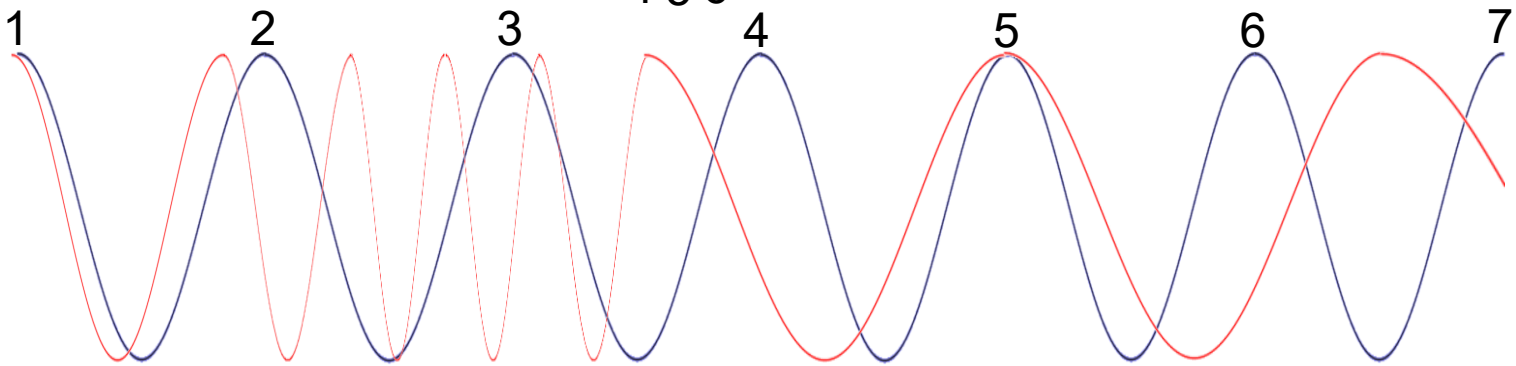

Fourier transform can be used to retrieve the data from the interferometer image

$$\mathbf{I}(x,y) = I_0(x,y) + m(x,y)\cos[2\pi\nu_0 x + \phi(x,y)] \qquad \cos(x) = \frac{e^{ix} + e^{-ix}}{2}$$

$$= I_0(x,y) + \frac{1}{2}m(x,y)\left(e^{i[2\pi\nu_0 x+\phi(x,y)]} + e^{-i[2\pi\nu_0 x+\phi(x,y)]}\right)$$

$$= I_0(x,y) + \frac{1}{2}m(x,y)e^{i\phi(x,y)}e^{i2\pi\nu_0 x} + \frac{1}{2}m(x,y)e^{-i\phi(x,y)}e^{-i2\pi\nu_0 x}$$

$$= I_0(x,y) + c(x,y)e^{i2\pi\nu_0 x} + c^*(x,y)e^{-i2\pi\nu_0 x}$$

$$c(x,y) \equiv \frac{1}{2}m(x,y)e^{i\phi(x,y)} \qquad \phi(x,y) = \tan^{-1}\left(\frac{\mathrm{Im}[c(x,y)]}{\mathrm{Re}[c(x,y)]}\right)$$

$$\hat{g}(f_x, y) \equiv \mathrm{FT}[g(x,y)]$$

$$\hat{g}(f_x - \nu_0, y) = \mathrm{FT}\left[g(x,y)e^{i2\pi\nu_0 x}\right]$$

$$\hat{I}(f_x, y) = \hat{I}_0(f_x, y) + \hat{c}(f_x - \nu_0, y) + \hat{c}^*(f_x + \nu_0, y)$$

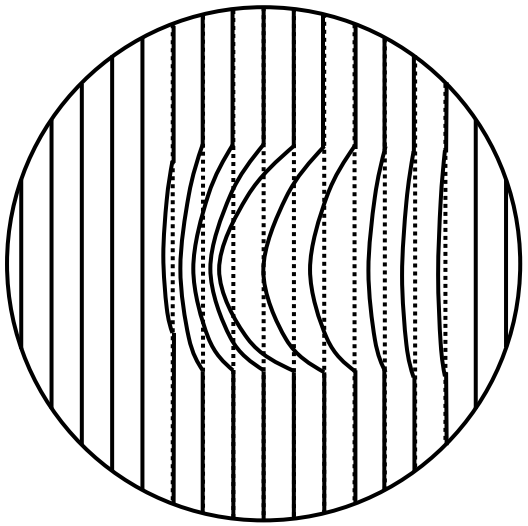

Basic knowledge of Fourier transform

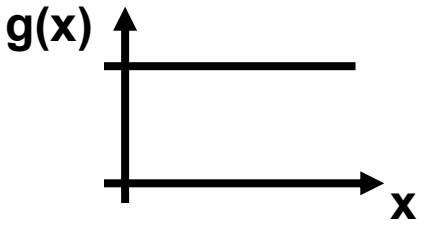

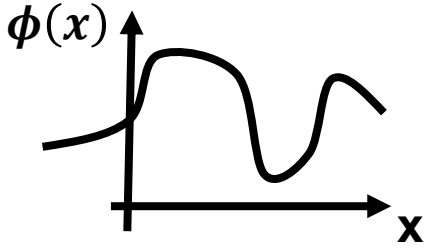

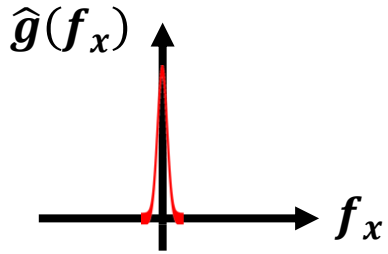

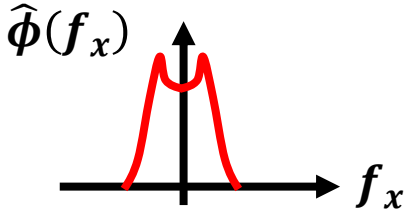

$$\mathbf{h}(x) = \phi(x) \times e^{-\mathrm{i}2\pi\nu_0 x}$$

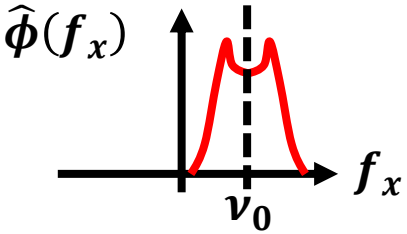

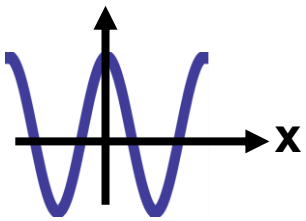

$$\mathbf{g}(x) = cos(2\pi\nu_0 x) = \frac{e^{\mathrm{i}2\pi\nu_0 x} + e^{-\mathrm{i}2\pi\nu_0 x}}{2}$$

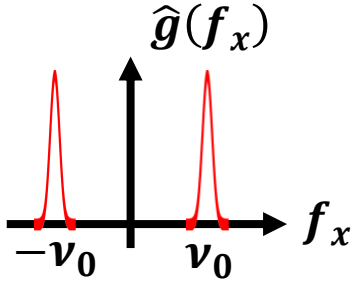

Procedure of retrieving data

$$\mathbf{I}(x) = I_0(x) + m(x)\cos[2\pi\nu_0 x + \phi(x)]$$
$$\equiv \cos[2\pi\nu_0 x + \phi(x)]$$
$$= c^*(x,y)e^{i2\pi\nu_0 x} + c(x,y)e^{-i2\pi\nu_0 x}$$

$$\hat{I}(f_x) = \hat{c}(f_x - \nu_0) + \hat{c}^*(f_x + \nu_0)$$

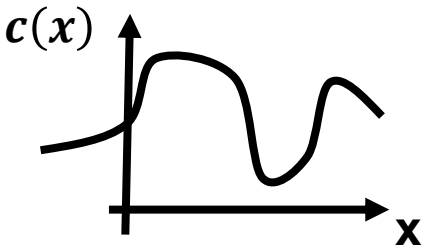

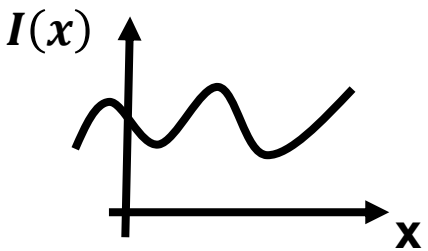

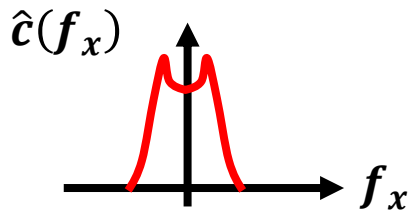

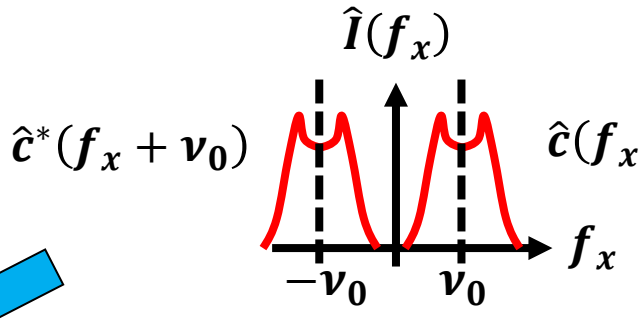

Filter

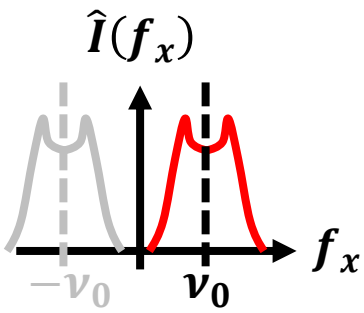

Shift

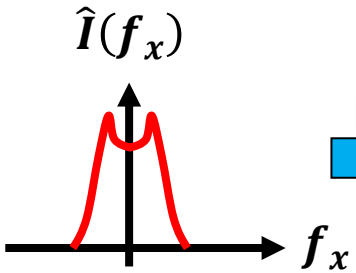

FT^{-1}

$$c(x,y) \equiv \frac{1}{2}e^{-i\phi(x,y)}$$

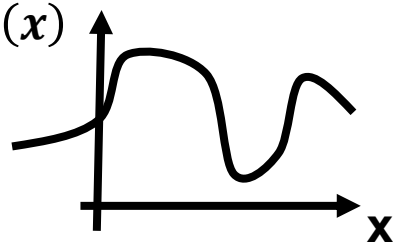

Example of retrieving data from 1D interferometer

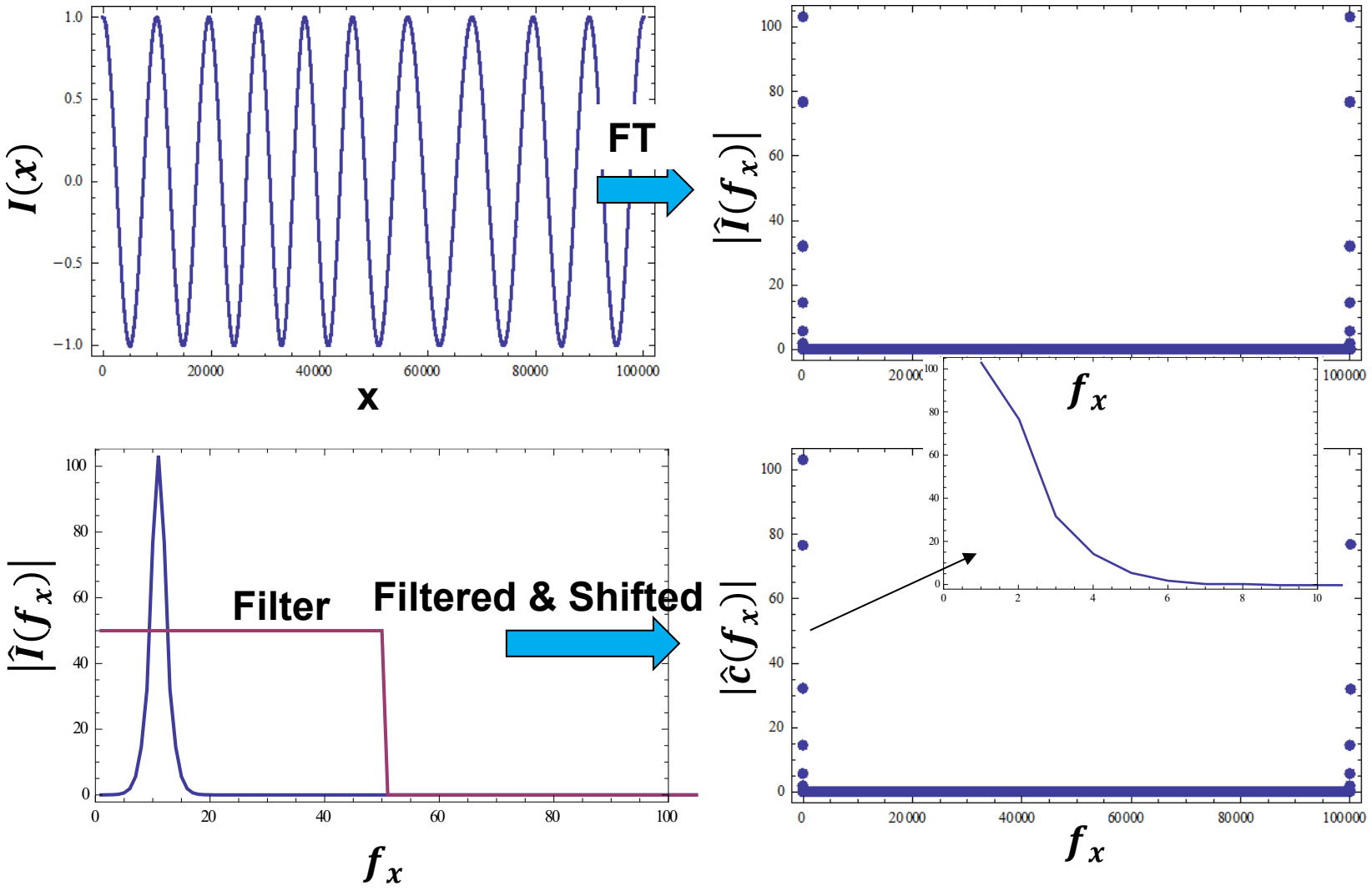

The retrieved data need to be modified if the phase change is too much

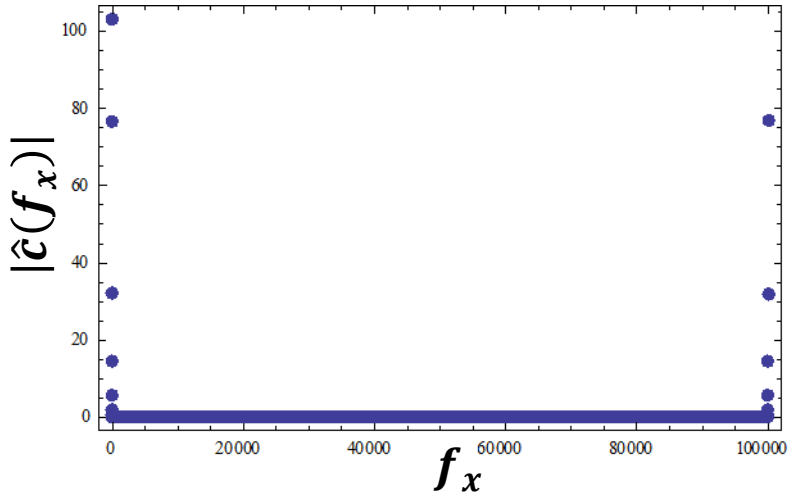

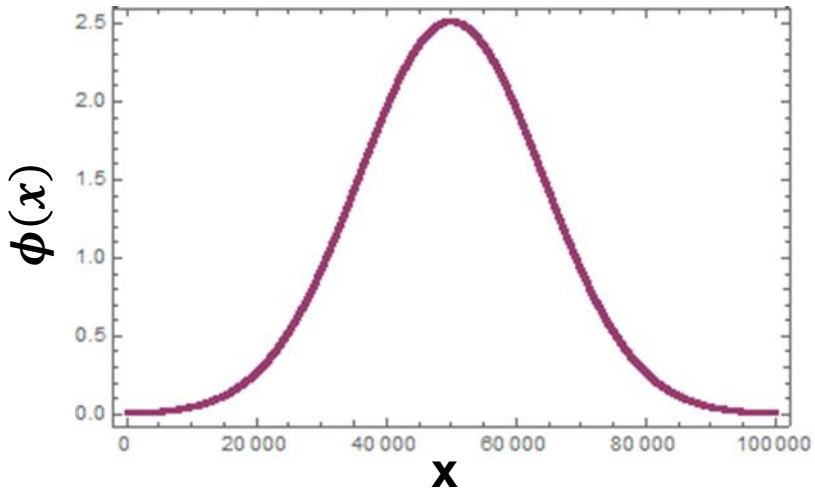

FT^{-1}& $\phi(x) = tan^{-1}\left(\frac{Im[c(x)]}{Re[c(x)]}\right)$

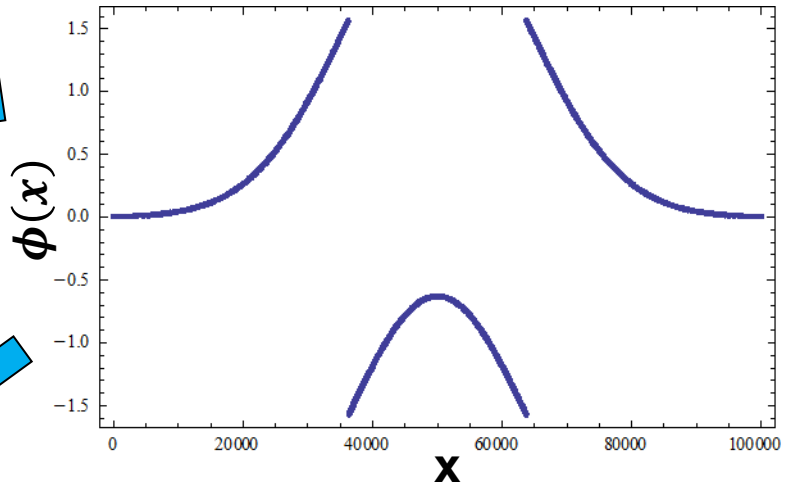

The final phase difference needs to be determined manually since it may exceeds 2π

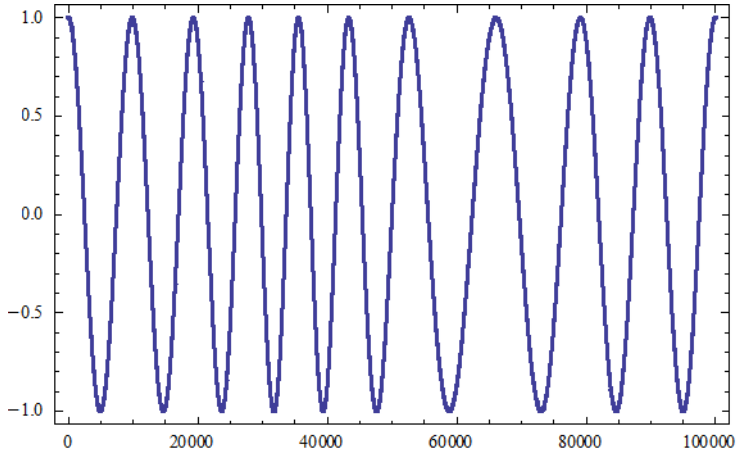

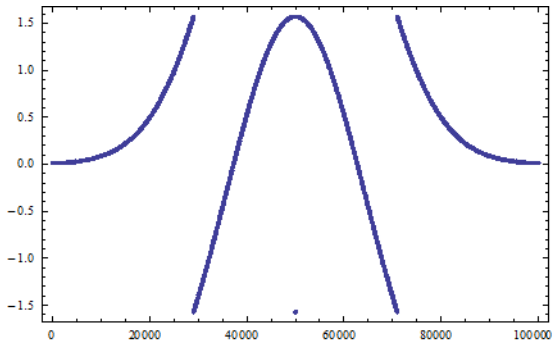

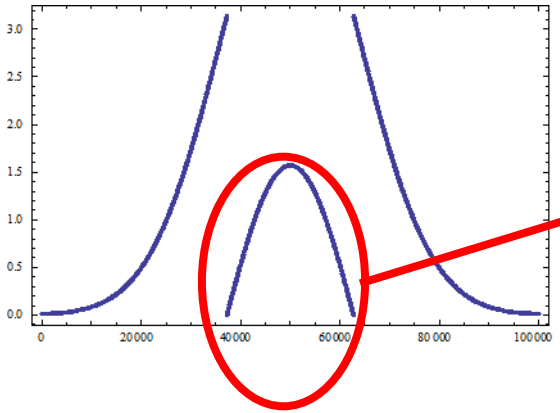

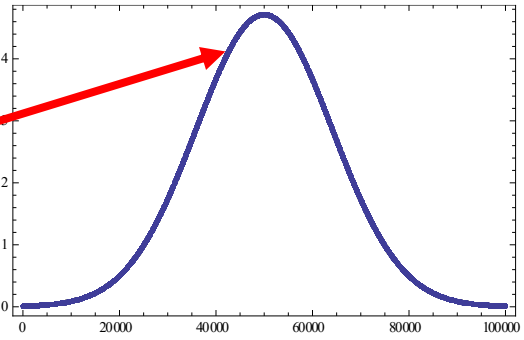

Example of retrieving data from 2D interferometer

$$\mathbf{I}(x,y) = \cos[2\pi\nu_0 x + \phi(x,y)]$$

$$\hat{I}(f_x, y) = \hat{c}(f_x - \nu_0, y) + \hat{c}^*(f_x + \nu_0, y)$$

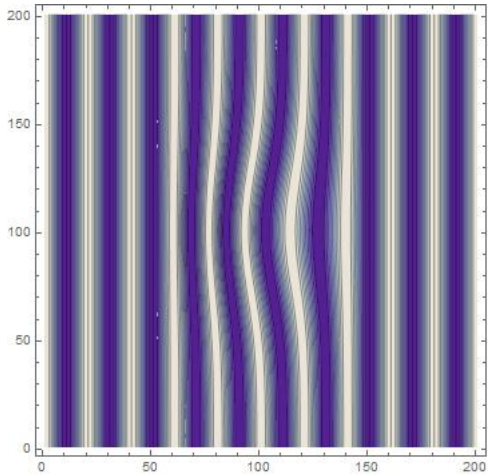

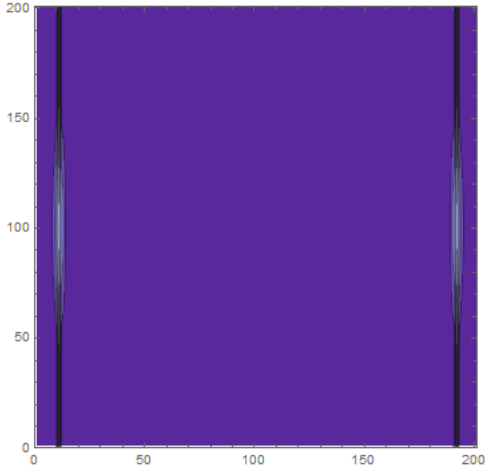

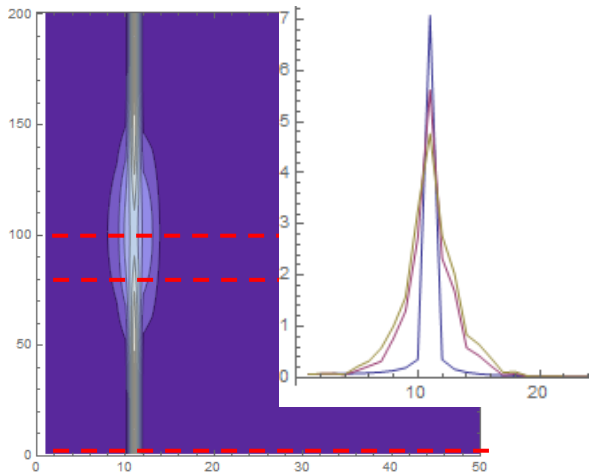

Filter

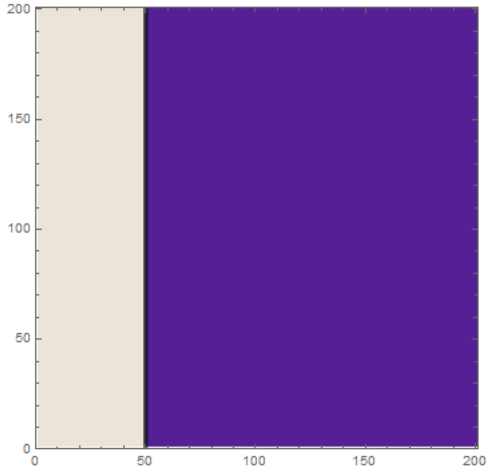

Filtered & Shifted

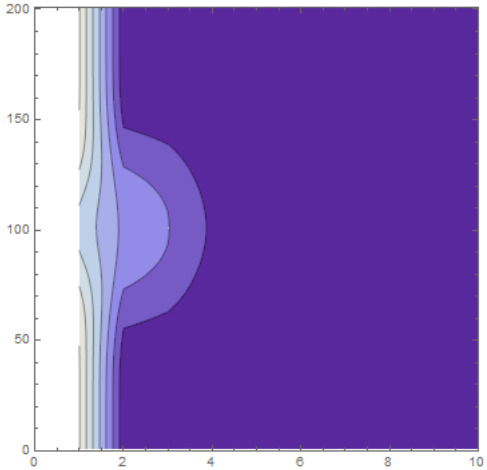

Retrieved data

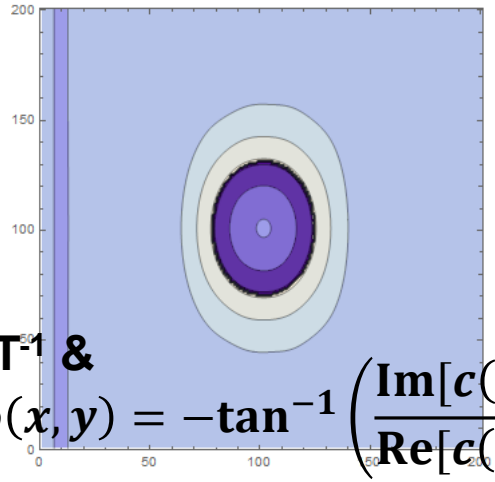

FT^{-1} &

$$\phi(x,y) = -\tan^{-1}\left(\frac{\mathrm{Im}[c(x,y)]}{\mathrm{Re}[c(x,y)]}\right)$$

The retrieved data may need to be modified if the phase change is too large

Retrieved data

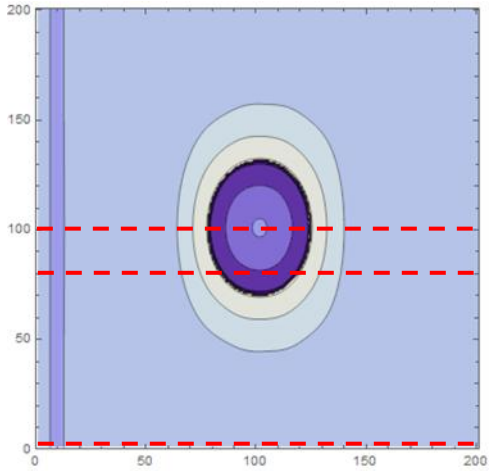

1D profile

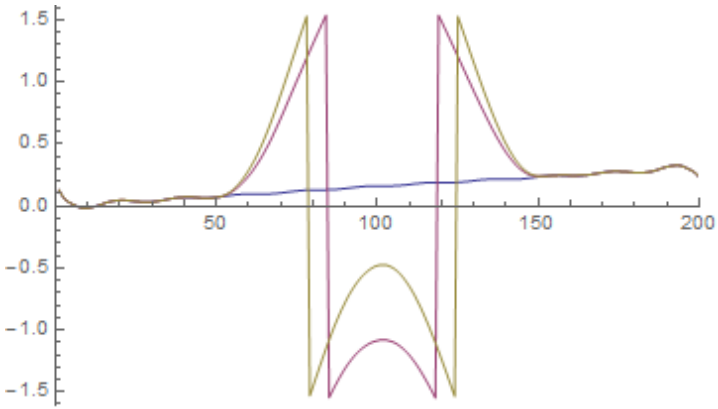

Modified result

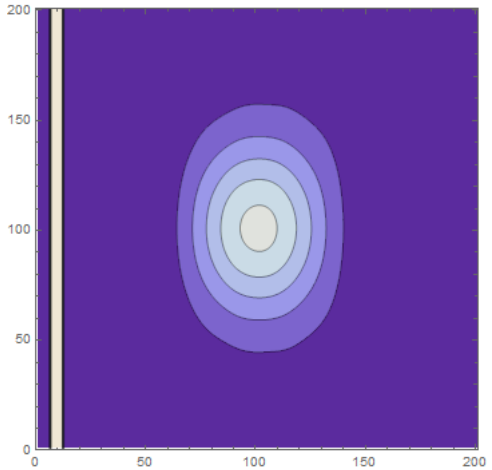

- **Noise came from low spatial resolution.**

Schlieren imaging system can detect density gradient

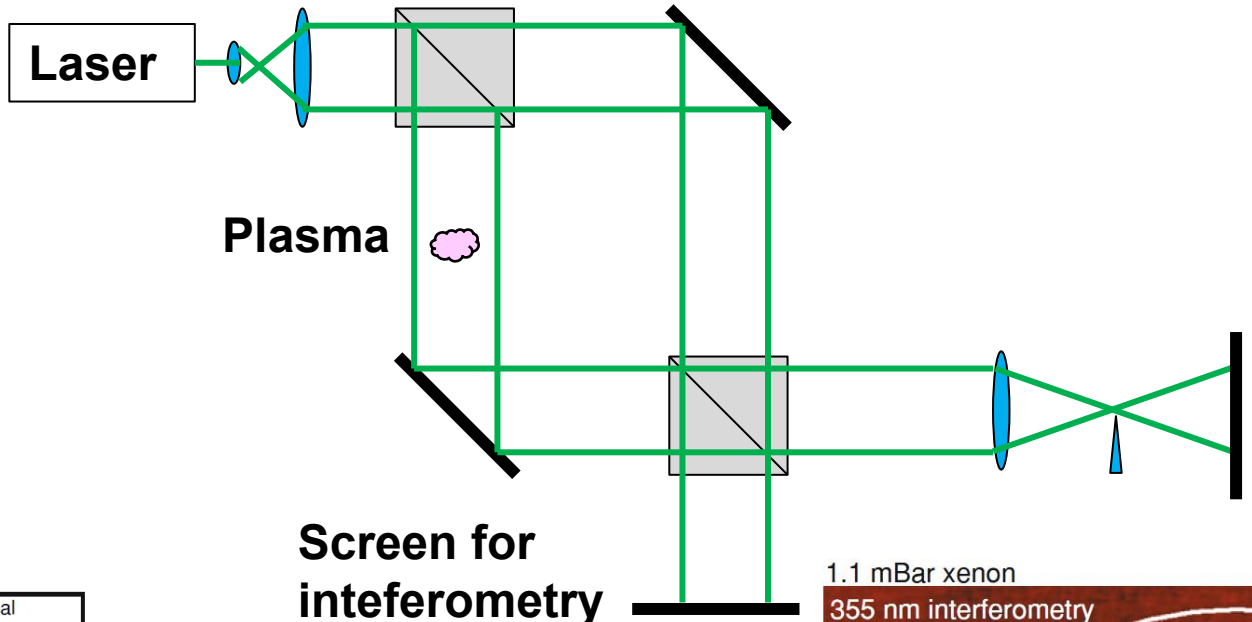

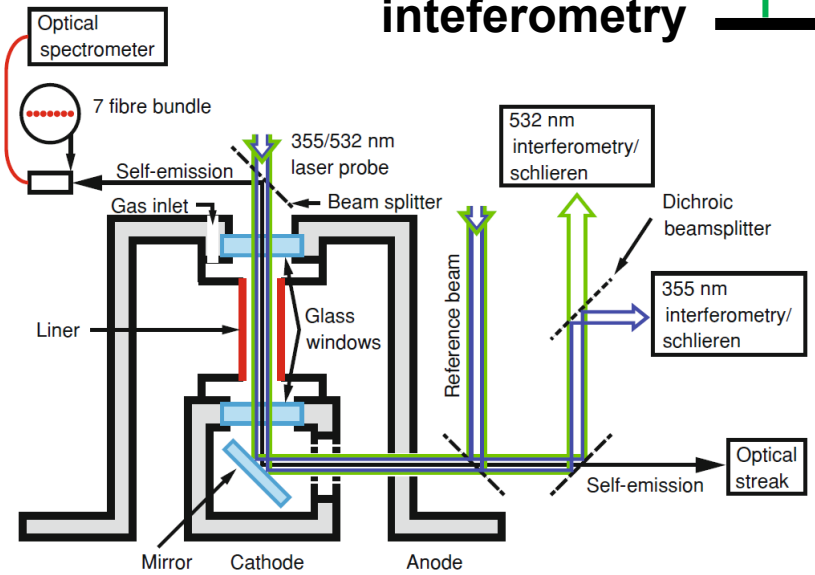

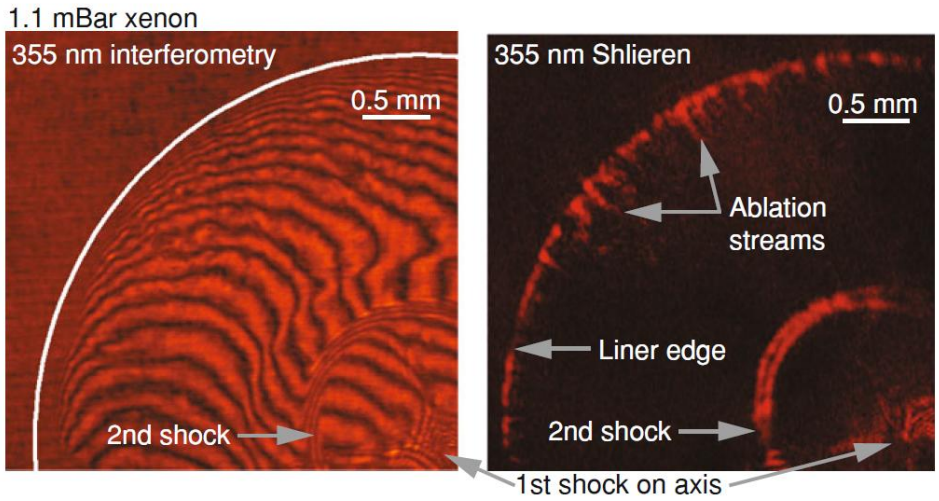

G. C. Burdiak, Cylindrical liner z-pinches as drivers for converging strong shock experiments

Angular filter refractometry (AFR) maps the refraction of the probe beam at TCC to contours in the image plane

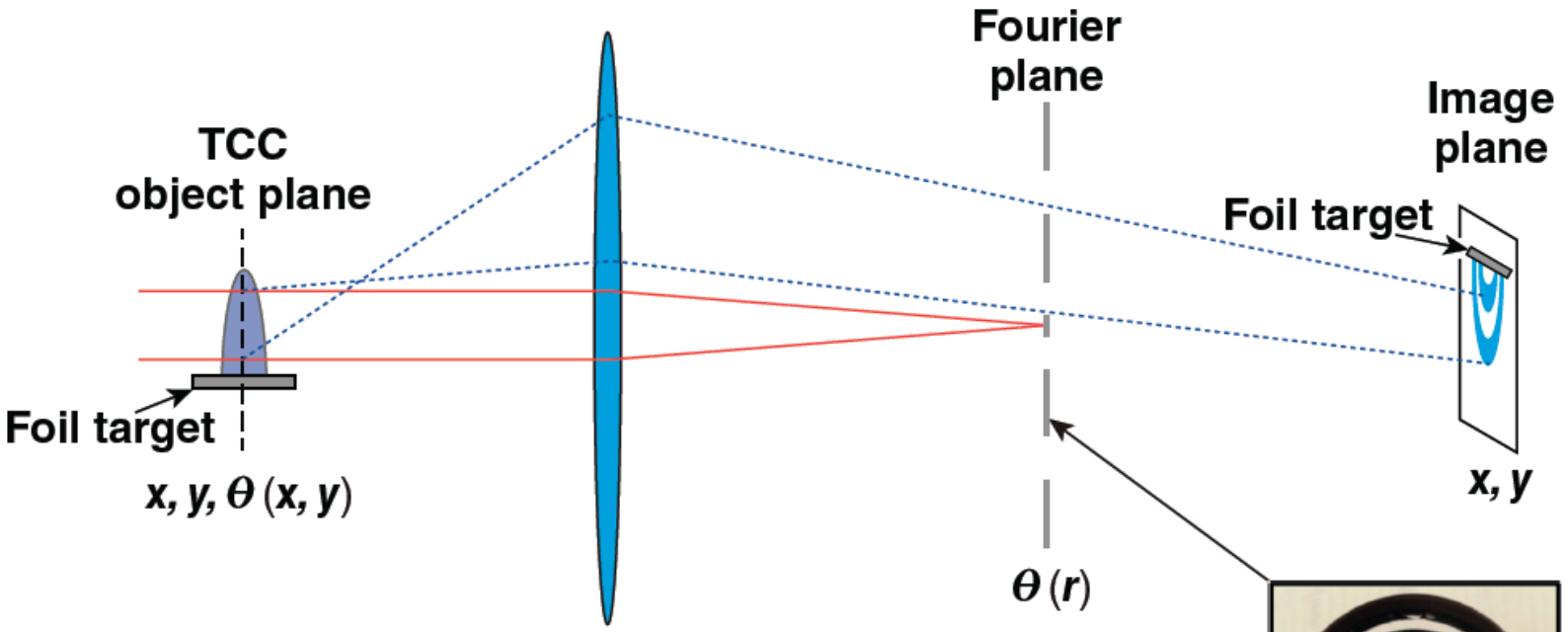

The edges of the rings map a certain refraction angle to the spatial location in the object plane.

Angular spectrum of plane waves can be used for diagnostic

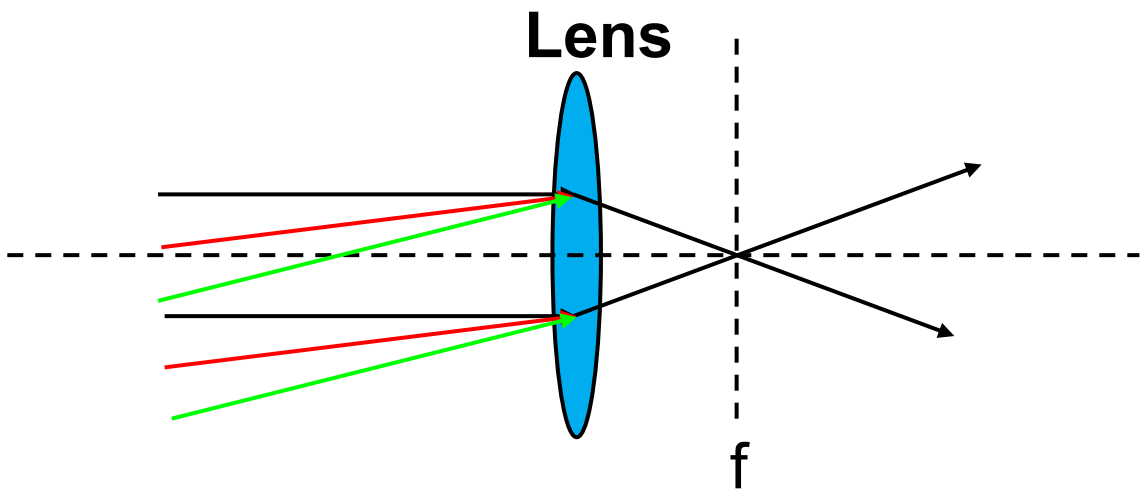

Angular spectrum of plane waves can be used for diagnostic

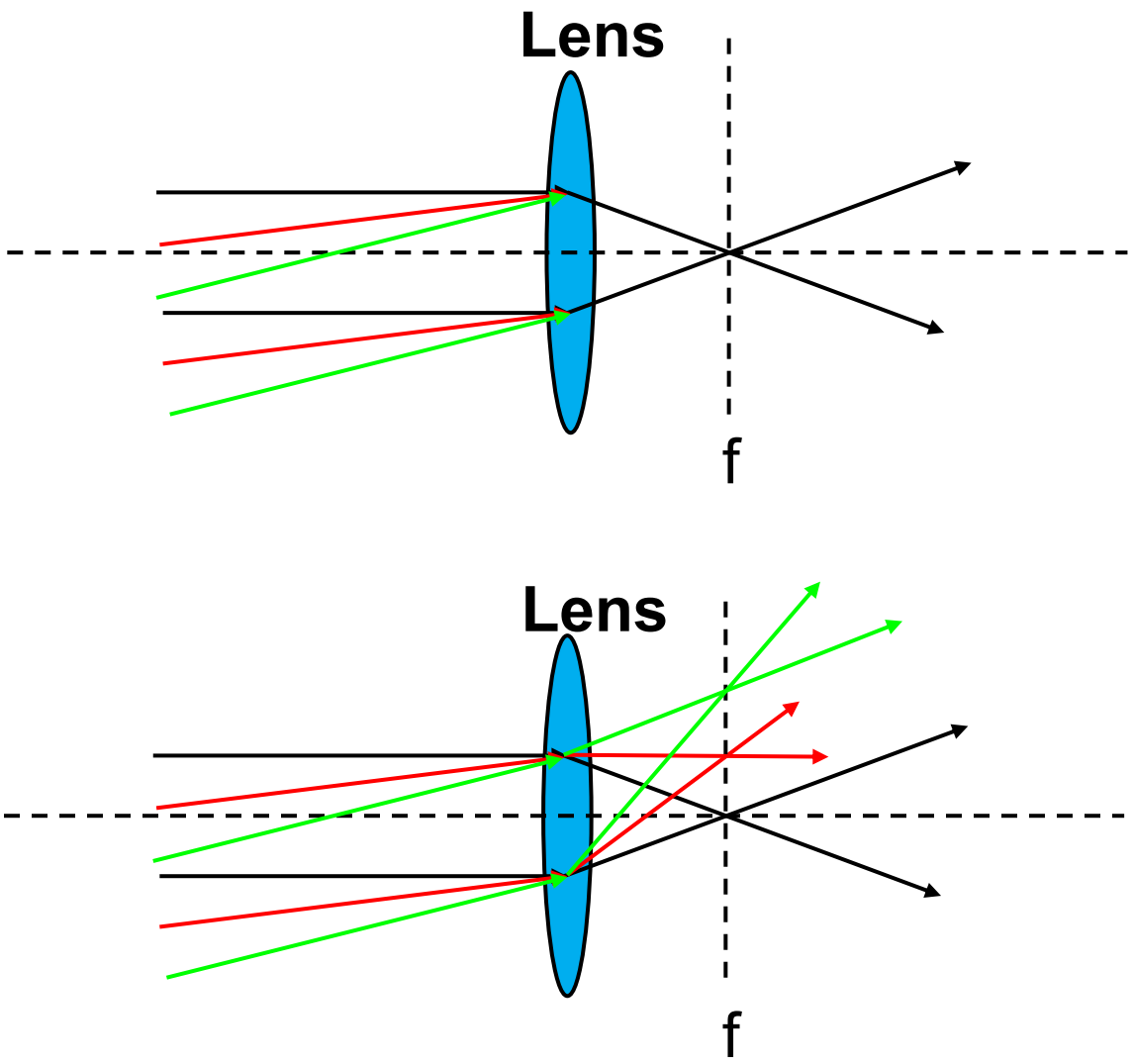

Rays with different angles go through different focal points on the focal points

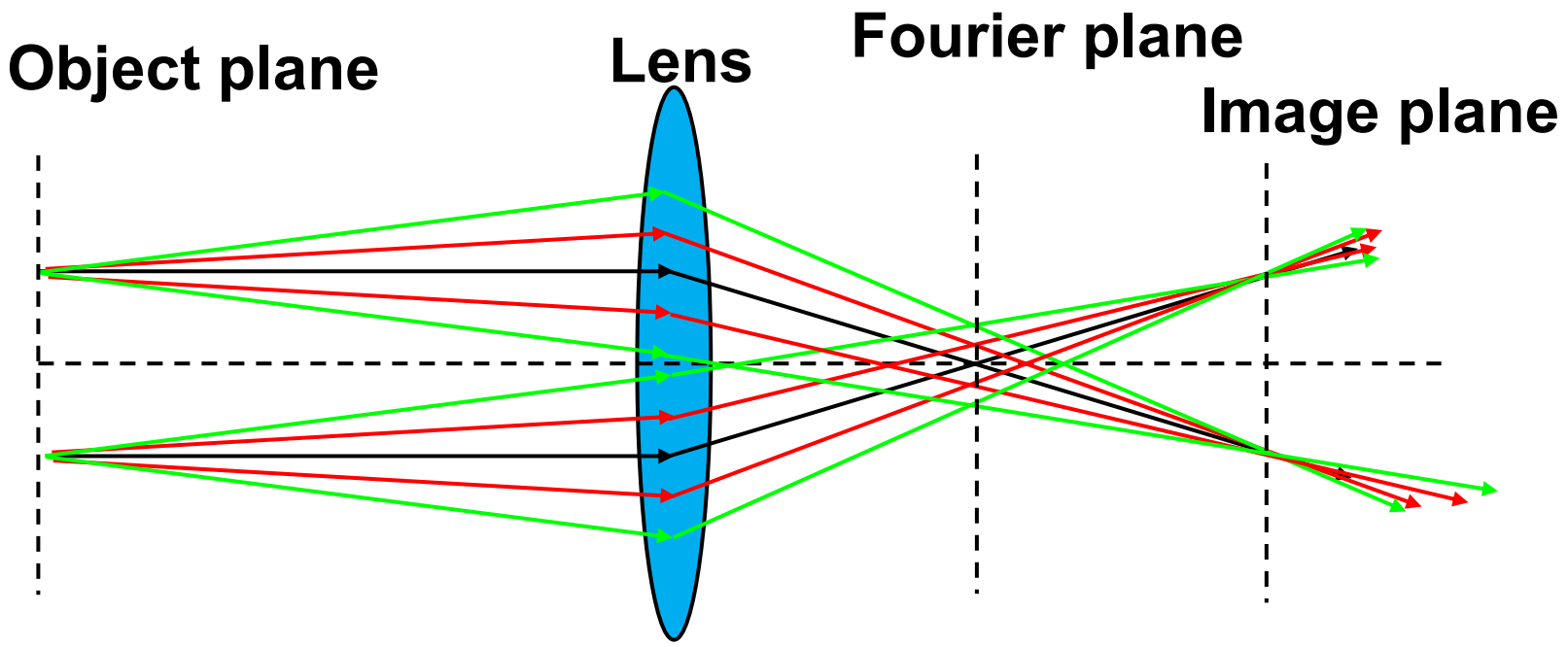

Rays with different angles can be selected by blocking different focal points

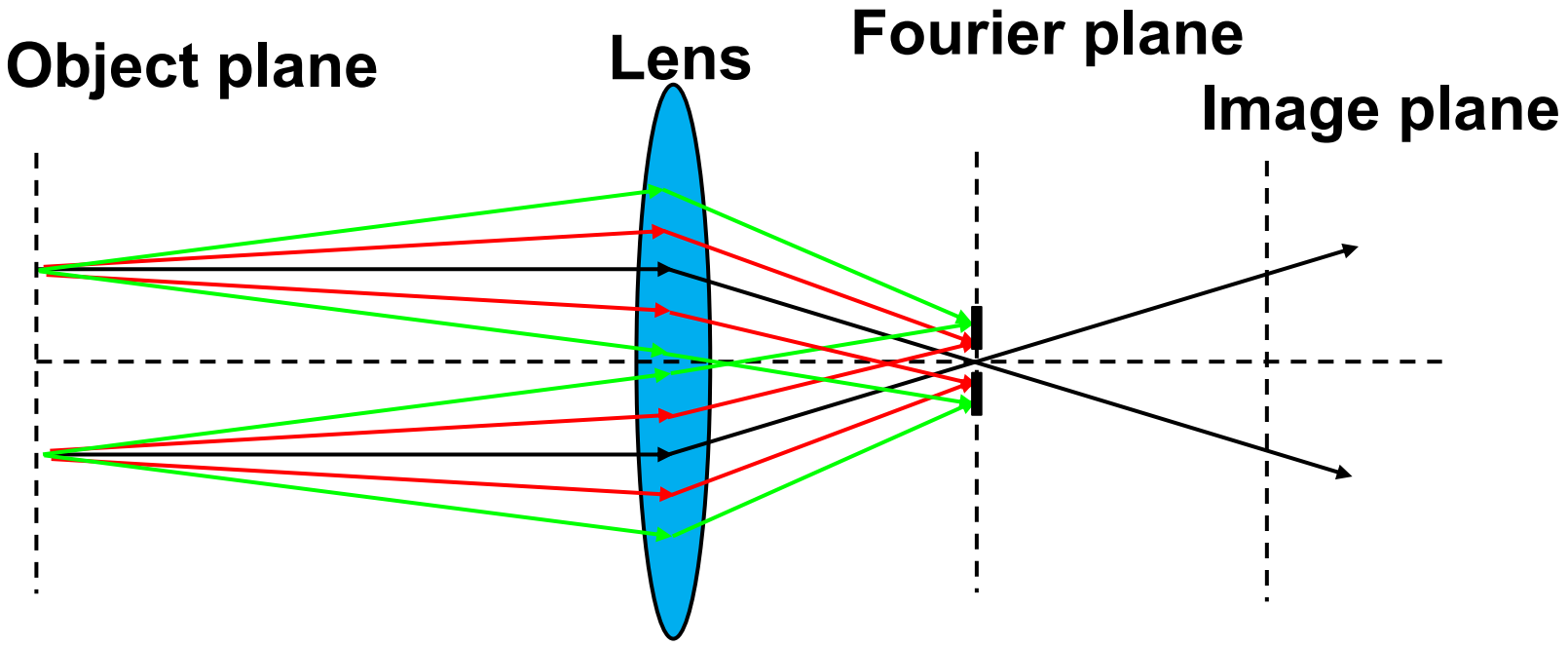

Rays with different angles go through different focal points on the focal points

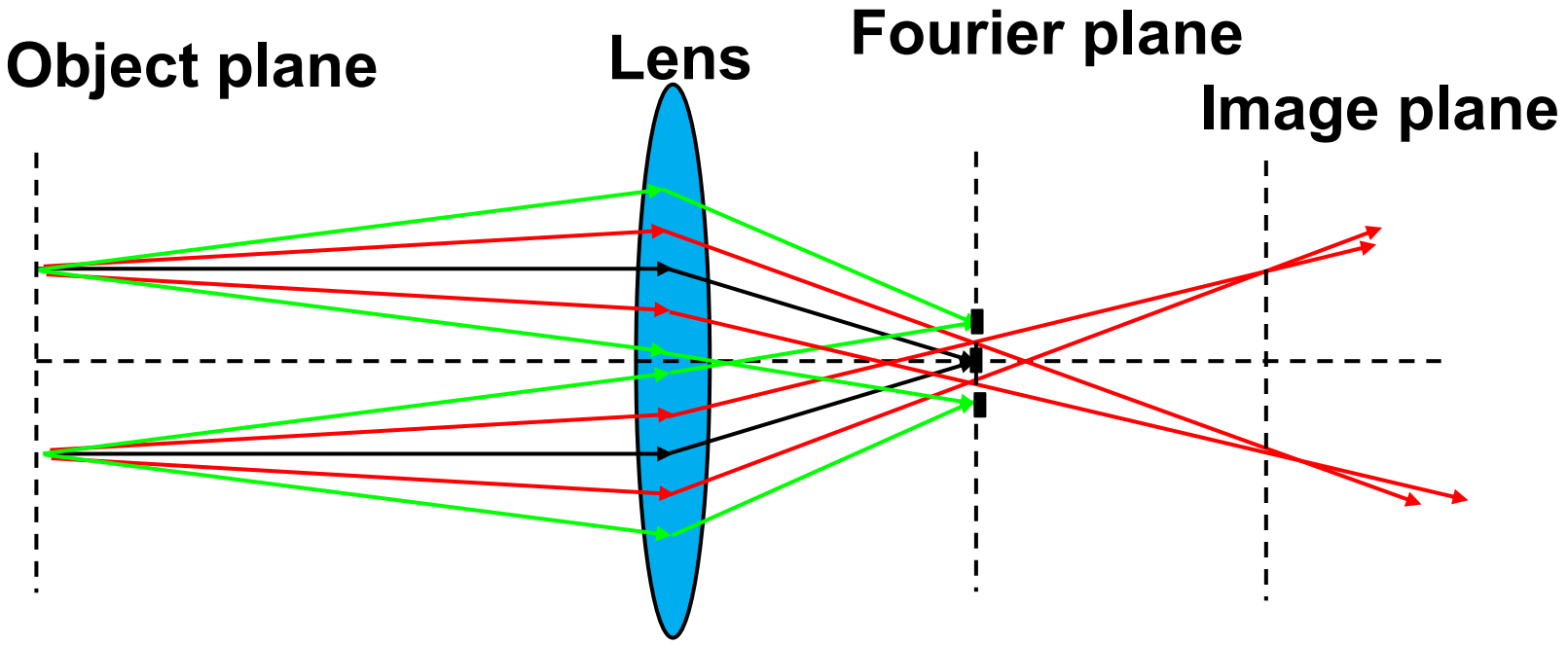

Rays with different angles go through different focal points on the focal points

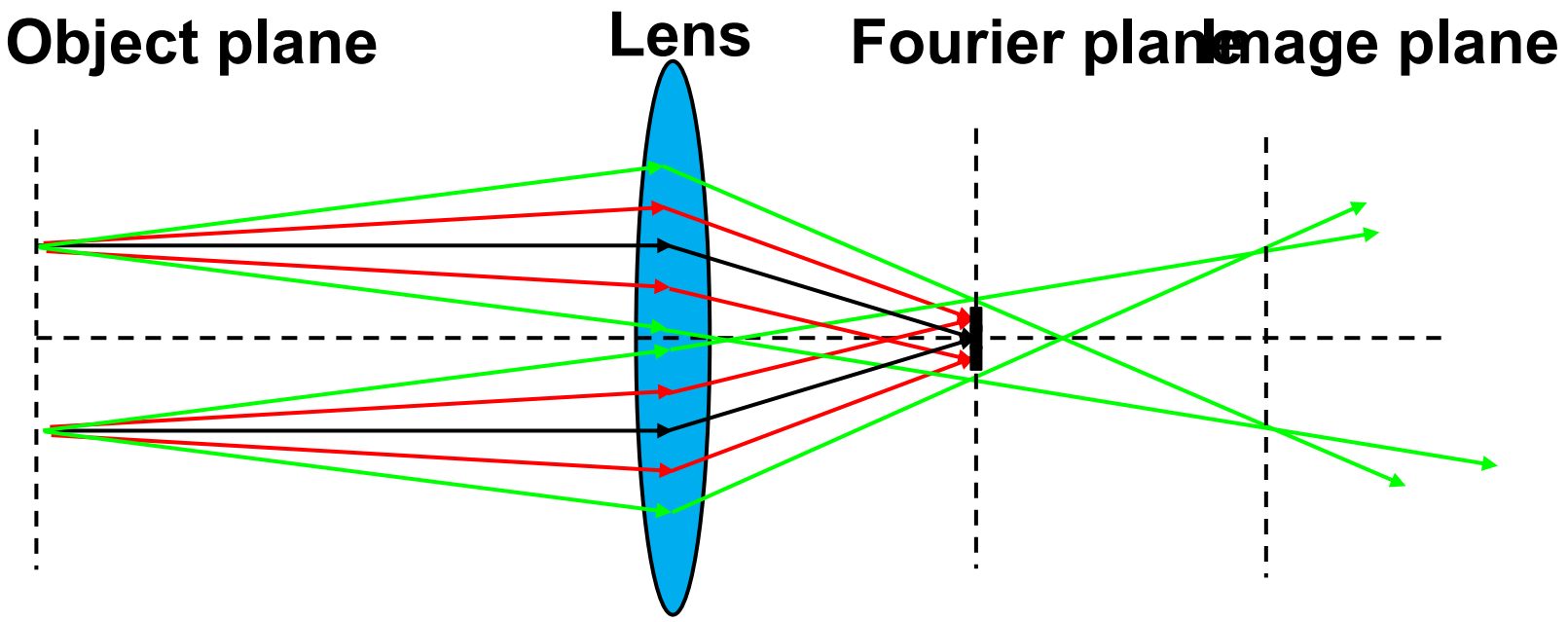

Angular filter refractometry (AFR) maps the refraction of the probe beam at TCC to contours in the image plane

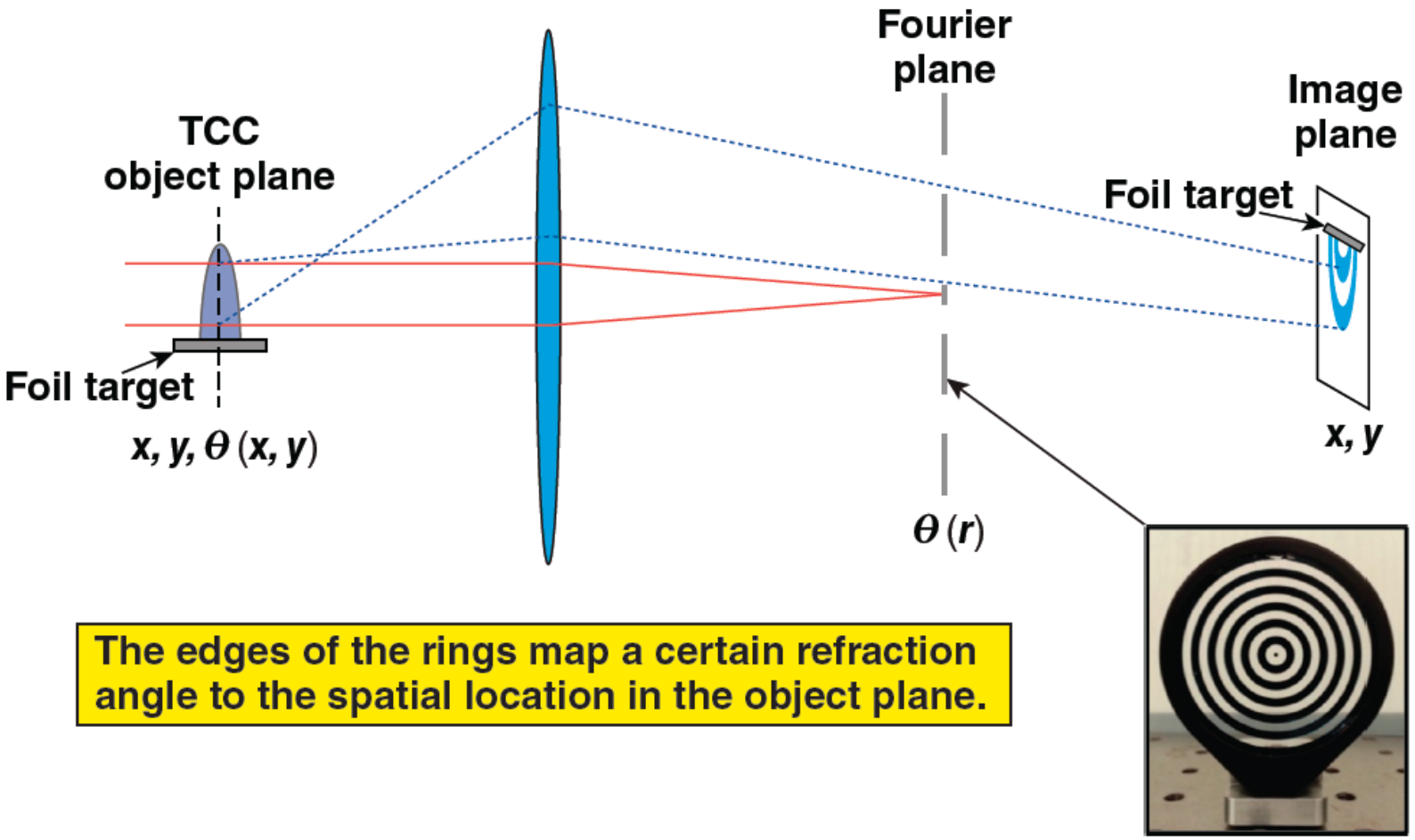

The edges of the rings map a certain refraction angle to the spatial location in the object plane.

Channeling of multi-kilojoule high-intensity laser beams in an inhomogeneous plasma was observed using AFR

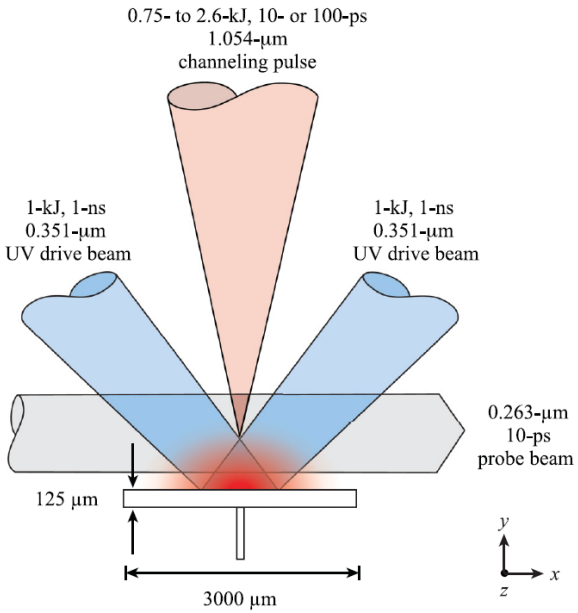

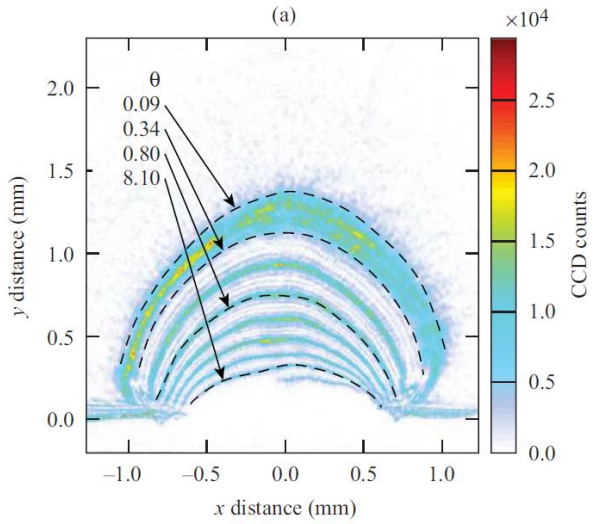

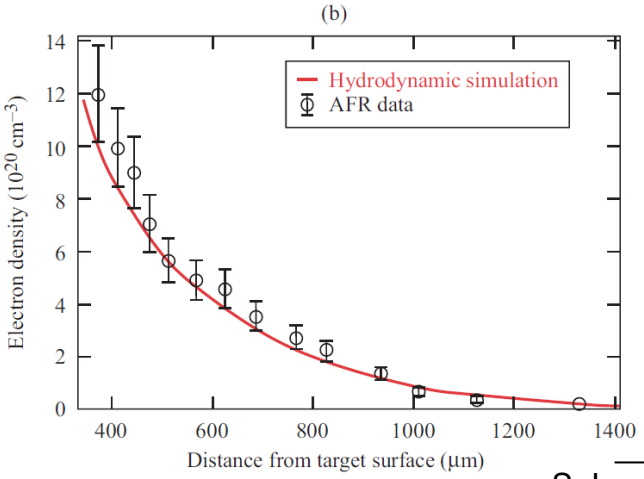

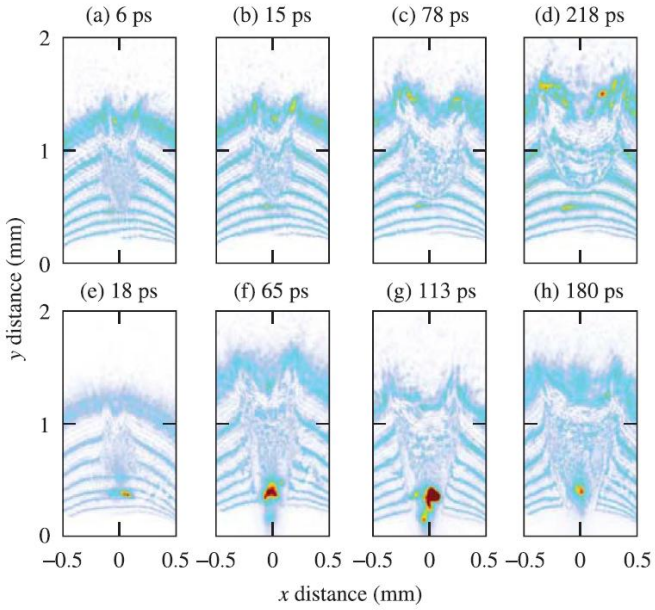

S. Ivancic *et al.*, Phys. Rev. E 91 , 051101 (2015)

Electromagnetic wave can be used to measure the density or the magnetic field in the plasma

- **Nonmagnetized isotropic plasma (interferometer needed):**

$$n^2 = 1 - \frac{X\left(1-X\right)}{1-X-\frac{1}{2}Y^2\sin^2\theta \pm \left[\left(\frac{1}{2}Y^2\sin^2\theta\right)^2 + \left(1-X\right)^2 Y^2\cos^2\theta\right]^{1/2}}$$

$$= 1 - X = 1 - \frac{\omega_{\mathrm{p}}^2}{\omega^2} = 1 - \frac{n_{\mathrm{e}}}{n_{\mathrm{cr}}} \qquad \left(\boldsymbol{Y \equiv \frac{\Omega}{\omega} \equiv 0}\right)$$

Note: $\omega_{\mathrm{p}}^2 = \dfrac{n_{\mathrm{e}}e^2}{\epsilon_0 m_{\mathrm{e}}}$ $\qquad n_{\mathrm{cr}} = \dfrac{\epsilon_0 m_{\mathrm{e}}\omega^2}{e^2}$

- **Magnetized isotropic plasma (Polarization detected needed):**

Parallel to B_0

$$n^2 = 1 - \frac{\omega_{\mathrm{p}}^2}{\omega\left(\omega \pm \Omega\right)} \qquad \frac{E_{\mathrm{x}}}{E_{\mathrm{y}}} = \pm i \qquad \Omega \equiv \frac{eB_0}{m_{\mathrm{e}}}$$

Faraday rotation: linear polarization rotation caused by the difference between the speed of LHC and RHC polarized wave.

Circular polarization

$$E_x = E_0 \exp(-i\omega t)$$

$$E_y = iE_x = iE_0 \exp(-i\omega t) = E_0 \exp\left(i\frac{\pi}{2}\right) \exp(-i\omega t) = E_0 \exp\left[-i\left(\omega t - \frac{\pi}{2}\right)\right]$$

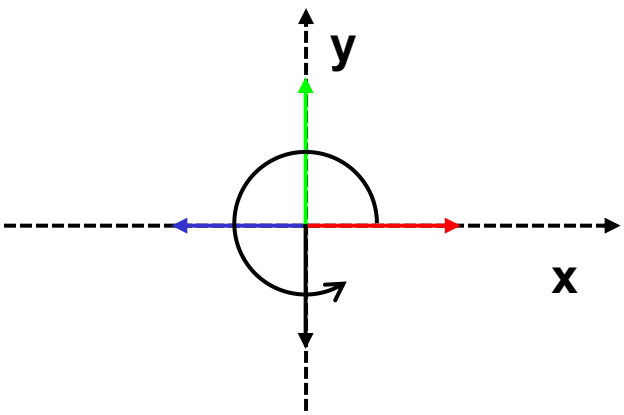

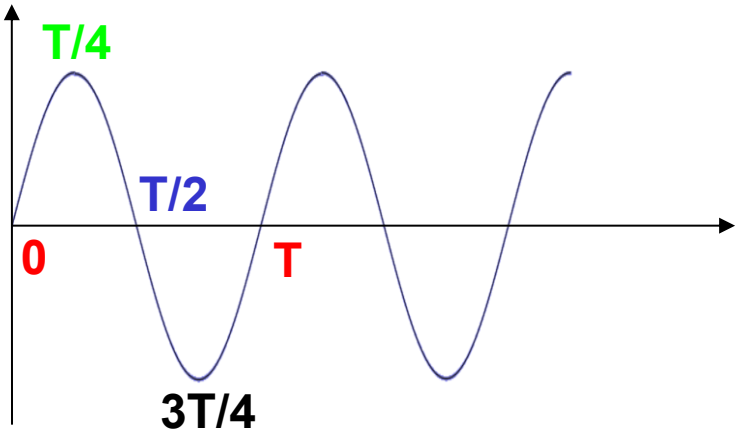

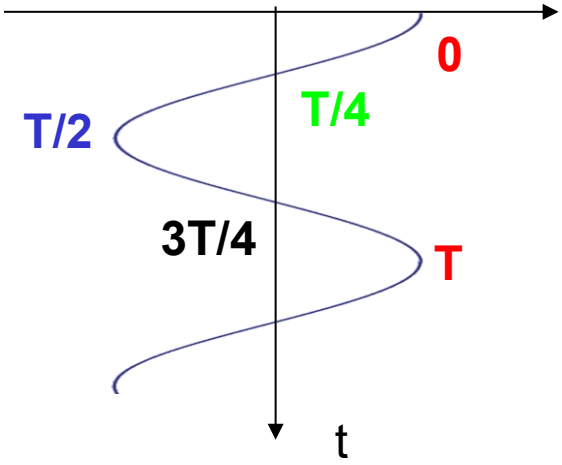

Linear polarization rotates as the wave propagates with different speed in LHC and RHC polarization

$$\vec{E} = E_0\hat{x} = \frac{E_0}{2}\left[(\hat{x}+i\hat{y})+(\hat{x}-i\hat{y})\right]$$

$$\vec{E}(z) = \vec{E}\exp(i\phi) \qquad \phi_{\mathrm{R}} \neq \phi_{\mathrm{L}} \qquad \bar{\phi} \equiv \frac{\phi_{\mathrm{R}}+\phi_{\mathrm{L}}}{2} \quad , \quad \Delta\phi = \frac{\phi_{\mathrm{R}}-\phi_{\mathrm{L}}}{2}$$

$$\begin{aligned}
\vec{E}(z) &= \frac{E_0}{2}\left[(\hat{x}+i\hat{y})\,e^{i\phi_{\mathrm{R}}}+(\hat{x}-i\hat{y})\,e^{i\phi_{\mathrm{L}}}\right] \\
&= \frac{E_0}{2}\left[\hat{x}\left(e^{i\phi_{\mathrm{R}}}+e^{i\phi_{\mathrm{L}}}\right)+\hat{y}i\left(e^{i\phi_{\mathrm{R}}}-e^{i\phi_{\mathrm{L}}}\right)\right] \\
&= \frac{E_0}{2}\left[\hat{x}\left(e^{i(\bar{\phi}+\Delta\phi)}+e^{i(\bar{\phi}+\Delta\phi)}\right)+\hat{y}i\left(e^{i(\bar{\phi}+\Delta\phi)}-e^{i(\bar{\phi}+\Delta\phi)}\right)\right] \\
&= E_0 e^{i\bar{\phi}}\left[\hat{x}\cos\left(\frac{\Delta\phi}{2}\right)+\hat{y}\sin\left(\frac{\Delta\phi}{2}\right)\right]
\end{aligned}$$

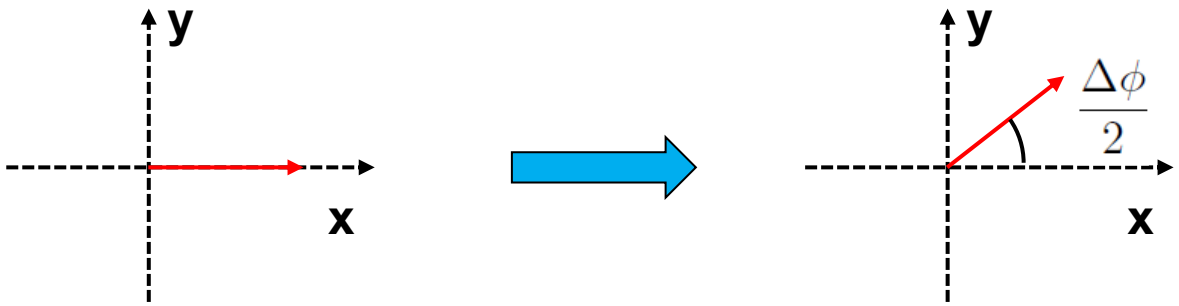

The rotation angle of the polarization depends on the linear integral of magnetic field and electron density

$$\phi = \int k dl = \int n \frac{\omega}{c} dl \qquad \alpha = \frac{\Delta\phi}{2} = \frac{\omega}{2c} \int (n_{\mathrm{R}} - n_{\mathrm{L}})\, dl$$

$$n_{\mathrm{R}} = \sqrt{1 - \frac{X}{1+Y}} \sim 1 - \frac{1}{2}\frac{X}{1+Y} \qquad X, Y << 1$$

$$n_{\mathrm{L}} \sim 1 - \frac{1}{2}\frac{X}{1-Y} \qquad \frac{X}{1 \pm Y} << 1$$

$$n_{\mathrm{R}} - n_{\mathrm{L}} \sim \frac{X}{2}\left(\frac{1}{1-Y} - \frac{1}{1+Y}\right) = \frac{XY}{1-Y^2} \sim XY$$

$$\alpha \sim \frac{\omega}{2c} \int XY\, dl = \frac{\omega}{2c} \int \frac{\omega_{\mathrm{p}}^2}{\omega^2}\frac{\Omega}{\omega} dl = \frac{1}{2c} \int \frac{n_{\mathrm{e}}}{n_{\mathrm{cr}}}\frac{eB}{m_{\mathrm{e}}} dl$$

$$= \frac{e}{2cm_{\mathrm{e}}n_{\mathrm{cr}}} \int n_{\mathrm{e}} B dl$$

The rotation angle of the polarization depends on the linear integral of magnetic field and electron density

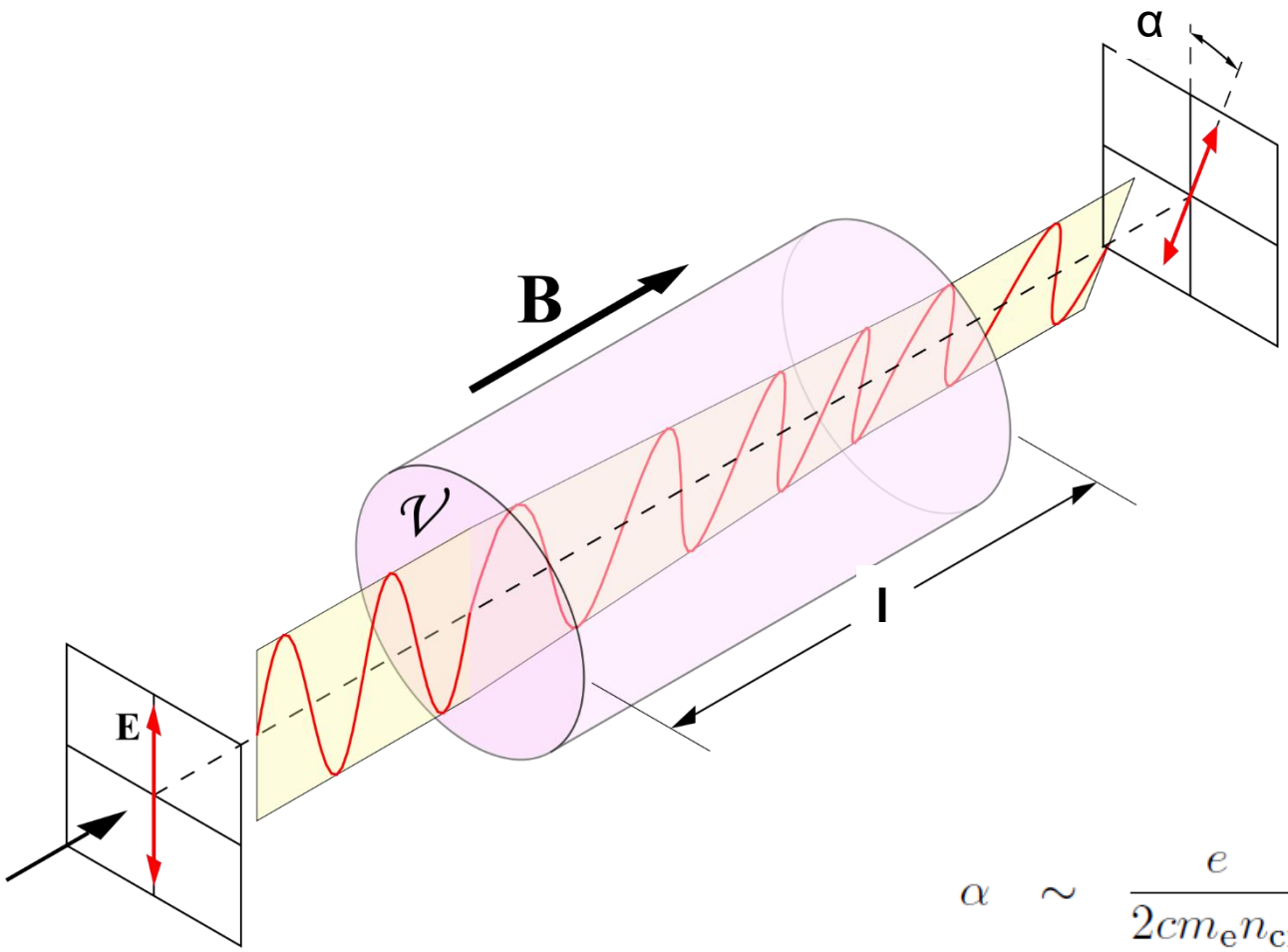

$$\alpha \sim \frac{e}{2cm_e n_{cr}} \int n_e B dl$$

Magnetic field can be generated when the temperature and density gradients are not parallel to each other

$$\frac{\partial \vec{B}}{\partial t} = \nabla \times \left[\underbrace{\vec{u} \times \vec{B}}_{\text{Convection term}} + \underbrace{\frac{1}{\sigma \mu_0} \nabla \times \vec{B}}_{\text{Diffusion term}} + \underbrace{\frac{\nabla p_\mathrm{e}}{n_\mathrm{e} e}}_{\text{self generated field}} \underbrace{- \frac{1}{\mu_0} \left(\frac{\nabla \times \vec{B}}{n_\mathrm{e} e} \times \vec{B} \right)}_{\text{Hall term}} \right]$$

$$\nabla \times \frac{\nabla p_\mathrm{e}}{n_\mathrm{e} e} = -\frac{k_\mathrm{B}}{e} \frac{\nabla n_\mathrm{e} \times \nabla T_\mathrm{e}}{n_\mathrm{e}}$$

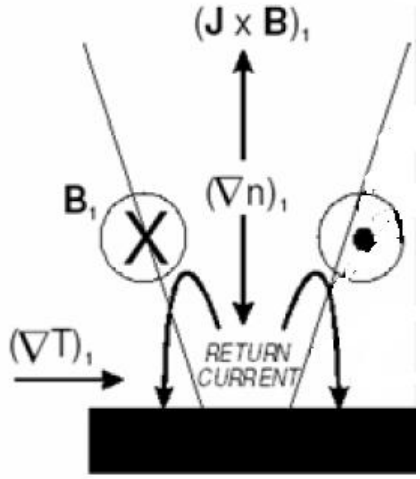

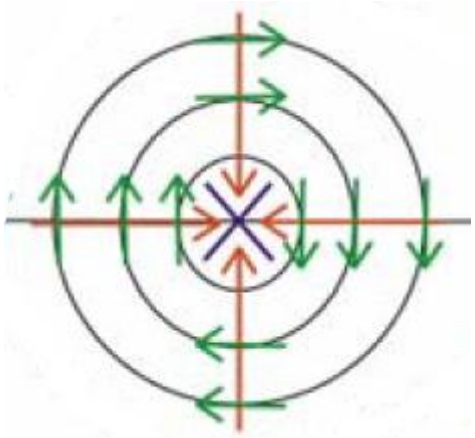

(grad n_e) × (grad T_e) ⟶ B field ⟶

P M Nilson *et al.*, Central Laser Facility Annual Report 2004/2005

Polarimetry diagnostic can be used to measure the magnetic field

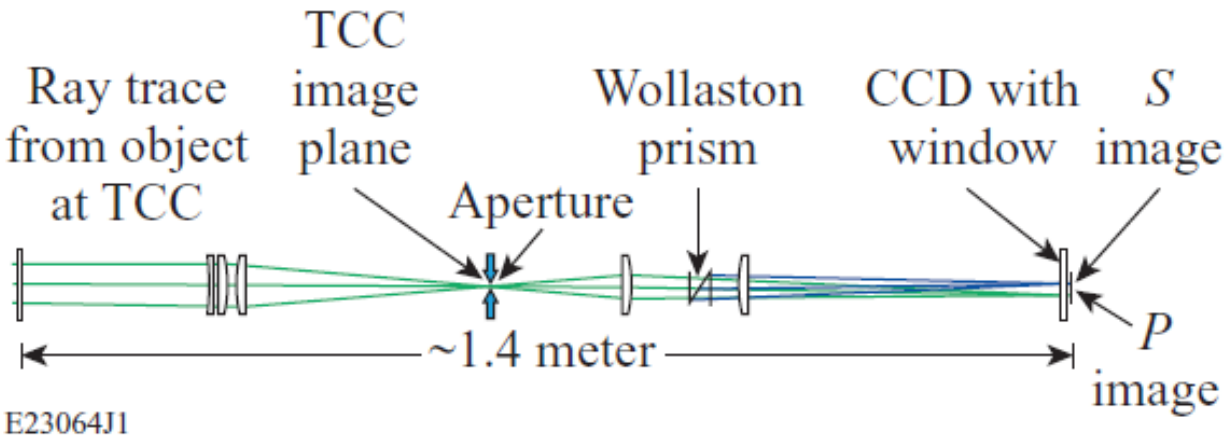

Wollaston prism

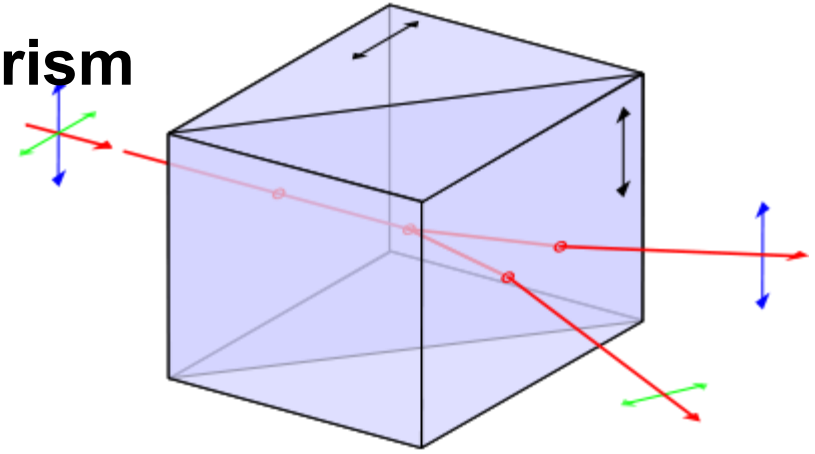

A. Davies *et al.*, Rev. Sci. Instrum. **85**, 11E611 (2014)

Self-generated field was suggested when multi-kilojoule high-intensity laser beams illuminated on an inhomogeneous plasma

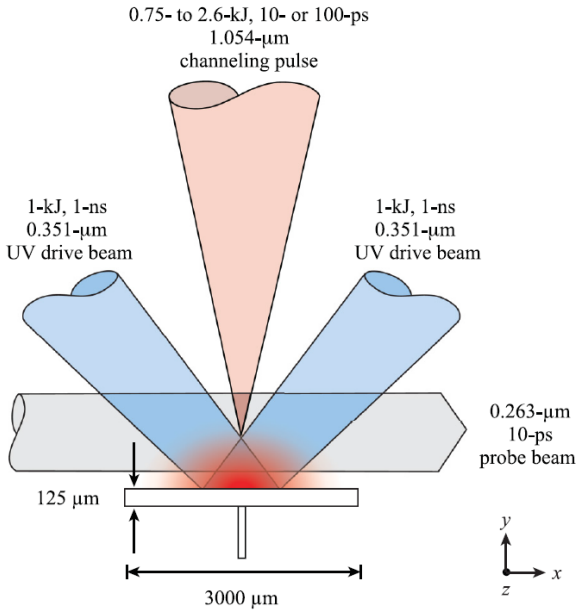

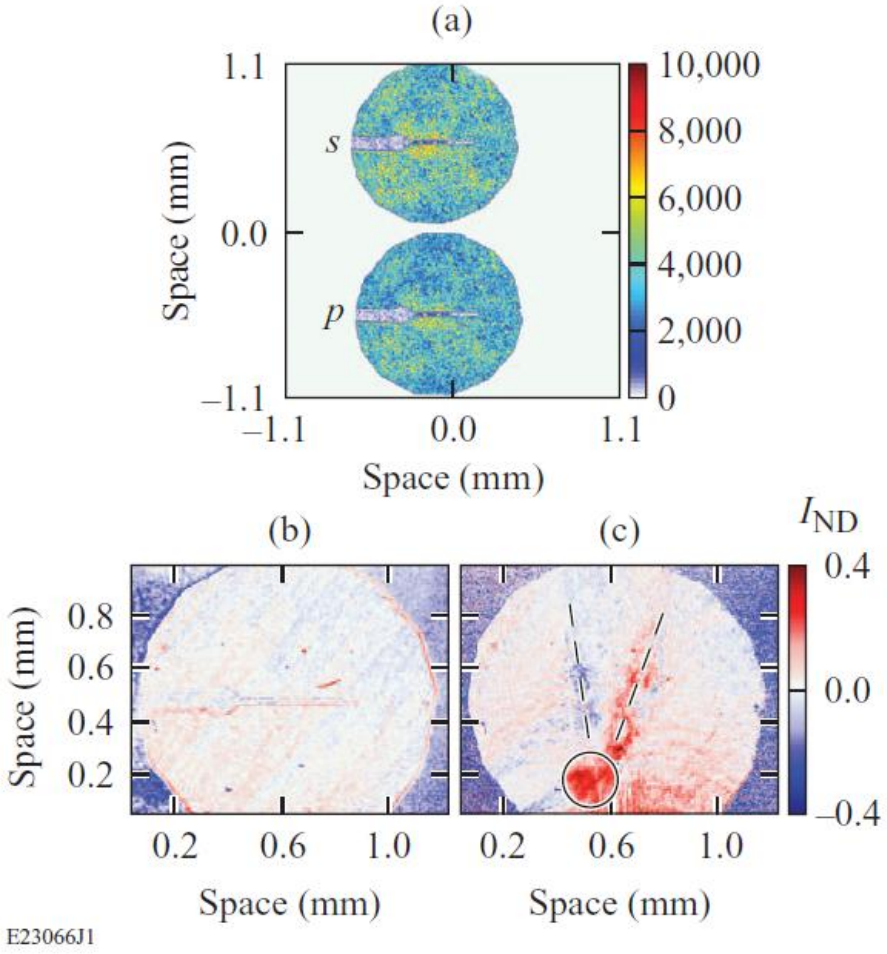

The magnetic field can be measured by measuring the deflected angle of charged particles

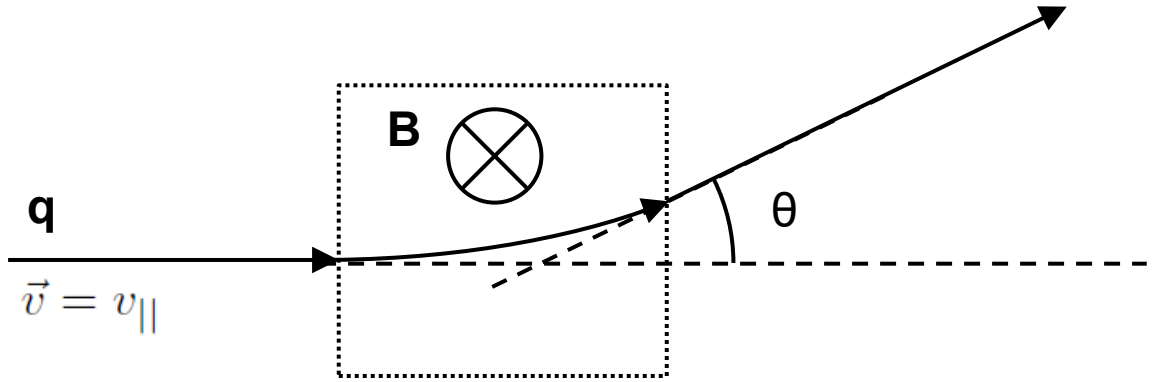

$$F_\perp = q\vec{v} \times \vec{B} = qv_{||}B = m\frac{dv_\perp}{dt}$$

$$v_\perp = \int \frac{qv_{||}B}{m}dt = \frac{qv_{||}}{m}\int Bdt\frac{dx}{dx} = \frac{qv_{||}}{m}\int \frac{B}{v_{||}}dx = \frac{q}{m}\int Bdx$$

$$\tan\theta = \frac{v_\perp}{v_{||}} = \frac{q}{mv_{||}}\int Bdx = \frac{q}{\sqrt{2mE}}\int Bdx \qquad \int Bdx = \frac{\sqrt{2mE}}{q}\tan\theta$$

Magnetic field was measured using protons

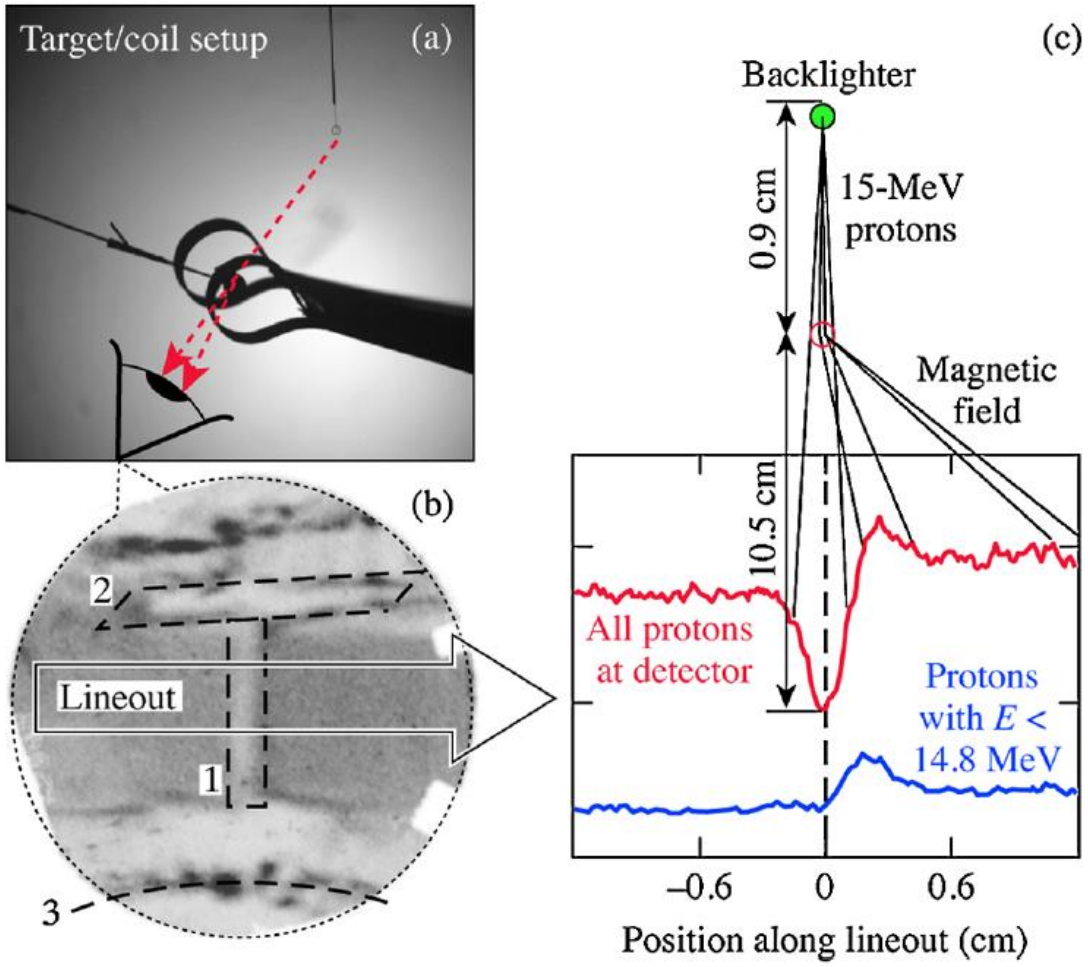

O. V. Gotchev *et al.*, Phys. Rev. Lett. **103**, 215004 (2009)

Protons can be generated from fusion product or copper foil illuminated by short pulse laser

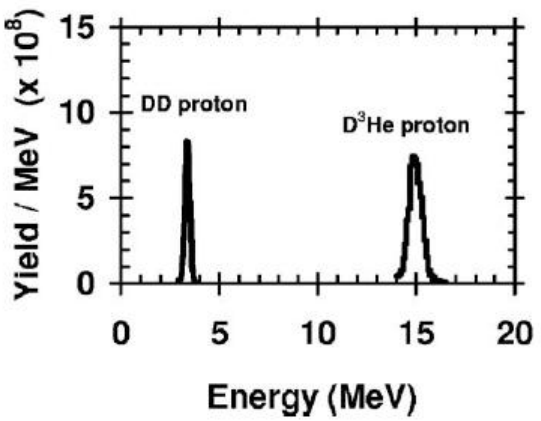

$$D + D \longrightarrow T(1.01\text{MeV}) + p(3.02\text{MeV})$$

$$D + \text{He}^3 \longrightarrow \text{He}^4(3.6\text{MeV}) + p(14.7\text{MeV})$$

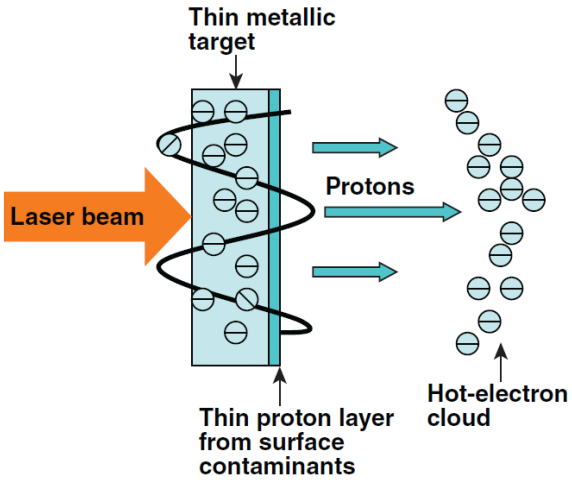

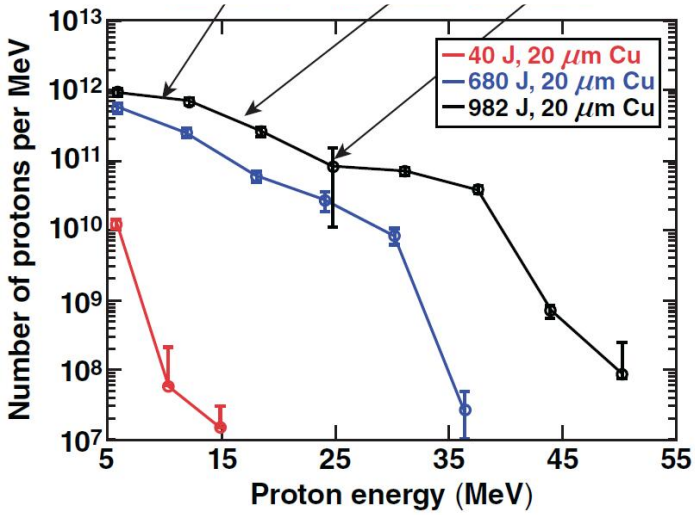

Target normal sheath acceleration (TNSA)

C. K. Li *et al.*, Rev. Sci. Instrum. **77**, 10E725 (2006)
L. Gao, PhD Thesis

Protons can leave tracks on CR39 or film

CR 39

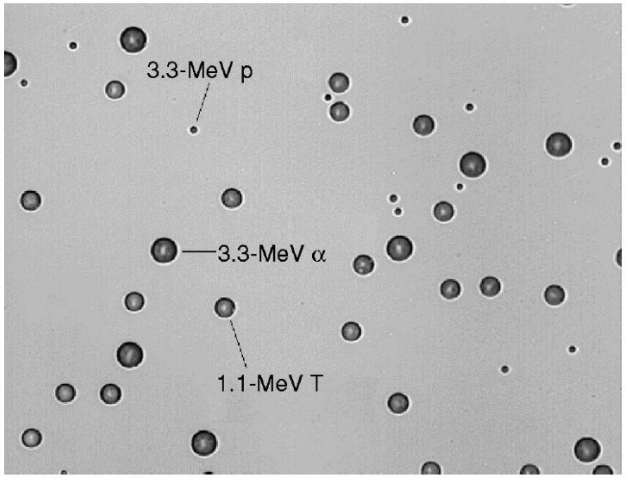

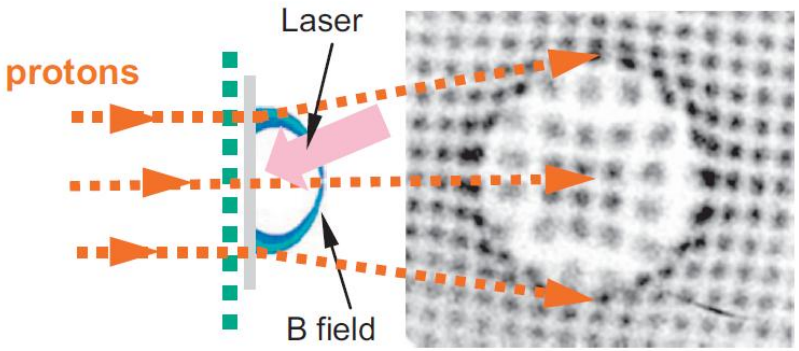

Radiochromic film pack

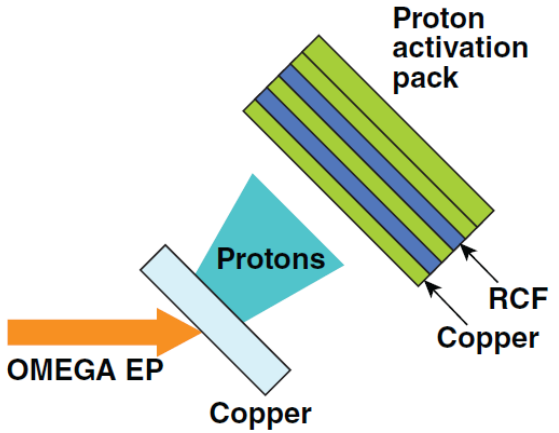

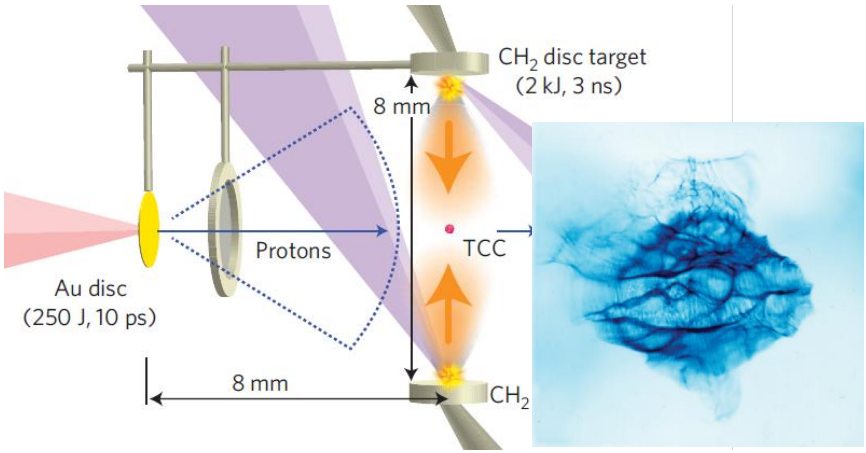

F. H. Seguin *et al.*, Rev. Sci. Instrum. **74**, 975 (2003)
C. K. Li *et al.*, Phys. Plasmas **16**,056304 (2009)
L. Gao, PhD Thesis
N. L. Kugland et al., Nature Phys. B, 809 (2012)

Time dependent magnetic field can be measured using B-dot probe

$$B = B(t)$$

$$\nabla \times \vec{E} = -\frac{\partial \vec{B}}{\partial t}$$

$$\int d\vec{A} \nabla \times \vec{E} = \oint \vec{E} d\vec{l} = V = -\int d\vec{A} \frac{\partial}{\partial t} \vec{B}$$

$$V \sim -A \frac{\partial B}{\partial t}$$

$$B = -\int \frac{V}{A} dt \sim -\frac{1}{A} \int V dt$$

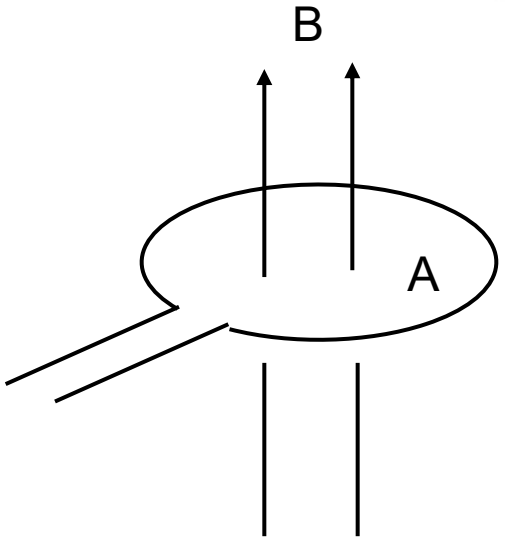

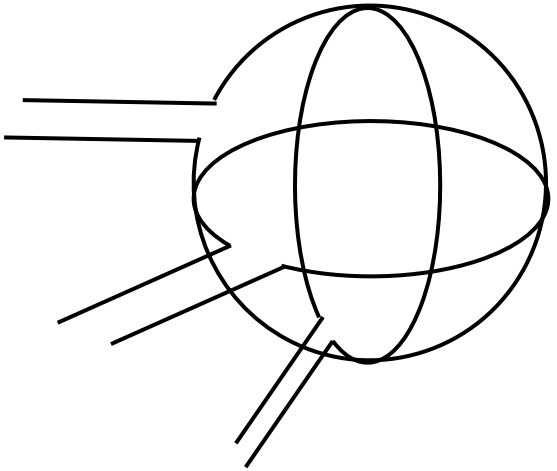

A Thomson parabola uses parallel electric and magnetic fields to deflect particles onto parabolic curves that resolve q/m

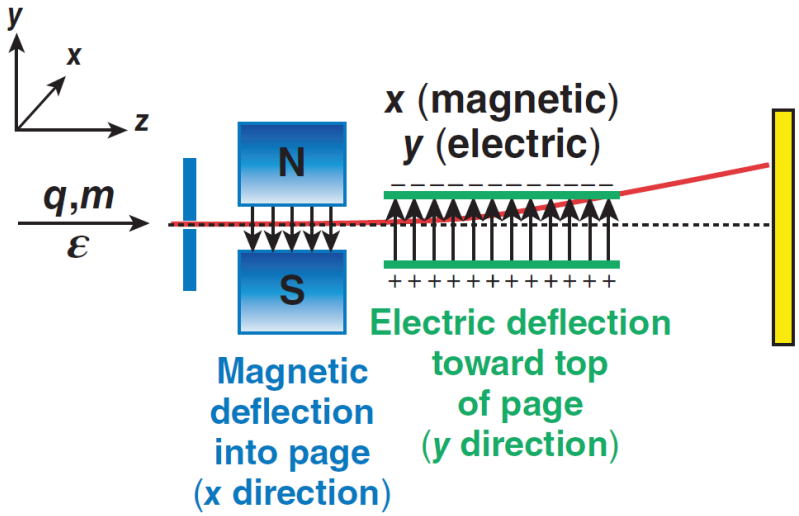

- Deflection caused by magnetic field ~q/p
- Deflection caused by electric field ~q/KE
- Ion traces form parabolic curves on detector plane

$$\tan \Delta\theta_x = \Delta\theta_x = \frac{qBL}{c\sqrt{2\,m\varepsilon}}$$

y deflection

$$F_\perp = qE$$

$$\varepsilon = \frac{q^2B^2L^2}{c^2 2m\Delta\theta_x^2}$$

$$\Delta m V_y = qE\tau = \frac{qEL}{V}$$

$$\tan\theta_y \sim \theta_y = \frac{\Delta m V_y}{mV} = \frac{qEL}{2\varepsilon}$$

$$y = \frac{mc^2E}{qLB^2}x^2$$

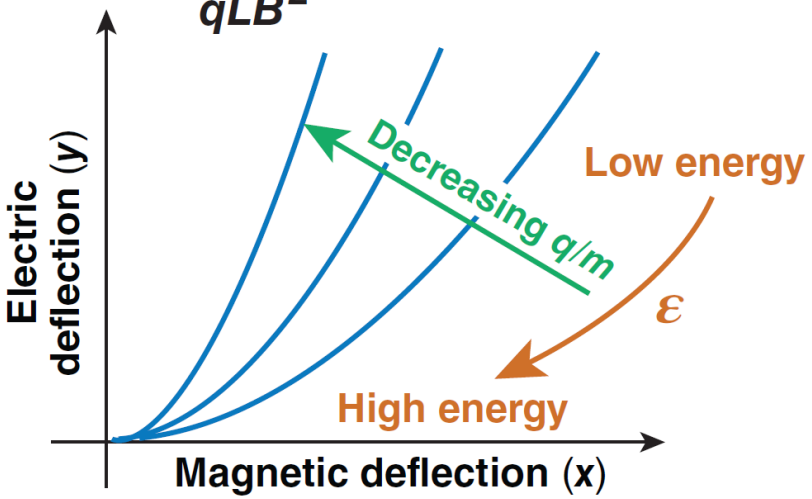

E16717b

A faraday cup measures the flux of charge particles

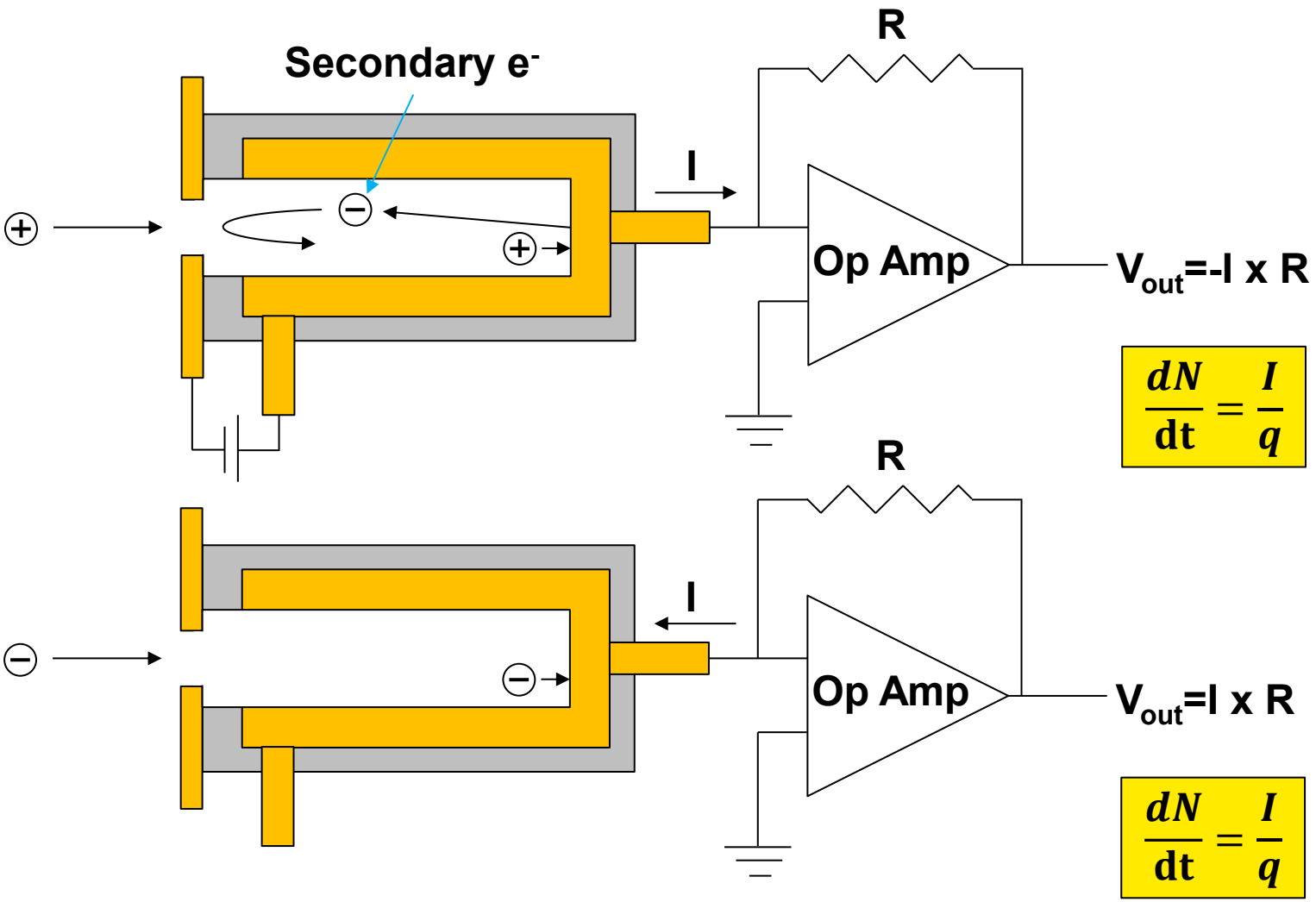

Retarding potential analyzer measures the energy / velocity distribution function

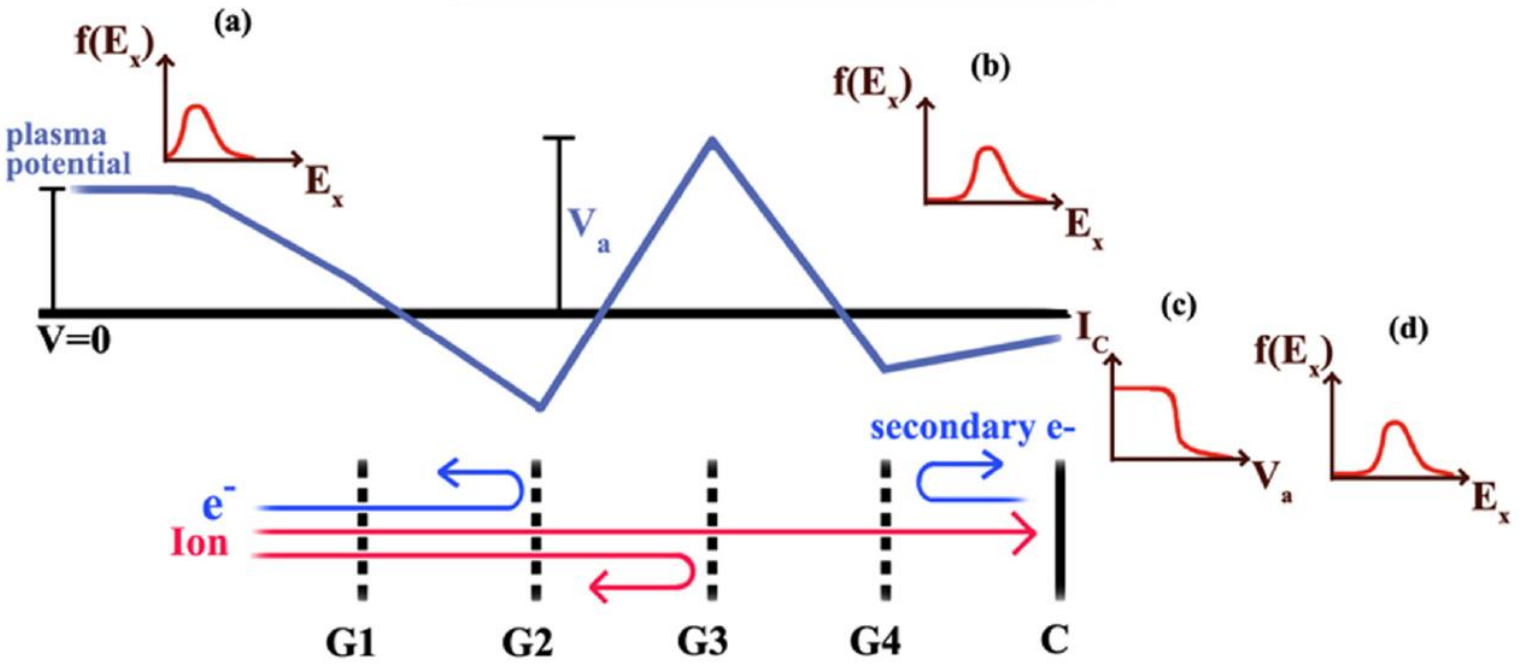

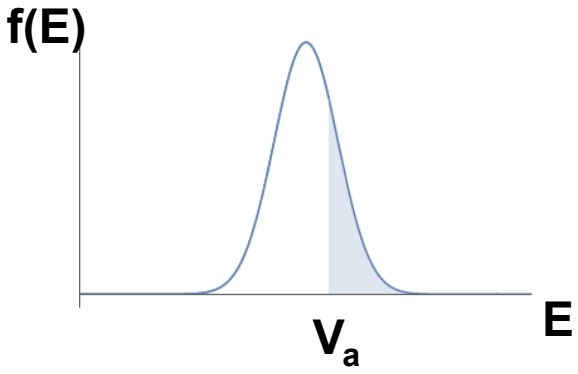

H.-K. Fang, 2015 NCKU Ph. D. Thesis, Ion measurements of ionosphere plasma in space plasma operation chamber

The photon energy spectrum provides valuable information

- Plasma conditions can be determined from the photon spectrum
  - visible light: absorption and laser-plasma interactions
  - x rays: electron temperature, density, plasma flow, material mixing
- There are three basic tools for determining the spectrum detected
  - filtering
  - grating spectrometer
  - Bragg spectrometer

Spectrum can be obtained using grating

- **Grating is used to disperse the light**

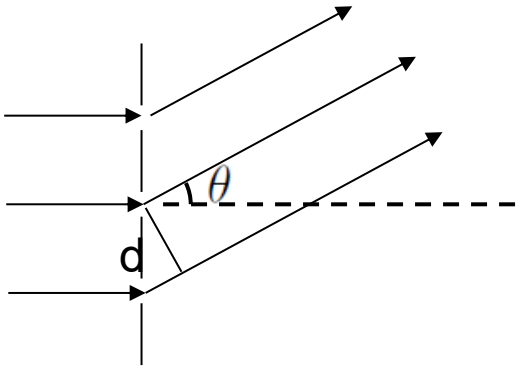

$$d\sin\theta = m\lambda$$

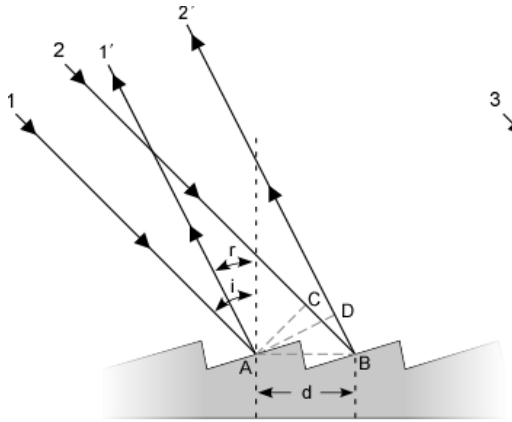

nλ = d(sin(i) + sin (r))

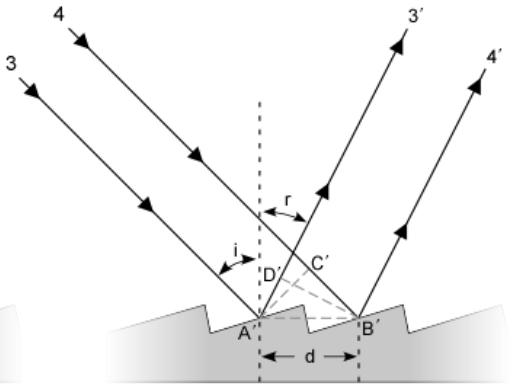

nλ = d(sin(i) - sin (r))

- **Bragg condition in the crystal is used for X-ray.**

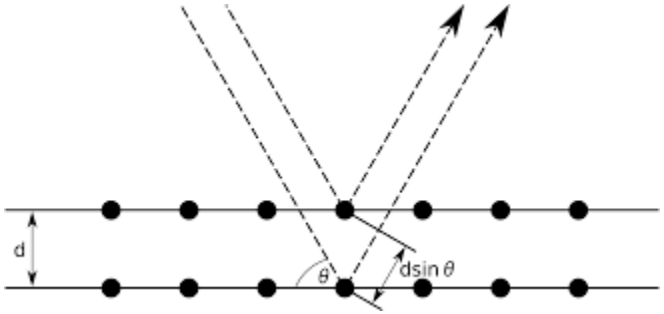

$$2d\sin\theta = m\lambda$$

Temperature and density can be obtained from the emission

Line emission

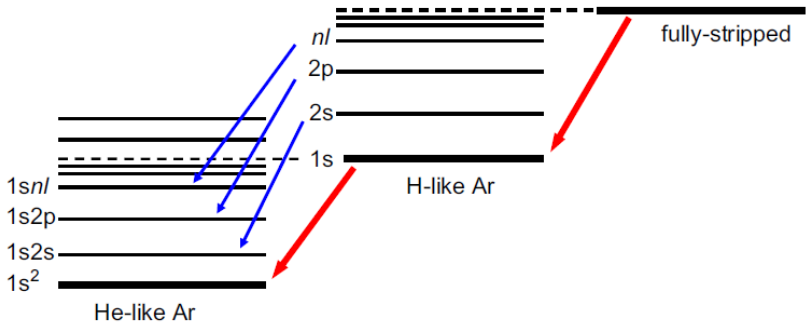

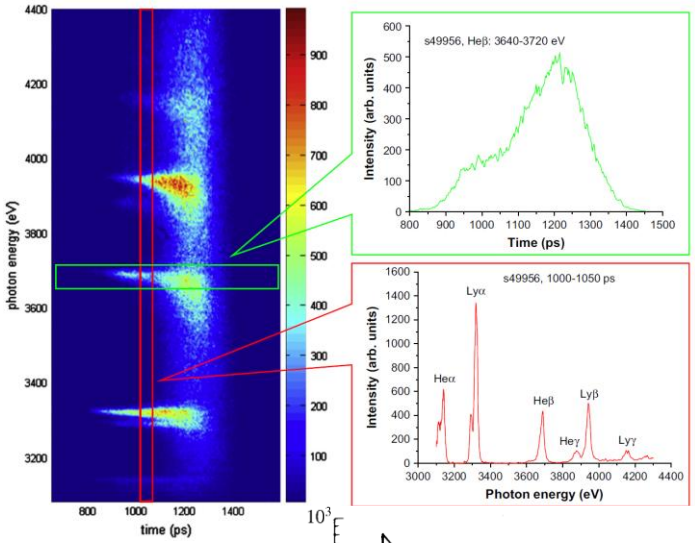

Bremsstrahlung emission

$$\eta_\nu = \frac{16\pi}{3\sqrt{6\pi}} \frac{e^6}{m_e^2 c^3} \frac{Z_i^2 n_e}{\sqrt{k_B T_e / m_e} A m_p} \exp\left(-\frac{h\nu}{k_B T_e}\right)$$

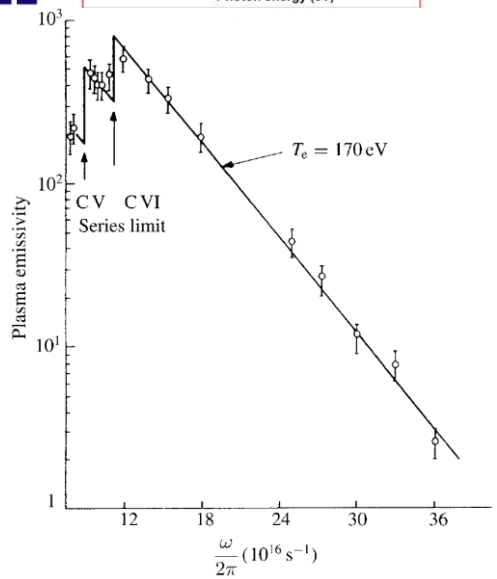

R. Florido *et al.*, High Energy Dens. Phys. **6**, 70 (2010)

Information of x-ray transmission or reflectivity over a surface can be obtained from the Center for X-Ray Optics

- **http://henke.lbl.gov/optical_constants/**

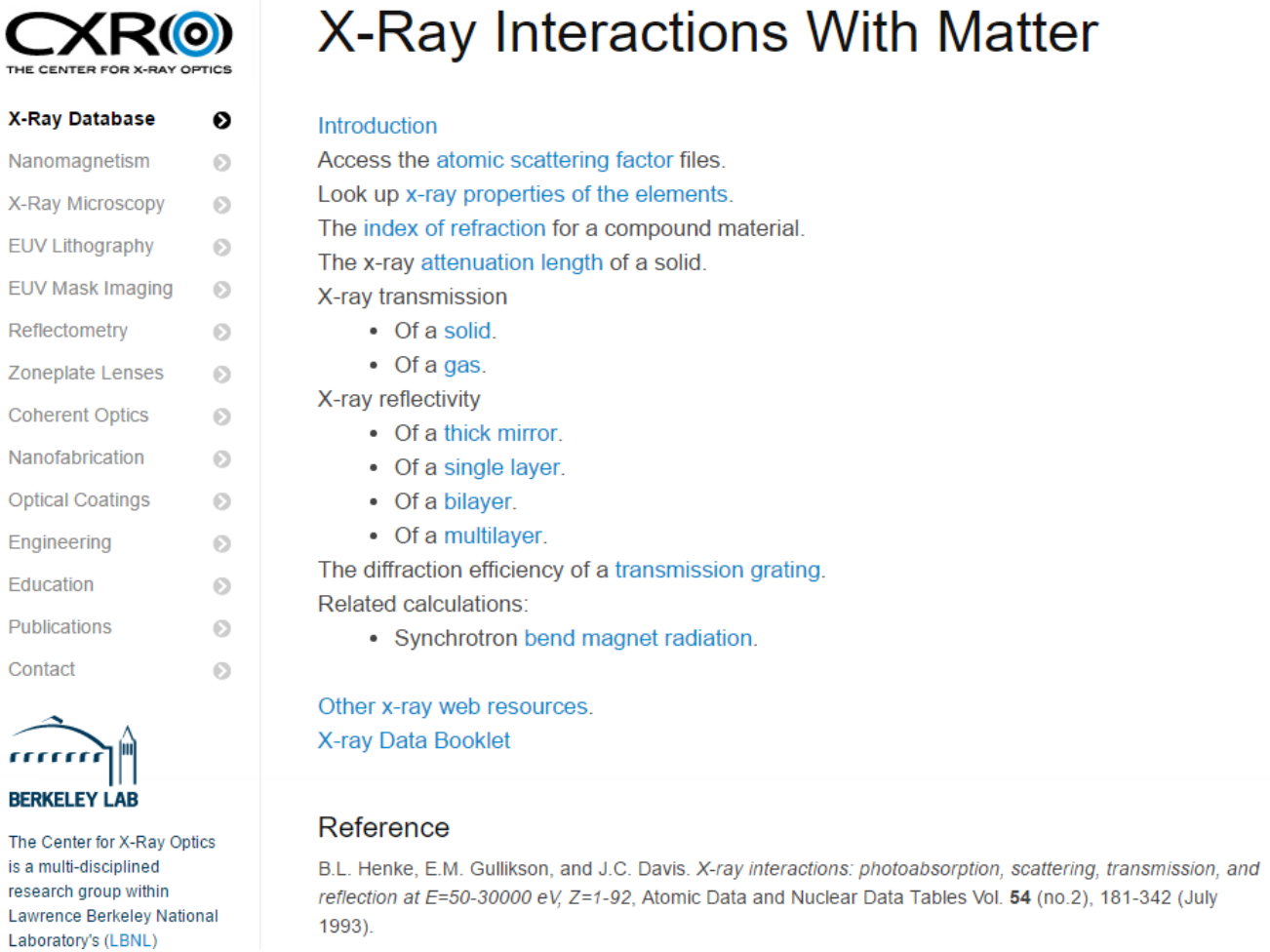

A band pass filter is obtained by combing a filter and a mirror

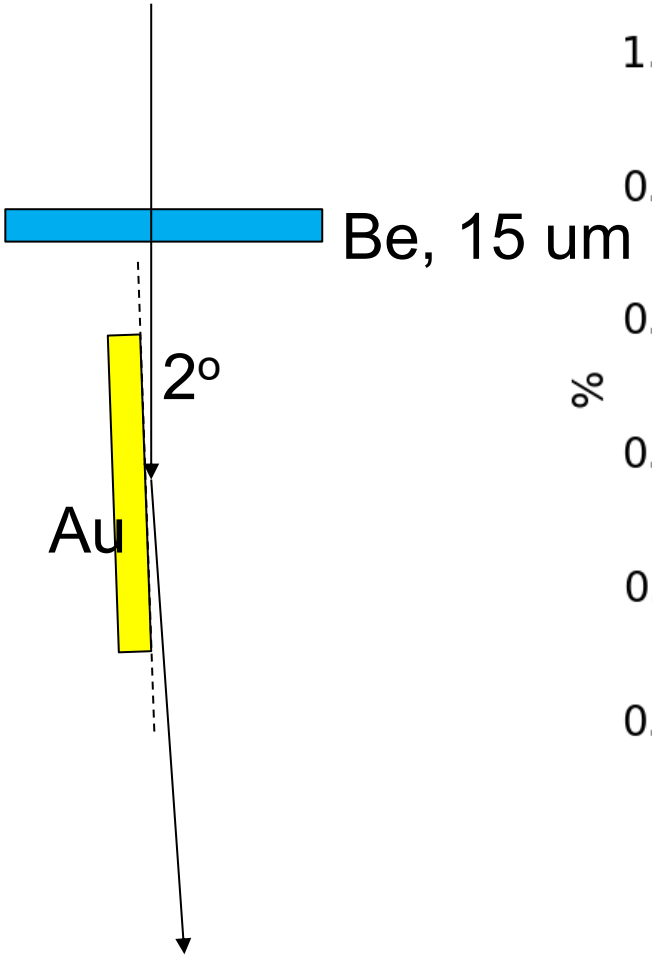

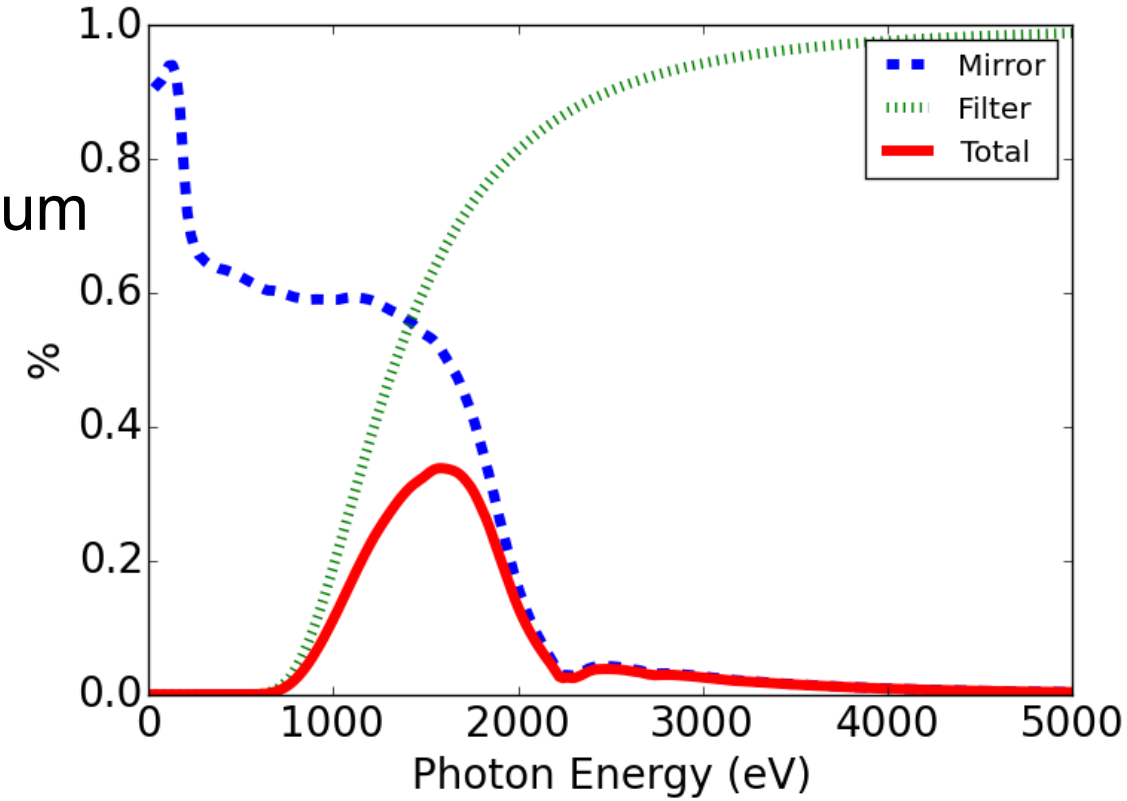

X rays can not be concentrated by lenses

- X-ray refractive indices are less than unity, $n \lesssim 1$
- For those with lower refractive indices, the absorption is also strong
- X-ray mirrors can be made through
  - Bragg reflection
  - External total reflection with a small grazing angle

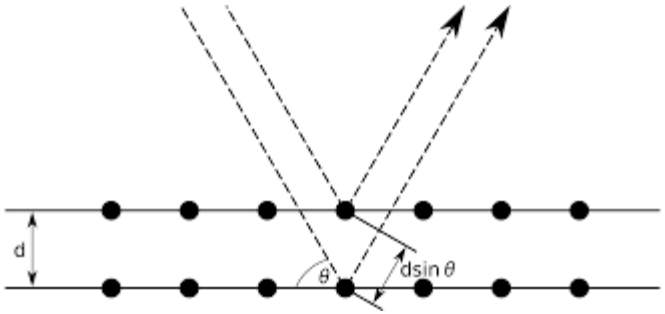

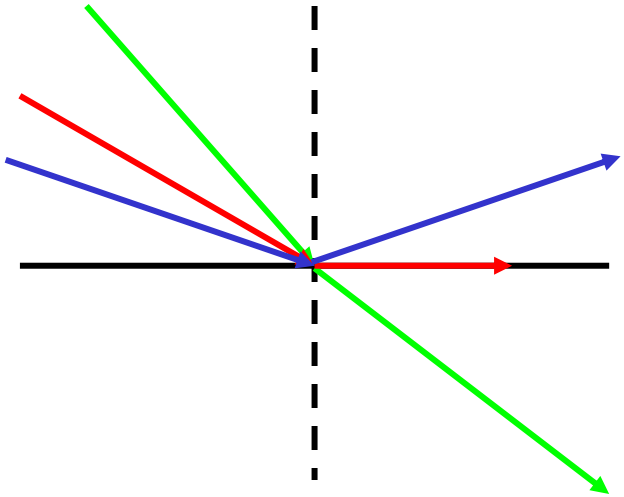

The simplest imaging device is a pinhole camera

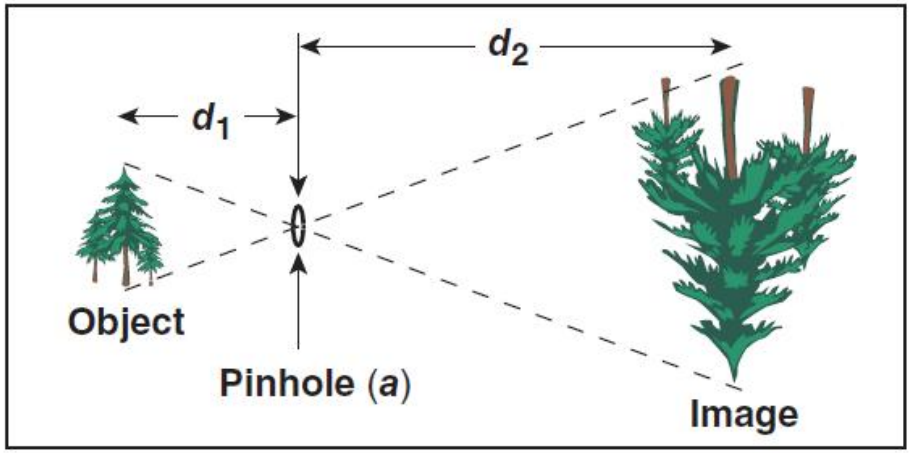

Kodak Brownie camera

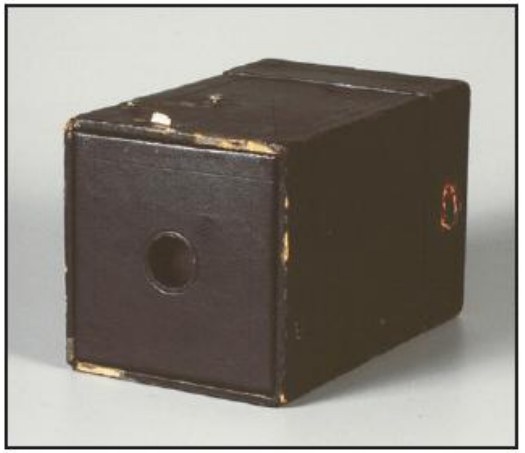

- Magnification = $\frac{d_2}{d_1}$
- Infinite depth of field (variable magnification)
- Pinhole diameter determines
  - resolution ~a
  - light collection: $\Delta\Omega = \frac{\pi}{4}\frac{a^2}{d_1^2}$

Imaging optics (e.g., lenses) can be used for higher resolutions with larger solid angles.

E13982a

2D images can be taken using charge injection device (CID) or charge coupled device (CCD)

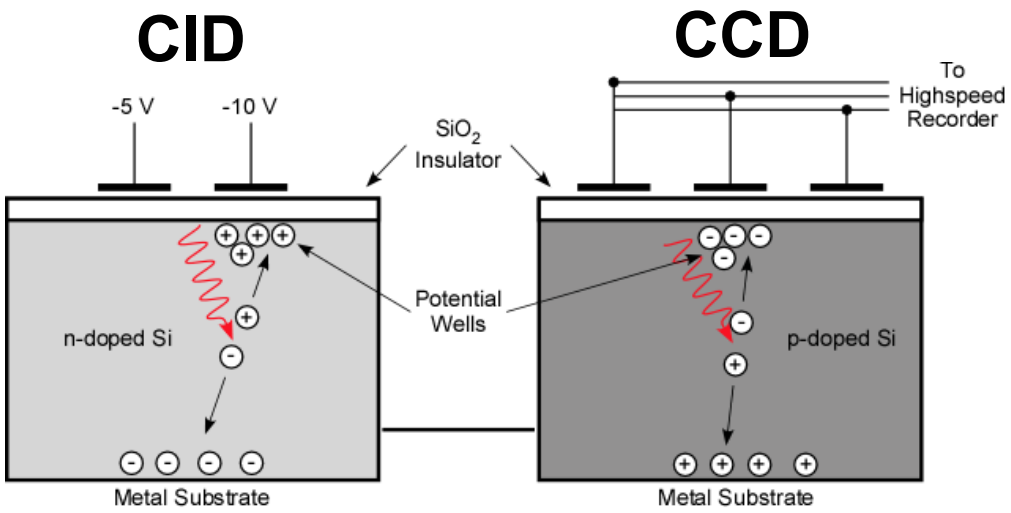

- Color mask is used for color image

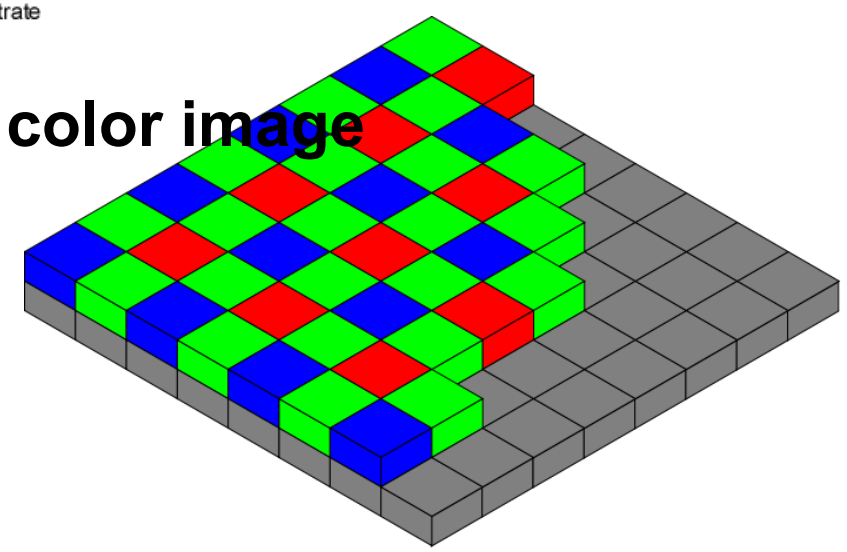

http://people.whitman.edu/~dunnivfm/FAASICPMS_Ebook/CH2/2_2_9.html
https://en.wikipedia.org/wiki/Charge-coupled_device

Charges are transferred along the array for readout in CCD

CCD readout:

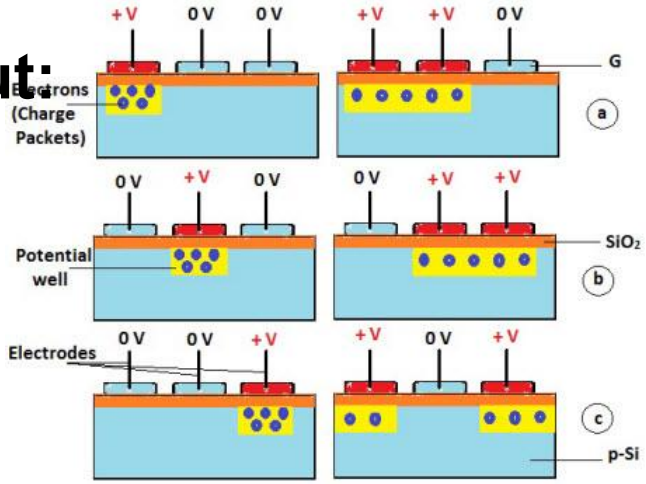

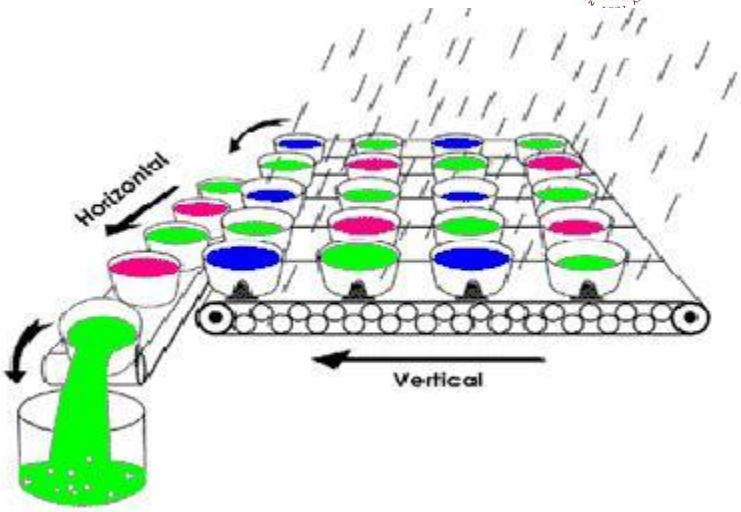

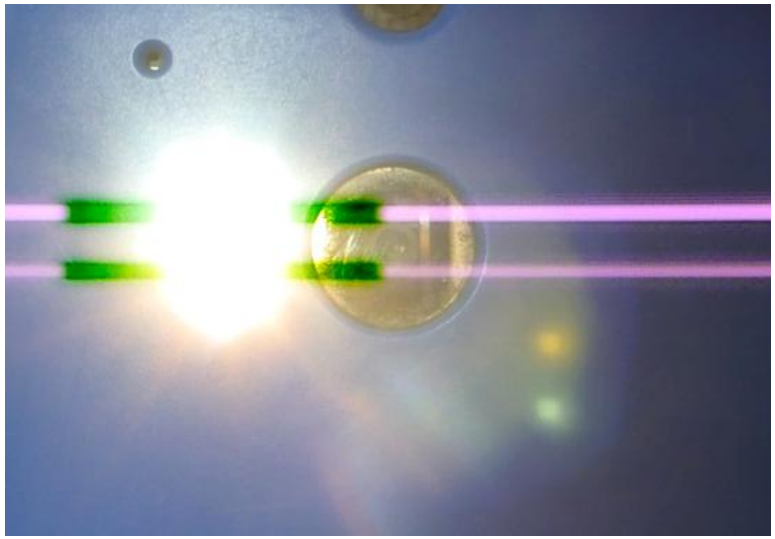

https://www.elprocus.com/know-about-the-working-principle-of-charge-coupled-device/
http://www.siliconimaging.com/ARTICLES/CMOS%20PRIMER.htm

Signal is readout individually in CMOS sensor

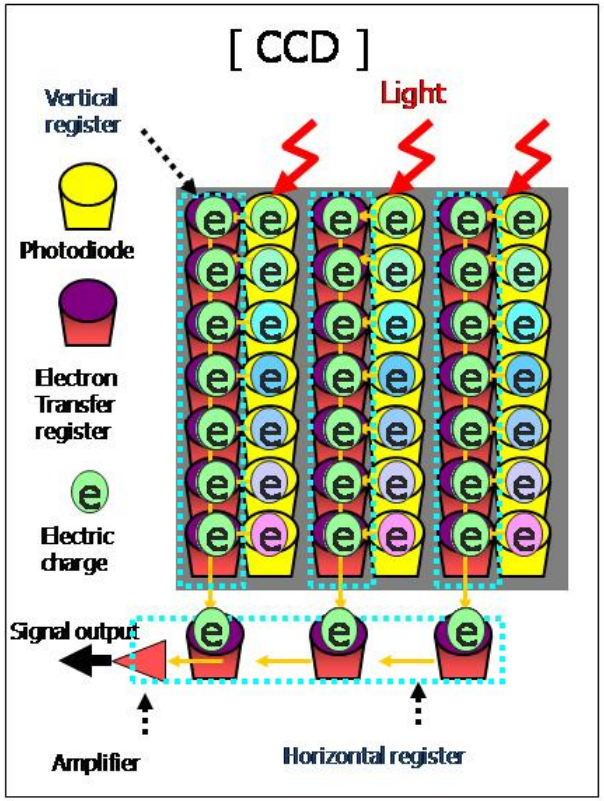

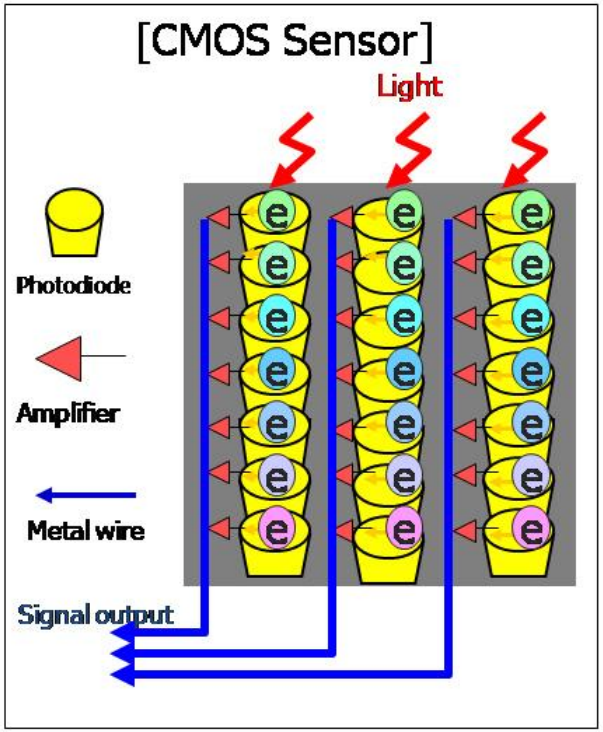

http://www.digitalbolex.com/global-shutter/

The number of electrons can be increased through photomultipliers or microchannel plate (MCP)

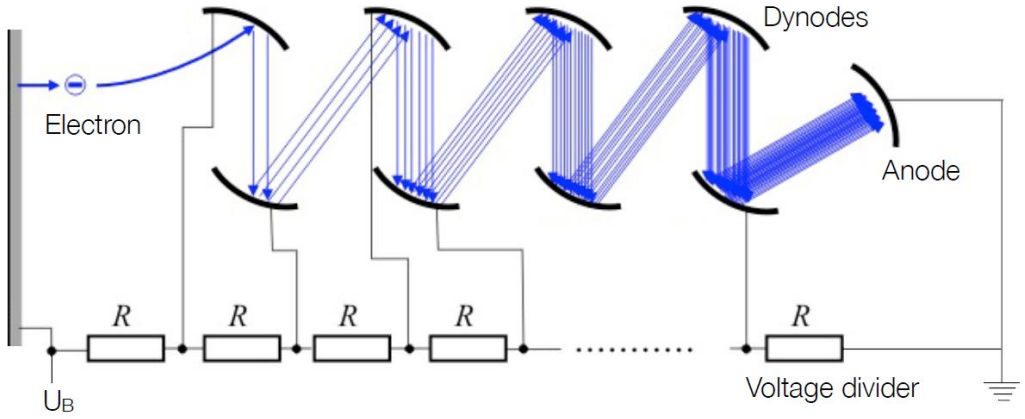

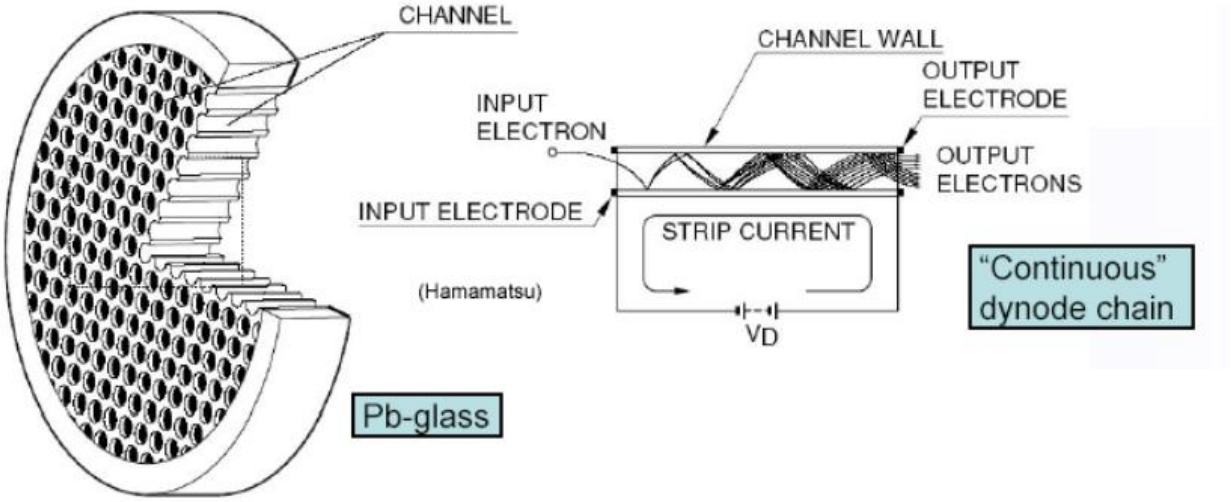

http://www.kip.uni-heidelberg.de/~coulon/Lectures/DetectorsSoSe10/

X-rays are imaged using photocathode, MCP, phosphor, and CCD

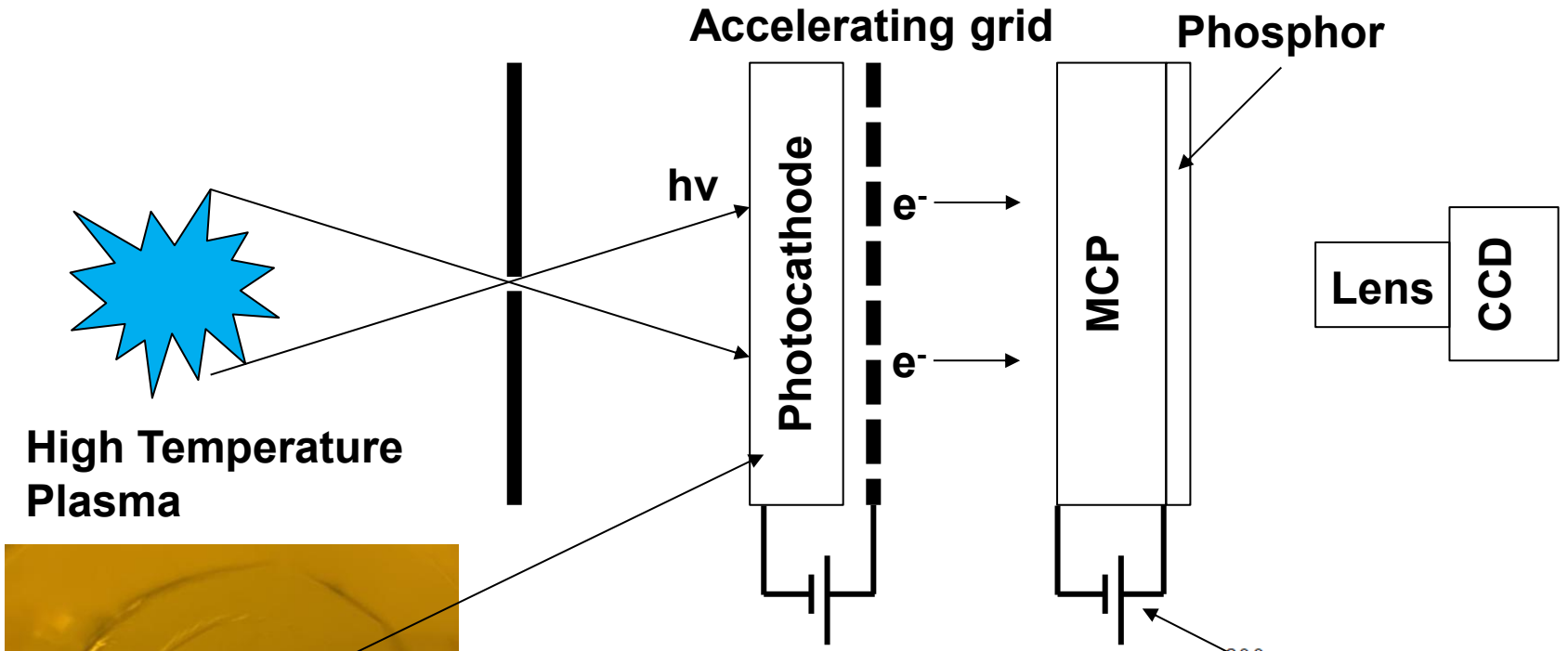

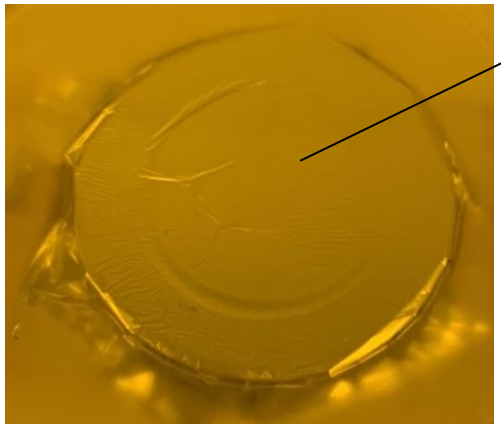

- CsI is used right now.
- Prof. Chou @ Photonics, NCKU is developing 50nm Au foil for us.

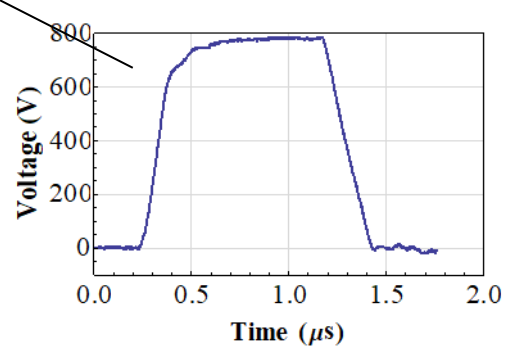

- Images can be gated using fast high voltage pulses.

A negative high-voltage pulse is used in our x-ray pinhole camera

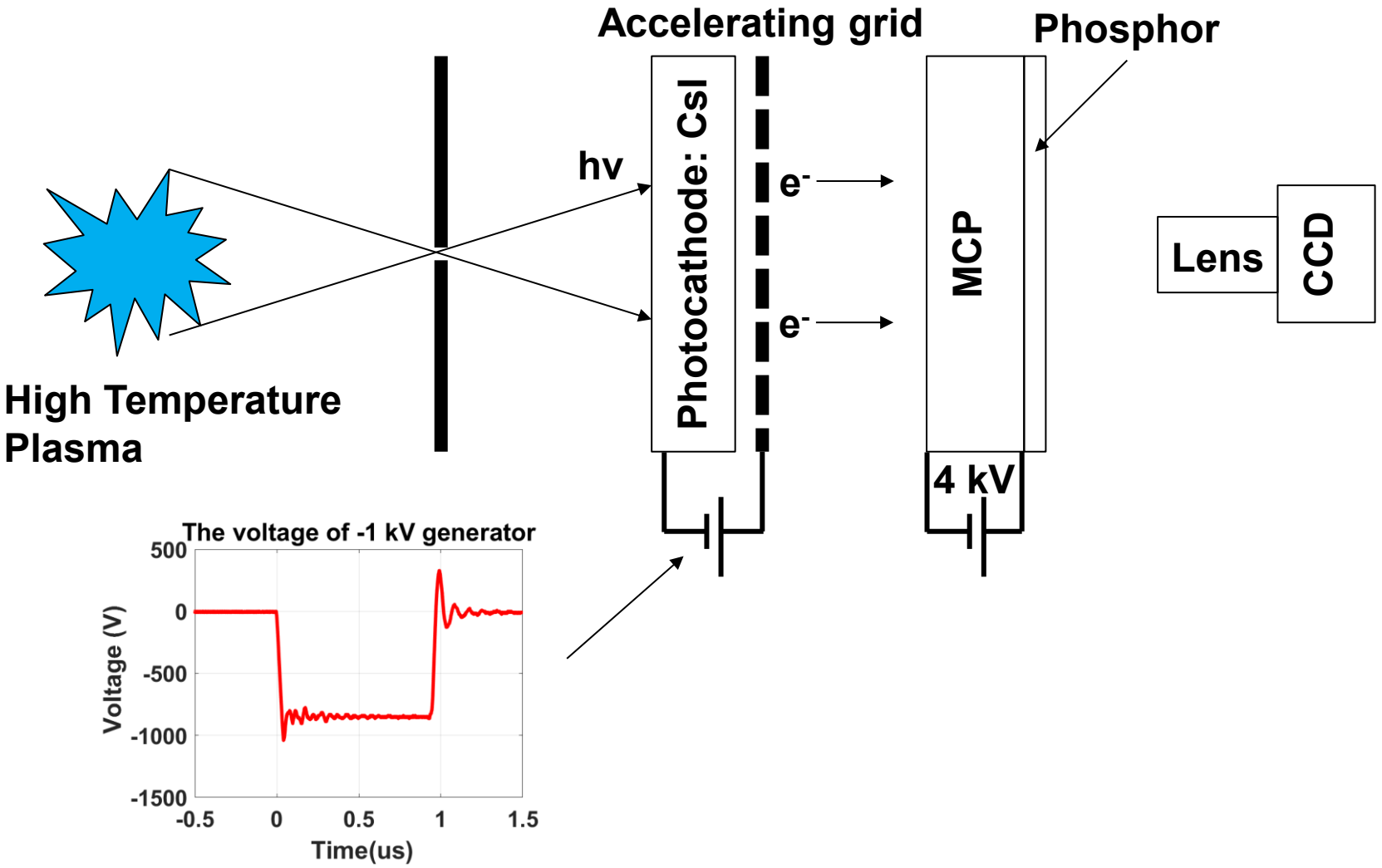

- **The x-ray camera with a shutter opening time of ≤ 10 ns will be built.**

A pinhole camera was designed and was built

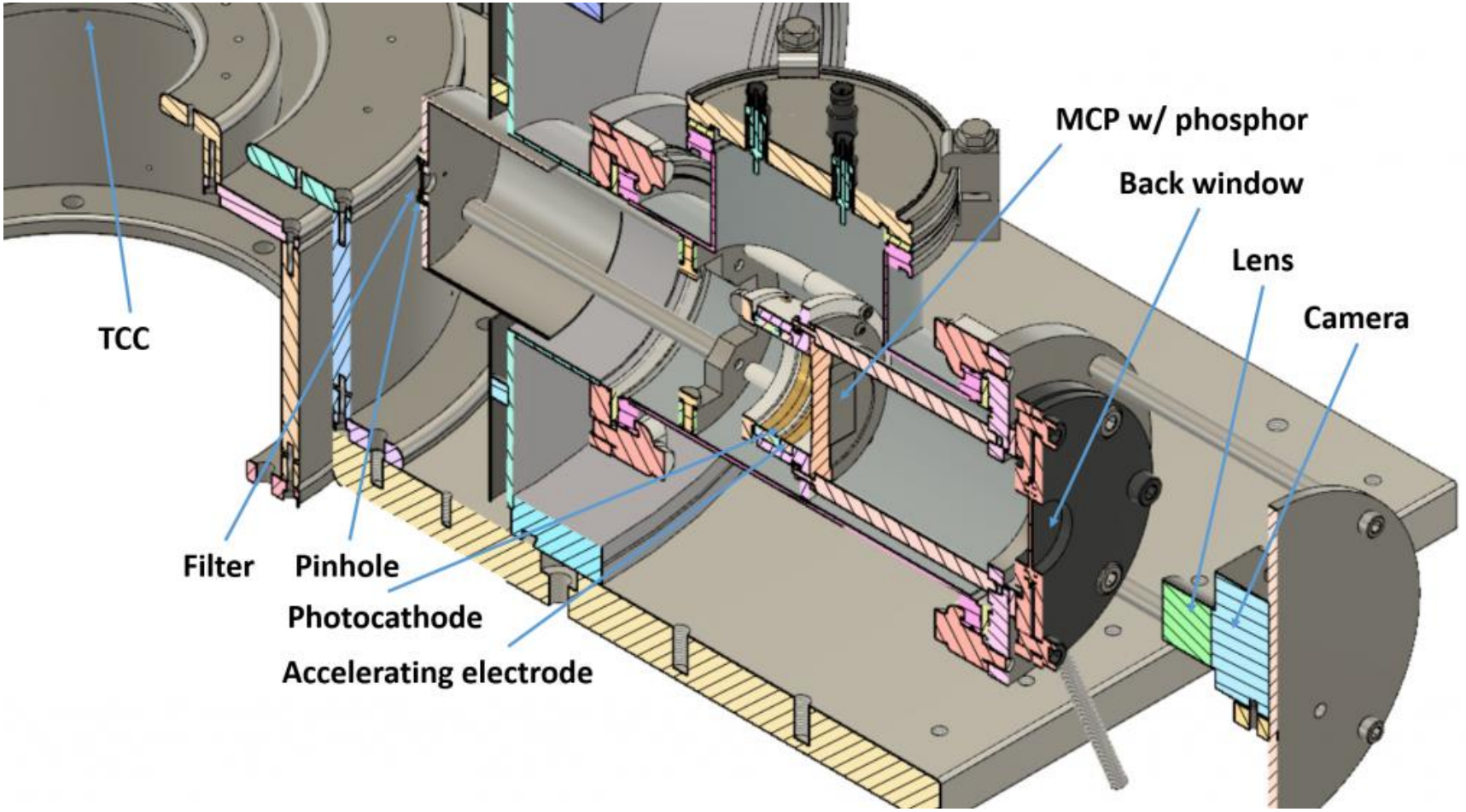

Electronic detectors provide rapid readout

- Electronic detectors are typically semiconductors or ionization-based stacks (e.g., photomultipliers)

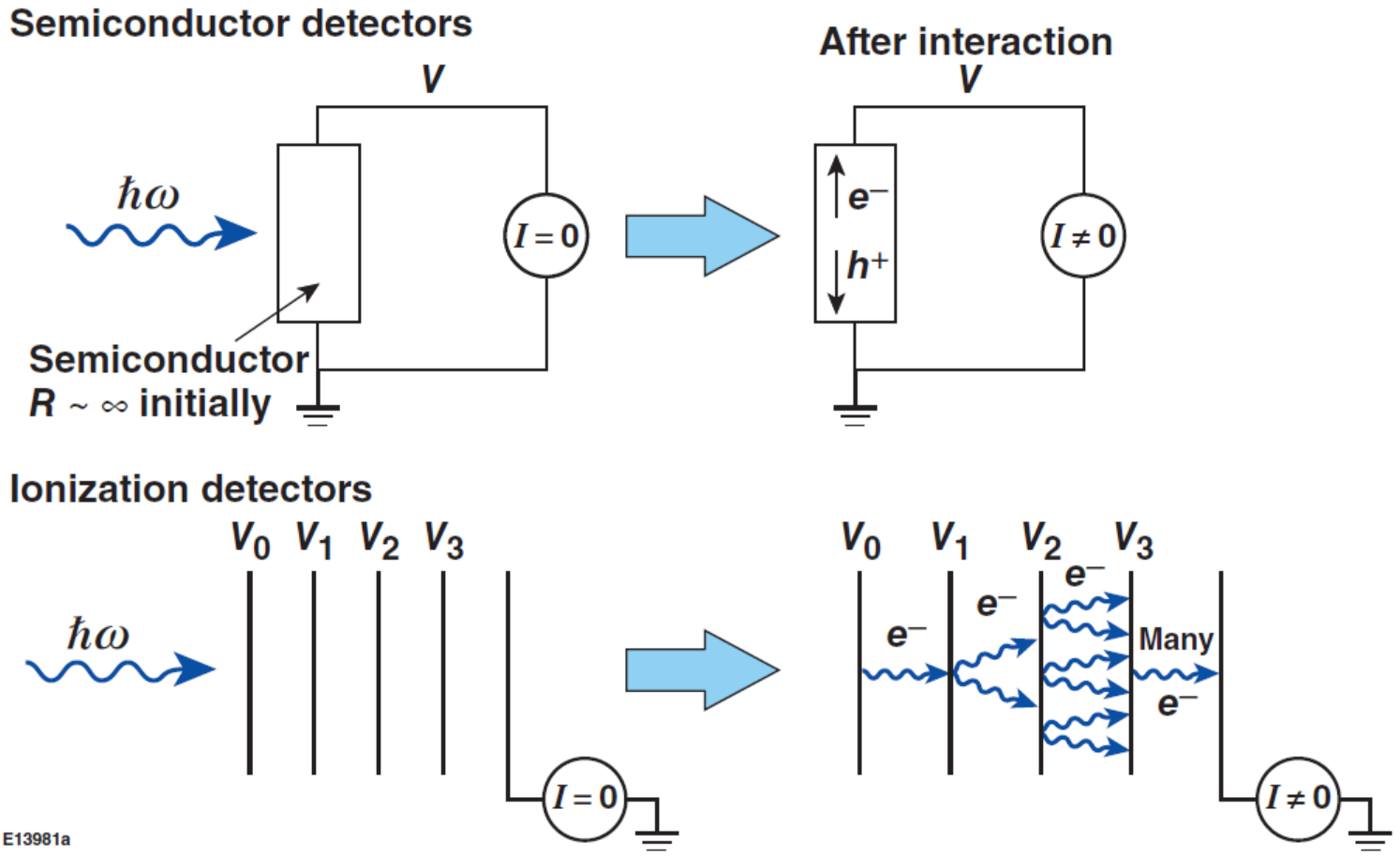

A framing camera provides a series of time-gated 2-D images, similar to a movie camera

- The building block of a framing camera is a gated microchannel-plate (MCP) detector
- An MCP is a plate covered with small holes, each acts as a photomultiplier

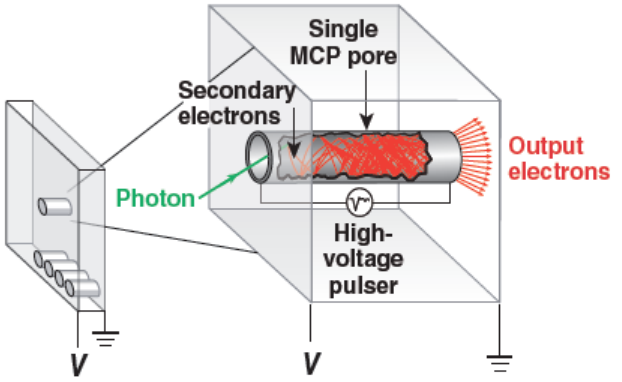

Multiple electrons are produced each time an electron or photon hits the wall

- A voltage pulse is sent down the plate, gating the detector

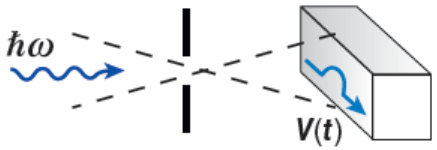

The detector is only on when the voltage pulse is present

E13986b

A framing camera detector consists of a microchannel plate (MCP) in front of a phosphor screen

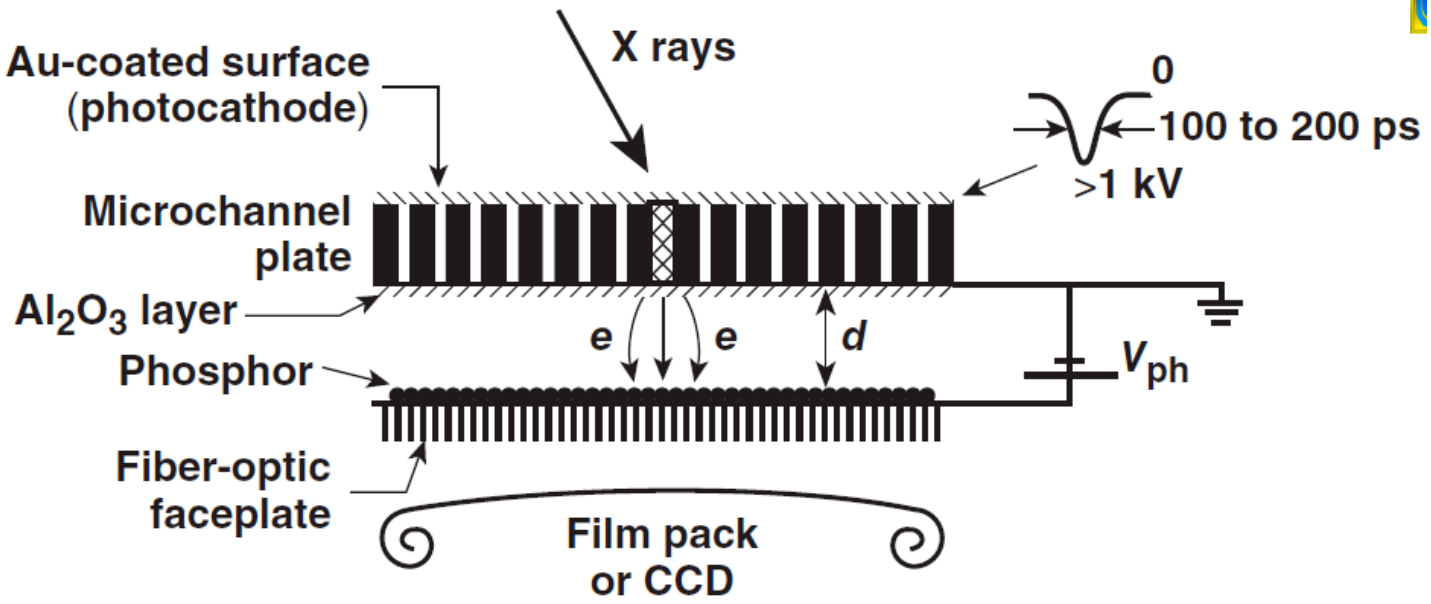

- Electrons are multiplied through MCP by voltage V_c
- Images are recorded on film behind phosphor
- Insulating Al_2O_3 layer allows for V_{ph} to be increased, thereby improving the spatial resolution of phosphor

E7795b

Two-dimensional time-resolved images are recorded using x-ray framing cameras

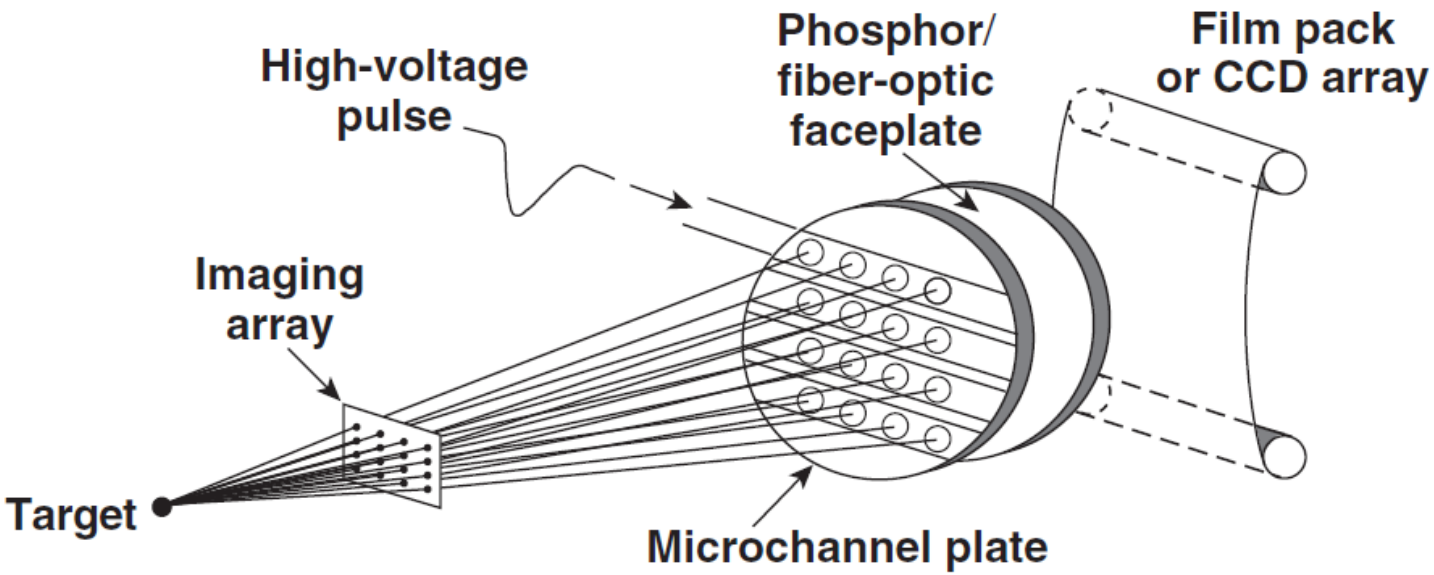

- Temporal resolution = 35 to 40 ps
- Imaging array: Pinholes: 10- to 12-μm resolution, 1 to 4 keV
- Space-resolved x-ray spectra can be obtained by using Bragg crystals and imaging slits

E7105b

X-ray framing cameras for recording two-dimensional time-resolved images will be built by the end of 2021

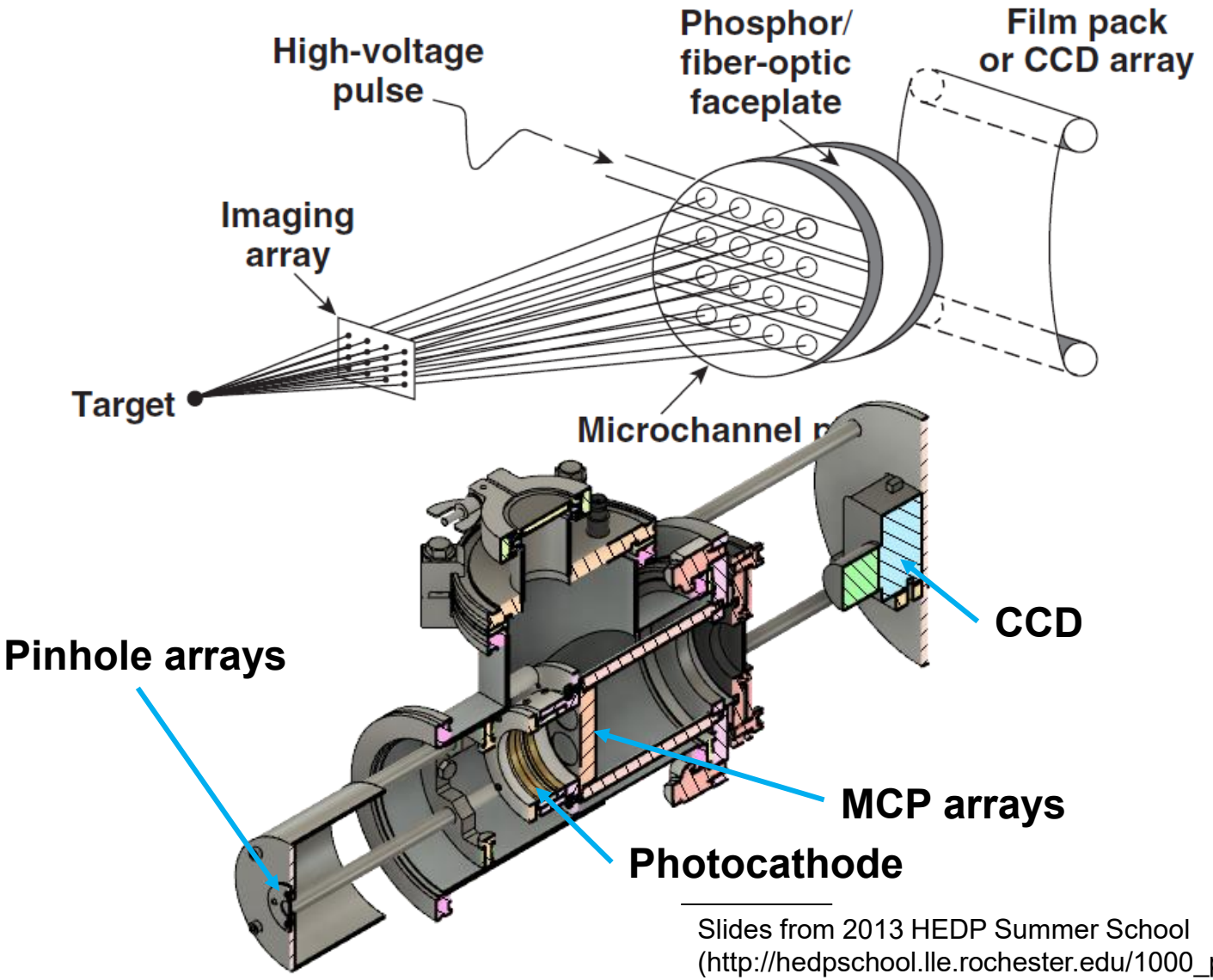

Slides from 2013 HEDP Summer School
(http://hedpschool.lle.rochester.edu/1000_proc2013.php)

Each pinhole camera will be triggered separately

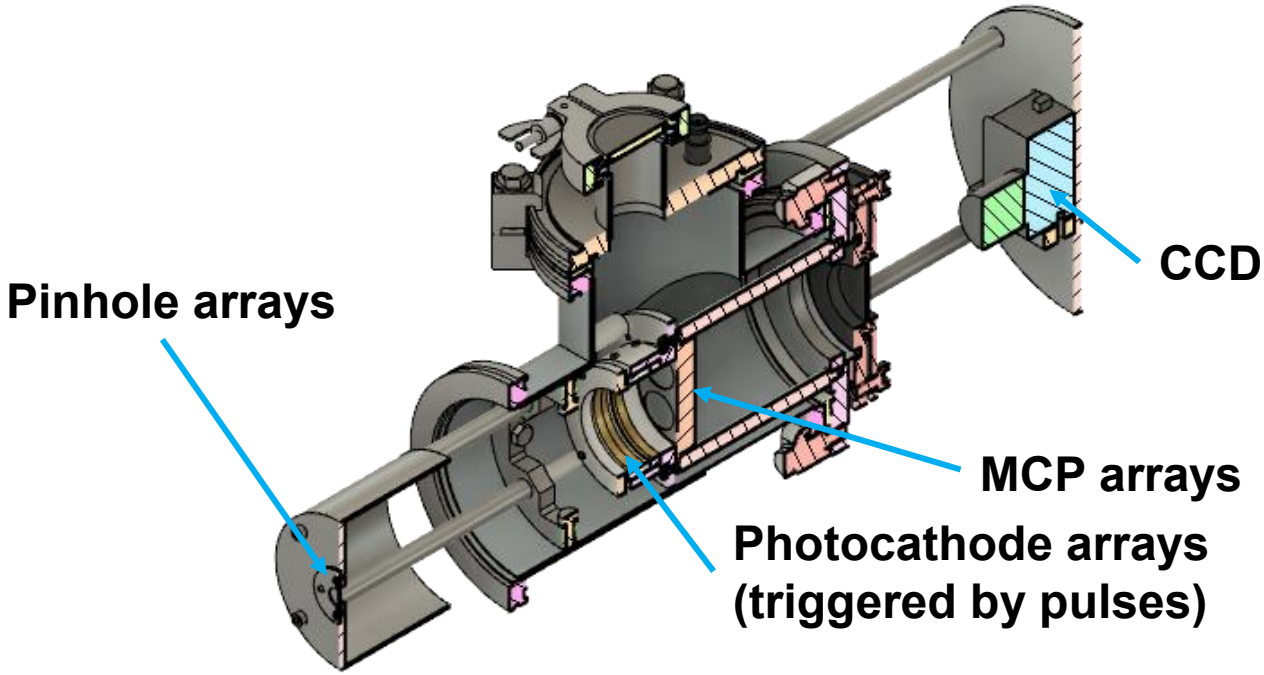

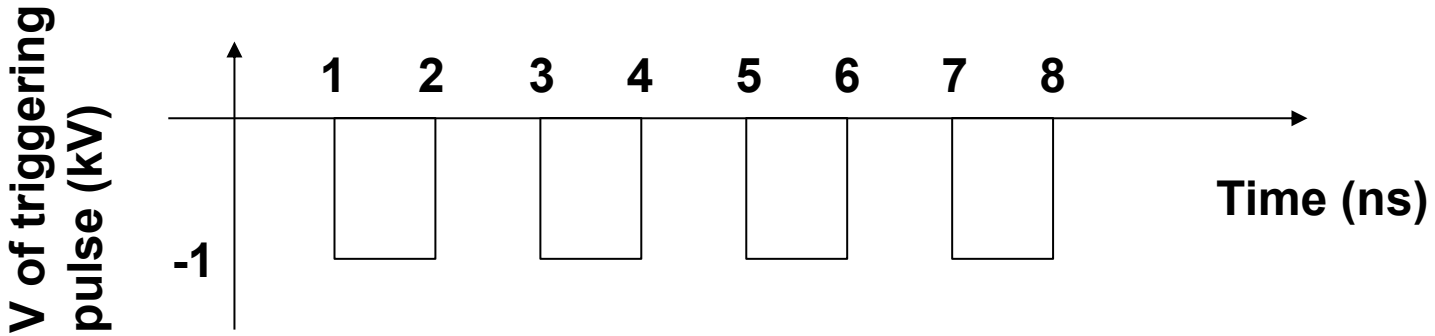

A streak camera provides temporal resolution of 1-D data

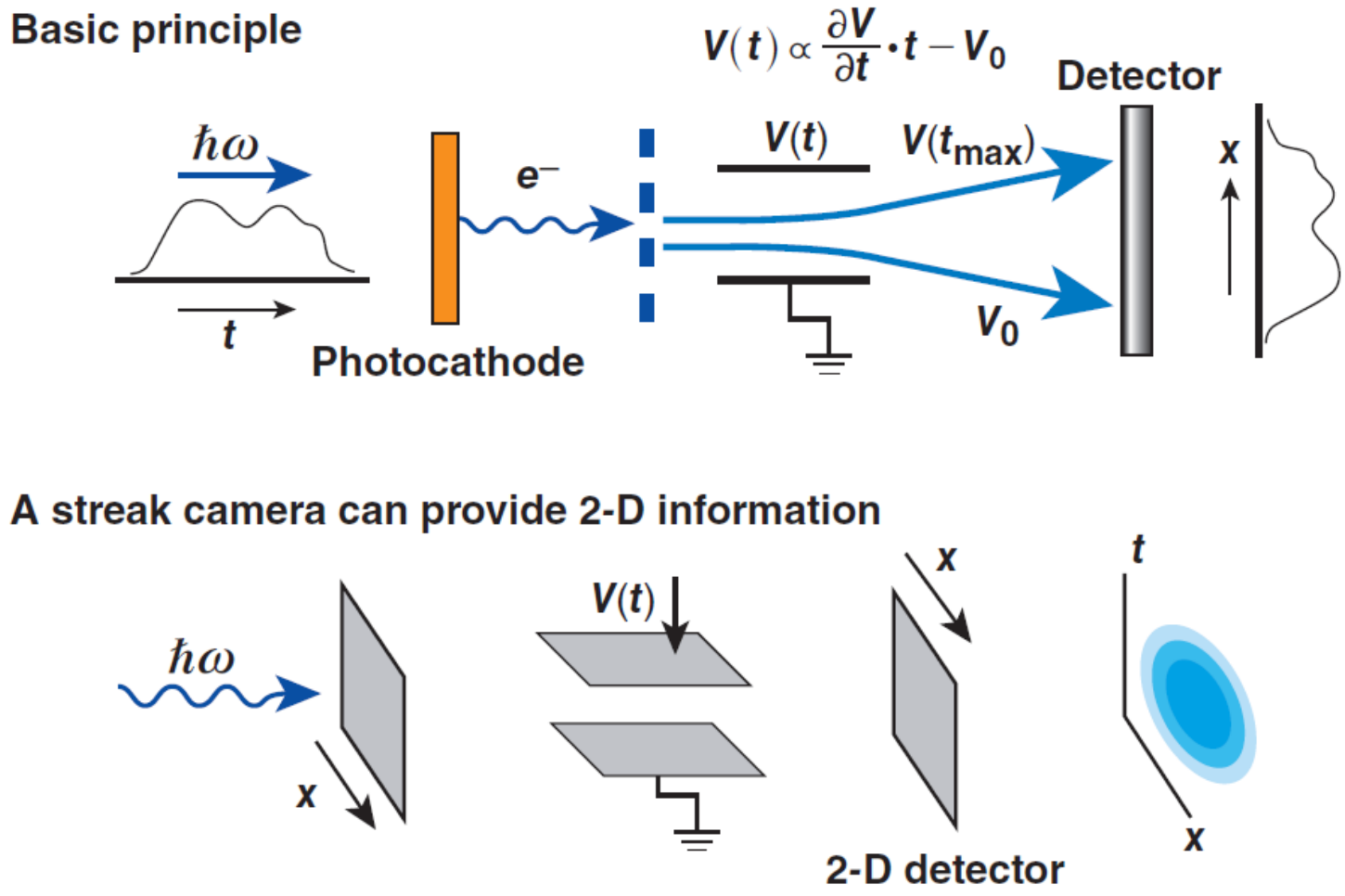

A temporal resolution higher than 15 ps is expected

Imaging system
- **Visible light: regular lens**
- **X rays: pinhole**

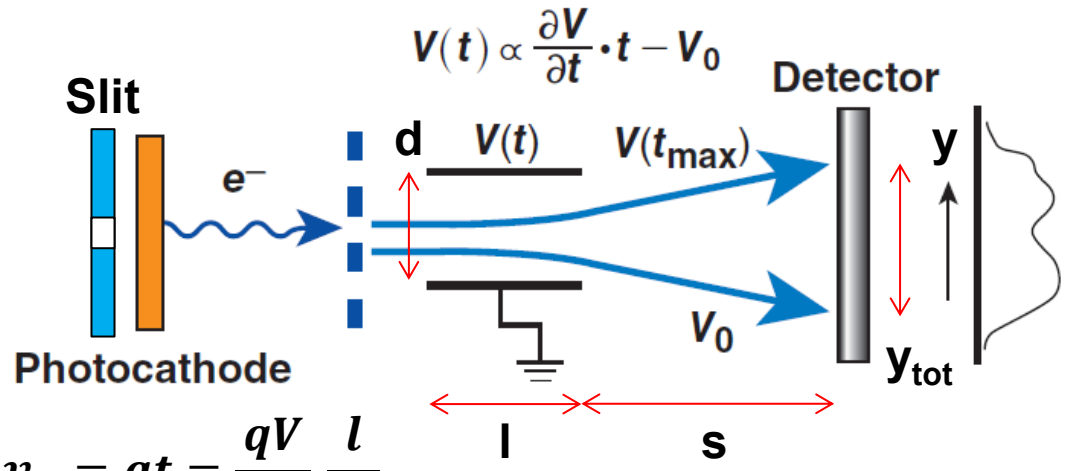

$$a = \frac{F}{m} = \frac{qE}{m} = \frac{qV}{md} \qquad v_{\perp} = at = \frac{qV}{md}\frac{l}{v_{||}}$$

$$y = s\,\mathrm{Tan}\theta = s\frac{V_{\perp}}{V_{||}} = \frac{1}{2E_k}\frac{l}{d}sqV = \frac{1}{2E_k}\frac{l}{d}sq(V_0 + V't)$$

- **Let d=10 mm, l=20 mm, s=50 mm, E_k=1 keV, V=-200 ~ 200 V**

$$V' \equiv \frac{V_{tot}}{t_{tot}} = 0.06\,\mathrm{kV/ns} \qquad y_{tot} = 15\mathrm{mm} \qquad y_{tot} = 15\mathrm{mm}$$

- **Temporal resolution:**

$$\delta t = \delta y \frac{2E_k d}{lsqV'} = 15\,\mathrm{ps} \quad \text{for} \quad \delta y = 45\mu\mathrm{m}$$

- **δt will be adjusted by changing E_k.**

A streak camera with temporal resolution of 15 ps has been developed

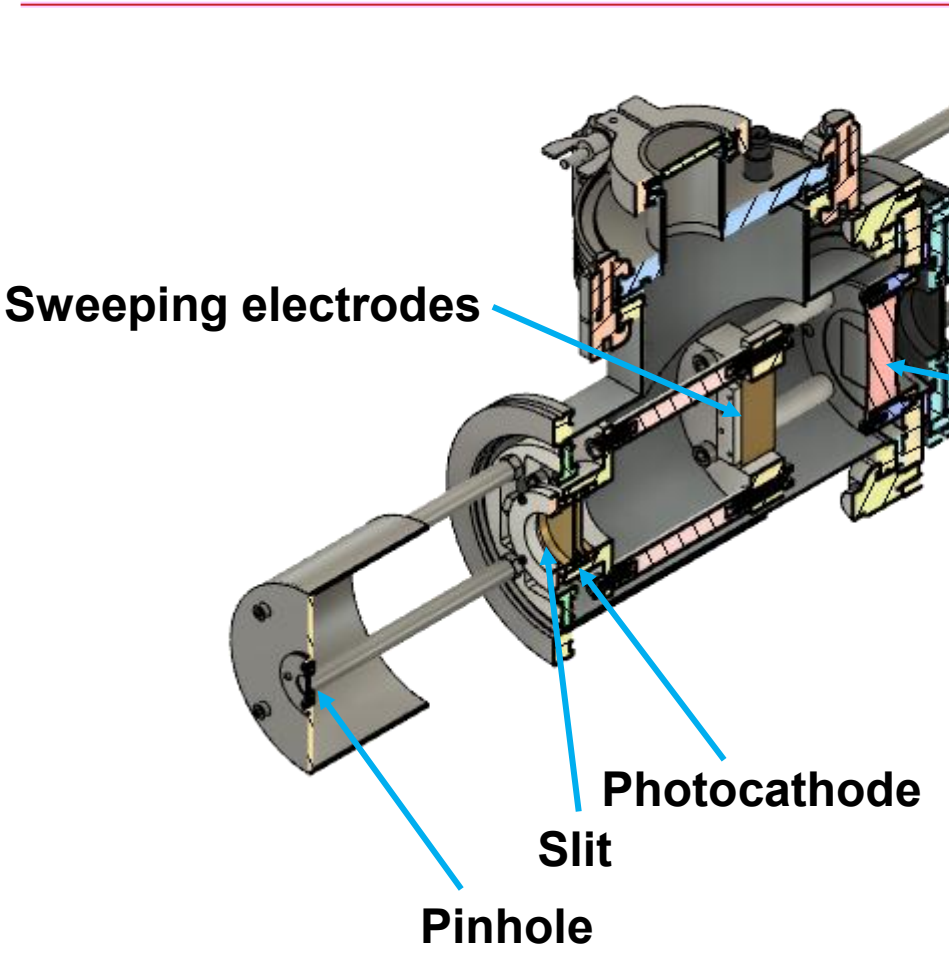

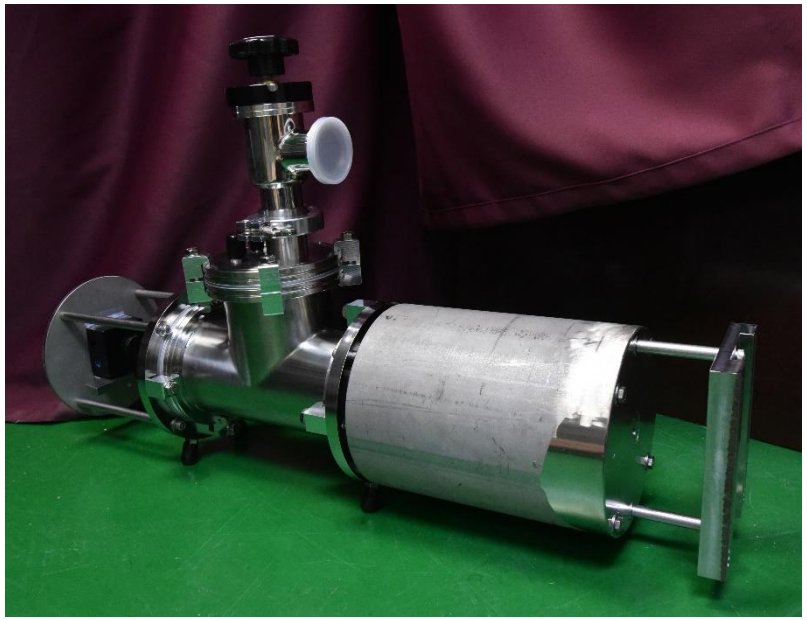

Shell trajectories can be measured using framing camera or streak camera

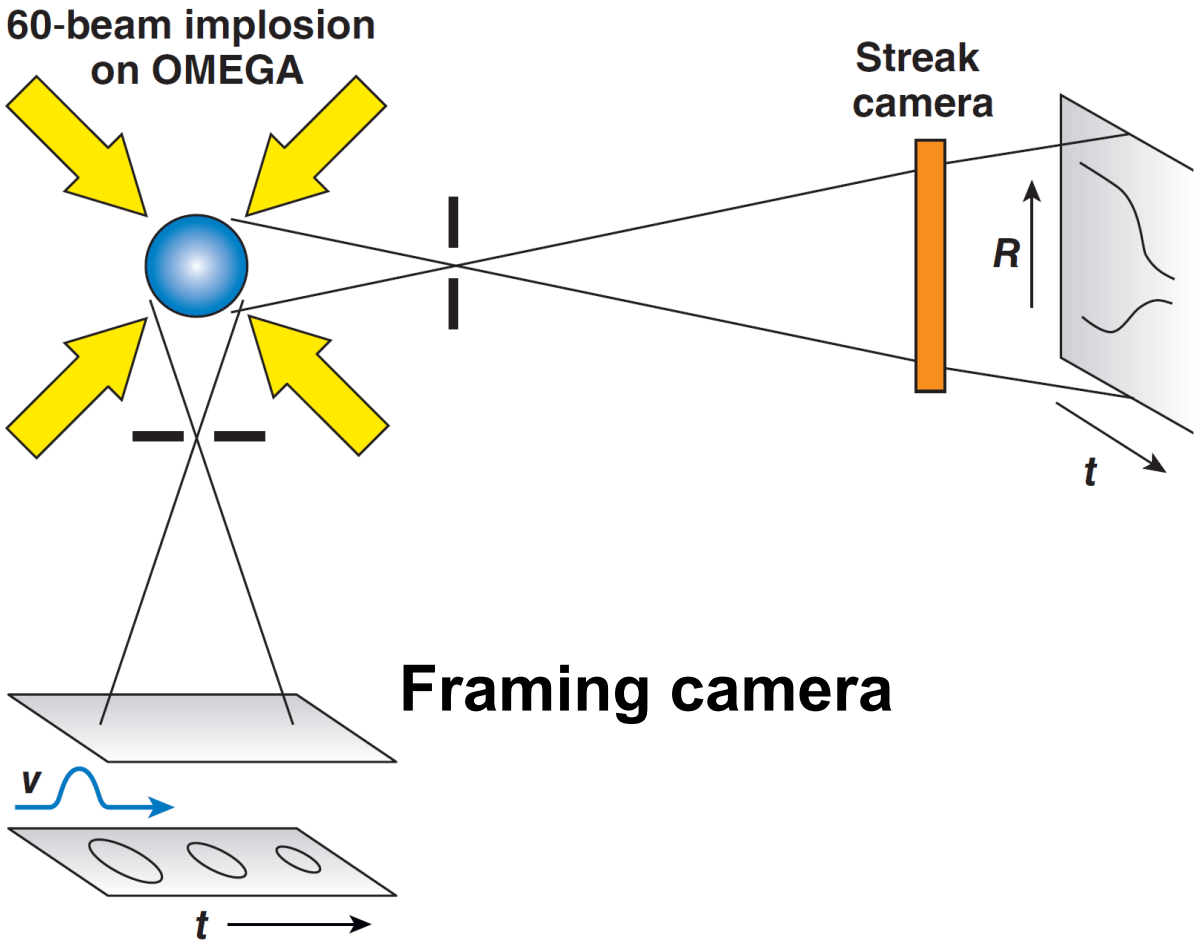

Comparison of images from framing camera versus streak camera

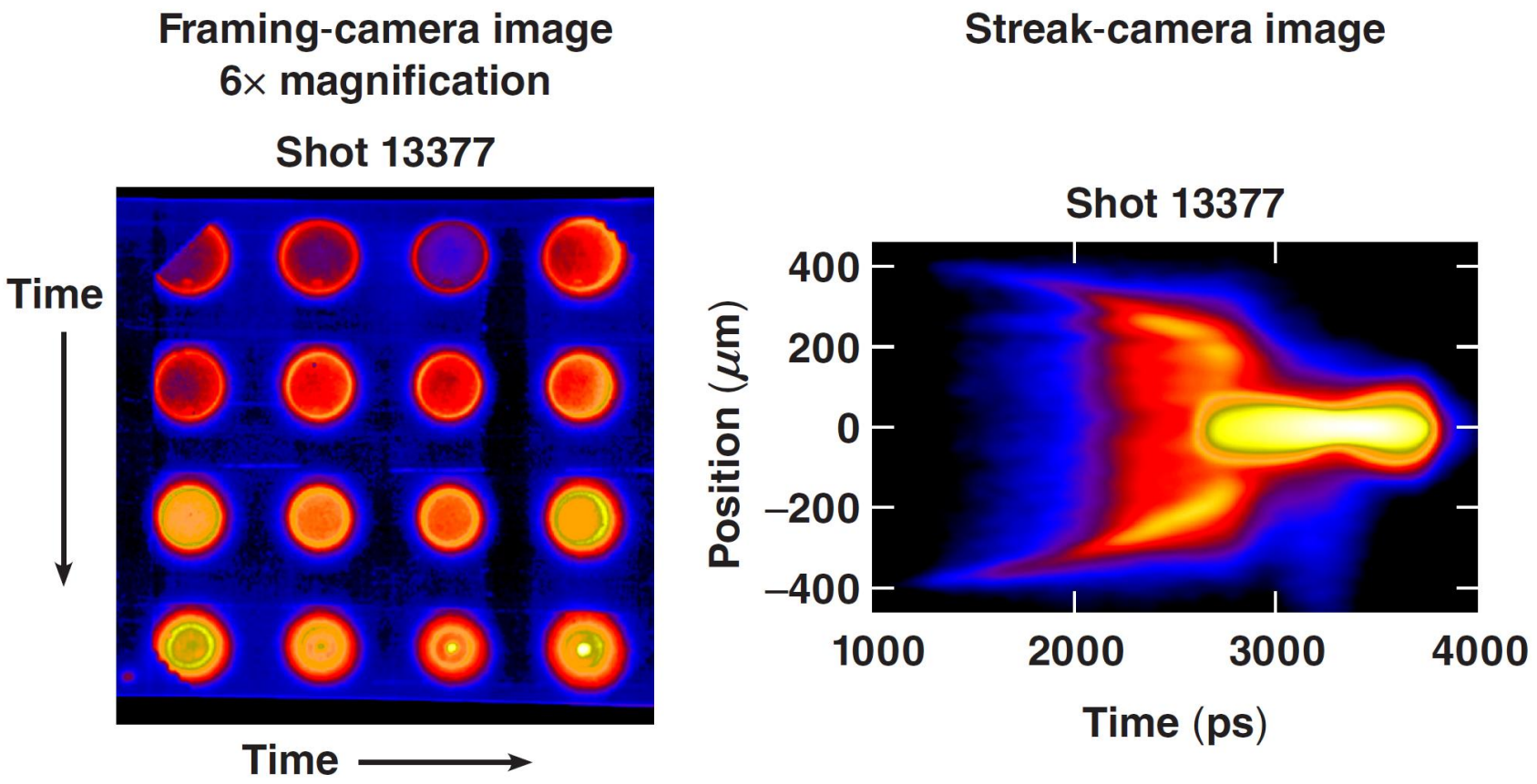

The optical density can be measured using the absorption of a backlighter

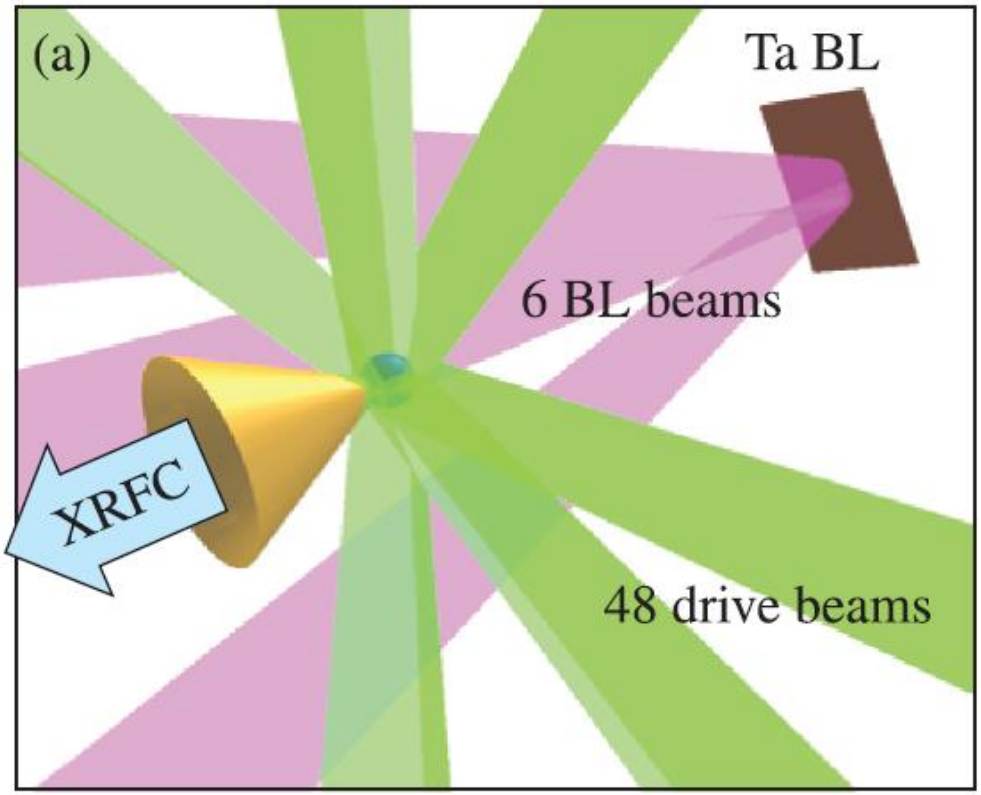

$$I = \int I(\varepsilon)\exp(-\mu(\varepsilon)\rho\delta)d\varepsilon$$

$$I = I_{\mathrm{BL}}\exp(-\bar{\mu}\rho\delta)$$

$$\ln I = \ln I_{BL} - \mu\rho r$$

G. Fiksel *et al.*, Phys. Plasmas **19**, 062704 (2012)

Shock velocities are measured using time-resolved Velocity Interferometer System for Any Reflector (VISAR)

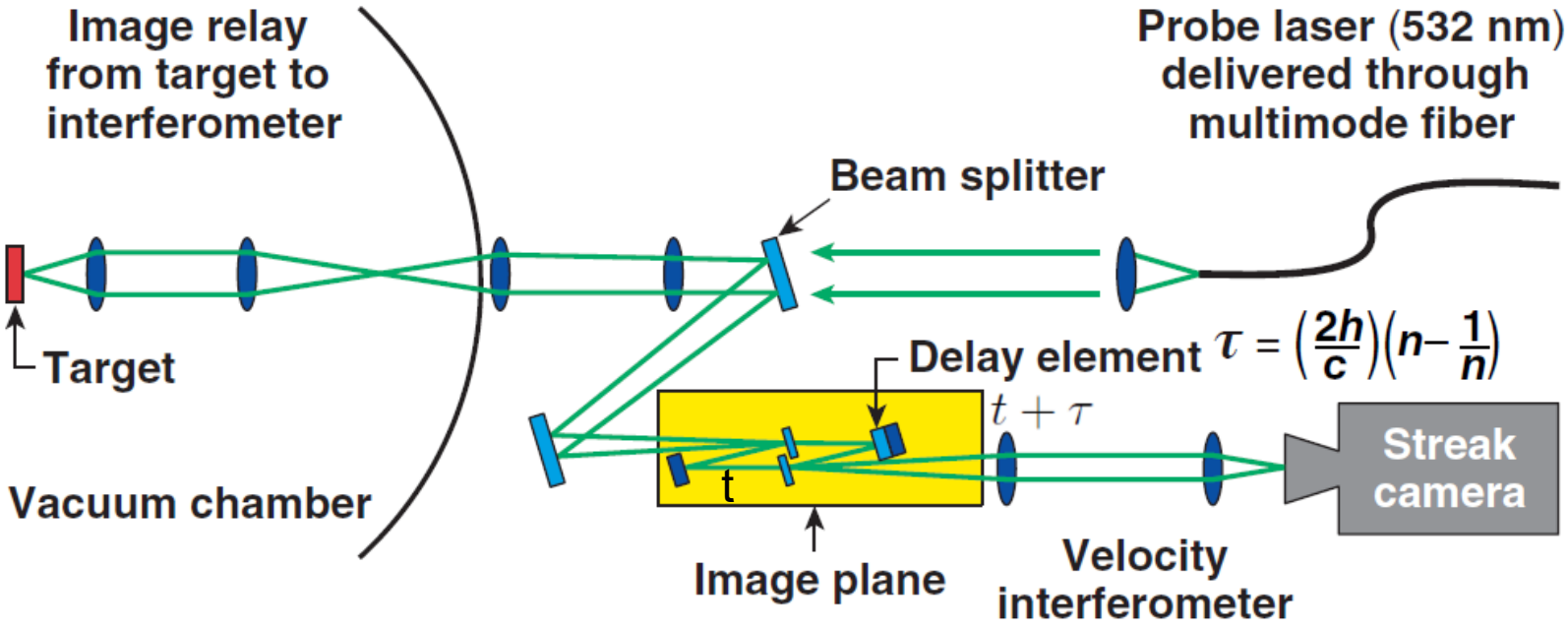

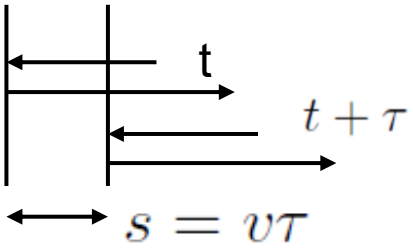

$$\Delta\phi = \frac{v\tau}{\lambda} \propto v$$

Neutron average temperature is obtained using Neutron Time of Flight (NToF)

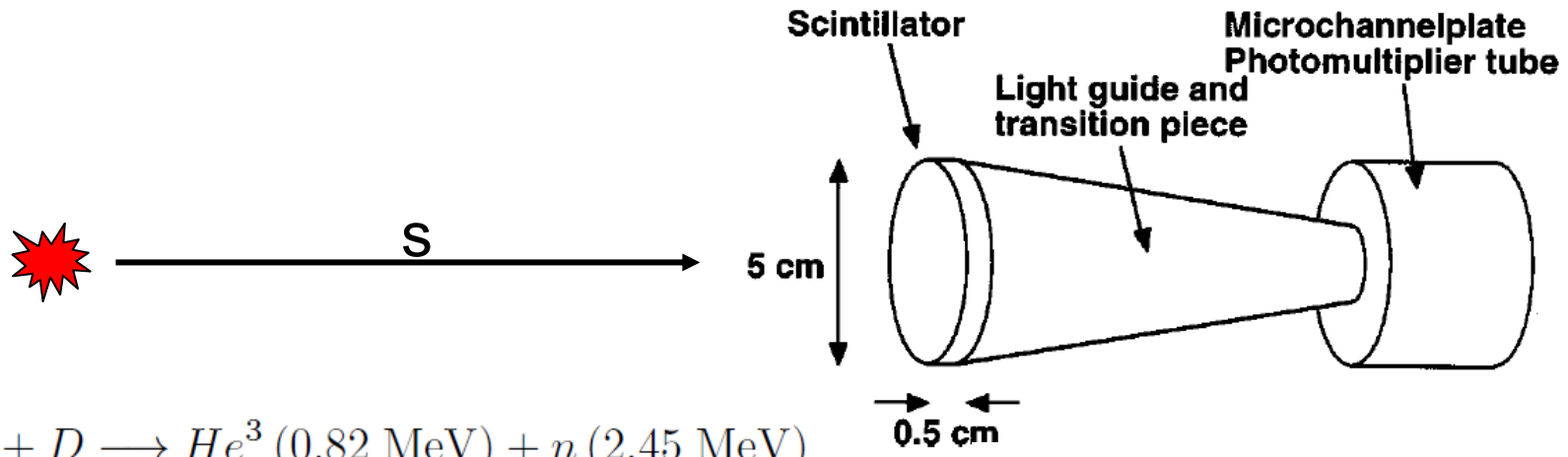

$$D + D \longrightarrow He^3\,(0.82\ \mathrm{MeV}) + n\,(2.45\ \mathrm{MeV})$$

$$D + T \longrightarrow He^4\,(3.5\ \mathrm{MeV}) + n\,(14.1\ \mathrm{MeV})$$

$$s = vt \qquad v = \frac{s}{t}$$

$$f(v) = \sqrt{\left(\frac{m}{2\pi kT}\right)}\exp\left(-\frac{mv^2}{2kT}\right)$$

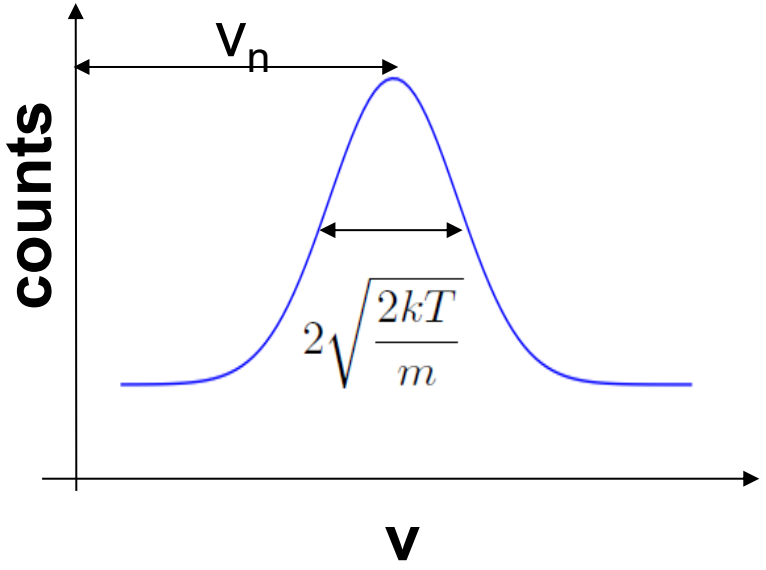

T. J. Murphy *et al.*, Rev. Sci. Instrum. **72**, 773 (2001)

The OMEGA Facility is carrying out ICF experiments using a full suite of target diagnostics

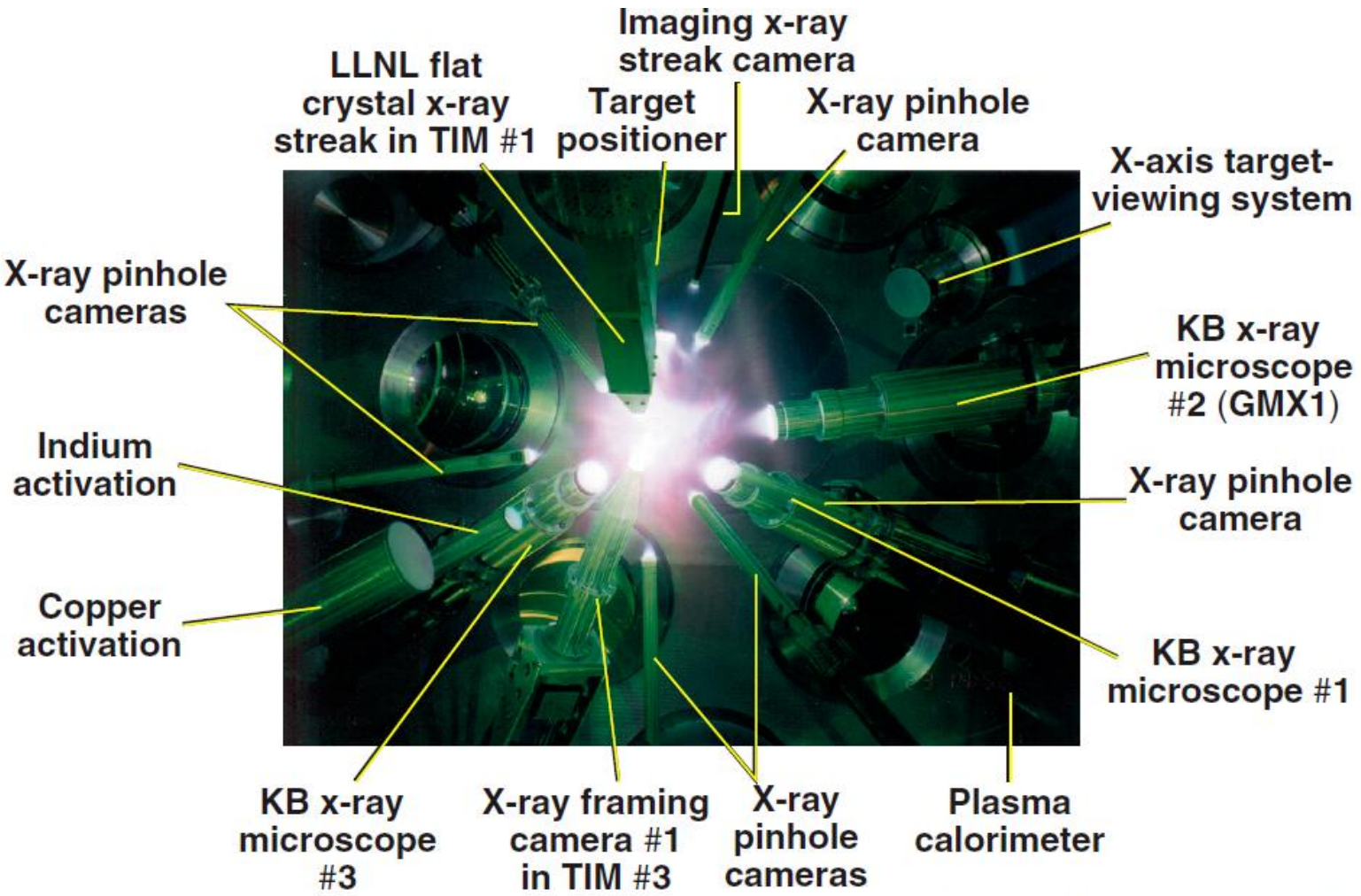

A suit of diagnostics in the range of (soft) x-ray are being built

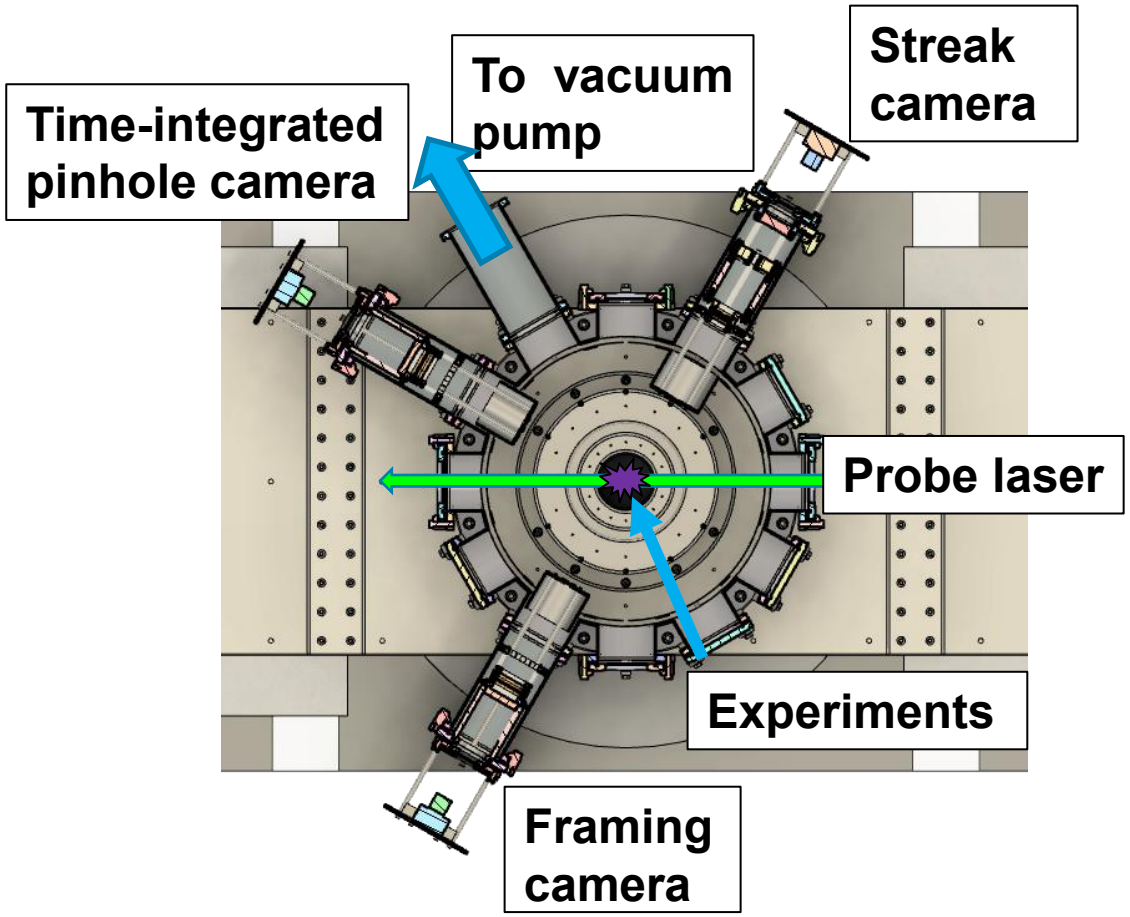

- CsI are used as the photocathode for all x-ray imaging system.
- Au photocathode may be used in the future.

- **Pinhole camera:**
  - Magnification: 1x
  - Exposure time: 1 us
- **Streak camera:**
  - Magnification: 1x
  - Temporal resolution: 15 ps
- **Framing camera:**
  - Magnification: 0.3x
  - Temporal resolution: ~ns using 4 individual MCPs
- **Laser probing:**
  - For interferometer, schlieren, shadowgraphy, Thomson scattering.
  - Temporal resolution: ~300 ps using stimulated brillouin scattering (SBS) pulse compression in water

Energetic charged particles losses most of its energy right before it stops

Momentum transfer:

$$\Delta p_\perp = \int F_\perp dt = \int F_\perp \frac{dt}{dx} dx = \int F_\perp \frac{dx}{v}$$

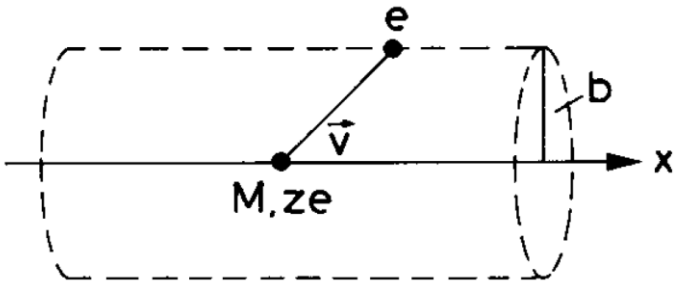

$$= \int_{-\infty}^{\infty} \frac{ze^2}{(x^2+b^2)} \cdot \frac{b}{\sqrt{x^2+b^2}} \cdot \frac{1}{v}\, dx = \frac{ze^2 b}{v} \left[\frac{x}{b^2\sqrt{x^2+b^2}} \right]_{-\infty}^{\infty} = \frac{2ze^2}{bv}$$

$\Delta p_\parallel$: averages to zero

$$\Delta E(b) = \frac{\Delta p^2}{2m_e} \qquad N_e = n \cdot (2\pi b) \cdot db\, dx$$

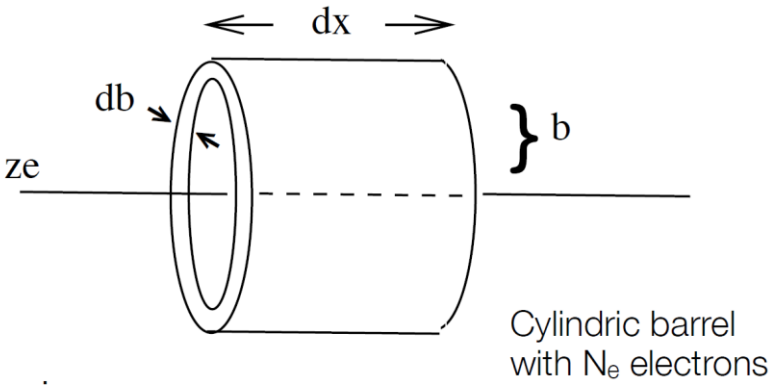

$$-dE(b) = \frac{\Delta p^2}{2m_e} \cdot 2\pi n b\, db\, dx$$

$$-\frac{dE}{dx} = \frac{4\pi\, n\, z^2 e^4}{m_e v^2} \cdot \int_{b_{min}}^{b_{max}} \frac{db}{b} = \frac{4\pi\, n\, z^2 e^4}{m_e v^2} \ln \frac{b_{max}}{b_{min}}$$

Proton therapy takes the advantage of using Bragg peak

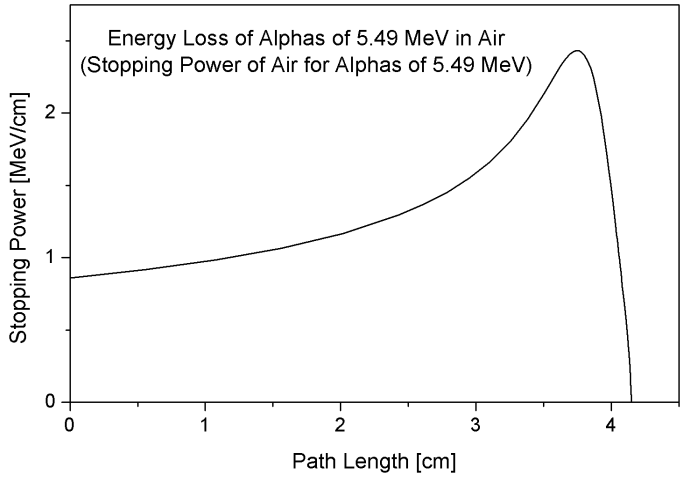

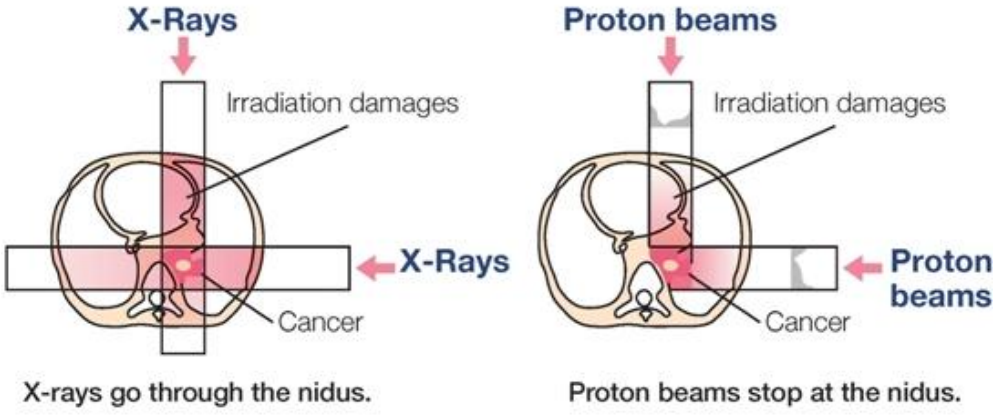

http://www.shi.co.jp/quantum/eng/product/proton/proton.html

There are two suggested website for getting the information of proton stopping power in different materials

http://www.nist.gov/pml/data/star/

NIST | NIST Time | NIST Home | About NIST | Contact Us | A-Z Site Index | Search

Physical Measurement Laboratory

About PML | Publications | Topic/Subject Areas | Products/Services | News/Multimedia | Programs/Projects | Facilities

NIST Home > PML > Physical Reference Data > Stopping-Power & Range Tables: e-, p+, Helium Ions

NISTIR 4999 | Version History | Disclaimer

Stopping-Power and Range Tables for Electrons, Protons, and Helium Ions

M.J. Berger, J.S. Coursey, M.A. Zucker and J. Chang
(NIST, Physical Measurement Laboratory)

estar | astar | pstar

Abstract:

The databases ESTAR, PSTAR, and ASTAR calculate stopping-power and range tables for electrons, protons, or helium ions, according to methods described in ICRU Reports 37 and 49. Stopping-power and range tables can be calculated for electrons in any user-specified material and for protons and helium ions in 74 materials.

Contents:

1. Introduction
2. ESTAR: Stopping Powers and Ranges for Electrons
3. PSTAR and ASTAR: for Protons and Helium Ions (alpha particles)

References

Appendix: Significance of Calculated Quantities

Access the Data:

1. Electrons
2. Protons

請選取語言 | SHARE

由「Google 翻譯」技術提供

© Creations/2010 Shutterstock.com

Access the Data

Electrons | Protons | Helium Ions

NIST Standard Reference Database 124
Rate our products and services.
Online: October 1998 - **Last update:** August 2005

Contact

Stephen Seltzer

http://www.srim.org/

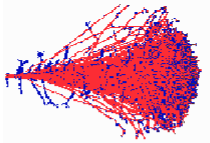

NEW! SRIM Textbook NEW!

Software	Science
SRIM / TRIM Introduction	Historical Review
Download SRIM-2013	Details of SRIM-2013
SRIM Install Problems	Experimental Data Plots Stopping of Ions in Matter
SRIM Tutorials	Stopping in Compounds
Download TRIM Manual Part-1, Part-2	Scientific Citations of Experimental Data
Stopping, Range and Damage	High Energy Stopping

The thickness of a filter can be decided from the range data from NIST website

COPPER

To download data in spreadsheet (array) form, choose a delimiter and use the checkboxes in the table heading. After downloading, save the output by using your browser's Save As feature.

Delimiter:
- space
- | (vertical bar)
- tab (some browsers may use spaces instead)
- newline

Download data | Reset

$\frac{dE}{\rho dx}$ ρx

(required) Kinetic Energy (MeV)	Stopping Power (MeV cm²/g)			Range		
	Electronic	Nuclear	Total	CSDA (g/cm²)	Projected (g/cm²)	Detour Factor Projected / CSDA
1.000E-03	3.490E+01	4.408E+00	3.931E+01	4.116E-05	5.620E-06	0.1365
1.500E-03	4.274E+01	4.231E+00	4.697E+01	5.267E-05	8.301E-06	0.1576
2.000E-03	4.935E+01	4.049E+00	5.340E+01	6.263E-05	1.101E-05	0.1759
2.500E-03	5.518E+01	3.876E+00	5.906E+01	7.152E-05	1.374E-05	0.1921
3.000E-03	6.045E+01	3.718E+00	6.416E+01	7.964E-05	1.647E-05	0.2068
4.000E-03	6.980E+01	3.440E+00	7.324E+01	9.419E-05	2.194E-05	0.2329
5.000E-03	7.804E+01	3.207E+00	8.124E+01	1.071E-04	2.739E-05	0.2556
6.000E-03	8.548E+01	3.010E+00	8.849E+01	1.189E-04	3.280E-05	0.2758
7.000E-03	9.233E+01	2.840E+00	9.517E+01	1.298E-04	3.817E-05	0.2940
8.000E-03	9.871E+01	2.692E+00	1.014E+02	1.400E-04	4.347E-05	0.3106
9.000E-03	1.047E+02	2.561E+00	1.073E+02	1.496E-04	4.872E-05	0.3258
1.000E-02	1.104E+02	2.445E+00	1.128E+02	1.587E-04	5.391E-05	0.3398

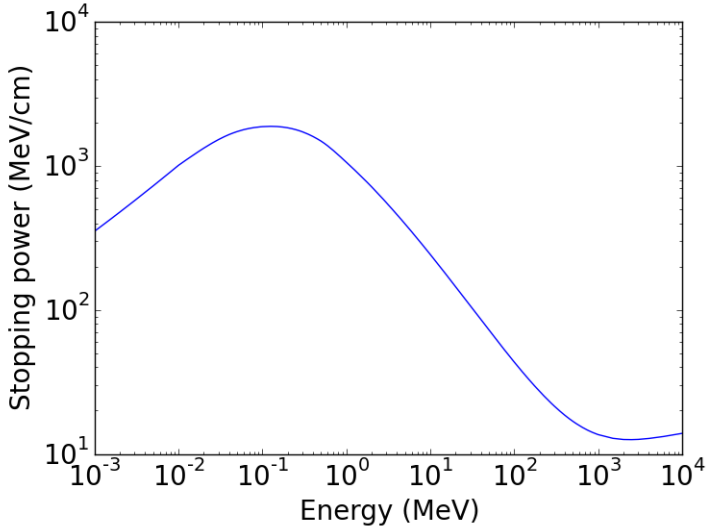

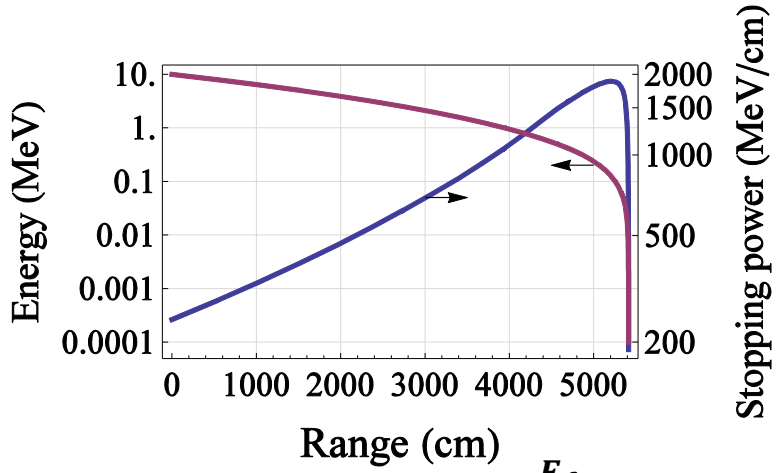

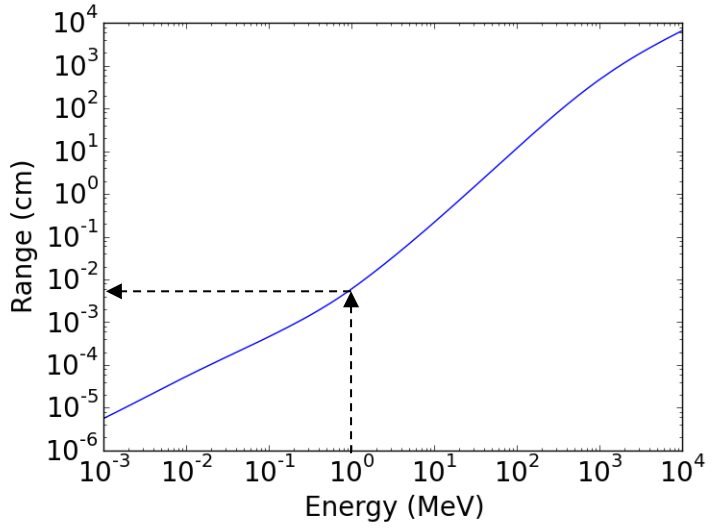

$$\frac{dE}{dx} = f(E) \Rightarrow x = \int_{E_i}^{E_f} \frac{dE}{f(E)}$$

Proton therapy takes the advantage of using Bragg peak

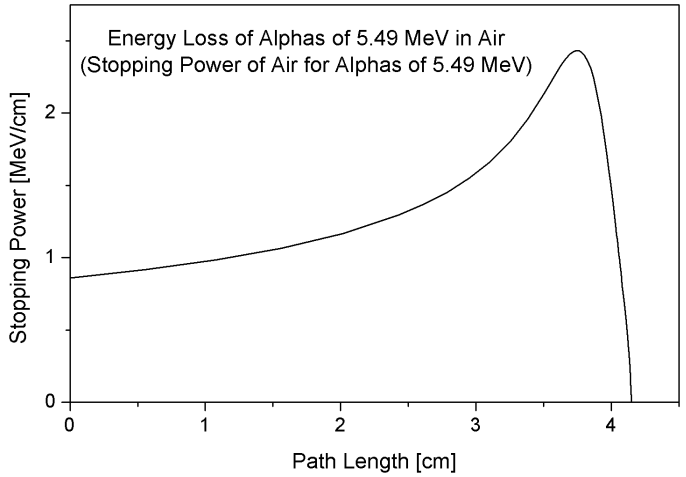

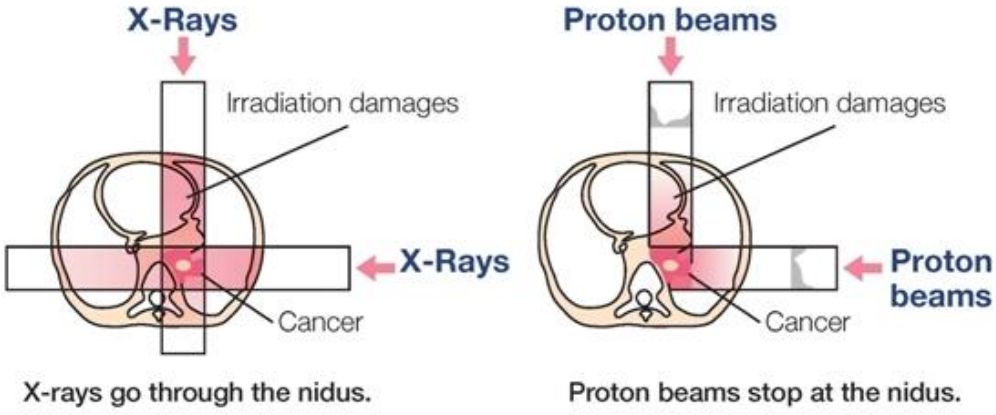

http://www.shi.co.jp/quantum/eng/product/proton/proton.html

Saha equation gives the relative proportions of atoms of a certain species that are in two different states of ionization in thermal equilibrium

$$\frac{n_{r+1}n_e}{n_r} = \frac{G_{r+1}g_e}{G_r}\frac{(2\pi m_e KT)^{3/2}}{h^3}\exp\left(-\frac{\chi_r}{KT}\right)$$

- n_{r+1}, n_r: Density of atoms in ionization state r+1, r (m^{-3})
- n_e: Density of electrons (m^{-3})
- G_{r+1}, G_r: Partition function of ionization state r+1, r
- g_e=2: Statistical weight of the electron
- m_e: Mass of the electron
- χ_r: Ionization potential of ground level of state r to reach to the ground level of state r+1
- T: Temperature
- h: Planck's constant
- K: Boltzmann constant

Supplement to Ch. 6 of Astrophysics Processes by Hale Bradt
(http://homepages.spa.umn.edu/~kd/Ast4001-2015/NOTES/n052-saha-bradt.pdf)

Some backgrounds of quantum mechanics

- **Planck blackbody function:**

$$u(\nu, T) = \frac{8\pi h\nu^3}{c^3}\frac{1}{e^{h\nu/KT} - 1}\left(W/m^3\,\mathrm{Hz}\right)$$

- **Boltzmann formula:**
  - **g_i, g_j: statistical weight**

$$\frac{n_i}{n_j} = \frac{g_i e^{-\epsilon_i/KT}}{g_j e^{-\epsilon_j/KT}} = \frac{g_i}{g_j} e^{-h\nu_{ij}/KT} \qquad \frac{g_i}{g_j} = \frac{2J_i + 1}{2J_j + 1}$$

    (J: angular momenta quantum number)
  - **Number in the ith state to the total atom:**

$$\frac{n_i}{n} = \frac{n_i}{\Sigma n_j} \equiv \frac{g_i e^{-\epsilon_i/KT}}{G} \qquad G \equiv \Sigma g_j e^{-\epsilon_j/KT}$$

G: partition function of statistical weight for the atom, taking into account all its excited states.

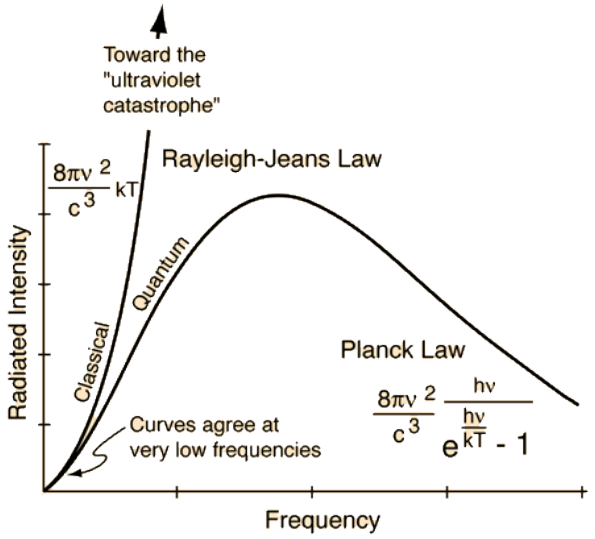

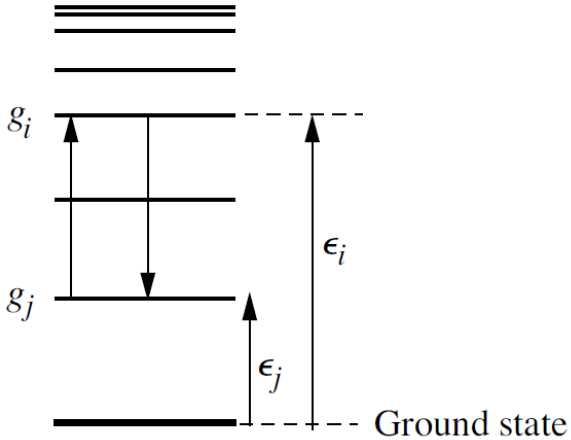

http://hyperphysics.phy-astr.gsu.edu/hbase/mod6.html

Einstein coefficient

- **Probability of electron energy transition:**
  - **Excitation (↑):** $P_{ji} = B_{ji}u(\nu, T)$
  - **De-excitation (↓):** $P_{ij} = A_{ij} + B_{ij}u(\nu, T)$
- **In thermal equilibrium:**

$$n_i\left(A_{ij} + B_{ij}u\right) = n_j B_{ji} u$$

$$\frac{g_i}{g_j} e^{-x}\left(A_{ij} + B_{ij}u\right) = B_{ji}u \qquad x \equiv \frac{h\nu}{KT}$$

$$u = a(e^x - 1)^{-1} \qquad a \equiv \frac{8\pi h\nu^3}{c^3}$$

$$a\left(e^x B_{ji} - \frac{g_i}{g_j} B_{ij}\right) = (e^x - 1)\frac{g_i}{g_j} A_{ij}$$

- **The Einstein coefficients are independent of T or v.**

$x \to 0, e^x \to 1$ $\qquad$ $x \to \infty, e^x \to \infty$

$$\frac{B_{ij}}{B_{ji}} = \frac{g_j}{g_i} \qquad aB_{ji} = \frac{g_i}{g_j} A_{ij} \qquad \frac{A_{ij}}{B_{ij}} = \frac{8\pi h\nu^3}{c^3}$$

- **Photoexcitation:**

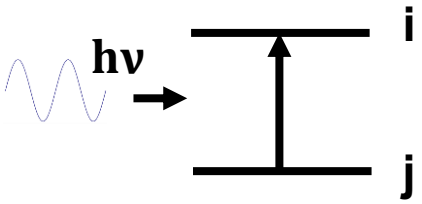

- **Induced radiation:**

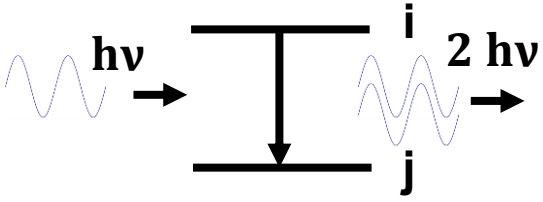

- **Spontaneous radiation:**

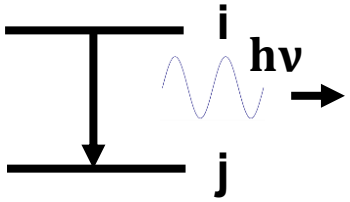

Saha equation is derived using the transition between different ionization states

- **Required photon energy for transition (1) from the ground state of r ionization state to the ground state of r+1 ionization state:**

$$h\nu = \chi_r + \frac{p^2}{2m}$$

Energy of the free electron

- **Required photon energy for transition (1) from the energy level k of r ionization state to the energy level j of r+1 ionization state:**

$$h\nu = \chi_r + \epsilon_{r+1,j} - \epsilon_{r,k} + \frac{p^2}{2m}$$

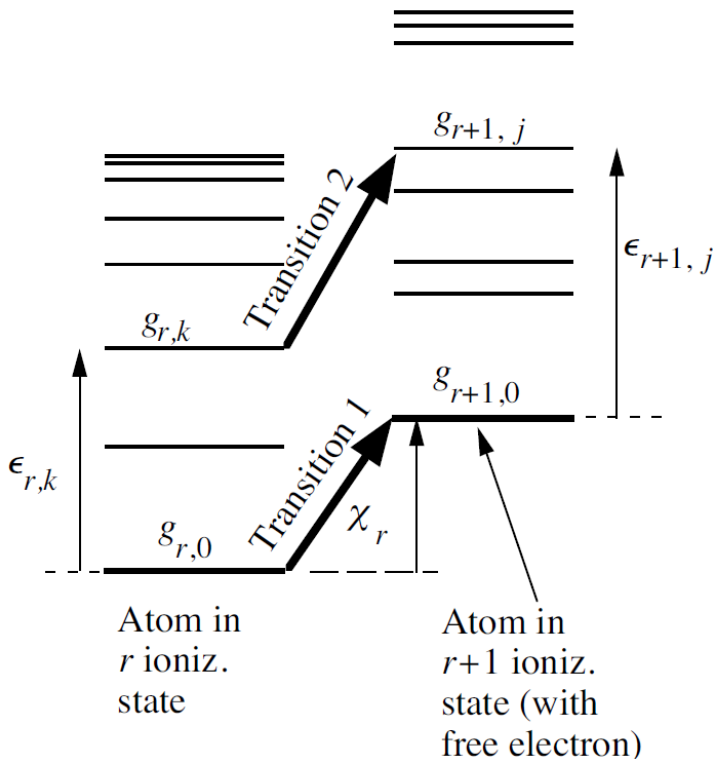

Saha equation is derived using the transition between different ionization states

- **Photoionization:**

$$R_{\mathrm{pi}} = n_{r,k} u(\nu) B_{r,k\to r+1,j}$$

- **Induced radiation:**

$$R_{\mathrm{ir}} = n_{r+1,j} n_{e,p}(p) u(\nu) B_{r+1,j\to r,k}$$

- **Spontaneous emission:**

$$R_{\mathrm{sr}} = n_{r+1,j} n_{e,p}(p) A_{r+1,j\to r,k}$$

- **In thermal equilibrium:**

$$n_{r+1,j} n_{e,p} A_{r+1,j\to r,k} + n_{r+1,j} n_{e,p} u B_{r+1,j\to r,k} = n_{r,k} u B_{r,k\to r+1,j}$$

- **Einstein coefficients:**

$$\frac{B_{r,k\to r+1,j}}{B_{r+1,j\to r,k}} = \frac{g_{r+1,j}}{g_{r,k}} \frac{g_e 4\pi p^2}{h^3} \qquad \frac{A_{r+1,j\to r,k}}{B_{r+1,j\to r,k}} = \frac{8\pi h \nu^3}{c^3}$$

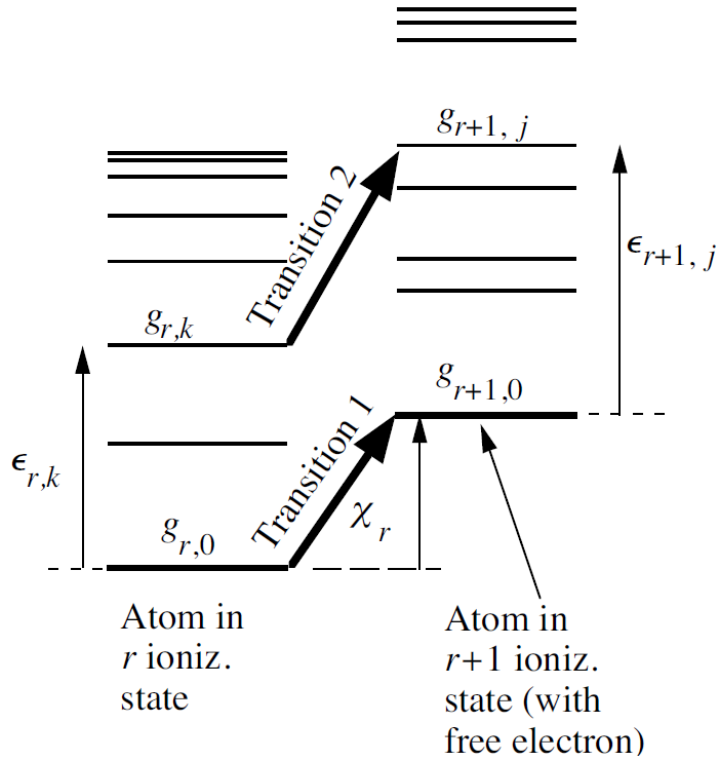

Saha equation - continued

$$n_{r+1,j}n_{e,p}A_{r+1,j\to r,k} + n_{r+1,j}n_{e,p}uB_{r+1,j\to r,k} = n_{r,k}uB_{r,k\to r+1,j}$$

$$n_{r+1,j}n_{e,p}\frac{A_{r+1,j\to r,k}}{B_{r+1,j\to r,k}} + n_{r+1,j}n_{e,p}u = n_{r,k}u\frac{B_{r,k\to r+1,j}}{B_{r+1,j\to r,k}}$$

$$\frac{n_{r+1,j}n_{e,p}}{n_{r,k}} = \left(\frac{A_{r+1,j\to r,k}}{uB_{r+1,j\to r,k}} + 1\right)^{-1}\frac{B_{r,k\to r+1,j}}{B_{r+1,j\to r,k}}$$

$$\frac{B_{r,k\to r+1,j}}{B_{r+1,j\to r,k}} = \frac{g_{r+1,j}}{g_{r,k}}\frac{g_e 4\pi p^2}{h^3}$$

$$n_{e,p}(p) = \frac{n_e 4\pi p^2}{(2\pi mKT)^{3/2}}\exp\left(-\frac{p^2}{2mKT}\right)$$

$$\frac{A_{r+1,j\to r,k}}{B_{r+1,j\to r,k}} = \frac{8\pi h\nu^3}{c^3}$$

$$\frac{n_{r+1,j}n_e}{n_{r,k}} = \frac{(2\pi mKT)^{3/2}}{4\pi p^2}\exp\left(\frac{p^2}{2mKT}\right)\left[\frac{c^3}{8\pi h\nu^3}\left(e^{h\nu/KT}-1\right)\frac{8\pi h\nu^3}{c^3}+1\right]^{-1}\frac{g_{r+1,j}}{g_{r,k}}\frac{g_e 4\pi p^2}{h^3}$$

$$\frac{n_{r+1,j}n_e}{n_{r,k}} = \frac{(2\pi mKT)^{3/2}}{h^3}\frac{g_{r+1,j}g_e}{g_{r,k}}\exp\left[\frac{1}{KT}\left(\frac{p^2}{2m}-h\nu\right)\right]$$

Saha equation - continued

$$\frac{n_{r+1,j}n_e}{n_{r,k}} = \frac{(2\pi mKT)^{3/2}}{h^3}\frac{g_{r+1,j}g_e}{g_{r,k}}\exp\left[\frac{1}{KT}\left(\frac{p^2}{2m} - h\nu\right)\right]$$

$$\frac{n_{r+1,j}n_e}{n_{r,k}} = \frac{(2\pi mKT)^{3/2}}{h^3}\frac{g_{r+1,j}g_e}{g_{r,k}}\exp\left[\frac{1}{KT}\left(\frac{p^2}{2m} - \chi_r - \epsilon_{r+1,j} + \epsilon_{r,k} - \frac{p^2}{2m}\right)\right]$$

$$\frac{n_{r+1,j}n_e}{n_{r,k}} = \frac{(2\pi mKT)^{3/2}}{h^3}\frac{g_{r+1,j}\exp\left(\frac{\epsilon_{r+1,j}}{KT}\right)g_e}{g_{r,k}\exp\left(\frac{\epsilon_{r,k}}{KT}\right)}\exp\left(-\frac{\chi_r}{KT}\right)$$

$$\frac{n_{r,k}}{n_r} = \frac{g_{r,k}e^{-\epsilon_{r,k}/KT}}{G_r} \qquad G_r = \Sigma g_{r,k}e^{-\epsilon_{r,k}/KT}$$

$$\frac{n_{r+1,j}}{n_{r+1}} = \frac{g_{r+1,j}e^{-\epsilon_{r+1,j}/KT}}{G_{r+1}} \qquad G_{r+1} = \Sigma g_{r+1,j}e^{-\epsilon_{r+1,j}/KT}$$

$$\frac{n_{r+1}n_e}{n_r} = \frac{G_{r+1}g_e}{G_r}\frac{(2\pi m_e KT)^{3/2}}{h^3}\exp\left(-\frac{\chi_r}{KT}\right)$$

Saha equation – example: hydrogen plasma of the sun

- **Photosphere of the sun – hydrogen atoms in an optically thick gas in thermal equilibrium at temperature T=6400 K.**
  - **Neutral hydrogen (r state / ground state)**

$$G_r = \Sigma g_{r,k} = g_{r,0} + g_{r,1}\exp\left(-\frac{\epsilon_{r,1}}{KT}\right) + \cdots = 2 + 8\exp\left(-\frac{10.2eV}{0.56eV}\right) + \cdots$$

$$= 2 + 9.8 \times 10^{-8} + \cdots \approx 2$$

  - **Ionized state (r+1 state)**

$$G_{r+1} = \Sigma g_{r+1,j} = g_{r+1,0} + g_{r+1,1}\exp\left(-\frac{\epsilon_{r+1,1}}{KT}\right) + \cdots \approx 1$$

  - **Other information:** $g_e = 2$ $\chi_r = 13.6eV; KT = 0.56eV$ $n_{r+1} = n_e$

$$\frac{{n_{r+1}}^2}{n_r} = 2.41 \times 10^{21}\frac{1 \times 2}{2}(6400)^{3/2}\exp\left(-\frac{13.6}{0.56}\right) = 3.5 \times 10^{16} m^{-3}$$

It is mostly neutral in the photosphere of the sun

- **Assuming 50 % ionization:**

$$n_{r+1} = n_r = 3.5 \times 10^{16} m^{-3} \qquad n = n_{r+1} + n_r = 7 \times 10^{16} m^{-3}$$

- **At lower densities n at the same temperature, there should be fewer collisions leading to recombination and thus the plasma to be more than 50 % ionization.**
- **In the photosphere of the sun:**

$$\rho \sim 3 \times 10^{-4}\,\mathrm{kg}/m^3 \rightarrow n = 2 \times 10^{23} m^{-3} \gg 7 \times 10^{16} m^{-3}$$

$\Rightarrow$ **Less than 50 % ionization**

- **Use the total number density to estimate the ionization percentage:**

$$n_{r+1} + n_r = 2 \times 10^{23}$$

$$\frac{n_{r+1}}{n_r} = 4 \times 10^{-4} @ 6400K$$